

Neuropeptidergic regulation of locomotion inhibition in *C. elegans*
studying stop and sleep neurons with (opto)genetics and fluorescence microscopy

Dissertation
zur Erlangung des Doktorgrades
der Naturwissenschaften

vorgelegt beim Fachbereich Biochemie, Chemie und Pharmazie
der Johann Wolfgang Goethe -Universität
in Frankfurt am Main

von
Petrus Van der Auwera
aus Diest, Belgien

Frankfurt 2022
(D 30)

Cotutelle PhD Thesis – KU Leuven – Goethe University Frankfurt

**NEUROPEPTIDERGIC REGULATION OF
LOCOMOTION INHIBITION IN *C. ELEGANS***
STUDYING STOP AND SLEEP NEURONS WITH
(OPTO)GENETICS AND FLUORESCENCE MICROSCOPY

Petrus VAN DER AUWERA

Supervisors:
Prof. Dr. Liliane Schoofs
Prof. Dr. Alexander
Gottschalk

Co-Supervisor:
Prof. Isabel Beets

Members of the
Examination Committee:
Prof. Dr. Hideaki Mizuno
Prof. Dr. Klaas Martinus Pos
Prof. Dr. Martin Grininger

Dissertation presented in partial
fulfilment of the requirements
for the degree of **Doctor of
Science (PhD): Biochemistry
and Biotechnology** or **PhD in
Natural Sciences (Dr. phil.
nat.)**

September 2022

vom Fachbereich Biochemie, Chemie und Pharmazie der
Johann Wolfgang Goethe - Universität als Dissertation angenommen.

Dekan: Prof. Dr. Clemens Glaubitz

Gutachter: Prof. Dr. Alexander Gottschalk, Prof. Dr. Liliane Schoofs, Prof. Dr. Klaas Martinus Pos,
Prof. Dr. Martin Grininger.

Datum der Disputation : 18 / 01 /2023

Cotutelle PhD Thesis – KU Leuven – Goethe University Frankfurt

Doctoraatsproefschrift aan de faculteit Wetenschappen van de KU Leuven

© 2022 Petrus Van der Auwera
Uitgegeven in eigen beheer, Petrus Van der Auwera, Leuven, Belgium

Alle rechten voorbehouden. Niets uit deze uitgave mag worden vermenigvuldigd en/of openbaar gemaakt worden door middel van druk, fotokopie, microfilm, elektronisch of op welke andere wijze ook zonder voorafgaandelijke schriftelijke toestemming van de uitgever.

All rights reserved. No part of the publication may be reproduced in any form by print, photoprint, microfilm, electronic or any other means without written permission from the publisher.

I. Preface

Explanation on the Joint/Dual Doctorate

This written dissertation is the exam piece that is used to assess the quality of doctoral research prepared by **Petrus Van der Auwera** at two Universities: (1) J.W. Goethe Universität, Frankfurt am Main, Germany and (2) KU Leuven, Leuven, Belgium. From November 2014 until 31th of December 2016, Petrus was employed as a PhD student at the Gottschalk lab (J.W. Goethe Universität, Frankfurt, Germany), and from the first of January 2017 until January 2020, his research continued in the Schoofs lab (KU Leuven, Leuven, Belgium).

For both Universities this dissertation is the single report that has to be presented in partial fulfilment of the requirements for the degree of “*Doctor of Science (PhD): Biochemistry and Biotechnology*” (KU Leuven, Belgium) or “*PhD in Natural Sciences (Dr. phil. nat.)*” (Johann Wolfgang Goethe – Universität, Frankfurt, Germany). The doctoral candidate has the right to carry the title in either the one or in the other form. However, no two independent doctoral titles will be awarded. Each of the two Universities issues a certificate. The certificates must state that the title is awarded on grounds of a joint supervision agreement (cotutelle), and that the certificates are only jointly valid.

To enable this cooperation between both universities a “Joint Supervision Cotutelle Agreement” (“Kooperationsvertrag zur Cotutelle”) was composed at the start of this PhD project and signed by the representatives of both parties.

This agreement is included below for the purposes of completeness and transparency.

Kooperationsvertrag zur Cotutelle

Präambel

Die *Goethe-Universität* Frankfurt am Main vertreten durch ihre Präsidentin, Prof. Birgitta Wolff, und die *Katholische Universität Leuven* (Belgien), vertreten durch ihren Rektor Rik Torfs, vereinbaren mit diesem Vertrag ein gemeinsames Promotionsverfahren von *Petrus Van der Auwera*, geboren in *Diest (Belgien)*, 2. 5. 1991.

Der Kooperationsvertrag wird unter Beachtung der folgenden Regularien geschlossen:

des *Codex Higher Education*; beschlossen am 11 October 2013;
des Beschlusses der Flämischen Regierung vom 11 Juni 2004, welcher die Art der Diplome und den Inhalt der begleitenden Diplom-Anhänge, wie sie von Anstalten der höheren Bildung in Flandern vergeben werden, insbesondere der Annexe 5 und 6;
der Regularien der Universität Leuven bezüglich Doktoratsstudien und der Doktorarbeit, des Doktorandenprogramms der Katholieke Universiteit Leuven, verabschiedet vom Akademischen Rat am 13. November 2006, und aktualisiert im Juli 2013;
der generellen Regularien der Arenberg Graduiertenschule für Naturwissenschaften, Ingenieurwissenschaften & Technologie der KU Leuven, verabschiedet vom Exekutivkomitee der Gruppe Naturwissenschaften, Ingenieurwissenschaften & Technologie am 20. März 2013;
gemäß der Promotionsordnung der Mathematisch-Naturwissenschaftlichen Fachbereiche der Goethe-Universität vom 26. Mai 1993 (ABL.1/94, S. 21), zuletzt geändert am 30. September 2014

I. Verwaltungstechnische Modalitäten

Die Einschreibung von *Petrus Van der Auwera* zur Cotutelle wird mit dem Inkrafttreten dieses Vertrages vorgenommen.

Er ist bereits als Doktorand eingeschrieben in Leuven, seit dem 2. September 2014.

Die voraussichtliche Dauer der Forschungsarbeit beträgt vier Jahre. Gegebenenfalls kann diese

Joint Supervision Cotutelle Agreement

Preamble

This agreement regulates a joint doctoral supervision for *Petrus Van der Auwera*, born in *Diest, Belgium*, 2nd of May, 1991, and is between *Goethe-University, Frankfurt am Main*, Germany, represented by its President, Prof. Brigitta Wolff, and *Katholieke Universiteit, Leuven*, Belgium, represented by its Rector, Prof. Rik Torfs.

The agreement has been approved in due observance of the following:

the *Codex Higher Education*; codified on 11 October 2013;
the Flemish Government's decision of 11 June 2004 establishing the form of the diplomas and the content of the accompanying diploma supplement awarded by institutions of higher education in Flanders, and annexes 5 and 6 in particular;
the University Regulations concerning pre-doctoral studies and the pre-doctoral examination; doctoral research and the doctorate; the doctoral programme and the doctoral school of the Katholieke Universiteit Leuven, approved by the Academic Council on 13 November 2006, as amended in July 2013;
the General Regulations of the Arenberg Doctoral School of Science, Engineering & Technology KU Leuven, approved by the executive committee of the Science, Engineering & Technology Group on 20 March 2013;
the Regulations of the Goethe University Frankfurt am Main, as laid down in the Promotionsordnung der Mathematisch-Naturwissenschaftlichen Fachbereiche der Goethe-Universität vom 26. Mai 1993 (ABL.1/94, S. 21), and amended on 30 September 2014

I. Administrative Details

Petrus Van der Auwera will be enrolled as Cotutelle PhD candidate with this agreement coming into effect in Frankfurt.

He has been enrolled in the Doctoral Program in Leuven since 2. September 2014.

The research project is carried out within an estimated period of 4 years, with a possible

Frist in Übereinstimmung mit den in beiden Fachbereichen gültigen Promotionsordnungen verlängert werden.

Die Vorbereitungsdauer der Dissertation verteilt sich zwischen den beiden betreuenden Hochschulen auf abwechselnde Aufenthalte in jedem der beiden Länder. Die Aufenthaltsdauer in den beiden Ländern steht in einem ausgewogenen Verhältnis.

Der Doktorand schreibt sich an jeder der beiden Hochschulen ein, ist aber an einer der beiden Hochschulen von der Zahlung der Einschreibegebühren befreit.

Die Einschreibegebühren werden bezahlt an der Goethe Universität, für die Zeit seines Aufenthaltes an der Goethe Universität.

Zu Beginn der Promotion wird er die vorgeschriebenen Einschreibegebühren der KU Leuven für das Promotionsprogramm der KU Leuven zahlen. Bei der Verteidigung wird er von der Zahlung der Einschreibegebühr der KU befreit.

Der Doktorand ist sozialversichert bei: Deutsche Sozialversicherung, für die Dauer seines Arbeitsvertrages an der Goethe Universität, z. Zt. 16.11.2014 - 15.11.2016.

Der Promotionsstudent wird die erforderlichen Maßnahmen ergreifen, um für seinen Krankenversicherungsschutz Sorge zu tragen. Der Doktorand muss sich jedes Jahr erneut an der Katholieke Universiteit Leuven einschreiben, ansonsten ist er nicht versichert. Der Versicherungsschutz verlängert sich durch die Einschreibung.

II. Studien- und Prüfungsmodalitäten

Der Schutz des Dissertationsthemas und deren Veröffentlichung, die Ausnutzung und der Schutz der Forschungsergebnisse, die gemeinsam in beiden Forschungseinrichtungen von dem/der Doktoranden/in erzielt worden sind, sind in Übereinstimmung mit den gültigen Promotionsordnungen an beiden Hochschulen abgesichert.

Die Forschungsergebnisse aus dem gemeinsamen Programm sollen nicht Inhalt eines Patentantrags oder einer kommerziellen Nutzung / Verwertung von nur einem der beiden Institutionen sein, ohne dass die schriftliche Einwilligung der anderen Einrichtung eingeholt wurde. Der Patentantrag soll, wenn möglich, gemeinsam eingereicht werden. Falls es erforderlich sein sollte, wird eine gesonderte Vereinbarung betreffend des

extension by mutual agreement, according to the relevant regulations.

The preparation of the dissertation will be carried out alternately in both supervising institutions in the two countries. The length of stay in each of the two countries is to be in equal proportion.

The candidate is enrolled in both universities but is exempt from tuition fees in one of the two universities. Tuition fees are paid at *Goethe University*, for the time of his stay at the Goethe University. At the start of the PhD, he shall pay the enrolment fees stipulated by KU Leuven for the doctoral programme to KU Leuven. At the defence, he shall be exempt from paying enrolment fees to KU Leuven.

The candidate is insured according to local social security regulations at German Social Insurance, or the duration of his work contract at Goethe University (currently 16.11. 2014 – 15.11.2016). The doctoral student shall comply with the obligation to take the necessary steps to be covered by health insurance. The doctoral candidate needs to (re)enrol as a doctoral student every year at Katholieke Universiteit Leuven, because otherwise, the doctoral candidate will not be insured. The insurance comes with the (re)enrolment.

II. Academic Details

The publication, exploitation and protection of the dissertation and the results of the Doctoral research, which have been accomplished in both research institutions, are protected according to the relevant policies of both universities. The findings resulting from the common research program shall not be subject of a patent application or a commercial use/exploitation by only one of the two institutions without having requested the written consent of the other institution. The patent applications shall be submitted jointly, if possible, by both institutions. If relevant, a separate agreement concerning intellectual property shall be made in annex to this agreement.

geistigen Eigentums als Anhang zu diesem Vertrag abgeschlossen.

Als Betreuer der Doktorarbeit werden festgelegt:

- an der Goethe-Universität: *Prof. Alexander Gottschalk*
- an der Universität Leuven: *Prof. Liliane Schoofs*

Beide Betreuer verpflichten sich, ihre Aufgabe als Betreuer gegenüber dem/der Doktoranden/in voll auszuüben und die hierzu erforderlichen Absprachen zu treffen.

Der Ort für die Verteidigung der Dissertation wird von den Beteiligten vereinbart.

Die Verteidigung wird von beiden Hochschulen anerkannt.

Die Promotionskommission wird in Übereinstimmung zwischen beiden Partnereinrichtungen ernannt. Sie wird in ausgewogenem Verhältnis mit Wissenschaftlern und Wissenschaftlerinnen aus beiden Ländern besetzt. Dabei werden die Prüfungsordnungen der beiden Länder und der beiden Universitäten berücksichtigt. Erfolgt die Verteidigung an der Goethe Universität, so soll ein zusätzliches Mitglied der Prüfungskommission aus dem Fachbereich 14 der Goethe Universität hinzugezogen werden. Externe Gutachter, die nicht einer der beiden Hochschulen angehören, können in die Promotionskommission eingeladen werden.

Die Mobilitätskosten für die Prüfer und Gutachter der Promotionskommission werden von den Prüfern und Gutachtern übernommen.

Die Dissertation wird in folgender Sprache geschrieben: Englisch.
Die Muttersprache des/der Kandidaten/in ist: Niederländisch
Die Sprache in der die Disputation durchgeführt wird: Englisch
Die Sprache/n der schriftlichen Zusammenfassung: Deutsch / Niederländisch / Englisch

Das Zeugnis:

Es ist nur ein einziger Prüfungsbericht vorzulegen. Es wird von jeder der beiden Universitäten eine Urkunde ausgestellt. Die *Goethe-Universität Frankfurt am Main* verleiht den Titel *Dr. phil nat.* Die *Katholieke*

Supervisors are:

- at Goethe-Universität: *Prof. Alexander Gottschalk*
- at the University of Leuven: *Prof. Liliane Schoofs*

Both supervisors will fully carry out their responsibilities in supervising the candidate and shall make the necessary arrangements.

The location for the disputation of the dissertation (private defense) will be arranged with all persons involved.

Both universities will recognize it.

The board of examiners will be nominated in consensus with both institutions. Scientists from both countries will be present in an appropriate relation. Relevant examination policies of both countries and Universities are considered. Should the defense take place at Goethe University, an additional member of the examination commission shall be called in from the Department 14 of Goethe University. External examiners, who are members of neither of the two Universities can be invited into the board of examiners.

Travel costs for examiners and reviewers are covered by examiners and reviewers themselves.

The dissertation will be written in the following language: English
The native language of the candidate is: Dutch
The language of the disputation is: English
The language of the written summary is: German/Dutch/English

Certification:

Only a single report has to be presented. Each of the two Universities issues a certificate. The *Goethe University* awards the title *Dr. phil. nat.* The *Katholieke Universiteit Leuven* awards the title *Doctor in Science: Biology.*

Universiteit Leuven verleiht den Titel *Doctor in Science: Biology*.

Es ist auf den Urkunden zu vermerken, dass es sich um ein gemeinsames Betreuungsverfahren (Cotutelle) handelt, und dass die Urkunde nur zusammen mit der jeweils anderen Urkunde gültig ist.

Der Promovierte hat das Recht, den Dokortitel entweder in der einen oder anderen Form zu führen. Es werden jedoch keine zwei Dokortitel vergeben.

Mit der Unterzeichnung des Vertrages verpflichten sich der Promotionsstudent und der Betreuer dazu die beiden Promotionsordnungen der beiden Partnereinrichtungen zu beachten, dies gilt sowohl für die Ordnung der Universität selbst als auch für die des Fachbereichs. Sollten sich die Ordnungen widersprechen, soll ein gemeinsamer Konsens darüber gefunden werden, welche Ordnung gilt.

Dieses Abkommen wird mit der Unterzeichnung durch die Leiter/innen beider Hochschulen gültig und endet am Ende des akademischen Jahres in welchem der Promotionsstudent seine Dissertation öffentlich verteidigt. Wenn eine Partei den Vertrag kündigen möchte, muss dies schriftlich erfolgen. Der Vertrag endet dann nach sechs Monaten, beginnend mit dem ersten Monat nach dem Zugang der schriftlichen Mitteilung. Um Zweifel, die möglicherweise während der Vertragslaufzeit oder der Erstellung des Vertrages auftauchen beizulegen, werden die Parteien ihr Bestes geben, um eine gemeinsame Lösung zu finden. Sollte dies unmöglich sein, werden die Parteien gemeinsam eine dritte natürliche Person benennen, die als Mediator fungieren wird.


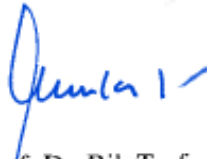







The certificates must state that the title is awarded on grounds of a joint supervision agreement (cotutelle), and that the certificates are only valid jointly.

The doctoral candidate has the right to carry the title in either the one or in the other form. However, there will not be two independent doctoral titles awarded.

By signing this agreement, the doctoral student and the supervisors pledge to act in accordance with the doctoral regulations enforced at each of both of the partner institutions; both the central university stipulations as well as the additional stipulations of the doctoral school and/or relevant faculty. In the event of contradictory stipulations, it shall be decided by mutual consent which regulations shall apply.

This agreement becomes effective when signed by the heads of both universities and shall end at the end of the academic year in which the doctoral student defends the doctoral dissertation publicly. If one of the parties wishes to terminate the agreement, it can do so with a written notice. The agreement will terminate after 6 months starting from the 1st of the month after the receipt of the written notice. Parties will still comply with all running engagements.

In order to settle any doubts that may arise under the performance or in the construction of this Agreement, the Parties shall exert their best efforts to arrive at a solution by mutual consent. In the event such consent is found to be impossible, the Parties shall jointly appoint a third party natural person, to act as mediator.

<p>Date: 06.07.2015</p>  <p>Prof. Brigitta Wolff, Präsident der Goethe-Universität; President of the Goethe-University</p>	<p>Date: JUN 0 5. 2015</p>  <p>Prof. Dr. Rik Torfs, Rector KU Leuven; Rektor der Universität Leuven</p>
<p>Date: 17.07.15</p>  <p>Prof. Dr. Karas, Dekan des Fachbereichs 14 (Biochemie, Chemie und Pharmazie) der Goethe- Universität; Dean of the Faculty of Biochemistry, Chemistry and Pharmacy of the Goethe- University</p>	<p>Date:</p>  <p>Prof. Dr. Johan Martens, Research Director, Science, Engineering & Technology, KU Leuven;</p>
<p></p>	<p>Date: 19/5/2015</p>  <p>Prof. Dr. Stefaan Vaes, Chair of the Doctoral Committee of the Faculty of Science KU Leuven</p>
<p>Date: 23.4.15</p>  <p>Prof. Dr. Alexander Gottschalk Betreuer Goethe-Universität; Supervisor at the Goethe-University</p>	<p>Date: JUN 0 5. 2015</p>  <p>Prof. Dr. Liliane Schoofs, Supervisor KU Leuven; Betreuerin: Universität Leuven</p>
<p>Date: 23/04/2015</p>  <p>Mr. Petrus van der Auwera, Doctoral student; Doktorand</p>	<p>Date: 23/04/2015</p>  <p>Mr. Petrus van der Auwera, Doctoral student; Doktorand</p>

II. Legal declaration

I hereby declare that I have submitted this dissertation entitled:

Neuropeptidergic regulation of locomotion inhibition in *C. elegans*
studying stop and sleep neurons with (opto)genetics and fluorescence microscopy

Except where stated otherwise by reference or acknowledgment, the work presented was generated by myself under the supervision of my advisors during my doctoral studies. All contributions from colleagues are explicitly referenced in the thesis (see below). The following parts of the thesis have been previously published and the material listed below was obtained in the context of collaborative research:

- Chapter 2:

Steuer Costa, W.*, Van der Auwera, P.*, Glock, C., Liewald, J. F., Bach, M., Schüler, C., Wabnig, S., Oranth, A., Masurat, F., Bringmann, H., Schoofs, L., Stelzer, E. H. K., Fischer, S. C. & Gottschalk, A. (2019). A GABAergic and peptidergic sleep neuron as a locomotion stop neuron with compartmentalized Ca²⁺ dynamics. *Nature Communications*, 10, 4095. <https://doi.org/10.1038/s41467-019-12098-5>

(* These authors contributed equally.)

This paper shows that in *Caenorhabditis elegans* the RIS neuron controls the termination of locomotion. Upon optogenetic stimulation, this neuron causes acute stopping behavior while muscle tone and body posture of nematodes are retained. For this, RIS requires GABA to induce behavioral arrest and FLP-11 neuropeptides to sustain the suppression of locomotion. Freely moving animals display spontaneous calcium activity in the axon of RIS which is compartmentalized and which correlates with stopping behavior. I contributed to this study by writing, generating mutant strains for neuropeptidergic signaling and testing these in the optogenetic stopping assay. In addition, I set up the automated microscope for the calcium imaging experiments in moving animals, performed them and analyzed the resulting data.

The contribution of colleagues in the figures presented in this work [percentage with respect to the entire figure] is as following:

Fig. 1: Photo-depolarization of the RIS neuron inhibits locomotion, by Wagner Steuer Costa [50%], Caspar Glock [40%], Sebastian Wabnig [10%] (Goethe Universität Frankfurt).

Fig. 2: RIS photoactivation stopped muscular Ca²⁺-dynamics, by Wagner Steuer Costa [50%], Caspar Glock [30%], Sebastian Wabnig [20%] (Goethe Universität Frankfurt).

Fig. 3: RIS photoactivation suppressed motor neuron (MN) synchrony and Ca²⁺ oscillations, by Jana F. Liewald [35%] and Wagner Steuer Costa [35%], Maximilian Bach [30%] (Goethe Universität Frankfurt).

Fig. 4: The stop phenotype induced by RIS photoactivation requires GABA and neuropeptide signalling, contributors: Wagner Steuer Costa [50%], Petrus Van der Auwera [30%], Caspar Glock [20%] (Goethe Universität Frankfurt).

Fig. 5: Ca²⁺ activity measured along the RIS axon in freely moving animals correlates with slowing and reversals, by Petrus Van der Auwera [90%], Sabine Fischer [10%] (Goethe Universität Frankfurt).

Fig. 6: RIS Ca²⁺ activity induces decreased forward locomotion and increased reversal probability, which requires FLP-11 neuropeptides, by Petrus Van der Auwera [85%] and Alexander Gottschalk [15%] (Goethe Universität Frankfurt).

Fig. 7: Compartmentalized Ca²⁺ dynamics in the RIS process, by Wagner Steuer Costa [60%] and Petrus Van der Auwera [40%] (Goethe Universität Frankfurt).

Fig. 8: Models summarizing stimulated and intrinsic activities of RIS and comparison of sleep and stop neurons across model systems, by Wagner Steuer Costa [30%], Alexander Gottschalk [30%] and Petrus Van der Auwera [30%] (Goethe Universität Frankfurt) and other authors [10%].

- Chapter 3:

Van der Auwera, P.*, Frooninckx, L.*, Buscemi, K., Vance, R. T., Nelson, M. D., Watteyne, J., Mirabeau, O., De Haes, W., Fancsalszky, L., Gottschalk, A., Raizen, D. M., Schoofs, L. & Beets, I (2020). RPamide neuropeptides NLP-22 and NLP-2 act through GnRH-like receptors to promote sleep and wakefulness in *C. elegans*. *Scientific Reports*, 10, 9929.

<https://doi.org/10.1038/s41598-020-66536-2>

(* These authors contributed equally.)

This article demonstrates that NLP-22 and NLP-2 neuropeptides, belonging to the RPamide family, opposingly regulate sleep-wake behavior in *Caenorhabditis elegans*. Gonadotropin-releasing hormone related receptors (GNRR) were identified *in vitro* as their signaling target. Somnogenic NLP-22 neuropeptides released from RIA interneurons function by activating GNRR-6 receptors, while the wake-promoting effects of NLP-2 neuropeptides require both GNRR-3 and GNRR-6. NLP-2 neuropeptides are expressed in AWA olfactory neurons and their transcripts cycle with developmental periodicity. For this study I rewrote the complete manuscript, I made most of the graphs, I generated mutant strains for *gnrr-6* that contained transgenic arrays for *nlp-2/22* overexpression and I identified the expressions patterns of both *nlp-2* and *gnrr-6*.

The contribution of colleagues in the figures presented in this work [percentage with respect to the entire figure] is as following:

Fig. 1: Maximum likelihood tree of vertebrate and invertebrate GnRH/AKH receptors, by Olivier Mirabeau [100%] (Institut Curie, Paris).

Fig. 2: NLP-2, NLP-22, and NLP-23 peptides activate GNRR-3 and GNRR-6 *in vitro*, by Petrus Van der Auwera [60%] and Lotte Frooninckx [40%] (KU Leuven).

Fig. 3: RPamide peptides are conserved among nematodes and share sequence similarity with GnRH/AKH peptides, by Petrus Van der Auwera [100%] (KU Leuven).

Fig. 4: GNRR-6, but not GNRR-3, is required for NLP-22 induced locomotion quiescence, contributors: Lotte Frooninckx [30%], Petrus Van der Auwera [20%] (KU Leuven) and Matthew D. Nelson [20%], Kristen

Buscemi [15%], Ryan T. Vance [15%] (Saint Joseph's University, Philadelphia). **Fig. 5:** GNRR-3 and GNRR-6 are required for the wake-promoting effects of nlp-2 overexpression, contributors: Lotte Frooninckx [30%], Petrus Van der Auwera [20%] (KU Leuven) and Matthew D. Nelson [20%], Kristen Buscemi [15%], Ryan T. Vance [15%] (Saint Joseph's University, Philadelphia).

Fig. 6: Expression of NLP-2 localizes to AWA neurons and cycles with larval periodicity, by Petrus Van der Auwera [55%], Lotte Frooninckx [25%] and Liesbet Temmerman [20%] (KU Leuven).

Both of these open access articles are licensed under a Creative Commons Attribution 4.0 International License (CC BY 4.0), which permits unrestricted use, sharing, adaptation, distribution and reproduction in any medium or format, as long as you give appropriate credit to the original author(s) and the source, provide a link to the Creative Commons license, and indicate if changes were made. You are not required to obtain permission to reuse these articles. The images or other third party material in this article are included in the article's Creative Commons license, unless indicated otherwise in a credit line to the material. If material is not included in the article's Creative Commons license and your intended use is not permitted by statutory regulation or exceeds the permitted use, you will need to obtain permission directly from the copyright holder. To view a copy of this license, visit <http://creativecommons.org/licenses/by/4.0/>.

The journals in which they are published are listed as RoMEO Green at www.sherpa.ac.uk.

In addition, I obtained permission, mainly by requesting written permissions at the Copyright Clearance Center (www.copyright.com), to reuse the following quote and figures in the introductory Chapter 1 of my academic dissertation:

The **quote** on page 3 of Chapter 1 from

Brenner, S. The genetics of *Caenorhabditis elegans*. *Genetics* 77, 71–94 (1974).

“Behavior is the result of a complex and ill-understood set of computations performed by nervous systems and it seems essential to decompose the problem into two: one concerned with the genetic specification of nervous systems and the other with the way nervous systems work to produce behavior. Both require that we must have some way of analyzing the structure of a nervous system.”

Fig. 1 on page 5 of Chapter 1 is a reuse of a drawing by Émile Maupas from:

Maupas, É. Modes et formes de reproduction des nématodes. *Arch. Zool. Exp. Gen.* ser.3 t.8, 463–624 (1900). <https://www.biodiversitylibrary.org/page/4460240>

and has no copyright as indicated on <https://www.biodiversitylibrary.org/bibliography/79165#/summary>

Fig. 2A on page 7 of Chapter 1 is a reuse of: Packer, J. S. et al. A lineage-resolved molecular atlas of *C. elegans* embryogenesis at single-cell resolution. *Science*. 365, (2019). Specifically, Figure 1A of this article.

Fig. 2B on page 7 of Chapter 1 is a reuse of: <http://browser.openworm.org>

Credit: Padraig Gleeson, UCL. Original data set from Christian Grove, Wormbase at Caltech. I received written permission from Stephen David Larsson (Co-founder of OpenWorm).

Fig. 3 on page 9 of Chapter 1 is a reuse of: Chalfie, M., Tu, Y., Euskirchen, G., Ward, W. W. & Prasher, D. C. Green fluorescent protein as a marker for gene expression. *Science*. 263, 802 LP – 805 (1994). Specifically, Figure 3 of this article.

Fig. 4A and **Fig. 4C** on page 11 of Chapter 1 are reuses of: Koldenkova, V. P., & Nagai, T. Genetically encoded Ca²⁺ indicators: Properties and evaluation. *Biochimica et Biophysica Acta (BBA)-Molecular Cell Research*. 1833(7), 1787-1797 (2013). Specifically, Figures 2A and 1A of this article, respectively.

Fig. 4B on page 11 of Chapter 1 is a reuse of: Wagner, S., De Bortoli, S., Schwarzländer, M., & Szabò, I. Regulation of mitochondrial calcium in plants versus animals. *Journal of Experimental Botany*, 67(13), 3809-3829 (2016). Specifically, Figure 3 of this article.

Fig. 4D on page 11 of Chapter 1 is a reuse of: Akerboom, J., Rivera, J. D. V., Guilbe, M. M. R., Malavé, E. C. A., Hernandez, H. H., Tian, L., Hires, S. A., Marvin, J. S., Looger, L. L., & Schreier, E. R. Crystal structures of the GCaMP calcium sensor reveal the mechanism of fluorescence signal change and aid rational design. *Journal of biological chemistry*, 284(10), 6455-6464 (2009). Specifically, Figure 1C of this article.

Fig. 5 on page 15 of Chapter 1 is a reuse of: Faumont, S., Rondeau, G., Thiele, T. R., Lawton, K. J., McCormick, K. E., Sottile, M., Griesbeck, O., Heckscher, E. S., Roberts, W. M., Doe, C. Q. & Lockery, S. R. An image-free opto-mechanical system for creating virtual environments and imaging neuronal activity in freely moving *Caenorhabditis elegans*. *PloS one*, 6(9), e24666 (2011). Specifically, Figure 1A of this article.

Fig. 6 on page 17 of Chapter 1 is a reuse of: Fenno, L., Yizhar, O., & Deisseroth, K. The development and application of optogenetics. *Annual review of neuroscience*, 34 (2011). Specifically, Figure 1 of this article.

Fig. 7A,C on page 21 of Chapter 1 is a reuse of: Wen, Q. et al. Proprioceptive coupling within motor neurons drives *C. elegans* forward locomotion. *Neuron* 76, 750–761 (2012). Specifically, Figure 1A and 1C of this article, respectively.

Fig. 7B on page 21 of Chapter 1 is a reuse of: Cohen, N. & Denham, J. E. Whole animal modeling: piecing together nematode locomotion. *Curr. Opin. Syst. Biol.* 13, 150–160 (2019). Specifically, Figure 1B of this article.

Fig. 7D on page 21 of Chapter 1 is a reuse of: Xu, T. et al. Descending pathway facilitates undulatory wave propagation in *Caenorhabditis elegans* through gap junctions. *Proc. Natl. Acad. Sci. U. S. A.* 115, E4493–E4502 (2018). Specifically, Figure 7B of this article.

Fig. 8 on page 22 of Chapter 1 is a reuse of: Wen, Q., Gao, S. & Zhen, M. *Caenorhabditis elegans* excitatory ventral cord motor neurons derive rhythm for body undulation. *Philos. Trans. R. Soc. B Biol. Sci.* 373, 20170370 (2018). Specifically, Figure 6 of this article.

Fig. 9A on page 25 of Chapter 1 is a reuse of: Grätsch, S., Büschges, A., & Dubuc, R. Descending control of locomotor circuits. *Current Opinion in Physiology*, 8, 94-98 (2019). Specifically, Figure 1 of this article.

Fig. 9B on page 25 of Chapter 1 is a reuse of: Grillner, S., & El Manira, A. Current principles of motor control, with special reference to vertebrate locomotion. *Physiological reviews*, 100(1), 271-320 (2020). Specifically, Figure 10 of this article.

Fig. 11 on page 30 of Chapter 1 and **Fig. 1-3** on pages 109, 1010, 1012 of Chapter 4, respectively, were made with the webapplication on <http://nemanode.org/> built by the lab of Prof. Mei Zhen: Witvliet, D., Mulcahy, B., Mitchell, J.K. et al. Connectomes across development reveal principles of brain maturation. *Nature* 596, 257–261 (2021).

Leuven, 15/09/2022

Petrus Van der Auwera

III. Scientific acknowledgements

This PhD project was realized thanks to collaboration with a number of colleagues. I had the fortune or maybe the guts and enthusiastic naivety to embark on this joint PhD plan, but found out that finishing a research project in Biosciences every two years is at least not particularly straightforward as I learnt that scientific publishing takes time. Luckily, I also discovered that passion for science and a common goal for enthusiastic colleagues can do extraordinary things as many hands make light work. So, I want to state this explicitly and resoundingly clear at the beginning of this dissertation already. Although this dissertation is my pride and joy, I really feel morally obliged to also honor all the hard work of my dear colleagues and fellow scientists to help me in becoming an independent researcher. To this purpose, I added detailed author contribution statements at the start of each results chapter.

Specifically, I would like to thank Dr. Wagner Steuer Costa and Caspar Glock who had discovered the RIS stopping phenotype and laid the groundwork for the follow-up experiments I performed. I am also very thankful to Prof. Alexander Gottschalk for putting his trust in me to live up to the task of studying this interesting topic in more detail.

I want to thank Dr. Lotte Frooninckx and Dr. Jan Watteyne who passionately trained me during my Master thesis work and from whom I learned most of the required practical skills to work in a laboratory. Furthermore, I sincerely hope that I did justice to the unfinished work of Dr. Lotte Frooninckx on GNRR receptors by diligently taking it up again until completion. In addition, I would like to thank Prof. Liliane Schoofs for her valuable guidance and persistent dedication.

I would also like to acknowledge all other co-authors, editors and reviewers of the manuscripts in this dissertation for their contribution and help in getting our scientific data peer-reviewed and published.

Finally, I would still like to thank the European Research Council (ERC) [grant GPT-C7144-ERC-2013-ADG-340318-PEPTIDELEARNING], KU Leuven, Goethe University and the Deutsche Forschungsgemeinschaft (DFG) [grants FOR1279 (GO1011/4-1, 4-2) and GO1011/13-1 to A.G. and EXC115 (Cluster of Excellence Frankfurt) to E.H.K.S. and A.G.] for funding the grants that realized for these interesting research projects (as is also mentioned in the respective publications).

IV. Personal word of thanks

Besides the more formal acknowledgement of the collaborations, guidance and direct help which I received during my PhD project, I am also extremely grateful for the unwavering support I received from many others. Both in and around the fantastic labs where I had the honor of working. I always felt surrounded by very welcoming, motivating and inclusive atmosphere. So first of all, I would explicitly like to thank Alex and Liliane for their enthusiasm, trust, unstoppable scientific drive and patience. I learned a lot from you throughout these past years both about academic science and life in general. You can both be very proud of the scientific environments filled with enthusiastic teams you shaped and guided over the years. Furthermore, I would like to thank Isabel and Liesbet for their valuable input and comments, for questioning my theories and for the fun interdisciplinary scientific discussions we often had.

Vielen Dank to all the Gottschies: Wagner, Oleg, Barbara, Negin, Alexandra, Basi, Jana, Liese, Jatin, Jonas, Szi-chieh, Christina, Max, Thilo, Martin, and others. I cherish the memories of countless jokes and smiles in the lab, BBQs, Birthday *kuchen*, Christmas parties and fun teambuilding activities like our hike in the Taunus area, cooking workshop or canoe trip on the Lahn river, the conference trip to Berlin or the workshop in Atlanta. Thanks to all of you Frankfurt now feels like a homely place abroad.

Also, *dikke merci* to all Lilianers and Jeffers: Evert, Jan, Charline, Sven, Lotte, Pieter, Bhavesh, Melissa, Stijn, Katleen, Ilayda, Michiel, Bram, Lucas, Brecht, Areta, Samantha and many others. I had a blast during each and every one of the lab activities: lab weekends, bowling nights, parties on the old market, lab brunches or Christmas parties.

Big thanks also to all technical staff that made working in the lab safe, fun and comfortable: Elke, Amanda, Heike, Luc, Fran, Marijke, Karen, Maria, Els. Thanks to the support of my current colleagues from LVCBT: Prof. Els Henckaerts, Bram, Marlies and Caroline and others.

In addition, I also want to thank the administrative personnel from both the Goethe University Frankfurt as well KU Leuven for allowing and arranging the Joint PhD agreement.

Then, I would like to thank my mum and dad, Hilde & Luc. They instigated my passion for questioning the world, they've put up with my worries and frustrations, they supported me throughout my studies, gave me the freedom to explore and never ceased to support me even when times were tough. Thank you for your pep talks, your confidence, your trust, your telephone calls on Friday nights and your love.

I really appreciate that my family: Nettie & Niels, Fons & Liesbeth, in-laws, aunts and uncles, nephews and nieces have always been curious and interested in why I would put this much energy in staring at these tiny worms. All your enthusiasm motivated me to live up to the task!

My friends, I would like to thank you all for distracting my thoughts from science with fun, games, drinks and parties when I absolutely needed it: Bernard, Pieter, Thomas, Evert, Veerle, Sara, Tom, Pablo, Maarten, Brent, An, Claudia, Noël, all the Flatermenschen and many others that encouraged me with the delightful question: *'How is your PhD going?'* I hope you will all enjoy the reception!

Last but not least, I would like to thank Signe, the strong woman who knows like no other what getting this PhD meant for me. You mean more to me than anyone could ever know.

V. Table of contents

<i>I. Preface</i>	<i>iii</i>
<i>II. Legal declaration</i>	<i>xi</i>
<i>III. Scientific acknowledgements</i>	<i>xv</i>
<i>IV. Personal word of thanks</i>	<i>xvi</i>
<i>V. Table of contents</i>	<i>xviii</i>
<i>VI. List of abbreviations</i>	<i>xx</i>
<i>VII. Summaries (in English, German and Dutch)</i>	<i>xxii</i>
Chapter 1:	1
Introduction	1
1.1 <i>General introduction</i>	1
1.1.1 Genetics: why we resemble our parents	1
1.1.2 Molecular neurobiology: how brains work	2
1.2 <i>C. elegans: a model organism ideal for molecular neurobiology</i>	3
1.2.1 Nature's gift to science	3
1.2.2 The advantages of performing research on <i>C. elegans</i>	3
1.2.3 The nervous system of <i>C. elegans</i> throughout development	6
1.3 <i>Let there be light beyond the connectome</i>	7
1.3.1 Functional neurotransmission: how neurons communicate	7
1.3.2 Analysis of mutant phenotypes	8
1.3.3 Fluorescence microscopy	8
1.3.3.1 Fluorescent proteins: observing proteins <i>in vivo</i>	9
1.3.4 Measuring brain activity non-invasively	10
1.3.4.1 Genetically encoded calcium indicators (GECIs)	11
1.3.4.2 Genetically encoded voltage indicators (GEVIs)	12
1.3.4.3 Advantages of fluorescent biosensors	13
1.3.4.4 Fluorescent biosensor imaging in <i>C. elegans</i>	13
1.3.4.5 Correlating neuronal activity with behavior	14
1.3.5 Optogenetics: neuronal activity manipulation with light	16
1.3.5.1 Optogenetic actuators	16
1.3.6 Optical molecular biology	18
1.4 <i>Coordination of locomotion</i>	18
1.4.1 Evolution: why fish swim	18
1.4.2 Muscle contraction: how fish swim	19
1.4.3 Neuronal control of locomotion: controlling spasms into locomotion	20
1.4.4 Locomotion control in <i>C. elegans</i>	20
1.5 <i>Locomotion inhibition</i>	23
1.5.1 Neuronal basis for locomotion inhibition	24
1.5.1.1 Stop neurons	24
1.5.1.2 Sleep neurons	26
1.5.2 Functional neurotransmission of locomotion inhibition	28
1.5.2.1 Neuropeptidergic regulation of neurotransmission	28
1.5.2.2 Neuropeptidergic regulation of locomotion inhibition in <i>C. elegans</i>	29
1.6 <i>Conclusions and aim of the project</i>	32
1.7 <i>References</i>	34
Chapter 2:	46
A GABAergic and peptidergic sleep neuron also functions as a locomotion stop neuron with compartmentalized Ca²⁺ dynamics	46
2.1 <i>Abstract</i>	48
2.2 <i>Introduction</i>	48
2.3 <i>Results</i>	51
2.3.1 Single-cell specific expression and photoactivation of ChR2 in RIS induces locomotion stop	51
2.3.2 RIS suppresses oscillatory activation of body wall muscle by affecting cholinergic neurons	53
2.3.3 RIS photostimulation effects are accelerated by GABA transmission	56

2.3.4 RIS photostimulation induces subsequent reversals via gap junctions	58
2.3.5 RIS photostimulation effects require neuropeptides	59
2.3.6 Recording of Ca ²⁺ activity in the RIS axon and soma in freely moving animals	59
2.3.7 RIS axonal Ca ²⁺ activity during locomotion is correlated with slowing and the onset of reversals	60
2.3.8 FLP-11 neuropeptides are required for RIS' effects on locomotion speed	64
2.3.9 Compartmentalized Ca ²⁺ dynamics in the RIS axon	65
2.4 Discussion	66
2.5 Methods	71
2.6 References	75
Chapter 3:	78
RPamide neuropeptides NLP-22 and NLP-2 act through GnRH-like receptors to promote sleep and wakefulness in <i>C. elegans</i>	78
3.1 Abstract	80
3.2 Introduction	80
3.3 Results	82
3.3.1 The <i>C. elegans</i> genome encodes eight GnRH/AKH-related receptors	82
3.3.2 RPamide neuropeptides activate GNRR-3 and GNRR-6 <i>in vitro</i>	83
3.3.4 NLP-22 RPamide neuropeptides induce locomotion quiescence through GNRR-6	87
3.3.5 NLP-2 RPamide neuropeptides reduce locomotion quiescence during L4 lethargus	88
3.3.6 GNRR-3 and GNRR-6 are required for wake-promoting effects of <i>nlp-2</i> overexpression	89
3.3.7 NLP-2 peptides do not modulate feeding quiescence and sensory arousal threshold during L4 lethargus	91
3.3.8 <i>nlp-2</i> expression cycles with a developmental clock	91
3.4 Discussion	93
3.5 Materials and Methods	97
3.6 References	100
Chapter 4:	106
Discussion	106
4.1 Discussion overview	106
4.2 Stop and sleep neurons in <i>C. elegans</i>	108
4.2.1 RIS	108
4.3 Neuropeptidergic modulation of locomotion inhibition	114
4.3.1 FLP-11 neuropeptidergic signaling	114
4.3.2 RPamide neuropeptidergic signaling	116
4.4 Outlook	120
4.4 References	122
<i>Erweiterte Zusammenfassung in Deutsch</i>	125
<i>Supplementary information and figures</i>	132
<i>List of publications</i>	133
<i>Curriculum vitae</i>	135

VI. List of abbreviations

3D	three-dimensional
$\Delta F/F_0$	change in fluorescence relative to baseline
AA	amino acid
AKH	adipokinetic hormone
APTF-2	transcription factor AP-2 domain-containing protein
ANOVA	analysis of variance
Arch	Archaeorhodopsin-3 light-activated proton pump protein
ATR	all-trans retinal
BLAST	basic local alignment search tool
BWM	body wall muscles
<i>C. elegans</i>	<i>Caenorhabditis elegans</i>
Ca ²⁺	calcium (ions)
CaMello-XR	calcium melanopsin local sensor light-activated GPCR
cAMP	cyclic adenosine monophosphate
CaMPARI	calcium modulated photoactivatable ratiometric integrator
CaViar	calcium and voltage indicator
CEPsh	cephalic sheath astrocyte-like glia
CFP	cyan fluorescent protein
CGC	Caenorhabditis Genetics Center
cGMP	cyclic guanosine monophosphate
CHO	chinese hamster ovary
ChR2	channelrhodopsin-2
Chx10+	positive in expressing visual system homeobox 2
cpFP	circularly permuted fluorescent protein
CPG	central pattern generators
DAF	abnormal dauer formation
DCV	dense core vesicle
DNA	deoxyribonucleic acid
DTS	developmentally-timed sleep
EC50	half maximal effective concentration
EEG	electroencephalogram
EMG	electromyograms
EPG	electropharyngeogram
EGF	epidermal growth factor
egl	egg-laying defective
EMG	electromyograms
Fig.	figure
flp	FMRFamide-like peptide gene
FP	fluorescent protein
FRET	Förster resonance energy transfer
FRPR	FMRFamide peptide receptor
FMRFamide	Phe-Met-Arg-Phe-amide
GABA	gamma-aminobutyric acid
GCaMP	green fluorescent calmodulin protein
GECI	genetically encoded calcium indicators
GEVI	genetically encoded voltage indicators
GFP	green fluorescent protein
Gi	gigantocellular reticular nucleus in the brainstem
GiA	alpha part of the gigantocellular nucleus of the medulla
GiV	ventral part of the gigantocellular nucleus of the medulla
GnIH	gonadotropin-inhibitory hormone
GnRH	gonadotropin-releasing hormone
gnrr	GnRH receptor related gene
GPCR	G protein coupled receptor
gtACR	Guillardia theta anion channelrhodopsin
HS	heat shock
Hz	hertz (s ⁻¹)
ins	insulin-like peptide gene
L1-L4	larval phase 1-4

L4L	lethargus subsequent to L4 larval phase
lin	abnormal cell lineage
LPGi	paragigantocellular nucleus of the medulla
M13	myosin light chain kinase peptide linker sequence
mAChR	muscarinic acetylcholine receptors
Mb	mega base pairs
MCH	melanin-concentrating hormone
MLR	mesencephalic locomotor region
mm	millimeter
MN	motor neurons
mPSCs	miniature postsynaptic currents
mRNA	messenger ribonucleic acid
n/N	number of (biological) replicates
ns	non significant
NeuroPAL	neuronal polychromatic atlas of landmarks
NGM	nematode growth medium
nlp	neuropeptide-like protein gene
NPVF	neuropeptide VF
Norm.	normalized
NpHR	Natronomonas pharaonis Halorhodopsin
NPR-1	neuropeptide receptor-1
OE	overexpression
PAC	photoactivated adenylyl cyclase
PCR	polymerase chain reaction
PDF(R)	pigment dispersing factor (receptor)
PDM-DN	posterior-dorsal-medial descending neurons
PIN	premotor interneuron
qRT-PCR	quantitative real-time polymerase chain reaction
RCaMP	red fluorescent calmodulin protein
REM	rapid eye movement
RFamide	Arg-Phe-amide
RFP	red fluorescent protein
RFRP	RFamide-related peptide
RGECO	red genetically encoded calcium indicators for optical imaging
RNA	ribonucleic acid
ROI	region of interest
RPamide	Arg-Pro-amide
RS	reticulospinal
sc-RNA-seq	single-cell ribonucleic acid sequencing
SCN	suprachiasmatic nucleus of the hypothalamus
SEZ-DN	subesophageal zone descending neurons
SEM	standard error of the mean
SIFamide	Ser-Ile-Phe-amide
SIS	stress-induced sleep
SLD	sublaterodorsal tegmental nucleus of the pons
tdc	tyrosine decarboxylase
TB	terminal bulb of the pharynx
UMAP	uniform manifold approximation and projection, a technique for dimension reduction of data
unc	uncoordinated
VLPO	ventrolateral preoptic area of the hypothalamus
vmM	ventromedial medulla
WT	wild type
YC	yellowameleon
YFP	yellow fluorescent protein

Some letter abbreviations in figures were not mentioned here as they are clearly explained in the dedicated figure legends below. For the meaning of the two or three letter identifiers of *C. elegans* neuron classes (such as RIS) I refer to: <https://www.wormatlas.org/neurons/Individual%20Neurons/Neuronframeset.html>

VII. Summaries (in English, German and Dutch)

Summary

Locomotion, the way animals independently move through space by active muscle contractions, is one of the most apparent animal behaviors. However, in many situations it is more beneficial for animals to actively prevent locomotion, for instance to briefly stop before reorienting with the aim of avoiding predators, or to save energy and recuperate from stress during sleep. The molecular and cellular mechanisms underlying such locomotion inhibition still remain elusive. So, the aim of this study was to utilize the practical genetic model organism *Caenorhabditis elegans* to efficiently tackle relevant questions on how animals are capable of suppressing locomotion.

Nerve cells, mostly called neurons, are known to control locomotion patterns by activating some and inhibiting other muscle groups in a spatiotemporal manner via local secretion of molecules known as neurotransmitters. This study particularly focuses on whether neuropeptides modulate such neurotransmission to prevent locomotion. Neuropeptides are small protein-like molecules that are secreted by specific neurons and that act in the brain by activating G protein-coupled receptors (GPCRs) expressed in other target neurons. They can act as hormones, neuromodulators or neurotransmitters. DNA sequences coding for neuropeptides and their cognate receptors are similar across diverse species and thus indicate evolutionary conservation of their molecular signaling pathways. This could potentially also imply that regulatory functions of specific neuropeptides are also similar across species and are thus meaningful to unravel more general mechanisms for instance underlying locomotion inhibition.

Specifically, we find that the modulatory interneuron RIS constitutes a dedicated stop neuron of which the activity is sufficient to initiate rapid locomotion arrest in *C. elegans* while maintaining its body posture. Similar to its known function in larval sleep, RIS requires RFamide neuropeptides encoded by the *flp-11* gene for this activity, in addition to GABA. Furthermore, we find that spontaneous calcium activity transients in RIS are compartmentalized and correlated with locomotion stop. These findings illustrate that a single neuron can regulate both stopping and sleeping phenotypes.

Secondly, we show that *C. elegans* RPamide neuropeptides encoded by *nlp-22* and *nlp-2* regulate sleep and wakefulness, respectively. We unexpectedly find that these peptides activate gonadotropin-releasing hormone (GnRH)-like receptors dose-dependently and we highlight their sequence resemblance to other bilaterian GnRH-like neuropeptides. In

addition, we show that these receptors are expressed in distinct subsets of neurons that are associated with motor behavior. Finally, we show that *nlp-22* encoded peptides signal through GNNR-6 receptors to regulate larval sleep and that *nlp-2* encoded peptides require both GNRR-3 and GNRR-6 receptors to promote wakefulness.

In sum, we find that locomotion inhibition in *C. elegans* is regulated by multiple, but evolutionary conserved RFamide and GnRH-like RPamide neuropeptidergic signaling pathways.

Zusammenfassung

Die Fortbewegung, das heißt die Art und Weise, wie sich Tiere mithilfe aktiver Muskelkontraktionen unabhängig durch den Raum bewegen, ist die Grundlage der meisten tierischen Verhaltensweisen. In vielen Situationen ist es für die Tiere jedoch vorteilhafter, ihre Fortbewegung aktiv zu stoppen, zum Beispiel um vor einer Neuorientierung kurz anzuhalten, um einem Raubtier auszuweichen, oder um Energie zu sparen und sich im Schlaf von Stress zu erholen. Die molekularen und zellulären Mechanismen, die dieser motorischen Hemmung zugrunde liegen, sind nur teilweise aufgeklärt. Diese Studie versucht anhand des genetischen Modellorganismus *Caenorhabditis elegans* die zentrale Forschungsfrage, wie Tiere die Fortbewegung hemmen, effizient zu beantworten.

Nervenzellen, gemeinhin als Neuronen bezeichnet, regulieren die Bewegungsmuster, indem sie über die lokale Ausschüttung von Molekülen, so genannter Neurotransmitter, bestimmte Muskelgruppen aktivieren und andere in räumlicher und zeitlicher Hinsicht hemmen. In dieser Arbeit wird speziell untersucht, ob Neuropeptide diese Neurotransmission vermitteln oder modulieren, um die Fortbewegung zu hemmen.

Neuropeptide sind kleine Proteinfragmente, die von bestimmten Neuronen abgesondert werden und G-Protein-gekoppelte Rezeptoren (GPCRs) in anderen (oder manchmal denselben) Neuronen im Organismus aktivieren. Die DNA-Sequenzen, die für manche Klassen von Neuropeptiden und ihre entsprechenden Rezeptoren kodieren, sind bei verschiedenen Tierarten ähnlich. Dies deutet auf die evolutionäre Konservierung ihrer molekularen Signalwege hin. Es könnte auch bedeuten, dass die regulatorischen Funktionen bestimmter Neuropeptide bei allen Arten ähnlich sind und dass es daher sinnvoll ist, allgemeinere Mechanismen aufzudecken, die beispielsweise dem aktiven Stoppen der Fortbewegung zugrunde liegen.

In dieser Studie zeige ich (mit Unterstützung meiner KollegInnen), dass das modulierende Interneuron RIS ein spezielles Stoppneuron ist. Dessen Aktivität reicht aus, um eine

schnelle Unterdrückung der Fortbewegung in *C. elegans* einzuleiten und gleichzeitig die Körperspannung aufrechtzuerhalten. Ähnlich wie bei der bekannten Funktion des RIS Neurons im schlafähnlichen Verhalten der Larven ist RIS, zusätzlich zu GABA, auf RFamid-Neuropeptide angewiesen, welche durch das *flp-11*-Gen kodiert werden. Unsere Experimente zeigen, dass die spontanen Kalziumtransienten in RIS kompartimentiert sind und mit dem Bewegungsstop korrelieren. Unsere Ergebnisse zeigen, dass ein einziges Neuron sowohl den Schlaf als auch die Beendigung der Fortbewegung steuern kann.

Darüber hinaus zeigen wir, dass die RPamid-Neuropeptide von *C. elegans*, welche von den Genen *nlp-22* und *nlp-2* kodiert werden, Schlaf und Wachphasen regulieren. Unerwarteterweise stellten wir fest, dass diese Peptide Gonadotropin-Releasing-Hormon (GnRH)-ähnliche Rezeptoren dosisabhängig aktivieren. Wir weisen in diesem Zusammenhang auf Sequenzähnlichkeiten mit anderen GnRH-ähnlichen Neuropeptiden in *Bilateria* hin. Wir zeigen, dass diese GnRH-Rezeptoren in verschiedenen Untergruppen von Neuronen exprimiert werden, die mit motorischem Verhalten in Verbindung stehen. Schließlich konnten wir zeigen, dass *nlp-22*-kodierte Peptide über GNNR-6-Rezeptoren signalisieren, um larvels Schlafverhalten zu regulieren, und dass *nlp-2*-kodierte Peptide sowohl GNRR-3- als auch GNRR-6-Rezeptoren benötigen, um das Wachsein zu fördern. Zusammenfassend lässt sich sagen, dass evolutionär konservierte RFamid- und GnRH-ähnliche RPamid-Neuropeptid-Signalwege an der Regulierung der motorischen Hemmung in *C. elegans* beteiligt sind.

Samenvatting

Voortbeweging, de manier waarop dieren zich zelfstandig door de ruimte bewegen door middel van actieve spiercontracties, vormt de basis van de meeste gedragingen bij dieren. In vele situaties is het voor dieren echter gunstiger om hun motoriek actief te verhinderen, om bijvoorbeeld kortstondig te stoppen alvorens zich te heroriënteren met als doel een roofdier te ontwijken, of om energie te besparen en te recupereren van stress tijdens slaap. De moleculaire en cellulaire mechanismen die aan de basis liggen van deze motorische inhibitie zijn nog steeds niet opgehelderd.

Deze studie tracht de centrale onderzoeksvraag over hoe dieren hun voortbeweging verhinderen, op efficiënte wijze te beantwoorden, hierbij gebruik makend van het genetisch modelorganisme *Caenorhabditis elegans*.

Zenuwcellen, meestal neuronen genoemd, reguleren patronen van voortbeweging door bepaalde spiergroepen te activeren en andere te inhiberen op een ruimtelijk en

tijdsgebonden manier, via plaatselijke secretie van moleculen die bekend staan als neurotransmitters. Deze thesis focust specifiek op de vraag of neuropeptiden zulke neurotransmissie reguleren om voortbeweging te verhinderen.

Neuropeptiden zijn kleine eiwitmoleculen die uitgescheiden worden door specifieke neuronen en die in andere (of soms ook dezelfde) neuronen in de hersenen G-proteïne gekoppelde receptoren (GPCRs) activeren. DNA-sequenties die coderen voor neuropeptiden en hun overeenkomstige receptoren zijn gelijkaardig in diverse diersoorten en duiden daarom op de evolutionaire conservatie van hun moleculaire signaalwegen. Dit kan mogelijks ook impliceren dat de regulatorische functies van specifieke neuropeptiden ook gelijkend zijn over diersoorten heen en dat het dus zinvol is om meer algemene mechanismen aan het licht te brengen die bijvoorbeeld onderliggend zijn aan de vermindering van de voortbeweging.

In deze studie tonen we aan dat het modulatorisch interneuron RIS een toegewijd stop-neuron is waarvan de activiteit voldoende is om een snelle onderdrukking van de voortbeweging te initiëren bij *C. elegans* en waarbij de lichaamshouding bovendien ondersteund blijft. Gelijktijdig aan de gekende functie van het RIS neuron in larvale slaap, doet RIS, naast GABA, hiervoor beroep op RFamide neuropeptiden die gecodeerd worden door het *flp-11* gen. Onze experimenten tonen aan dat de spontane transiënte calcium activiteiten in RIS onderverdeeld zijn in compartimenten en gecorreleerd zijn met het stoppen van voortbeweging. Onze bevindingen illustreren dat één neuron zowel slaap als het stoppen van voortbeweging kan reguleren.

Daarnaast tonen we ook aan dat *C. elegans* RPamide neuropeptiden gecodeerd door *nlp-22* en *nlp-2* respectievelijk slaap en waakzaamheid reguleren. We vinden onverwachts dat deze peptiden gonadotropine-vrijzettend hormoon (GnRH)-gelijkende receptoren activeren op een dosisafhankelijke wijze en we benadrukken de sequentiegelijkenissen met andere GnRH-gelijkende neuropeptiden. We tonen aan dat deze GnRH receptoren in afzonderlijke subgroepen van neuronen tot expressie komen die geassocieerd zijn met motorisch gedrag. Finaal brachten we aan het licht dat de *nlp-22* gecodeerde peptiden via GNNR-6 receptoren signaleren om larvale slaap te reguleren en dat *nlp-2* gecodeerde peptiden zowel GNRR-3 als GNRR-6 receptoren vereisen om waakzaamheid te bevorderen.

Samengevat, evolutionair geconserveerde RFamide en GnRH-gelijkende RPamide neuropeptiderge signaalwegen zijn betrokken bij de regulatie van motorische inhibitie bij *C. elegans*.

NEUROPEPTIDERGIC REGULATION OF LOCOMOTION INHIBITION IN *C. ELEGANS*

STUDYING STOP AND SLEEP NEURONS WITH (OPTO)GENETICS AND FLUORESCENCE MICROSCOPY

Chapter 1:

Introduction

1.1 General introduction

Cell division is the defining characteristic of life. All living organisms are composed out of cells¹: small lipid bilayer bubbles full of water, sugars, proteins and nucleic acids (DNA and RNA). Phospholipid membranes form a hydrophobic barrier that allows to maintain an intracellular homeostatic equilibrium. Sugars provide energy to a cellular metabolic system. Proteins are the functional molecules regulating homeostasis and proliferation through multiple mechanisms: membrane transport, catalyzing metabolic reactions, cell signaling or composition of the cytoskeleton and its rearrangements that establish cell division. DNA encodes the heritable sequence information that RNA relays to build proteins.^{2,3} Cell proliferation during development leads to cell differentiation when cells start differing in their expressed protein content.

1.1.1 Genetics: why we resemble our parents

Animals perceive their environment via specialized sensory cells that express receptor proteins and they manage to respond in appropriate ways due to evolutionary adaptations that were often already fit in past generations. Studying how observable traits of organisms are inherited to their offspring has long been a fundamental biological question.^{4,5} In 1905, the first experimental observations were provided that such phenotypic traits were

dependent on the type of chromosomes present in cell nuclei.⁶ Frans Alfons Janssens demonstrated by 1909 that recombination of chromosomes could occur during meiosis.^{7,8} In subsequent years, these insights allowed Thomas Hunt Morgan and his students to systematically map the determinants of phenotypic traits of fruit flies on specific locations of chromosomes.^{9,10} Afterwards, these determinants were named genes, and thus genetics, the scientific study of genes, had been founded.¹¹ Genes were later shown to consist out of DNA sequences on a molecular level. Once the central dogma of molecular biology was generally accepted, studying cells on a molecular level opened up a plethora of novel insights and new ways to achieve them.^{2,3,12}

1.1.2 Molecular neurobiology: how brains work

Cells communicate with each other on a molecular level via cell junctions, electrical signals, chemical synaptic connections, endocrine signals or pheromones. Their cellular response options generally fall into 1) metabolism and growth, 2) selective transport across the membranes which includes both secreting or taking up chemical substances as well as the opening of selective ion channels to change their membrane potential and 3) relative movement of the cytoskeleton fibers to change cell shape thus allowing for cell division and cell motility.

The most well-known active cellular shape changes establishing animal motility are muscle contractions.¹³ Muscle cells can shorten their length by the rapid action of pulling myosin filaments that actively move along the aligned actin cytoskeleton.¹⁴ Similar proteins are part of the cytoskeleton in all eukaryotic cells and motor proteins have even been identified in Bacteria too. Muscle contractions are the principal underlying mechanism of most animal behaviors: from running, over bowel movements, to mating, singing and smiling. Animals employ neuronal cells (also known as neurons) to coordinate both muscle contraction strength and timing to result in the organism's behavior¹⁵. This same fundamental principle underlies a vast array of behaviors: from the tube feet movements of arctic deep-sea starfish to fine tuning a vast philharmonic orchestra in creating a classical music masterpiece.

In sum, animals adequately optimize the problem of “*when and how to move (?)*” in order to survive in changing environments and to increase their sustainable reproductive potential. In contrast, an equally interesting question to study is: “*When and why it is beneficial for an animal not to move?*”. Depending on the environmental context or life history, animals often actively stop (rhythmic) movements. The molecular regulation of such locomotion inhibition was studied in this PhD project in the roundworm *Caenorhabditis elegans*.^{16,17}

1.2 *C. elegans*: a model organism ideal for molecular neurobiology

1.2.1 Nature's gift to science¹⁸

Brains are remarkable things. They are the intricate networks of neurons that coordinate complex animal behavior. The human brain consists of an estimated 86.000.000.000 neurons and even a small fruit fly like *Drosophila melanogaster* has a brain of about 135.000 neurons.^{19,20} Neurons mainly communicate with each other through synapses; connections across which electrical stimuli or chemical molecules, called neurotransmitters, are transmitted. The fact that each neuron can form thousands of synaptic connections to as many other neurons gives rise to the inconceivably vast complexity of a brain.

To commence our understanding of such complexity scientists first had to combine cutting-edge biochemical and technical tools with a thorough understanding of the genetic code of life.¹² Since genetic research only came of age in the beginning of the twentieth century, Molecular Neurobiology is still an exciting multidisciplinary field of research to this day.^{2,3,12} Sidney Brenner (1927-2019) was among the first scientist that tried to tackle the questions of Neurobiology systematically with genetics²¹. He formulated one of the fundamental research questions of Neuroscience as followed:

“Behavior is the result of a complex and ill-understood set of computations performed by nervous systems and it seems essential to decompose the problem into two: one concerned with the genetic specification of nervous systems and the other with the way nervous systems work to produce behavior. Both require that we must have some way of analyzing the structure of a nervous system.”

S. Brenner, Genetics, 1974

This landmark publication²¹ pioneered a new genetic research field as in it Sidney Brenner introduced a small roundworm: *Caenorhabditis elegans* (Maupas, 1899).^{17,22} In the following decades astonishing biological discoveries were made thanks to this tiny worm that even were recognized as part of two Nobel Prizes in Physiology or Medicine (2002 and 2006) and one in Chemistry (2008).

1.2.2 The advantages of performing research on *C. elegans*

C. elegans is a member of the *Rhabditidae* family and by extension of the phylum *Nematoda* (roundworms).¹⁷ Adult animals are only about 1 mm long, about 70 µm wide and are translucent. *C. elegans* is a non-parasitic soil nematode with a global distribution.

Nematodes are ecdysozoan worms that shed their cuticular layer during larval development. *C. elegans* goes through four larval stages (L1-L4) before reaching reproductive adulthood.²³ During each of the molting interphases larvae display behavioral quiescence that meets all the defined criteria of sleep and that is called lethargus.²⁴ At 20°C temperature (standard in the lab) they have a generation time of about 65 hours.²⁵

C. elegans appears as one of two sexes with distinct anatomical features: hermaphrodite or male (**Fig. 1**). While hermaphrodites are diploid animals as they contain two X sex chromosomes besides the five pairs of autosomes common to both sexes, males only retain a single copy of the X sex chromosome. Hermaphrodites sexually reproduce by either self-fertilization or by mating with males.²⁶ This versatile characteristic is very useful to maintain genotypically homogeneous strains as well as to selectively generate strains of distinct progeny with novel allele combinations by crossing of diverse known strains to each other.²⁷

Furthermore, animals can be viably stored for many decades at -196°C in small vials, until they could be of use again for future research.²¹ Strains can also be deposited at or retrieved from the *Caenorhabditis* Genetics Center (CGC).²⁸ Animals are cultured in incubators on nematode growth medium (NGM) agar plates seeded with a lawn of *Escherichia coli* OP50 bacteria. Feeding is attained by sucking these bacteria from their environment with the pharynx, a neuromuscular tubular organ in the head that mechanically grinds food and transports it from their mouth to their intestine.²³ *C. elegans*' short generation time, its optional cross progeny and its relatively low maintenance costs due to its small size, made it become an ideal model organism for genetics.

No wonder that *C. elegans* was the first multicellular eukaryote for which the complete genome (the nucleotide sequence of all chromosomes of an organism) with a total length of 100,286 Mb has been sequenced.²⁹ Currently, its annotated protein count comprises 28469 proteins (GenBank Annotation report of genome assembly accession GCA_000002985.3).

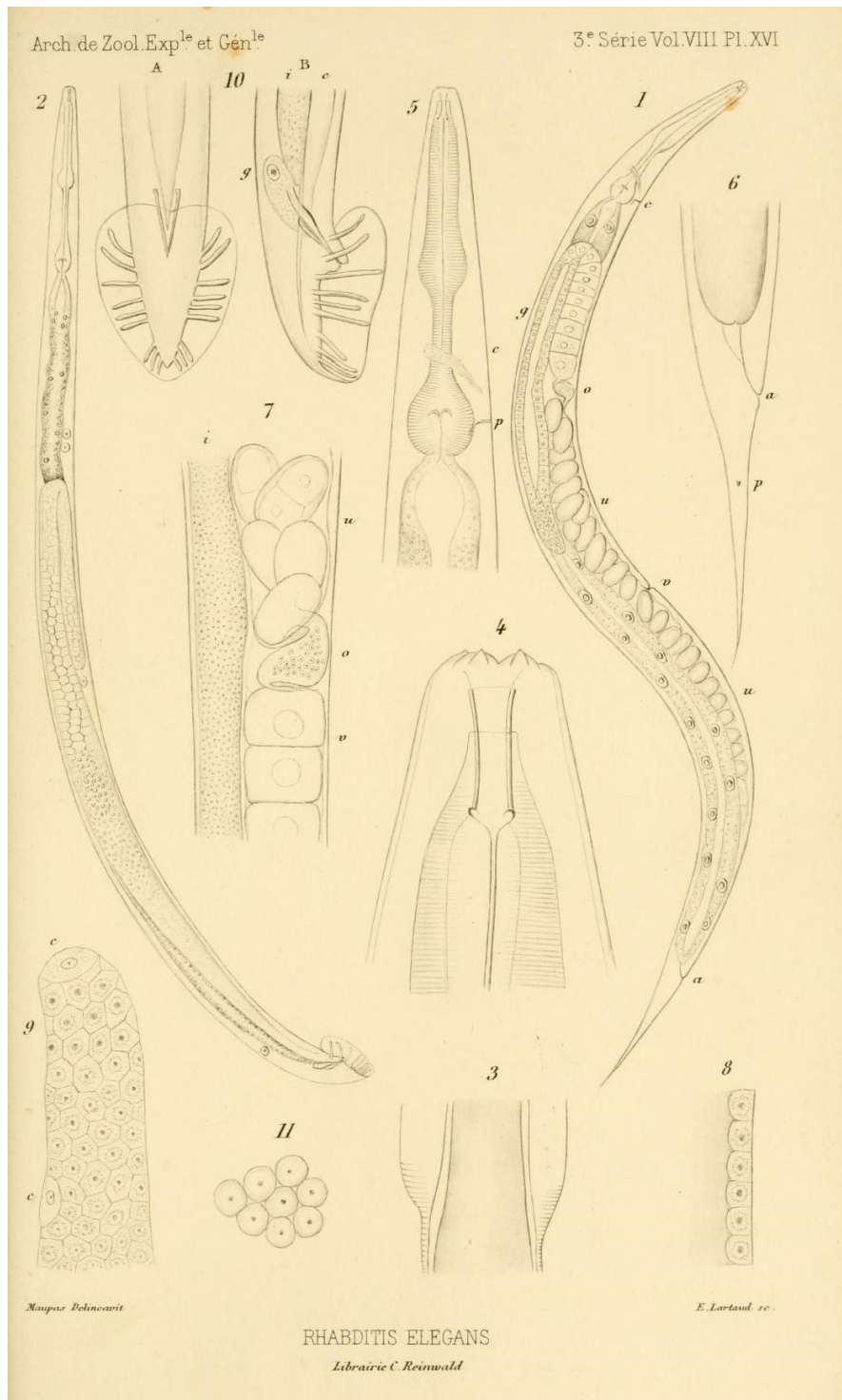


Figure 1: First drawings of both *Caenorhabditis elegans* sexes by Émile Maupas.¹⁶

“(1) Adult hermaphrodite: v, vulva; c, nerve ring and excretory pore; a, anus; u, uterus; o, oviduct; o, ovarium [150x]. (2) Adult male [150x]. (3) Body section with undoubled cuticula due to the action of acetic acid [335x]. (4) Mouth, buccal cavity and anterior extremity of the esophagus [1510x]. (5) Esophagus: c, nerve ring; p, excretory pore [335x]. (6) Hermaphroditic tail: a, anus; p, phasmid sensillar opening [355x]. (7) The oviduct o, assembles vitellogenin v to the uterus, u. The oviduct which is bulged in a pocket serves as a spermatheca; i, intestine [335x]. (8) Germ cells lining the ovary wall as an epithelium and enveloping an amorphous shaft [800x]. (9) Blind extremity of the ovarium: cc, cells of terminus and the tunica intima; g, germ cells [800x]. (10) A, B. Front and profile view of the male tail fan and copulatory spicules: i, intestine; c, vas deferens; g, rectal gland [395x]. (11) Spermatozooids [1510x].” Text translated from original French figure legend. Square brackets do not reflect exact scaling, but indicate at which magnification drawn features are resolvable.

1.2.3 The nervous system of *C. elegans* throughout development

After fertilization, the *C. elegans* zygote undergoes determinate cleavages as it develops from an embryo into an L1 larva consisting of about 600 cells when it hatches from its eggshell in a mere 14 hours.³⁰ During this embryogenesis, cells start differentiating to distinct cell types depending on the transcription factors and microRNAs expressed in each cell.³¹ Adult animals stop somatic cell divisions once terminally differentiated and thus comprise an invariant number of stereotyped somatic cells. Hermaphrodites are composed out of exactly 959 somatic cells of which 302 have a neuronal fate. Males are made up of 1033 somatic cells, of which 385 are neurons.^{30,32,33} *C. elegans* was the first animal of which the complete invariant cell lineage has been mapped.^{30,34} State-of-the-art advances in single-cell RNA sequencing (sc-RNA-seq) now even allow us to reconstruct dynamical transcriptome profiles of such cell fate trajectories along the developmental stages of the maturing embryo (**Fig. 2A**).^{35,36}

Furthermore, also the complete connectome(s), the network(s) of more than 6000 (or 7000) anatomical connections (consisting of either chemical synapses or gap junctions) between all 302 (or 385) neurons in the nervous system, have been accurately mapped for both adult hermaphrodite³⁷ and male³⁸ animals respectively, and even data for connectome remodeling during larval development will soon be published.^{39,40} At present, *C. elegans* is still the only animal model for which the complete adult connectome is known, although it will soon be joined by the fruit fly *Drosophila melanogaster*.⁴¹ By combining data of such connectomes with cell fate transcriptomes scientists can now acquire increasing knowledge on the “genetic specification” and the “structure of the nervous system” (the two prerequisites mentioned in Sidney Brenner’s quote²¹) that will eventually allow them to unravel how exactly “complex neuronal computations” result in animal behavior.⁴² Furthermore, an international collaboration of bio-informaticians, named OpenWorm Foundation, is programming frameworks towards integrating all the available data into models that simulate *C. elegans in silico* (**Fig. 2B**).^{43,44}

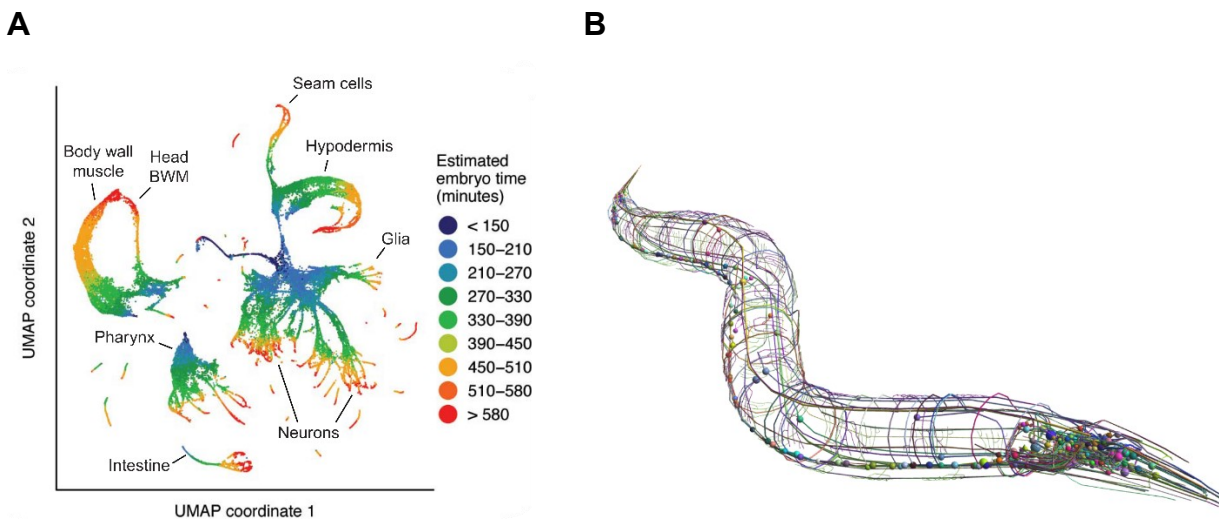


Figure 2: Lineage-resolved single-cell transcriptome and nervous system visualizations. (A) UMAP projection of sc-RNA-seq data points indicate developmental cell differentiation trajectories. [originating from Packer *et al.*, 2019.]³⁵ (B) 3D spatial representation of the hermaphrodite nervous system consisting of 302 neurons generated with the OpenWorm browser (<http://browser.openworm.org>)⁴⁴

1.3 Let there be light beyond the connectome⁴⁵

For over thirty years, the connectome of *C. elegans* was generally assumed to be more or less invariant (as no corroborative experimental data was available to contradict such assumption since the landmark publication by John White *et al.*, 1986).³⁷ Recent studies now put this position in perspective as newly generated connectome datasets seem to diverge more than initially assumed. A useful web application, <http://nemanode.org> (built by the lab of Prof. Zhen), aims to collect all the available electron microscopy connectome datasets.⁴⁰ The connectome-based neural circuit models (C1Fig. 10 and C4Figs. 1-3) generated with this tool and their accompanying consequences and positions in the Discussion of this dissertation are thus based on the neuronal circuit connections identified to this day. The validity of connections still remains to be verified further by extensive data collection in the future.

1.3.1 Functional neurotransmission: how neurons communicate

However, knowing how a genetically characterized nervous system physically interconnects in a static manner still does not explain how it dynamically functions to integrate a continuous stream of ever-changing sensory stimuli from its environment into behavioral output.^{45,46} The latter also requires functional knowledge on the variety of molecular mechanisms that different neuron classes use to communicate. The anatomical connectome is thus only the first of multiple interacting functional layers that control animal behavior.⁴⁷ Chemical synapses can for instance be either excitatory or inhibitory (even for the same

neurotransmitter) depending on the expressed post-synaptic receptors.^{48,49} In addition, neurotransmitters are known to modulate neuronal circuits extrasynaptically.^{47,50,51} Also, electrical synapses can be rectifying⁵² and can display developmental plasticity.⁵³ Although cell morphology and laser ablations studies already gave some first clues of the function of a few neuron types,⁵⁴ innovative molecular tools now enable us to functionally study neurotransmission with molecular detail (*ut infra*).

1.3.2 Analysis of mutant phenotypes

To identify proteins involved in neurotransmission, scientists developed techniques for genetic analysis and selected model organisms, like *C. elegans* and *Drosophila*, that are especially amenable for this daunting task.^{55,56} The classical and most straightforward method to identify novel genes that function in the nervous system is a genetic screen for mutant phenotypes.⁵⁷ Genetic mutations are alterations in the nucleotide sequence of a genome due to erroneous DNA replication or DNA damage by radiation or genotoxic chemicals. Mutations can potentially affect an animal's phenotype by altering expression of proteins, their amino acid sequence, their structure or function. Thus, correlating identified mutations with morphological, molecular and behavioral phenotypes of organisms provides valuable insights about the function of their associated proteins. Initially, forward mutagenesis genetic screens, such as the ones performed by Sidney Brenner,²¹ mainly identified genes associated with obvious morphological or behavioral phenotypes (phenotype to genotype), but more modern genetic techniques, like targeted mutagenesis strategies such as CRISPR/Cas9, now also allow for a reverse genetic approach (genotype to phenotype) to test for specific protein domains in more subtle molecular phenotypes.^{58–60} Furthermore, comparative studies of genome data revealed a high degree of sequence similarity across species which is indicative of potential evolutionary conservation of protein function and enables using knowledge obtained from working with convenient genetic model organisms for translational neuroscience.⁶¹

1.3.3 Fluorescence microscopy

One of the crucial driving factors to verify scientific theories are innovative technical developments.⁶² The discovery of chromosomes and the founding theories of genetics at the beginning of the 20th century for instance were only enabled by novel developments in classical light microscopes and staining techniques.⁶³ Therefore, I will now highlight modern

biochemical tools that accelerated functional studies in molecular neurobiology and that were also essential for this study.

1.3.3.1 Fluorescent proteins: observing proteins *in vivo*

A major technical leap forward in studying gene function was the transgenic expression of green fluorescent protein (GFP) in *C. elegans* to visualize the cellular expression pattern of genes (**Fig. 3**).⁶⁴ Fluorescent molecules can reemit light that they absorb.⁶⁵ The emission spectrum of fluorescent light displays wavelengths that are red-shifted relative to the absorbed excitation light due to vibrational relaxation. By insertion of a suitable long-pass filter in the optical light path of a microscope the excitation light can be filtered out. In contrast to conventional light microscopy, detection of only the reemitted wavelengths allows for very sensitive detection of fluorescent signals with high resolution on a dark background.⁶⁵ GFP from the jellyfish *Aequorea victoria* was the first fluorescent protein (FP) that was both structurally and genetically characterized.^{66–68} It displays maximal absorption at 475 nm (blue light) and peak emission at 509 nm (green light). Even detection of single molecules is feasible.⁶⁹

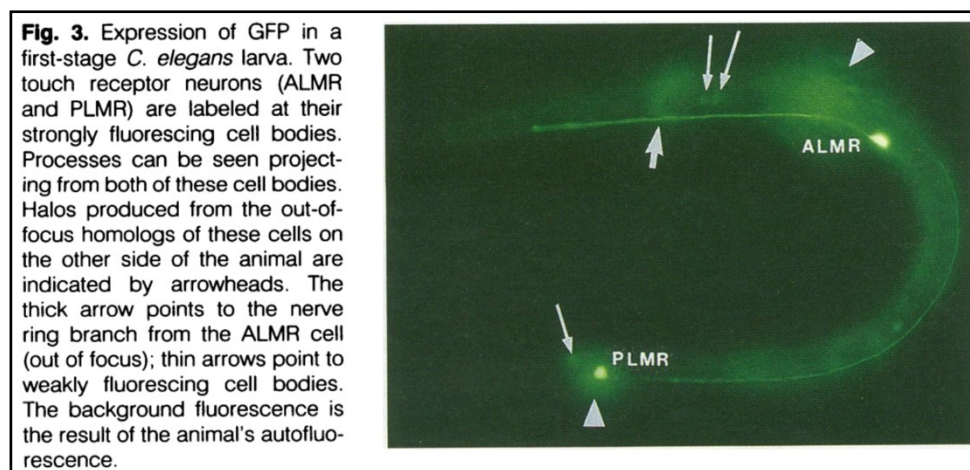


Figure 3: Transgenic expression of green fluorescent protein (GFP) in *C. elegans*

This figure was the first published image of the use of GFP as a marker for gene expression patterns.⁶⁴ It allows for visualization of the expression pattern under control of the promoter of the *mec-7* gene in living animals and can be transmitted to progeny.

One of the major advantages of genetically-encoded fluorescent markers over fluorescent dyes or labeled antibodies is that one can achieve (even subcellular) localization in genetically specified cell types, or at subcellular location of identified proteins, that is transmitted to transgenic offspring.^{70,71}

Since its discovery a variety of GFP-derived molecular tools have been developed to study cell biology.^{72,73} The best-known examples comprise spectral variants of GFP that fluoresce in cyan (CFP), yellow (YFP) and red (RFP) and thus enable multicolor imaging in distinct fluorescent channels.⁷⁴ Besides GFP, also many other FPs were developed, like for instance the photo-transformable FPs called Kaede⁷⁵, EosFP⁷⁶ and Dronpa⁷⁷ that are useful for super-resolution microscopy.^{78,79}

Fluorescent proteins enable to identify the cell types where specific genes are expressed by cellular morphology or by colocalization with spectrally distinct fluorescent markers of already known gene expression.^{80–82} Correlations of either overlapping or differential protein expression patterns can provide valuable clues for both cellular and protein functions. The NeuroPAL transgene (Neuronal Polychromatic Atlas of Landmarks) is a promising novel tool in *C. elegans* research as it differentially expresses four spectrally distinct FPs to generate a colorful whole-brain map with unique cell type identifiers based on (pseudo-)color and relative position. This innovative approach will soon enable rapid and automated neuronal cell type identification in *C. elegans* of any fluorescent expression pattern of interest.⁸³ Technological advances in fluorescence microscopy and digital image acquisition have revolutionized the scientific visualization of the molecular processes of life enormously.^{84–86} Although correlation of *in vivo* gene expression with neuron type on a subcellular level can pinpoint a role for specific proteins in neurotransmission it still does not enable to determine how such proteins functionally affect neurotransmission.

1.3.4 Measuring brain activity non-invasively

While electrophysiology techniques do allow for highly accurate quantitative measurements of electrical cellular activity, their tissue invasiveness often hampers straightforward correlation with natural behavior.^{87,88} Although still feasible, additional complications for neuronal electrophysiology methods in *C. elegans* (like the small size of its neurons and its tough protective cuticula that supports its hydrostatic skeleton) make it very challenging.⁸⁹ The advent of synthetic fluorescent dyes enabled non-invasive visualization of cellular activity like changing cytosolic calcium levels or membrane potential, but tissue permeability or neuron selectivity were still problematic.^{90–92} Similarly to such functionally-sensitive fluorescent dyes, genetically encoded FP tools were designed that change fluorescence intensity depending on the physicochemical properties in their cellular micro-environment.

1.3.4.1 Genetically encoded calcium indicators (GECIs)

The first generation of genetically encoded indicators, so called cameleons, make use of Förster Resonance Energy Transfer (FRET) to visualize changes in intracellular calcium levels.⁹³ FRET is the physicochemical phenomenon that an excited donor fluorophore nonradiatively transfers energy to a spectrally red-shifted acceptor fluorophore in close proximity.⁹⁴ This means that the fluorescence intensity of this acceptor fluorophore is dependent on the distance, the relative angular orientation and the overlap of its excitation spectrum with the emission spectrum of the donor fluorophore.

Yellow cameleon (YC) calcium indicators are fusion proteins that are composed of a CFP donor and YFP acceptor module that are tethered together by a calcium sensitive linker domain (**Fig. 4A,B**). This domain consists of M13 and calmodulin subdomains that change conformation upon calcium binding to form a Ca^{2+} -calmodulin-M13 complex and physically bring the fluorophores closer together, thereby increasing the YFP fluorescence intensity while simultaneously decreasing the fluorescence intensity of CFP.⁹³ This allows for accurately and non-invasively measuring intracellular calcium fluctuations in living animals in real-time.⁹⁵ Subsequently, also other indicator tool designs have been optimized. GCaMP is based on a single GFP molecule and displays a larger dynamic calcium affinity range and faster dynamics (**Fig. 4C,D**).^{96–98} RCaMP and RGECO are red-shifted GECIs.^{99–101} CaMPARI is photo-transformable and allows for mapping of active neuronal circuits.^{102,103}

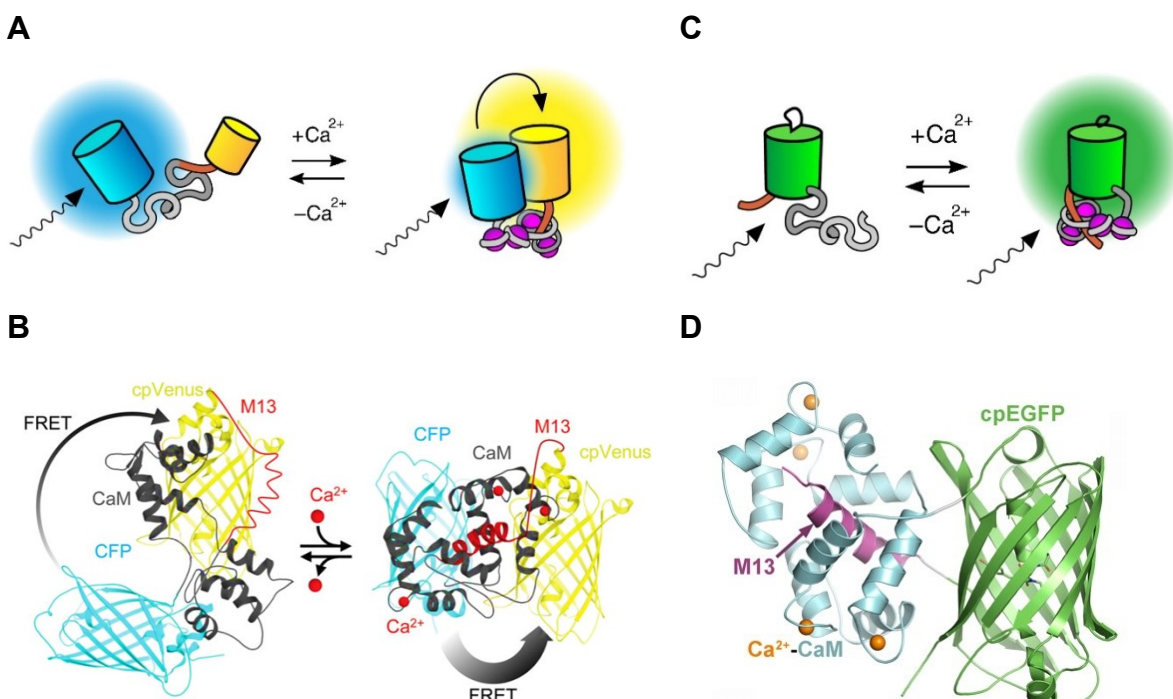


Figure 4: Schematic representations and structural protein models of genetically encoded calcium indicators. (A,C) Simplified diagrams visualizing the working principle of genetically encoded calcium

indicators such as FRET for the ratiometric Yellow Cameleon series (**A**) and intramolecular conformational change increasing the absorption spectra for the intensimetric GCaMP series (**C**). (**B,D**) Hypothetical protein structure models of the respective sensors: YC 3.6 (**C**) and GCaMP2 (**D**). Cyan fluorescent protein CFP (blue/cyan), circularly permuted enhanced green fluorescent protein cpEGFP domain (green), CaM calmodulin domain (grey), calcium ions (lila/red/orange), M13 domain (orange/red/purple), yellow fluorescent protein YFP or cpVenus (yellow). [Fig. panels **A** and **C** are modified from Koldenkova *et al.*, 2013¹⁰⁴ and Fig. panels **B** and **D** are from Wagner *et al.*, 2016¹⁰⁵ and Akerboom *et al.*, 2009¹⁰⁶, respectively.]

1.3.4.2 Genetically encoded voltage indicators (GEVIs)

Similarly, genetically encoded indicators that report changes in electrical membrane potential, also known as voltage sensors or GEVIs, have been developed.^{107,108} Initial GEVI designs contained a voltage sensing domain fused to a pair of FPs that allow for FRET sensing.¹⁰⁹ Optimization of this type of GEVI, mostly via circular permutation (cp) of the FP, led to a variety of monochromatic GEVIs with just one cpFP.¹¹⁰ A second type of GEVIs is based on the microbial rhodopsin Arch that incorporates retinal as a chromophore.^{111,112} This allows for fluorescence in the far-red spectrum which prevents spectral overlap with other commonly used FPs. As their dim intrinsic fluorescence requires high excitation light intensities novel rhodopsin-based GEVI designs use electrochromic FRET to decrease the fluorescence intensity of a fused donor FP upon depolarization.¹¹³ This also lead to spectral diversification similar to FP tools.^{114,115} I refer to Bando *et al.*, 2019 for a comparison of the advantages of specific GEVIs.¹¹⁶

By fusion of a GCaMP-type GEVI to an Arch-based GEVI even a transgenic reporter tool, named CaViar, was created that reports both calcium and voltage independently.¹¹⁷ The prospect of optimizing such GEVI-GEVI dual function imaging to study how calcium signaling and membrane potential interact in a spatiotemporal manner seems extremely promising.^{118,119} In contrast to GEVIs, GEVIs can also report hyperpolarization.¹²⁰ As calcium is often incorrectly presumed to be just an indirect surrogate for membrane potential, I would like to highlight the importance of calcium as an evolutionary ancient secondary messenger¹²¹ that serves crucial functions in neurotransmission that are distinct from voltage, both pre-synaptically (vesicle fusion for neurotransmitter release)¹²² and post-synaptically (calcium/calmodulin-dependent protein kinases)¹²³, as well as in cytoskeleton rearrangements such as muscle contractions.¹²⁴ In this manner, calcium links chemosensory input to developmental and behavioral output.

1.3.4.3 Advantages of fluorescent biosensors

Besides calcium many other signaling molecules affect neuronal activity, protein expression and plasticity. Therefore, fluorescent biosensors are also being developed to study these diverse cellular signaling mechanisms.¹²⁵ Notable examples include cGMP sensor FlincG3,¹²⁶ glutamate sensor iGluSnFR,¹²⁷ gamma-aminobutyric acid (GABA) sensor iGABASnFR,¹²⁸ chloride sensor SuperClomeleon,¹²⁹ pH sensor pHluorin,¹³⁰ and the G protein-coupled receptor (GPCR) activity reporter system Tango.^{131,132} This functional diversity to study neurotransmission is another crucial advantage of genetically encoded biosensor imaging over electrophysiology techniques. Furthermore, multiplexing functionally diverse and spectrally distinct sensors enables studying how signaling molecules interact.¹¹⁷ Another strength of biosensor imaging in neurons is that it allows to concomitantly study the spatiotemporal extent of neurotransmission by visualizing the dynamic spreading of voltage or calcium transients over time.^{118,133} Neurons are known to display subcellular compartmentalization.¹³⁴ By fusing short signal sequence peptides to biosensor proteins one can also target indicators to membranes or subcellular compartments like the nucleus,¹³⁵ the cell soma,¹³⁶ the endoplasmatic reticulum,¹³⁷ synapses^{138,139} or axons.¹⁴⁰ With state-of-the-art microscopy one can measure activity in large brain volumes multidimensionally (i. e. the subcellular distribution of signaling molecules in multiple neurons in 3D with multiple spectrally distinct biosensor channels).^{135,141,142}

1.3.4.4 Fluorescent biosensor imaging in *C. elegans*

C. elegans neurons are thought to mainly display graded electrical potentials^{143,144} although calcium action potentials are observed in muscle cells^{145,146} and the AWA sensory neurons.¹⁴⁷ Potentially, more neurons might display calcium action potentials, but the notoriously challenging use of electrophysiology in the nematode slows down conclusions. Obviously, the translucency and compact nervous system of *C. elegans* are extremely convenient for biosensor imaging. Although GECIs are already widely used in *C. elegans* neurobiological research, GEVI measurements are unfortunately still rather rare.^{112,148,149} Furthermore, neuron class-specific promoters are available for most of the 118 hermaphroditic neuron classes.^{150,151} Combinatorial expression systems that should allow for cell type-specific expression in the remaining neuron types are well established too.^{152,153} Even whole-brain^{135,154–157} and whole nervous system^{86,158} calcium imaging have been shown to be feasible. However, unambiguous annotation of the 302 neurons has been

challenging.^{159–161} Automated annotation efforts and the NeuroPAL strain⁸³ promise substantial improvements.^{162–165}

Compartmentalization of neurons has also been observed in *C. elegans*.¹³⁴ Differential calcium dynamics in compartments along the axons of the RIA interneurons encode dorsoventral head movements.^{166,167} Upon odor stimulation AWC olfactory neurons display transiently decreased levels of cGMP in their sensory cilia while levels in dendrites and soma subsequently increase.¹⁶⁸

1.3.4.5 Correlating neuronal activity with behavior

During calcium imaging, nematodes are often immobilized with glue or beads for practical reasons and to exclude motion artefacts.¹⁶⁹ Also, microfluidic chips specifically designed for *C. elegans* can enable long-term immobilization and control of sensory stimulation during imaging.^{170–174} However, molecular neurobiology also studies how neuronal signaling mechanisms generate natural behavior.¹⁷⁵ So, neurobiologists try to find correlations between brain activity and accurately measured, but unrestrained animal behavior. Accurate quantitative measurements of *C. elegans* locomotion behavior require a tracking system that enables continuously monitoring behavior.¹⁷⁶ To allow for simultaneous brain activity monitoring with genetically encoded biosensors, such a tracking system needs to be integrated in a fluorescence microscope.¹⁷⁷

Prior to the start of this work, only relatively few studies had achieved neuronal calcium imaging in freely moving *C. elegans*.^{177–185} The first and most used approach for automated tracking employs custom-built computer vision systems that rely on digital image acquisition to calculate the oriented deviation of the brightest fluorescent signal in the field of view (FOV) and reposition it to the FOV center by means of a motorized microscopy stage.^{177,179,181,182,185}

Subsequently, an analogous method that uses a four-quadrant photomultiplier tube (PMT) for faster recentering of the fluorescent region of interest (ROI) was developed and commercialized (**Fig. 5**).¹⁸⁰ This method uses a beam splitter inserted in the light path to divert a fraction of the emitted fluorescent signal that is being tracked (away from the camera) towards the middle of a two-by-two array of four PMT channels. An iris diaphragm is used to restrict the aperture such that each PMT channel detects only a quarter of the circular fluorescent signal when centered in the FOV. Dedicated electrical firmware then uses the differences in currents generated in each PMT channel to analogously calculate the two-dimensional deviation of the fluorescent signal from its desired FOV center position.

So, such tracking does not depend on digital image acquisition. This reduces the latency time for each automated stage position correction to about 2 ms. The latter method was also used in this work.¹⁵³ To improve the reliability of our *C. elegans* tracking performance in combination with a 25x air objective, I used nematodes with FP marker expression in the terminal bulb of the pharynx of *C. elegans* to obtain a brighter fluorescent signal for tracking.

Today, functional aspects of many *C. elegans* neuron types have been characterized in molecular detail by correlating calcium dynamics of these genetically tractable cells with behavioral motifs.^{154,186,187} However, the functional role of many more proteins involved in neurotransmission still remains unknown. Just three studies have been published that managed to perform whole-brain calcium imaging in freely moving nematodes.^{86,155,156} Furthermore, GEVI studies in unrestrained nematodes have not been performed yet to my knowledge. So, the future perspectives of studying complex behaviors such as learning and memory with fluorescent biosensors in freely moving *C. elegans* still seem extremely promising.

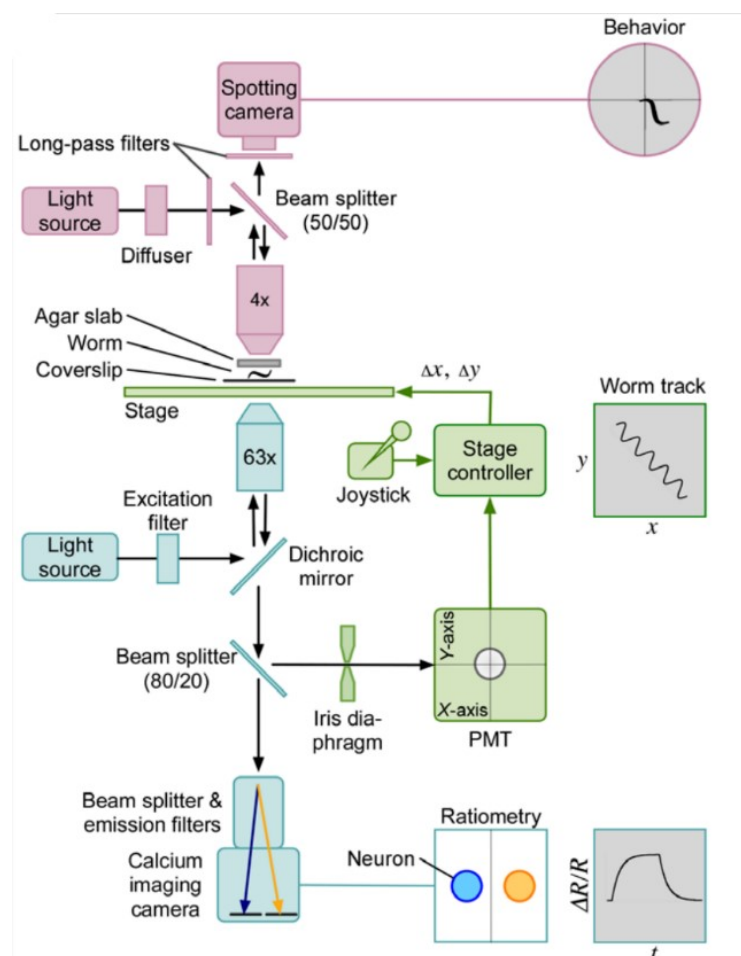


Figure 5: Automated tracking system for neuronal calcium imaging in freely moving *C. elegans* animals¹⁸⁰ Schematic diagram representing the components of the microscopic set up for automated calcium imaging as featured in Faumont *et al.*, 2011.¹⁸⁰ The blue subcomponents represent the reflective light path

required for image acquisition of fluorescent light emitted by neuronally expressed genetically encoded ratiometric biosensors in two color channels simultaneously on the same high resolution camera. The purple subcomponents visualize the light path for acquiring the (locomotion) behavior of the complete body of a worm in 4x magnification. The green subcomponents allow for constantly repositioning the fields of view to recenter the moving fluorescent neuron by means of an automated microscope stage that rapidly corrects the offset of the fluorescent signal detected by a four-quadrant photomultiplier tube.

1.3.5 Optogenetics: neuronal activity manipulation with light

Another approach to study how neurotransmission regulates animal behavior is by actively manipulating neurotransmission and observing the resulting behavior. Besides monitoring brain activity, electrophysiology techniques also enable electrical stimulation of single neurons.^{188–190} Similarly to optical biosensors such as GEVIs, genetically encoded optical techniques were developed for the direct activity manipulation of selected cells with light.^{191–193} In 2006, these groundbreaking photomanipulation methods were termed optogenetics.¹⁹⁴

1.3.5.1 Optogenetic actuators

With the electrical and molecular characterization of light-absorbing rhodopsin-like proteins from microbes the idea of genetically encoded direct photomanipulation of electrical cellular activity became a possibility.^{195–197} One of such microbial rhodopsins, Channelrhodopsin-2 (ChR2) from *Chlamydomonas reinhardtii*, is a cation channel that opens upon conformational change induced by absorption of blue light and isomerization of its *all-trans* retinal (ATR) chromophore (**Fig. 6**).¹⁹⁸ Upon transgenic expression of ChR2 in cultured neurons, they reliably undergo depolarization upon photostimulation.¹⁹⁹ *C. elegans* was the first intact freely moving animal of which the behavior was optogenetically manipulated with a ChR2 variant. By transgenetically expressing a mutant of ChR2 in selected mechanosensory neurons, their electrical membrane potentials and the resulting behavioral response were directly altered with light.²⁰⁰ Application of ChR2 in many other animal models followed soon thereafter and is adopted widely now.^{201–203} Again, many genetic variants have been designed to generate channelrhodopsins with different spectral characteristics and kinetics such as the red-shifted Chrimson^{204,205} and step-function ChR2(C128S)^{206,207}, respectively. Combination of Chrimson with the blue-shifted Chronos allows independent photodepolarization of distinct neurons expressing only one of both with either red or blue light, respectively.²⁰⁴

In addition to ChR2 photodepolarization, also optogenetic inhibitors have been developed that hyperpolarize neurons upon illumination. Halorhodopsin, NpHR, from

Natronomonas pharaonis is a chloride pump that actively transfers chloride ions intracellularly (**Fig. 6**),^{195,208} while archaerhodopsin-3 (Arch) and the fungal opsin Mac are proton pumps that relocate protons extracellularly.²⁰⁹ Nowadays, more potent photohyperpolarizing proteins are available like the algal *Guillardia theta* anion channelrhodopsins (gtACRs).^{210–212} As NpHR is spectrally distinct from ChR2, they can be differentially addressed to bidirectionally steer membrane potential and to fine-tune electrochemical gradients across membranes.²¹³ For an extensive review on microbial rhodopsin-based optogenetic tools in *C. elegans* I refer to Bergs *et al.*, 2018.²¹⁴

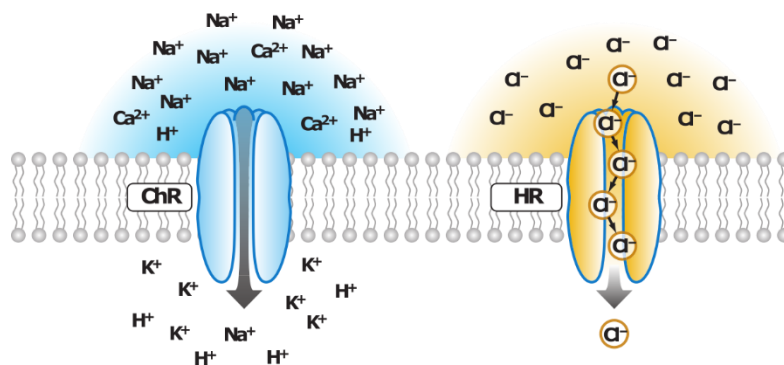


Figure 6: Optogenetic actuator proteins enable manipulation of cellular membrane potential by controlled exposure to light with specific wavelengths Schematic representation of stereotypic channelrhodopsin (ChR) or halorhodopsin (HR) proteins inserted in the membrane of a cell. Upon exposure to blue light channelrhodopsins change conformation allowing positive ions like Ca²⁺ to move through a central channel into the cytoplasm, which in turn depolarizes cells. Upon exposure to yellow light halorhodopsins pump chloride ions intracellularly, which then hyperpolarizes cells. [Figure adapted from Fenno *et al.*, 2011]²¹⁵

Similar to the functional diversity of fluorescent biosensors, a wide variety of optogenetic actuators that manipulate biomolecular cell signaling processes have become available.^{216,217} Notable examples include photo-induced gene expression systems²¹⁸ and optogenetic tools for directed manipulation of GPCR signaling cascades. The latter comprise optoXR_s,²¹⁹ the Japanese lamprey parapainopsin UVLamP,²²⁰ and tools that rapidly increase either cAMP or cGMP levels like photoactivated adenylyl cyclases (PACs)^{221,222} or CyclOps²²³, respectively.

At first, either invasive conventional electrophysiology or behavioral quantification were used as readout for optogenetic manipulation of neurotransmission.^{200,224} In this study, tracking and quantification of optogenetically induced behaviors was predominantly performed with the Single Worm Tracker and its accompanying LabVIEW scripts (developed by Jeffrey N. Stirman).²²⁴ However, optogenetic actuators can also be utilized in combination with fluorescent biosensors.²²⁵ *C. elegans* was the first animal in which optogenetic perturbation

and calcium imaging were combined with quantitative analysis of unrestrained locomotion behavior.¹⁸⁵ In sum, optimization and further development of diverse non-invasive optical molecular tools allows us to functionally study molecular neurotransmission with light in freely moving animals.^{62,226} In addition, optogenetics also offers great potential for therapeutic applications.²²⁷

1.3.6 Optical molecular neurosciences

All the above mentioned historically acquired knowledge and exciting state-of-the-art optical research techniques highlight the feasibility, adequacy and relevance of studying fundamental molecular mechanisms of neurotransmission with a user-friendly genetic model organism. *C. elegans* research thus allows us to effectively tackle relevant questions on what genetic and molecular mechanisms the nervous system employs to elicit complex animal behaviors such as locomotion, sleep or learning and memory.^{153,212,228,229} In sum, the invaluable wealth of knowledge generated by the rich history of *C. elegans* research and the vast biochemical data sets in web-accessible integrated databases that accompanied it, established this microscopically small and seemingly simple animal model as an indispensable asset for neurobiological research of the future.⁴³

1.4 Coordination of locomotion

As motion inherently attracts our mind's attention the most obvious and most appealing of all animal behaviors must be locomotion.

1.4.1 Evolution: why fish swim

To survive the test of time, organisms need to keep the lead in the competition on how to gain energy and organic resources efficiently to grow and reproduce durably while simultaneously preventing harm from both abiotic and biotic perturbations.⁴ Dispersal of progeny safeguards the continued survival of many multicellular species. The efficiency of undirected, passive dispersal by gravity, wind or ocean currents is limited as it heavily depends on random chance. When suitable habitats or potential mates are scarce and far apart, large progeny dispersal distances would be favored. During evolution animals managed to increase their progeny dispersal distances and to direct it to suitable habitats.^{230,231} Animals mainly did this by making use of active muscle-driven motility to which I will refer as locomotion behavior.^{232,233} Locomotion even enables animals to migrate

vast distances through water, air or soil or over land and ice in a well-timed and targeted fashion across oceans²³⁴ and continents²³⁵. Self-propelled locomotion allows animals to dynamically relocate to more optimal life-sustaining microhabitats, to gather food or catch prey, to search for suitable mates and to avoid predators.

1.4.2 Muscle contraction: how fish swim

All bilaterian animals have muscle cells that enable them to independently move their bodies to disperse through their environment in at least some phase of their development.²³⁶ As most molecular components that control muscle contraction are conserved across bilaterian species, their last common ancestor must have already utilized similar mechanisms to spontaneously move through space about 650 million years ago.^{237,238} Although gut peristalsis can already be established by myogenic muscle contractions without the need for neuronal input, somatic muscle contractions do require temporal control by specialized neuronal circuits to generate suitable behavioral responses for survival.^{237,239}

Locomotion strategies for active animal relocation are thus dependent 1) on the relative arrangement of muscle tissues (potentially anchored to mineralized skeleton components) and 2) on the temporal control by motor neuron circuits to generate the resulting collective mechanic force sequence that enables body displacement. Therefore, locomotion strategies are major determinants for animal morphology and their vast variety is thus also embodied by the diversity of animal shapes.²³³ These range from pulsatile hydrojet propulsion or vortex ring generation by jellyfish (Cnidaria),^{240,241} to upside down climbing by Gecko lizards (Chordata)²⁴² and to backward flight in dragonflies (Arthropoda)²⁴³ and hummingbirds (Chordata).²⁴⁴

To relocate, nematodes like *C. elegans* use undulation, the principal locomotion strategy used by elongated limbless animals to swim and crawl.^{245,246} Undulation is the active propagation of rhythmic travelling waves along the antero-posterior body axis by alternating opposing muscle contractions to generate thrust by pushing against the surrounding medium (**Fig. 7A**).^{232,247} Undulation allows for energy-efficient navigation in liquid media with varying viscosity as well as through a rigid three-dimensional terrestrial maze of soil or vegetation by adjusting the frequency and wavelength of the body waves.^{248,249} Undulation most likely represents the ancestral locomotion strategy of all vertebrate animals.^{250,251} However, undulatory locomotion mostly evolved convergently in diverse animal taxa like nematodes, leeches, tunicate larvae, lampreys, caecilians or snakes and thus evidently

clear differences are apparent.²⁵² While divergent neuronal circuit architectures across taxa do exist,²⁵³ fundamental molecular features of neuronal control might still be conserved.^{254–256}

1.4.3 Neuronal control of locomotion: controlling spasms into locomotion

Muscle contraction sequences underlying vertebrate undulatory locomotion are generated by dedicated neuronal networks located in the spinal cord, called central pattern generators (CPGs).^{257,258} These CPG networks intrinsically regulate contraction-relaxation rhythms by periodically timing the discharge of motor neurons that control muscle groups along the elongated body axis.²⁵⁹ CPGs establish such oscillatory activity by reciprocal inhibition even in the absence of patterned sensory input or sensory feedback.²⁶⁰ Besides locomotion, pattern-generating circuits can also regulate respiration, swallowing or pyloric rhythms among others.^{259,261} CPG networks have been heavily studied and their concept can also be applied to the generation of more complex fixed action patterns like bird songs.²⁶² However, how CPG networks are modulated or interrupted to actively stop or prevent locomotion is still poorly understood.²⁶³ From behavioral observations it is evident that locomotion inhibition is omnipresent in animals and can be linked to metabolic, developmental and behavioral contexts, like (stress-induced) sleep,²⁶⁴ molting²⁶⁵ and predator avoidance.^{266–268} So, studying the neurotransmission that induce locomotion inhibition in a model organism like *C. elegans* provides (1) fundamental insight to how animals actively prevent locomotion, (2) clues to how locomotion inhibition might have evolved, and (3) potential new leads to generalize molecular mechanisms underlying suppression of complex fixed action patterns.

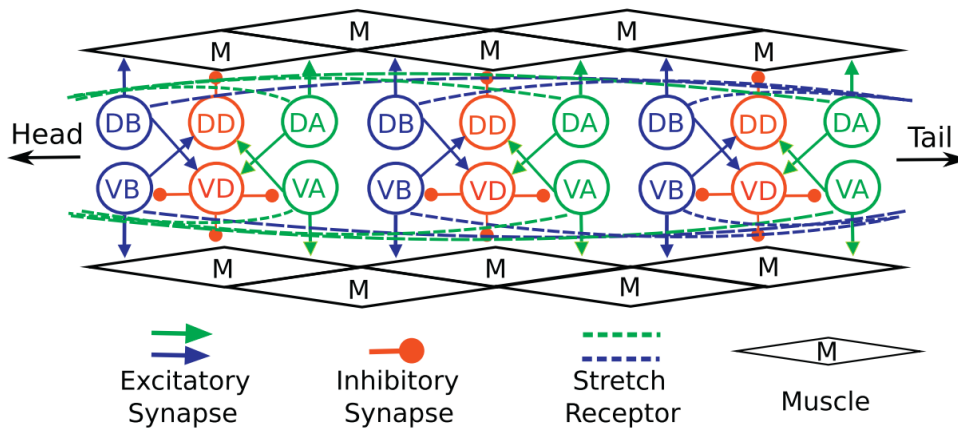
1.4.4 Locomotion control in *C. elegans*

In the last decade, the CPG networks that regulate rhythmic undulatory wave propagation in *C. elegans* (**Fig. 8**) have been functionally characterized *in vivo* by means of calcium imaging and optogenetic experiments.¹⁸⁶ Excitatory motor neurons (MNs) in the ventral nerve cord function as distributed non-bursting local CPG circuits to coordinate undulation along its elongated body axis.¹⁸⁶ Midbody B-type MNs coordinate forward motor patterns,²⁶⁹ while A-type MNs act as intrinsic oscillators for backward locomotion (**Fig. 7B**).¹⁸⁷

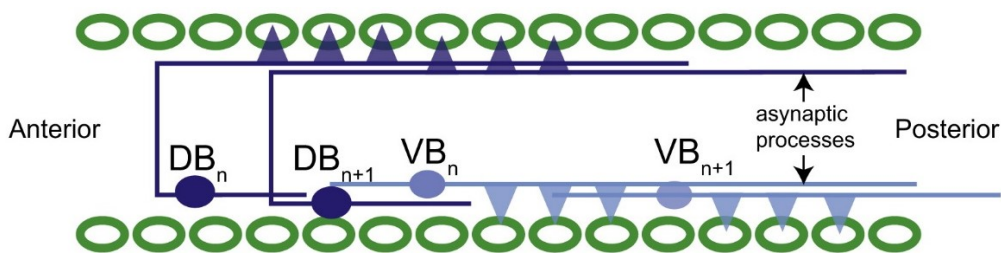
A



B



C



D

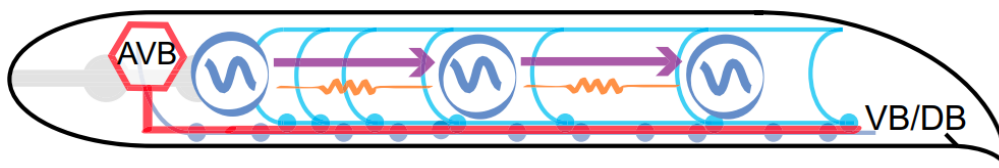


Figure 7: *C. elegans* body wall muscles and their motor circuits

(A) *C. elegans* undulation is orchestrated by alternating waves of dorsoventrally opposing muscle contraction and relaxation cycles travelling through the four bundles of along its longitudinal body axis. Empty green circles indicate relaxed body wall muscle (BWM) cells and filled green circles indicate contracted BWM cells. [Figure adapted from Wen *et al.*, 2012]²⁷⁰ (B) Simplified representation of three repeating motor neuron circuit units that innervate BWMs in adjacent body regions. Dorsal (DA) or ventral (VA) excitatory A-type motor neurons are indicated in green. Dorsal (DB) or ventral (VB) excitatory B-type motor neurons are indicated in blue. A-type motor neurons display cell-autonomous oscillatory activity. Dorsal (DD) or ventral (VD) inhibitory D-type motor neurons are indicated in red. Individual rhomboid-shaped BWM cells are indicated with capital letters 'M'. [Figure adapted from Cohen *et al.*, 2019]²⁷¹ (C) B-type motor neurons primarily form neuromuscular junctions to BWMs where they overlap with the anterior processes of their posterior neighboring ($n+1$) motor neurons of the same neuron class. These anterior processes are presumed to be capable of sensing mechanical bending. This leads to proprioceptive coupling of the activity of motor circuit units to the activity of their anterior

neighbors. [Figure adapted from Wen *et al.*, 2012]²⁷⁰ (D) For forward locomotion, the coordination of neighboring body regions is controlled by electrical inputs from AVB premotor interneurons (PINs, red) that couple to B-type motor neuron CPG circuits (blue) via gap junctions. Together with proprioceptive coupling (purple arrows) and weak electrical coupling of motor neurons themselves (orange signal lines), this coordinates the propagation of body bending waves from head to tail that make up forward undulation in *C. elegans*. [Figure adapted from Xu *et al.*, 2018]²⁶⁹

Proprioceptive coupling of oscillating MNs to adjacent body segments²⁷⁰ enables entrainment and phase-coupling (**Fig. 7C**), while gap junctions inputs from either AVA or AVB premotor interneurons (PINs) promote forward or backward wave propagation, respectively (**Fig. 7D and 8B**).^{181,269} Transitioning from forward to backward locomotion and vice versa might be determined by motor command brain state sequences with distinct neuronal activity patterns (**Fig. 8A**).¹⁵⁴ In comparison to other major MN types in the ventral nerve chord, the AS-type MNs are asymmetric in the sense that they only project to dorsal body wall muscles. Intriguingly, it is still not confirmed nor excluded yet that also AS-type MNs could display CPG activity.²¹² These cholinergic MNs are nonetheless essential for proper coordination of dorso-ventral body bending and antero-posterior wave propagation during locomotion as optogenetic manipulations of their activity and their ablations severely disrupts locomotor patterns. (More detailed information can be found in the publication Tolstenkov *et al.*, 2018²¹² in the supplemental information; Annex I). In contrast to vertebrate locomotor CPGs which were presumed to predominantly reside in spinal PINs,²⁵⁹ *C. elegans* functionally compresses CPG activity and proprioception into MNs to incorporate behavioral complexity in an anatomically compact nervous system.¹⁸⁶

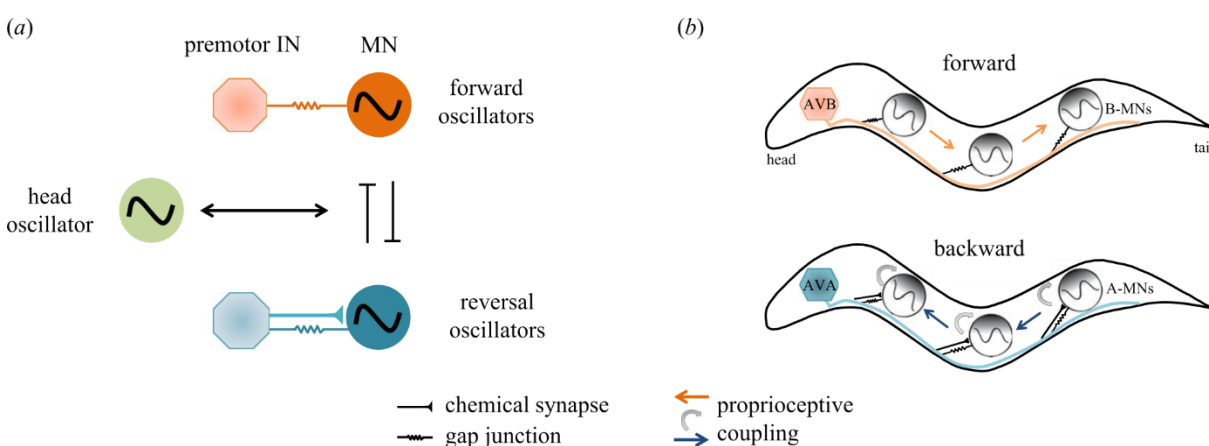


Figure 8: Schematics of a model of *C. elegans* locomotion

“(a) Head oscillation and body undulation are separately controlled. Descending inputs and directional phase-couplings allow distributed local oscillators to drive body undulation during forward and backward locomotion, respectively. A mutually inhibitory motif is introduced to flexibly control the two motor program sub-circuits. Head–body undulation can be bi-directionally coupled with the forward or backward body undulation to generate different motor programs. (b) The spatial layout of descending projection-premotor interneurons, local

motor neuron CPGs and proprioceptive couplings between motor neurons for body undulation that drive forward and backward movements.” [Figure copied and its legend quoted from Wen *et al.*, 2018.]¹⁸⁶

All the above has led us to develop a thorough, but still incomplete understanding of locomotor rhythm generation and basic pattern coordination in *C. elegans*. For extensive review, I recommend Wen *et al.*, 2018 and Cohen & Denham, 2019.^{186,271} Combining this knowledge with whole-brain calcium imaging data¹⁵⁴ gives us promising perspectives to study how more complex behavioral motor patterns are generated in the compact nervous system of *C. elegans*²⁷² and how sensorimotor integration might orchestrate such behavioral responses.²⁷³ In sum, to establish versatile bi-directional undulation *C. elegans* employs two opposing descending PIN pathways (dedicated to either forward or backward motor programs) which are integrated by local oscillating MNs and entrained via gap junction coupling together with direct proprioceptive feedback (**Fig. 8**).¹⁸⁶ How the interaction is coordinated between the abovementioned opposing descending PIN pathways (controlling body undulations) and an independent head oscillator circuit (controlling head casts) to generate more complex motor sequences like transitioning from forward to backward locomotion (or vice versa) is currently still under research (**Fig. 8A**). As a potential stepping stone to approach this question, I investigated how (forward) locomotion is actively prevented on a cellular and molecular level in *C. elegans*. In particular, I hypothesized that the brief intermediate stopping pauses upon such directional transitions (as proposed by Roberts, *et al.* 2016)²⁷⁴ could potentially be regulated by similar neuronal circuit mechanisms as halting behavior or sustained motor inactivity.

Now that we roughly understand which neuronal circuits generate *C. elegans* locomotion, let us question what neurons *C. elegans* employs to actively halt locomotion. Particularly, it still remains unclear 1) whether both of these descending pathways are simultaneously suppressed or whether they are carefully balanced to acutely induce and subsequently sustain locomotion inhibition and 2) what molecular signals functionally regulate the transition between locomotion and its active inhibition.

1.5 Locomotion inhibition

Just as is obvious in a zoo, animals that do not move are generally granted considerably less attention. Neurotransmission in animals at rest has often been dismissed as the mere absence of excitatory locomotor input.

Locomotion inhibition, the active suppression of animal locomotion behavior, is a term that covers a specific aspect of behavioral output,^{263,275} but it can be evolutionary beneficial for

diverse reasons nonetheless depending on the ecological niche of a species.^{276,277} Furthermore, locomotion inhibition comprises physiologically distinct behaviors over a large range of timescales. Depending on its duration it is included in definitions of animal quiescence and dormancy (e.g. hibernation,²⁷⁸ diapause,²⁷⁹ or seasonal inactivity in general), developmentally timed or circadian sleep,²⁶⁴ rest and freezing²⁸⁰ or stopping²⁷⁵ behavior. Previous research has predominantly focused on how all the preceding behaviors differ, while very little is known about how they might relate evolutionarily and if underlying molecular mechanisms might have been conserved.^{281,282} However, one might assume that diverse descending neuronal pathways that prevent locomotion for differential purposes most probably still all converge on the same CPG networks to enable similar suppression of motor output.²⁵⁹

Now, let us finally discuss what is already known about molecular neurotransmission regulating the two best studied types of locomotion inhibition: stopping behavior and sleep.

1.5.1 Neuronal basis for locomotion inhibition

1.5.1.1 Stop neurons

In vertebrates, reticulospinal (RS) neurons in the hindbrain strongly innervate and directly command CPG networks in the spinal cord.²⁵⁷ These RS neurons themselves receive synaptic input from the mesencephalic locomotor region (MLR) that on its turn is innervated by higher brain regions that specify complex motor programs.^{259,263} Neurons in these descending reticulospinal tracts were found to display functional heterogeneity. Specifically, intermingled populations of RS neurons each control distinct aspects of locomotor behavior.^{263,283} Bouvier *et al.*, 2015 discovered that optogenetic activation of Chx10⁺ glutamatergic V2a RS neurons in the caudal pons or rostral medulla, specifically the gigantocellular reticular nucleus (Gi), actively halts locomotion in freely-moving mice by indirectly inhibiting premotor networks.²⁷⁵ More recent calcium imaging data now show that V2a Gi neurons consist of functionally heterogeneous subpopulations of which some are indeed active during locomotor arrest while others seem to regulate distinct motor patterns (like grooming or locomotor initiation).²⁸⁴ Furthermore, Capelli *et al.*, 2017 have shown that inhibitory glycinergic RS neurons in the lateral paragigantocellular nucleus (LPGi) and the alpha part of the gigantocellular nucleus (GiA) in the caudal medulla also halt locomotion.²⁸⁵ In lampreys, the termination of undulatory swimming is also regulated by glutamatergic RS neurons in the hindbrain, similarly to V2a neurons in mice. These RS stop neurons are even known to display a transient burst of spikes at the end of locomotion bouts.²⁸³ This

termination burst is induced by glutamatergic projections from the MLR.²⁸⁶ However, as swimming bouts still terminate even when glutamatergic signaling is blocked, other descending pathways must exist that might differentially regulate distinct types of locomotion inhibition.^{285,286} Optogenetic activation of GABAergic populations in the MLR of mice also seems to impede locomotion, potentially by hyperpolarizing local glutamatergic neurons.²⁸⁷

In sum, information from higher brain regions is integrated by descending pathways comprising the MLR and stop neurons in brainstem RS tracts to inhibit CPG activity in the spinal cord thereby suppressing locomotion while maintaining body posture (**Fig. 9**).²⁶³

A critical behavioral distinction between stopping locomotion and sleep (besides its duration) concerns body posture. During brief stopping behavior muscle tone is maintained, while during sleep animals adopt characteristic body postures and their muscles often relax substantially.^{288,289} For instance, photoactivation of glycinergic neurons in the Gi leads to rapid locomotion arrest in mice, but in addition induces body collapse and spasms.²⁸⁵

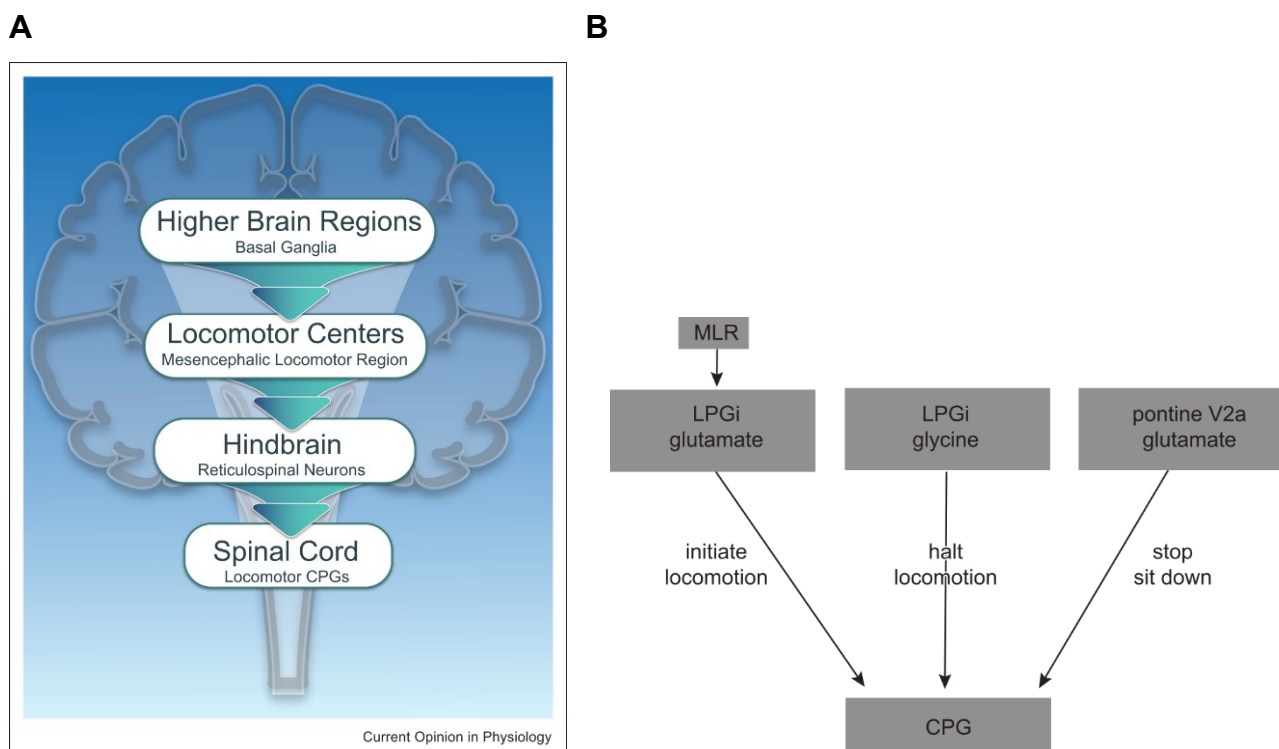


Figure 9: Schematics of known vertebrate neurocircuits controlling locomotion and its inhibition (A) Important brain areas of the known descending pathways hierarchically controlling motor patterns underlying locomotion behavior in vertebrates as displayed in Grätsch *et al.*, 2019.²⁶³ (B) Areas of the brainstem known to contain characteristic stop neurons that can induce locomotion inhibition in vertebrates as featured in Grillner & El Manira, 2020.²⁵⁹

In protostomian animals, dedicated stop neurons have only been characterized in *Drosophila* larvae. Their peristaltic motion is inhibited by optogenetic activation of a pair of

bilaterally symmetric cholinergic posterior-dorsal-medial descending neurons (PDM-DN). These neurons activate GABAergic subesophageal zone descending neurons (SEZ-DN) that themselves inhibit A27h premotor neurons in posterior segments.²⁹⁰ Prior to our study, no dedicated stop neurons were known in *C. elegans*. The GABAergic ALA modulatory⁴⁰ interneuron was shown to be required for an artificial pausing phenotype.²⁹¹ This suggests at least that it contributes to suppressing locomotion. Optogenetic activation of the ALA interneuron only reduces adult locomotion activity though, but does not elicit complete locomotion arrest.^{292,293}

1.5.1.2 Sleep neurons

Sleep is an essential behavioral and physiological state of animal quiescence^{294,295} related to both brain function²⁹⁶ and metabolism.²⁹⁷ Obtaining a conclusive scientific understanding of the ultimate functions which make sleeping behavior evolutionary beneficial across the animal kingdom will require a multidisciplinary approach that studies its neuronal and molecular regulation in diverse model organisms. By definition, sleep encompasses several behavioral aspects among which prolonged, but rapidly reversible locomotion inhibition is one. Other behavioral consensus criteria for sleep include a stereotypical quiescence body posture, reduced sensory responsiveness and homeostatic regulation.²⁹⁵ *C. elegans* sleep conforms to all these criteria which makes it an efficient model organism to study this complex behavior in a straightforward manner. Circadian regulation is often linked to sleep despite that it is not a prerequisite for sleep.²⁹⁸ Infradian forms of sleep or locomotion inhibition are often grouped under the term dormancy (similar to dormancy in plants). Such elongated infradian periods of animal dormancy usually display, depending on their duration, even more drastic changes in metabolism (often severely reducing or even stopping animal growth) or developmental alterations in anatomy. In mammals, physiologically distinct types of sleep are additionally characterized by measuring brain and muscle activity with electroencephalograms (EEG) and electromyograms (EMG), respectively.^{299,300} Although a potential core function of sleep³⁰¹ is still heavily debated^{302–305} due to the vast diversity of sleep traits across animal taxa,²⁸² a fundamental role for suppression of motor activity is irrefutable.³⁰⁰

In contrast to the central descending pathways controlling stopping behavior,²⁶³ sleep-promoting neurons are found in distributed networks spanning multiple brain regions.^{264,300,306} Especially the role of the hypothalamus has been intensively studied in

vertebrates. It comprises GABAergic/peptidergic sleep-active neurons in the ventrolateral preoptic area (VLPO) that inhibit brainstem neurons and that are themselves regulated by central circadian clock neurons in the suprachiasmatic nucleus (SCN).^{299,307}

Intriguingly, deep sleep in mammals is characterized by loss of muscle tone that results in a stereotypic sleep posture while rapid eye movements (REM) are promoted.^{299,308,309} Sleep pathways innervate glutamatergic neurons in the pontine sublaterodorsal tegmental nucleus (SLD) that are known to induce muscle atonia and to suppress limb movements during REM sleep.^{308,310–312} These SLD neurons primarily innervate inhibitory RS neurons in the LPGi, GiA and the ventral part of the gigantocellular nucleus (GiV) as well as spinal neurons.^{299,310,313–315} In mice, optogenetic stimulation of glycinergic RS neurons in GiV again leads to rapid locomotion arrest, but also induces concomitant muscle atonia in their limbs and thus temporarily results in a sleep like posture.²⁸⁵ Such glycinergic RS premotor interneurons in the ventromedial medulla (vmM), including GiV and GiA, are thus essential for muscle atonia and are thought to hyperpolarize motor neurons synergistically with GABA inputs to enable immobilization during sleep.^{285,316–318} For a comprehensive review I refer to Liu & Dan, 2019.³⁰⁰

Just as for any other animal, the distinction between stopping behavior and sleep in *C. elegans* might seem somewhat ambiguous on a behavioral level as animals transition from one to the other during spontaneous behavior. However, clear differences are apparent on a physiological level: such as reduced sensory responsiveness, altered brain activity or endocrine levels, and reduced muscle tone. *C. elegans* primarily displays developmental sleep during phases of larval molting.²⁴ This developmentally-timed sleep (DTS), also called lethargus, is known to be induced by the GABAergic RIS modulatory interneuron.^{319,320} Furthermore, also the glutamatergic RIA interneurons are known to promote sleep during lethargus via neuropeptides although their optogenetic activation stimulates motor activity.³²¹ Lastly, the ALA modulatory interneuron plays a crucial somnogenic role in stress-induced sleep.^{292,322–326} Brainwide nuclear calcium imaging has characterized *C. elegans* sleep in immobilized animals as a global brain state that induces inactivity of the majority of the wake-active neurons when arousing stimuli are absent. On the contrary, sleep-active neurons like RIS display stationary increased calcium levels. Although ALA retains transient activity bouts during quiescence^{327,328} it still remains uncertain if it constitutes a genuine sleep-active neuron.²⁶⁴ Interestingly, sleep entry mainly develops out of the forward locomotor brain state.³²⁷

However, whether these stop and sleep interneurons in *C. elegans* communicate either via electrical or synaptic connections, and then which ones in particular, or via chemical endocrine signaling to interfere with the descending PIN pathways controlling locomotion (1.4.4 and **Fig. 8**) is still poorly understood. Therefore, it was one of the investigation aims in this thesis.

1.5.2 Functional neurotransmission of locomotion inhibition

While still relatively little is known about functional neurotransmission of stop neurons,²⁵⁹ a plethora of conserved neuromodulators have already been involved in the molecular control of sleep in higher brain regions like the hypothalamus.³⁰⁶ Notable examples include adenosine, melanin-concentrating hormone (MCH) and galanin. Thus, besides conventional neurotransmitters (like acetylcholine, glutamate, GABA or glycine) also other important signaling molecules like neuropeptides are known to regulate sleep-wake behavior.^{306,329,330}

1.5.2.1 Neuropeptidergic regulation of neurotransmission

Neuropeptides are oligopeptides, short protein-like chains of (potentially modified) amino acids, that are secreted by neurons and that function as endocrine modulators of neuronal circuits by binding G protein-coupled receptors (GPCRs).^{331–333} In contrast to other neurotransmitters, neuropeptides are thus encoded in the genome as neuropeptide precursor genes which is valuable for comparative studies.^{334–336} By transcription of these genes and subsequent translation preproteins are produced that undergo proteolytic processing and post-translational modifications to generate mature bioactive peptides that are eventually secreted via dense core vesicles (**Fig. 10**).³³⁷ These features make them the most diverse class of neurotransmitters.^{331,338} In *C. elegans* neuropeptide genes are categorized in three major families: the FMRFamide (Phe-Met-Arg-Phe-amide)-like peptide (*flp*) family, insulin-like peptide (*ins*) family and the remaining neuropeptide-like protein (*nlp*) family.³³⁹ Currently, 126 neuropeptide precursor genes have been predicted in the *C. elegans* genome presumably encoding over 400 bioactive peptides of which 270 have already been identified with mass spectrometry so far [personal communication with Sven Van Bael].³³⁷ It has been speculated that *C. elegans* employs this many modulatory neuropeptidergic transmitters as a means of compressing the neuronal regulation for an extensive behavioral repertoire into a relatively compact nervous system. Consequently,

neuropeptides are known to regulate a wide variety of physiological processes and behaviors ranging from energy metabolism to locomotion, sleep, and learning and memory.^{330,338,340–342} (More detailed information on salt learning can be found in the publication Watteyne *et al.*, 2020²²⁸ in the supplemental information; Annex II).

>FLP-11, isoform a (K02G10.4a.1)

MTQFSALALLLIVFVAASEFAQSYDDVSAEKRAMRNALVRFGRASGGMRNALVRFGKRSPLDEEDFA
PESPLQGRNGAPQPFVRFGRSGQLDHMHDLSTLQKLFANNK

Figure 10: Representative neuropeptide precursor sequence. The amino acid residues of the longest known protein isoform of the *flp-11* gene (K02G10.4a.1) are represented with their one letter amino acid code. The predicted signal peptide that targets neuropeptides for secretion via dense core vesicles is indicated in yellow and the presumed proprotein convertase cleavage sites are indicated in green. Mature peptides that were identified with mass spectrometry³³⁷ are underlined and indicated in red. The N-terminal glycine residues of these four peptides are post-translationally amidated.

GPCRs are seven transmembrane domain (7TM) proteins that transduce the detection of an external stimulus across the cell membrane.^{333,343} GPCRs are found in all animals, are thus evolutionary ancient and are activated by diverse stimuli comprising light, odorants, metabolites, mechanical stimuli and peptides.^{344–346} Upon neuropeptide binding GPCRs change conformation and thereby activate heterotrimeric G proteins that initiate multiple intracellular signaling cascades.³⁴⁷ More than 5% of all *C. elegans* genes are predicted to code for GPCRs of which at least 128 are presumed to code for neuropeptide receptors.^{61,333}

The vast diversity of neuropeptidergic signaling and its differential functionality presumably arose through genetic duplication events, subsequent coevolution and differentiation into specialized neuronal cell types.^{336,348,349} Neuropeptides function as modulators of neurotransmission and in addition regulate (developmental) plasticity of the nervous system.^{45,350–352} Neuropeptidergic modulation of neuronal networks thus enables adaptive integration of sensory input, metabolic states, developmental programs and past experience to generate appropriate animal behaviors, including locomotion^{222,353–357} and thus as a consequence potentially also its inhibition. In addition, GPCRs are interesting drug targets which makes neuropeptide receptors exciting candidates for therapeutic applications.³⁵⁸

1.5.2.2 Neuropeptidergic regulation of locomotion inhibition in *C. elegans*

As prior to this study no dedicated stop neurons were known in *C. elegans*, a potential role for neuropeptides in the regulation of brief locomotion inhibition remained unstudied.

Intriguingly, ablation of astrocyte-like CEPsh glial cells that ensheath the synapses relaying the major output from the modulatory ALA interneurons to the AVE backward locomotion command interneurons leads to ectopic pausing behaviors in adult animals (**Fig. 11**).²⁹¹ Although a suggested direct role for neuropeptides secreted from the required ALA neuron could not yet be shown in this study, it still remains plausible that unidentified neuropeptides might regulate this artificial locomotion inhibition phenotype. In addition, the calcium activity of the DVA modulatory interneurons has been associated with prolonged pausing behavior (among multiple other behavioral correlates).³⁵⁵ However, optogenetic activation of DVA rather induces reorientations related to local search behavior in a *nlp-12/ckr-1* dependent manner.³⁵⁹ This indicates that DVA is most likely not a dedicated stop neuron, but rather suggests that it utilizes neuropeptides to regulate body posture during locomotion.^{355,360,361}

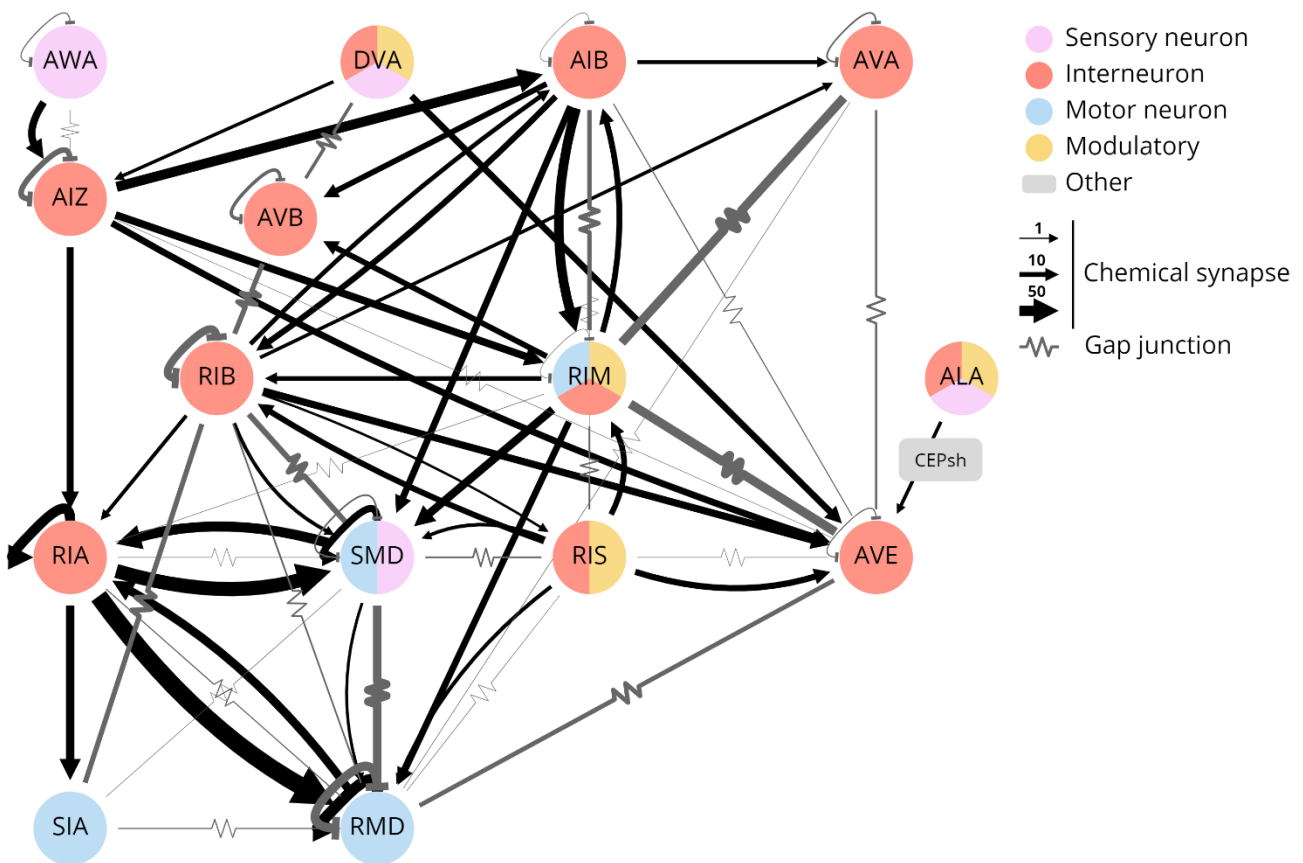


Figure 11: Connectome-based neural circuit model of head neurons known to participate in the inhibition of locomotion during sleep, slowing or stopping behaviors. Color codes of neuron types are indicated on the right. Black arrows represent the synaptic connections between neuron classes. Grey jagged lines represent gap junctions between neurons. The thickness of these symbols indicates the number of synapses or junctions, respectively. Generated with <http://nemanode.org> (built by <http://zhenlab.com>)⁴⁰

On the other hand, the role of neuropeptides in locomotion suppression during *C. elegans* sleep is well established. NLP-22-derived neuropeptides were the first somnogenic neuropeptides identified in *C. elegans*.³²¹ They are expressed in the RIA interneurons and

their expression cycles with larval molting periodicity. However, potential receptors for NLP-22 neuropeptides remained unknown. The sleep-active RIS modulatory interneuron is known to release both GABA and neuropeptides although it only requires neuropeptidergic signaling to induce larval sleep.³¹⁹ Predominantly, RFamide neuropeptides encoded by the *flp-11* gene have been involved although other neuropeptides might also contribute to establish sleep.³²⁰ As FLP-11 neuropeptides are able to activate many receptors *in vitro*, it still remains unclear whether they signal through multiple redundant receptors *in vivo* or if a more potent receptor has yet to be identified.^{320,360} Furthermore, the somnogenic ALA modulatory interneuron controls stress-induced sleep (SIS) by secretion of neuropeptides encoded by *flp-13*, *flp-24* and *nlp-8* genes that are thought to inhibit wake-promoting neurons.^{292,325,362} *flp-13* encoded peptides signal through DMSR-1 to induce SIS.³⁶² However, it is suggested that they can also activate other receptors, like FRPR-4, in addition or that other transmitters might signal through DMSR-1 too. Subsequently, *flp-13* encoded peptides were found to inhibit locomotion by reducing cAMP levels in the DVA neuron, potentially preventing it from releasing wake-promoting signals or affecting proprioception and body posture.³⁶³ A similar mechanism is proposed for *flp-24* encoded neuropeptides reducing intracellular cAMP in RIF interneurons. Furthermore, somnogenic *flp-18* and *flp-21* encoded peptides signaling through NPR-1 are known to increase the sensory arousal threshold associated with sleep by inhibiting arousing signals.^{291,327,364,365}

In sum, ample evidence indicates a crucial role for neuropeptides in the regulation of a quiescent brain state underlying *C. elegans* sleep.³²⁷ In accordance, orthologs of both *flp-11* and *nlp-22* encoded peptides in the parasitic nematode *Ascaris suum* have also been involved in motor inhibition.^{366,367} Similarly, somnogenic functions for RFamide neuropeptides were shown in *Drosophila*.^{368,369} Together these insights lead to the discovery that the vertebrate RFamide neuropeptide NPVF is involved in larval sleep of zebrafish.³⁷⁰ All these data emphasize a fundamental function for RFamide neuropeptides in sleep regulation that is evolutionary conserved across distantly related species. However, it still remains to be studied 1) how RFamide neuropeptides mechanistically establish locomotion inhibition in *C. elegans*, 2) in which neurocircuits the control of stopping and sleeping phenotypes is generated, 3) whether they are differentially controlled and 4) if also other neuropeptidergic signaling pathways might be involved.

1.6 Conclusions and aim of the project

To conclude, this dissertation aims at identifying and characterizing neuropeptidergic regulators of locomotion inhibition in *C. elegans*. As little is known about neuronal mechanisms that actively stop locomotion, genetic screening approaches were used to identify and characterize molecular pathways that actively prevent locomotion.

In the first results chapter, we investigated how the stop neuron RIS achieves to actively halt locomotion while simultaneously maintaining muscle tone. A genetic candidate screen was used to identify the molecular factors that the RIS modulatory interneuron requires to induce this locomotion stop phenotype in adult animals. This was achieved by screening selected genomic mutants in an optogenetic behavioral assay. Next, spontaneous activity of the RIS modulatory interneuron was studied using calcium imaging to probe if its neuronal activity during locomotion corresponds in time to reducing forward locomotion speed up to a halt prior to reversal events. We found that the calcium activity along the axonal process that runs around nerve ring displays compartmentalization. For this reason, I optimized the tracking performance and data-analysis pipeline of a fluorescence microscope built for Ca²⁺ imaging of freely moving worms with subcellular resolution.

In the second results chapter, we studied whether gonadotropin-releasing hormone (GnRH)-like signaling in *C. elegans* is involved in regulating locomotion inhibition. We identified sequence similarities of 7 novel GnRH receptor related (*gnrr*) genes in the *in silico* *C. elegans* genome. By screening these receptors in an *in vitro* calcium mobility receptor assay, we identified RPamide neuropeptides derived from *nlp-2*, *nlp-22* and *nlp-23* genes as their cognate ligands. We sought to uncover how their endocrine function affected behavior. For this, a reverse genetic screen was employed by means of mutant and overexpression analysis to pinpoint the role of these unstudied neuropeptide systems with sequence similarities to the GnRH signaling system. Led by the known function of NLP-22 neuropeptides in inducing sleep upon overexpression, we questioned through which receptors they exert their somnogenic function. Furthermore, we also assessed if similar RPamide peptides with physiologically relevant binding affinities encoded by *nlp-2* and *nlp-23* have comparable functions in the sleep-wake state control during lethargus. Next, I also studied through which neuronal circuits the GnRH-like signaling systems exert their function. Transgenic expression of genetically encoded fluorescent markers under the control of their native promoters allowed visualizing their expression patterns. In addition, I sought confirmation for the identified cell types in publicly available sc-RNA-seq databases.

In the final chapter, I elaborate on these findings and speculate on their potential implications for future research. Specifically, I will discuss the similarities and differences between stop neurons and sleep neurons. In addition, I discuss how neuropeptides might regulate stopping and sleeping behavior by neuromodulation of sensorimotor circuits.

1.7 References

1. Ribatti, D. An historical note on the cell theory. *Exp. Cell Res.* **364**, 1–4 (2018).
2. Crick, F. H. C. On protein synthesis. *Symp. Soc. Exp. Biol.* **12**, 138–163 (1958).
3. Crick, F. H. C. Central dogma of molecular biology. *Nature* **227**, 561–563 (1970).
4. Darwin, C. *On the origin of species by means of natural selection, or preservation of favoured races in the struggle for life.* (1859).
5. Bateson, W. & Mendel, G. W. B. *Mendel's principles of heredity.* (Cambridge University Press, 1902).
6. Ogilvie, M. B. & Choquette, C. J. Nettie Maria Stevens (1861-1912): her life and contributions to cytogenetics. *Proc. Am. Philos. Soc.* **125**, 292–311 (1981).
7. Janssens, F. A., Koszul, R. & Zickler, D. La theorie de la chiasmotypie nouvelle interprétation des cinèses de maturation. *Genetics* **191**, 319–346 (2012).
8. Koszul, R., Meselson, M., Van oninck, K., Vandenhaute, J. & Zickler, D. The centenary of Janssens's Chiasmatype theory. *Genetics* **191**, 309–317 (2012).
9. Morgan, T. H. Sex limited inheritance in *Drosophila*. *Science* **32**, 120–122 (1910).
10. Sturtevant, A. H. The linear arrangement of six sex-linked factors in *Drosophila*, as shown by their mode of association. *J. Exp. Biol.* **14**, 43–59 (1913).
11. Ganetzky, B. & Hawley, R. S. The centenary of GENETICS: Bridges to the future. *Genetics* **202**, 15–23 (2016).
12. Crick, F. H. C. The genetic code--yesterday, today, and tomorrow. *Cold Spring Harb. Symp. Quant. Biol.* **31**, 1–9 (1966).
13. Miyata, M. *et al.* Tree of motility – A proposed history of motility systems in the tree of life. *Genes to Cells* **25**, 6–21 (2020).
14. Szent-Györgyi, A. G. Milestone in physiology: The early history of the biochemistry of muscle contraction. *J. Gen. Physiol.* **123**, 631–641 (2004).
15. López-Muñoz, F., Boya, J. & Alamo, C. Neuron theory, the cornerstone of neuroscience, on the centenary of the Nobel Prize award to Santiago Ramón y Cajal. *Brain Res. Bull.* **70**, 391–405 (2006).
16. Maupas, É. Modes et formes de reproduction des nématodes. *Arch. Zool. Exp. Gen.* **ser.3 t.8**, 463–624 (1900).
17. Bezerra, T. N. *et al.* *Caenorhabditis elegans* (Maupas, 1899). *Nemys: World Database of Nematodes.* (2019).
18. Brenner, S. Nature's gift to science. in *The Nobel Prizes 2002* (ed. Tore Frängsmyr) 274–282 ([Nobel Foundation], 2003).
19. Herculano-Houzel, S. The remarkable, yet not extraordinary, human brain as a scaled-up primate brain and its associated cost. *Proc. Natl. Acad. Sci. U. S. A.* **109**, 10661–10668 (2012).
20. Bates, A. S., Janssens, J., Jefferis, G. S. & Aerts, S. Neuronal cell types in the fly: single-cell anatomy meets single-cell genomics. *Curr. Opin. Neurobiol.* **56**, 125–134 (2019).
21. Brenner, S. The genetics of *Caenorhabditis elegans*. *Genetics* **77**, 71–94 (1974).
22. Maupas, É. La mue et l'enkystement chez les nématodes. *Arch. Zool. Exp. Gen.* **ser.3 t.7**, 563–628 (1899).
23. Altun, Z. F. *et al.* WormAtlas.
24. Raizen, D. M. *et al.* Lethargus is a *Caenorhabditis elegans* sleep-like state. *Nature* **451**, 569–572 (2008).
25. Byerly, L., Scherer, S. & Russell, R. L. The life cycle of the nematode *Caenorhabditis elegans*. *Dev. Biol.* **51**, 34–48 (1976).
26. Zarkower, D. Somatic sex determination. in *WormBook* (ed. The *C. elegans* Research Community) (WormBook, 2006). doi:doi/10.1895/wormbook.1.84.1
27. Fay, D. S. *Classical genetic methods.* *WormBook* (Wormbook, 2013). doi:10.1895/wormbook.1.1
28. Stiernagle, T. Maintenance of *C. elegans*. in *WormBook* (eds. Fay, D. S. & Ambros, V.) doi/10.1895/wormbook.1.101.1 (The *C. elegans* Research Community, 2006). doi:10.1895/wormbook.1.101.1
29. The *C. elegans* sequencing consortium. Genome Sequence Platform of the Nematode *C. elegans*: A Platform for Investigating Biology. *Science*. **282**, 2012–2018 (1998).
30. Sulston, J. E., Schierenberg, E., White, J. G. & Thomson, J. N. The embryonic cell lineage of the nematode *Caenorhabditis elegans*. *Dev. Biol.* **100**, 64–119 (1983).
31. Hobert, O. Gene regulation by transcription factors and MicroRNAs. *Science*. **319**, 1785–1786 (2008).
32. Sammut, M. *et al.* Glia-derived neurons are required for sex-specific learning in *C. elegans*. *Nature* **526**, 385–390 (2015).
33. Hart, M. P. & Hobert, O. Sexual dimorphism: mystery neurons control sex-specific behavioral plasticity. *Curr. Biol.* **25**, R1170–R1172 (2015).
34. Sulston, J. E. & Horvitz, H. R. Post-embryonic cell lineages of the nematode, *Caenorhabditis elegans*. *Dev. Biol.* **56**, 110–156 (1977).
35. Packer, J. S. *et al.* A lineage-resolved molecular atlas of *C. elegans* embryogenesis at single-cell resolution. *Science*, **365**, eaax1971 (2019).
36. Taylor, S. R. *et al.* Expression profiling of the mature *C. elegans* nervous system by single-cell RNA-Sequencing. *bioRxiv* 737577 (2019). doi:10.1101/737577
37. White, J. G., Southgate, E., Thomson, J. N. & Brenner, S. The structure of the nervous system of the nematode *Caenorhabditis elegans*. *Philos. Trans. R. Soc. B Biol. Sci.* **314**, 1–340 (1986).
38. Cook, S. J. *et al.* Whole-animal connectomes of both *Caenorhabditis elegans* sexes. *Nature* **571**, 63–71 (2019).
39. Mulcahy, B. *et al.* A pipeline for volume electron microscopy of the *caenorhabditis elegans* nervous system. *Front. Neural Circuits* **12**, (2018).
40. Witvliet, D., Mulcahy, B., Mitchell, J.K. *et al.* Connectomes across development reveal principles of brain maturation. *Nature* **596**, 257–261 (2021). <https://doi.org/10.1038/s41586-021-03778-8>
41. Scheffer, L. K. *et al.* A connectome and analysis of the adult *Drosophila* central brain. *ELife* **9**, e57443 (2020).

42. Hammarlund, M., Hobert, O., Miller, D. M. & Sestan, N. The CeNGEN Project: the complete gene expression map of an entire nervous system. *Neuron* **99**, 430–433 (2018).
43. Larson, S. D., Gleeson, P. & Brown, A. E. X. Connectome to behaviour: Modeling *Caenorhabditis elegans* at cellular resolution. *Philos. Trans. R. Soc. B Biol. Sci.* **373**, 8–10 (2018).
44. Sarma, G. P. *et al.* OpenWorm: overview and recent advances in integrative biological simulation of *Caenorhabditis elegans*. *Philos. Trans. R. Soc. B Biol. Sci.* **373**, 20170382 (2018).
45. Bargmann, C. I. Beyond the connectome: How neuromodulators shape neural circuits. *BioEssays* **34**, 458–465 (2012).
46. Bargmann, C. I. & Marder, E. From the connectome to brain function. *Nat. Methods* **10**, 483–490 (2013).
47. Bentley, B. *et al.* The Multilayer Connectome of *Caenorhabditis elegans*. *PLoS Computational Biology* **12**, (2016).
48. Schuske, K., Beg, A. A. & Jorgensen, E. M. The GABA nervous system in *C. elegans*. *Trends Neurosci.* **27**, 407–414 (2004).
49. Jobson, M. A. *et al.* Spillover transmission is mediated by the excitatory GABA receptor LGC-35 in *C. elegans*. *J. Neurosci.* **35**, 2803–2816 (2015).
50. de Bono, M. & Villu Maricq, A. Neuronal substrates of complex behaviors in *C. elegans*. *Annu. Rev. Neurosci.* **28**, 451–501 (2005).
51. Shen, Y. *et al.* An extrasynaptic GABAergic signal modulates a pattern of forward movement in *Caenorhabditis elegans*. *ELife* **5**, 1–25 (2016).
52. Liu, P., Chen, B., Mailler, R. & Wang, Z. W. Antidromic-rectifying gap junctions amplify chemical transmission at functionally mixed electrical-chemical synapses. *Nat. Commun.* **8**, (2017).
53. Bhattacharya, A., Aghayeva, U., Berghoff, E. G. & Hobert, O. Plasticity of the electrical connectome of *C. elegans*. *Cell* **176**, 1174–1189.e16 (2019).
54. Bargmann, C. I. & Avery, L. Laser killing of cells in *Caenorhabditis elegans*. *Methods Cell Biol.* **48**, 225–250 (1995).
55. Ankeny, R. A. The natural history of *Caenorhabditis elegans* research. *Nat. Rev. Genet.* **2**, 474–479 (2001).
56. Bellen, H. J., Tong, C. & Tsuda, H. 100 years of *Drosophila* research and its impact on vertebrate neuroscience: a history lesson for the future. *Neuroscience* **11**, 514–522 (2010).
57. Jorgensen, E. M. & Mango, S. E. The art and design of genetic screens: *Caenorhabditis elegans*. *Nat. Rev. Genet.* **3**, 356–369 (2002).
58. Jansen, G., Hazendonk, E., Thijssen, K. L. & Plasterk, R. H. A. Reverse genetics by chemical mutagenesis in *Caenorhabditis elegans*. *Nat. Genet.* **17**, 119–121 (1997).
59. Boulin, T. & Hobert, O. From genes to function: The *C. elegans* genetic toolbox. *Wiley Interdiscip. Rev. Dev. Biol.* **1**, 114–137 (2012).
60. Nance, J. & Frøkjær-Jensen, C. *The caenorhabditis elegans transgenic toolbox*. *Genetics* **212**, (2019).
61. Bargmann, C. I. Neurobiology of the *Caenorhabditis elegans* genome. *Science* **282**, 2028–2033 (1998).
62. Cohen, A. E. Optogenetics: turning the microscope on its head. *Biophys. J.* **110**, 997–1003 (2016).
63. Wollman, A. J. M., Nudd, R., Hedlund, E. G. & Leake, M. C. From Animaculum to single molecules: 300 years of the light microscope. *Philos. Trans. R. Soc. London* **5**, 150019 (2015).
64. Chalfie, M., Tu, Y., Euskirchen, G., Ward, W. W. & Prasher, D. C. Green fluorescent protein as a marker for gene expression. *Science* **263**, 802 LP – 805 (1994).
65. Lichtman, J. W. & Conchello, J. A. Fluorescence microscopy. *Nat. Methods* **2**, 910–919 (2005).
66. Shimomura, O. Structure of the chromophore of *Aequorea* green fluorescent protein. *FEBS Lett.* **104**, 220–222 (1979).
67. Prasher, D. C., Eckenrode, V. K., Ward, W. W., Prendergast, F. G. & Cormier, M. J. Primary structure of the *Aequorea victoria* green-fluorescent protein. *Gene* **111**, 229–233 (1992).
68. Ormö, M. *et al.* Crystal structure of the *Aequorea victoria* green fluorescent protein. *Science* **273**, 1392–1395 (1996).
69. Shashkova, S. & Leake, M. C. Single-molecule fluorescence microscopy review: Shedding new light on old problems. *Biosci. Rep.* **37**, 1–19 (2017).
70. Sengupta, P., Chou, J. H. & Bargmann, C. I. odr-10 Encodes a seven transmembrane domain olfactory receptor required for responses to the odorant diacetyl. *Cell* **84**, 899–909 (1996).
71. Tursun, B., Patel, T., Kratsios, P. & Hobert, O. Direct conversion of *C. elegans* germ cells into specific neuron types. *Science* **331**, 304–308 (2011).
72. Specht, E. A., Braselmann, E. & Palmer, A. E. A critical and comparative review of fluorescent tools for live-cell imaging. *Annu. Rev. Physiol.* **79**, 93–117 (2017).
73. Romei, M. G. & Boxer, S. G. Split green fluorescent proteins: scope, limitations, and outlook. *Annu. Rev. Biophys.* **48**, 19–44 (2019).
74. Zhang, J., Campbell, R. E., Ting, A. Y. & Tsien, R. Y. Creating new fluorescent probes for cell biology. *Nat. Rev. Mol. Cell Biol.* **3**, 906–918 (2002).
75. Ando, R., Hama, H., Yamamoto-Hino, M., Mizuno, H. & Miyawaki, A. An optical marker based on the UV-induced green-to-red photoconversion of a fluorescent protein. *Proc. Natl. Acad. Sci. U. S. A.* **99**, 12651–12656 (2002).
76. Wiedenmann, J. *et al.* EosFP, a fluorescent marker protein with UV-inducible green-to-red fluorescence conversion. *Proc. Natl. Acad. Sci.* **101**, 15905–15910 (2004).
77. Ando, R., Mizuno, H. & Miyawaki, A. Regulated fast nucleocytoplasmic shuttling observed by reversible protein highlighting. *Science* **306**, 1370–1373 (2004).
78. Betzig, E. *et al.* Imaging intracellular fluorescent proteins at nanometer resolution. *Science* **313**, 1642–1645 (2006).
79. Duwé, S. & Dedecker, P. Optimizing the fluorescent protein toolbox and its use. *Curr. Opin. Biotechnol.* **58**, 183–

- 191 (2019).
80. Rongo, C., Whitfield, C. W., Rodal, A., Stuart K, K. & Kaplan, J. M. LIN-10 is a shared component of the polarized protein localization pathways in neurons and epithelia. *Cell* **94**, 751–759 (1998).
 81. Nathoo, A. N., Moeller, R. A., Westlund, B. A. & Hart, A. C. Identification of neuropeptide-like protein gene families in *Caenorhabditis elegans* and other species. *Proc. Natl. Acad. Sci.* **98**, 14000–14005 (2001).
 82. Kim, K. & Li, C. Expression and regulation of an FMRFamide-related neuropeptide gene family in *Caenorhabditis elegans*. *J. Comp. Neurol.* **475**, 540–550 (2004).
 83. Yemini, E. *et al.* NeuroPAL: a multicolor atlas for whole-brain neuronal identification in *C. elegans*. *Cell* **184**, 272–288.e11 (2021).
 84. Chen, B. C. *et al.* Lattice light-sheet microscopy: Imaging molecules to embryos at high spatiotemporal resolution. *Science* **346**, (2014).
 85. Royer, L. A. *et al.* Adaptive light-sheet microscopy for long-term, high-resolution imaging in living organisms. *Nat. Biotechnol.* **34**, 1267–1278 (2016).
 86. Voleti, V. *et al.* Real-time volumetric microscopy of in vivo dynamics and large-scale samples with SCAPE 2.0. *Nat. Methods* **16**, 1054–1062 (2019).
 87. Avery, L., Raizen, D. & Lockery, S. Electrophysiological Methods. *Methods Cell Biol.* **48**, 251–269 (1995).
 88. Gonzales, D. L. *et al.* Scalable electrophysiology in intact small animals with nanoscale suspended electrode arrays. *Nat. Nanotechnol.* **12**, 684–691 (2017).
 89. Goodman, M. B., Lindsay, T. H., Lockery, S. R. & Richmond, J. E. Electrophysiological methods for *Caenorhabditis elegans* neurobiology. *Methods in Cell Biology* **107**, (Elsevier Inc., 2012).
 90. Tsien, R. Y. New calcium indicators and buffers with high selectivity against magnesium and protons: design, synthesis, and properties of prototype structures. *Biochemistry* **19**, 2396–2404 (1980).
 91. Loew, L. M., Cohen, L. B., Salzberg, B. M., Obaid, A. L. & Bezanilla, F. Charge-shift probes of membrane potential. Characterization of aminostyrylpyridinium dyes on the squid giant axon. *Biophys. J.* **47**, 71–77 (1985).
 92. Dal Santo, P., Logan, M. A., Chisholm, A. D. & Jorgensen, E. M. The inositol triphosphate receptor regulates a 50-second behavioral rhythm in *C. elegans*. *Cell* **98**, 757–767 (1999).
 93. Miyawaki, A. *et al.* Fluorescent indicators for Ca²⁺ based on green fluorescent proteins and calmodulin. *Nature* **388**, 882–887 (1997).
 94. Förster, T. Zwischenmolekulare Energiewanderung und Fluoreszenz. *Ann. Phys.* **437**, 55–75 (1948).
 95. Kerr, R. *et al.* Optical imaging of calcium transients in neurons and pharyngeal muscle of *C. elegans*. *Neuron* **26**, 583–594 (2000).
 96. Nakai, J., Ohkura, M. & Imoto, K. A high signal-to-noise Ca²⁺ probe composed of a single green fluorescent protein. *Nat. Biotechnol.* **19**, 137–141 (2001).
 97. Chen, T. W. *et al.* Ultrasensitive fluorescent proteins for imaging neuronal activity. *Nature* **499**, 295–300 (2013).
 98. Dana, H. *et al.* High-performance calcium sensors for imaging activity in neuronal populations and microcompartments. *Nat. Methods* **16**, 649–657 (2019).
 99. Zhao, Y. *et al.* An expanded palette of genetically encoded Ca²⁺ indicators. *Science* **333**, 1888 LP – 1891 (2011).
 100. Akerboom, J. *et al.* Genetically encoded calcium indicators for multi-color neural activity imaging and combination with optogenetics. *Front. Mol. Neurosci.* **6**, 1–29 (2013).
 101. Dana, H. *et al.* Sensitive red protein calcium indicators for imaging neural activity. *ELife* **5**, 1–24 (2016).
 102. Fosque, B. F. *et al.* Labeling of active neural circuits in vivo with designed calcium integrators. *Science* **347**, 755–760 (2015).
 103. Moeyaert, B. *et al.* Improved methods for marking active neuron populations. *Nat. Commun.* **9**, 1–12 (2018).
 104. Pérez Koldenkova, V. & Nagai, T. Genetically encoded Ca²⁺ indicators: Properties and evaluation. *Biochim. Biophys. Acta - Mol. Cell Res.* **1833**, 1787–1797 (2013).
 105. Wagner, S., De Bortoli, S., Schwarzländer, M. & Szabó, I. Regulation of mitochondrial calcium in plants versus animals. *J. Exp. Bot.* **67**, 3809–3829 (2016).
 106. Akerboom, J. *et al.* Crystal structures of the GCaMP calcium sensor reveal the mechanism of fluorescence signal change and aid rational design. *J. Biol. Chem.* **284**, 6455–6464 (2009).
 107. Xu, Y., Zou, P. & Cohen, A. E. Voltage imaging with genetically encoded indicators. *Curr. Opin. Chem. Biol.* **39**, 1–10 (2017).
 108. Knöpfel, T. & Song, C. Optical voltage imaging in neurons: moving from technology development to practical tool. *Nat. Rev. Neurosci.* **20**, 719–727 (2019).
 109. Dimitrov, D. *et al.* Engineering and characterization of an enhanced fluorescent protein voltage sensor. *PLoS One* **2**, 2–6 (2007).
 110. Kannan, M., Vasan, G. & Pieribone, V. A. Optimizing strategies for developing genetically encoded voltage indicators. *Front. Cell. Neurosci.* **13**, 1–17 (2019).
 111. Kralj, J. M., Douglass, A. D., Hochbaum, D. R., MacLaurin, D. & Cohen, A. E. Optical recording of action potentials in mammalian neurons using a microbial rhodopsin. *Nat. Methods* **9**, 90–95 (2012).
 112. Piatkevich, K. D. *et al.* A robotic multidimensional directed evolution approach applied to fluorescent voltage reporters article. *Nat. Chem. Biol.* **14**, 352–360 (2018).
 113. Zou, P. *et al.* Bright and fast multicoloured voltage reporters via electrochromic FRET. *Nat. Commun.* **5**, (2014).
 114. Gong, Y. *et al.* High-speed recording of neural spikes in awake mice and flies with a fluorescent voltage sensor. *Science* **350**, 1361 LP – 1366 (2015).
 115. Kannan, M. *et al.* Fast, *in vivo* voltage imaging using a red fluorescent indicator. *Nat. Methods* **15**, 1108–1116 (2018).
 116. Bando, Y., Sakamoto, M., Kim, S., Ayzenshtat, I. & Yuste, R. Comparative evaluation of genetically encoded voltage indicators. *Cell Rep.* **26**, 802–813.e4 (2019).

117. Hou, J. H., Kralj, J. M., Douglass, A. D., Engert, F. & Cohen, A. E. Simultaneous mapping of membrane voltage and calcium in zebrafish heart *in vivo* reveals chamber-specific developmental transitions in ionic currents. *Front. Physiol.* **5** AUG, 1–10 (2014).
118. Yang, H. H. H. *et al.* Subcellular imaging of voltage and calcium signals reveals neural processing *in vivo*. *Cell* **166**, 245–257 (2016).
119. Fan, L. Z. *et al.* All-optical synaptic electrophysiology probes mechanism of ketamine-induced disinhibition. *Nat. Methods* **15**, 823–831 (2018).
120. Piao, H. H., Rajakumar, D., Kang, B. E., Kim, E. H. & Baker, B. J. Combinatorial mutagenesis of the voltage-sensing domain enables the optical resolution of action potentials firing at 60 Hz by a genetically encoded fluorescent sensor of membrane potential. *J. Neurosci.* **35**, 372–385 (2015).
121. Brunet, T. & Arendt, D. From damage response to action potentials: Early evolution of neural and contractile modules in stem eukaryotes. *Philos. Trans. R. Soc. B Biol. Sci.* **371**, (2016).
122. Rizo, J. & Rosenmund, C. Synaptic vesicle fusion. *Nat. Struct. Mol. Biol.* **15**, 665–674 (2008).
123. Bayer, K. U. & Schulman, H. CaM Kinase: Still Inspiring at 40. *Neuron* **103**, 380–394 (2019).
124. Zot, A. S. & Potter, J. D. Structural aspects of troponin-tropomyosin regulation of skeletal muscle contraction. *Annu. Rev. Biophys. Biophys. Chem.* **16**, 535–559 (1987).
125. Kim, E. H., Chin, G., Rong, G., Poskanzer, K. E. & Clark, H. A. Optical probes for neurobiological sensing and imaging. *Acc. Chem. Res.* **51**, 1023–1032 (2018).
126. Woldemariam, S. *et al.* Using a robust and sensitive GFP-Based cGMP sensor for real-time imaging in intact *Caenorhabditis elegans*. *Genetics* **213**, 59–77 (2019).
127. Marvin, J. S. *et al.* An optimized fluorescent probe for visualizing glutamate neurotransmission. *Nat. Methods* **10**, 162–170 (2013).
128. Marvin, J. S. *et al.* A genetically encoded fluorescent sensor for *in vivo* imaging of GABA. *Nat. Methods* **16**, 763–770 (2019).
129. Grimley, J. S. *et al.* Visualization of synaptic inhibition with an optogenetic sensor developed by cell-free protein engineering automation. *J. Neurosci.* **33**, 16297–16309 (2013).
130. Miesenböck, G., De Angelis, D. A. & Rothman, J. E. Visualizing secretion and synaptic transmission with pH-sensitive green fluorescent proteins. *Nature* **394**, 192–195 (1998).
131. Barnea, G. *et al.* The genetic design of signaling cascades to record receptor activation. *Proc. Natl. Acad. Sci. U. S. A.* **105**, 64–69 (2008).
132. Katow, H., Takahashi, T., Saito, K., Tanimoto, H. & Kondo, S. Tango knock-ins visualize endogenous activity of G protein-coupled receptors in *Drosophila*. *J. Neurogenet.* **33**, 44–51 (2019).
133. Hochbaum, D. R. *et al.* All-optical electrophysiology in mammalian neurons using engineered microbial rhodopsins. *Nat. Methods* **11**, 825–833 (2014).
134. Donato, A., Kagias, K., Zhang, Y. & Hilliard, M. A. Neuronal sub-compartmentalization: a strategy to optimize neuronal function. *Biol. Rev.* **94**, 1023–1037 (2019).
135. Schrödel, T., Prevedel, R., Aumayr, K., Zimmer, M. & Vaziri, A. Brain-wide 3D imaging of neuronal activity in *Caenorhabditis elegans* with sculpted light. *Nat. Methods* **10**, 1013–1020 (2013).
136. Piatkevich, K. D. *et al.* Population imaging of neural activity in awake behaving mice. *Nature* **574**, 413–417 (2019).
137. Palmer, A. E., Jin, C., Reed, J. C. & Tsien, R. Y. Bcl-2-mediated alterations in endoplasmic reticulum Ca²⁺ analyzed with an improved genetically encoded fluorescent sensor. *Proc. Natl. Acad. Sci.* **101**, 17404–17409 (2004).
138. Voglmaier, S. M. *et al.* Distinct endocytic pathways control the rate and extent of synaptic vesicle protein recycling. *Neuron* **51**, 71–84 (2006).
139. Ventimiglia, D. & Bargmann, C. I. Diverse modes of synaptic signaling, regulation, and plasticity distinguish two classes of *C. elegans* glutamatergic neurons. *ELife* **6**, 1–25 (2017).
140. Broussard, G. J. *et al.* In vivo measurement of afferent activity with axon-specific calcium imaging. *Nat. Neurosci.* **21**, 1272–1280 (2018).
141. Ahrens, M. B., Orger, M. B., Robson, D. N., Li, J. M. & Keller, P. J. Whole-brain functional imaging at cellular resolution using light-sheet microscopy. *Nat. Methods* **10**, 413–420 (2013).
142. Lecoq, J., Orlova, N. & Grewe, B. F. Wide. Fast. Deep: Recent advances in multiphoton microscopy of *in vivo* neuronal activity. *J. Neurosci.* **39**, 9042–9052 (2019).
143. Liu, Q., Hollopeter, G. & Jorgensen, E. M. Graded synaptic transmission at the *Caenorhabditis elegans* neuromuscular junction. *Proc. Natl. Acad. Sci. U. S. A.* **106**, 10823–10828 (2009).
144. Lockery, S. R. & Goodman, M. B. The quest for action potentials in *C. elegans* neurons hits a plateau. *Nat. Neurosci.* **12**, 377–378 (2009).
145. Raizen, D. M. & Avery, L. Electrical activity and behavior in the pharynx of *Caenorhabditis elegans*. *Neuron* **12**, 483–495 (1994).
146. Gao, S. & Zhen, M. Action potentials drive body wall muscle contractions in *Caenorhabditis elegans*. *Proc. Natl. Acad. Sci. U. S. A.* **108**, 2557–2562 (2011).
147. Liu, Q., Kidd, P. B., Dobosiewicz, M. & Bargmann, C. I. *C. elegans* AWA Olfactory Neurons Fire Calcium-Mediated All-or-None Action Potentials. *Cell* **175**, 57–70 (2018).
148. Flytzanis, N. C. *et al.* Archaelhodopsin variants with enhanced voltage-sensitive fluorescence in mammalian and *Caenorhabditis elegans* neurons. *Nat. Commun.* **5**, (2014).
149. Hashemi, N. A. *et al.* Rhodopsin-based voltage imaging tools for use in muscles and neurons of *Caenorhabditis elegans*. *Proc. Natl. Acad. Sci. U. S. A.* **116**, 17051–17060 (2019).
150. Hobert, O., Glenwinkel, L. & White, J. Revisiting neuronal cell type classification in *Caenorhabditis elegans*. *Curr. Biol.* **26**, R1197–R1203 (2016).

151. Lorenzo, R., Onizuka, M., Defrance, M. & Laurent, P. Combining single-cell RNA-sequencing with a molecular atlas unveils new markers for *Caenorhabditis elegans* neuron classes. *Nucleic Acids Res* **48**, 7119–7134 (2020).
152. Schmitt, C., Schultheis, C., Husson, S. J., Liewald, J. F. & Gottschalk, A. Specific expression of Channelrhodopsin-2 in single neurons of *Caenorhabditis elegans*. *PLoS One* **7**, (2012).
153. Steuer Costa, W. *et al.* A GABAergic and peptidergic sleep neuron as a locomotion stop neuron with compartmentalized Ca²⁺ dynamics. *Nat. Commun.* **10**, 4095 (2019).
154. Kato, S. *et al.* Global brain dynamics embed the motor command sequence of *Caenorhabditis elegans*. *Cell* **163**, 656–669 (2015).
155. Nguyen, J. P. *et al.* Whole-brain calcium imaging with cellular resolution in freely behaving *Caenorhabditis elegans*. *Proc. Natl. Acad. Sci. U. S. A.* **113**, E1074–E1081 (2016).
156. Venkatachalam, V. *et al.* Pan-neuronal imaging in roaming *Caenorhabditis elegans*. *Proc. Natl. Acad. Sci. U. S. A.* **113**, E1082–E1088 (2016).
157. Kotera, I. *et al.* Pan-neuronal screening in *Caenorhabditis elegans* reveals asymmetric dynamics of AWC neurons is critical for thermal avoidance behavior. *ELife* **5**, 1–19 (2016).
158. Prevedel, R. *et al.* Simultaneous whole-animal 3D imaging of neuronal activity using light-field microscopy. *Nat. Methods* **11**, 727–730 (2014).
159. Tokunaga, T. *et al.* Automated detection and tracking of many cells by using 4D live-cell imaging data. *Bioinformatics* **30**, 43–51 (2014).
160. Toyoshima, Y. *et al.* Accurate automatic detection of densely distributed cell nuclei in 3D space. *PLoS Comput. Biol.* **12**, 1–20 (2016).
161. Toyoshima, Y. *et al.* Neuron ID dataset facilitates neuronal annotation for whole-brain activity imaging of *C. elegans*. *BMC Biol.* **18**, 1–20 (2020).
162. Wu, S. *et al.* An ensemble learning approach to auto-annotation for whole-brain *C. elegans* imaging. 1–14 (2017). doi:10.1101/180430
163. Mena, G. *et al.* Semi-automated cell identification in NeuroPAL *C. elegans* strains. 1–31 (2019). doi:https://doi.org/10.1101/2020.03.10.986356
164. Bubnis, G., Ban, S., DiFranco, M. D. & Kato, S. A probabilistic atlas for cell identification. (2019).
165. Chaudhary, S., Lee, S. A., Li, Y., Patel, D. S. & Lu, H. Graphical-model framework for automated annotation of cell identities in dense cellular images. *eLife* **10**, e60321 (2021).
166. Hendricks, M., Ha, H., Maffey, N. & Zhang, Y. Compartmentalized calcium dynamics in a *C. elegans* interneuron encode head movement. *Nature* **487**, 99–103 (2012).
167. Ouellette, M.-H., Desrochers, M. J., Gheta, I., Ramos, R. & Hendricks, M. A gate-and-switch model for head orientation behaviors in *Caenorhabditis elegans*. *Eneuro* **5**, ENEURO.0121-18.2018 (2018).
168. Shidara, H., Hotta, K. & Oka, K. Compartmentalized cGMP responses of olfactory sensory neurons in *Caenorhabditis elegans*. *J. Neurosci.* **37**, 3753–3763 (2017).
169. Suzuki, H. *et al.* *In vivo* imaging of *C. elegans* mechanosensory neurons demonstrates a specific role for the MEC-4 channel in the process of gentle touch sensation. *Neuron* **39**, 1005–1017 (2003).
170. Chronis, N., Zimmer, M. & Bargmann, C. I. Microfluidics for *in vivo* imaging of neuronal and behavioral activity in *Caenorhabditis elegans*. *Nat. Methods* **4**, 727–731 (2007).
171. Stirman, J. N., Brauner, M., Gottschalk, A. & Lu, H. High-throughput study of synaptic transmission at the neuromuscular junction enabled by optogenetics and microfluidics. *J. Neurosci. Methods* **191**, 90–93 (2010).
172. Turek, M., Besseling, J. & Bringmann, H. Agarose microchambers for long-term calcium imaging of *Caenorhabditis elegans*. *J. Vis. Exp.* 1–8 (2015). doi:10.3791/52742
173. Cho, Y., Oakland, D. N., Lee, S. A., Schafer, W. R. & Lu, H. On-chip functional neuroimaging with mechanical stimulation in: *Caenorhabditis elegans* larvae for studying development and neural circuits. *Lab Chip* **18**, 601–609 (2018).
174. Rouse, T., Aubry, G., Cho, Y., Zimmer, M. & Lu, H. A programmable platform for sub-second multichemical dynamic stimulation and neuronal functional imaging in *C. elegans*. *Lab Chip* **18**, 505–513 (2018).
175. Gray, J. M., Hill, J. J. & Bargmann, C. I. A circuit for navigation in *Caenorhabditis elegans*. *Proc. Natl. Acad. Sci.* **102**, 3184–3191 (2005).
176. Husson, S. J., Steuer Costa, W., Wagner Schmitt, C. & Gottschalk, A. Keeping track of worm trackers. in *WormBook* (Community, 2012). doi:doi/10.1895/wormbook.1.156.1
177. Ben Arous, J., Tanizawa, Y., Rabinowitch, I., Chatenay, D. & Schafer, W. R. Automated imaging of neuronal activity in freely behaving *Caenorhabditis elegans*. *J. Neurosci. Methods* **187**, 229–234 (2010).
178. Clark, D. A., Gabel, C. V., Gabel, H. & Samuel, A. D. T. Temporal activity patterns in thermosensory neurons of freely moving *Caenorhabditis elegans* encode spatial thermal gradients. *J. Neurosci.* **27**, 6083–6090 (2007).
179. Piggott, B. J., Liu, J., Feng, Z., Wescott, S. A. & Xu, X. Z. S. The neural circuits and synaptic mechanisms underlying motor initiation in *C. elegans*. *Cell* **147**, 922–933 (2011).
180. Faumont, S. *et al.* An Image-Free Opto-Mechanical system for creating virtual environments and imaging neuronal activity in freely moving *Caenorhabditis elegans*. *PLoS One* **6**, (2011).
181. Kawano, T. *et al.* An imbalancing act: Gap junctions reduce the backward motor circuit activity to bias *C. elegans* for forward locomotion. *Neuron* **72**, 572–586 (2011).
182. Zheng, M., Cao, P., Yang, J., Xu, S. X. Z. & Feng, Z. Calcium imaging of multiple neurons in freely behaving *C. elegans*. *J. Neurosci. Methods* **206**, 78–82 (2012).
183. Larsch, J., Ventimiglia, D., Bargmann, C. I. & Albrecht, D. R. High-throughput imaging of neuronal activity in *Caenorhabditis elegans*. *Proc. Natl. Acad. Sci.* **110**, (2013).
184. Busch, K. E. *et al.* Tonic signaling from O₂ sensors sets neural circuit activity and behavioral state. *Nat. Neurosci.* **15**, 581–591 (2012).
185. Shipley, F. B., Clark, C. M., Alkema, M. J. & Leifer, A. M. Simultaneous optogenetic manipulation and calcium

- imaging in freely moving *C. elegans*. *Front. Neural Circuits* **8**, 1–8 (2014).
186. Wen, Q., Gao, S. & Zhen, M. *Caenorhabditis elegans* excitatory ventral cord motor neurons derive rhythm for body undulation. *Philos. Trans. R. Soc. B Biol. Sci.* **373**, 20170370 (2018).
 187. Gao, S. *et al.* Excitatory motor neurons are local oscillators for backward locomotion. *ELife* **7**, 1–32 (2018).
 188. Mainen, Z. F., Sejnowski, T. J., Series, N. & Jun, N. Reliability of spike timing in neocortical neurons reliability of spike timing in neocortical neurons. *Science* **268**, 1503–1506 (1995).
 189. Doron, G. & Brecht, M. What single-cell stimulation has told us about neural coding. *Philos. Trans. R. Soc. B Biol. Sci.* **370**, (2015).
 190. Ronchi, S. *et al.* Single-cell electrical stimulation using CMOS-based high-density microelectrode arrays. *Front. Neurosci.* **13**, (2019).
 191. Zemelman, B. V., Lee, G. A., Ng, M. & Miesenböck, G. Selective photostimulation of genetically chARGed neurons. *Neuron* **33**, 15–22 (2002).
 192. Banghart, M., Borges, K., Isacoff, E., Trauner, D. & Kramer, R. H. Light-activated ion channels for remote control of neuronal firing. *Nat. Neurosci.* **7**, 1381–1386 (2004).
 193. Qiu, X. *et al.* Induction of photosensitivity by heterologous expression of melanopsin. *Nature* **433**, 745–749 (2005).
 194. Zhang, F., Wang, L. P., Boyden, E. S. & Deisseroth, K. Channelrhodopsin-2 and optical control of excitable cells. *Nat. Methods* **3**, 785–792 (2006).
 195. Schobert, B. & Lanyi, J. K. Halorhodopsin is a light-driven chloride pump. *J. Biol. Chem.* **257**, 10306–10313 (1982).
 196. Nagel, G. *et al.* Channelrhodopsin-1: A light-gated proton channel in green algae. *Science* **296**, 2395–2398 (2002).
 197. Nagel, G. *et al.* Channelrhodopsin-2, a directly light-gated cation-selective membrane channel. *Proc. Natl. Acad. Sci.* **100**, 13940–13945 (2003).
 198. Müller, M., Bamann, C., Bamberg, E. & Kühlbrandt, W. Projection structure of channelrhodopsin-2 at 6 Å resolution by electron crystallography. *J. Mol. Biol.* **414**, 86–95 (2011).
 199. Boyden, E. S., Zhang, F., Bamberg, E., Nagel, G. & Deisseroth, K. Millisecond-timescale, genetically targeted optical control of neural activity. *Nat. Neurosci.* **8**, 1263–1268 (2005).
 200. Nagel, G. *et al.* Light activation of Channelrhodopsin-2 in excitable cells of *Caenorhabditis elegans* triggers rapid behavioral responses. *Curr. Biol.* **15**, 2279–2284 (2005).
 201. Li, X. *et al.* Fast noninvasive activation and inhibition of neural and network activity by vertebrate rhodopsin and green algae channelrhodopsin. *Proc. Natl. Acad. Sci.* **102**, 17816–17821 (2005).
 202. Bi, A. *et al.* Ectopic expression of a microbial-type Rhodopsin restores visual responses in mice with photoreceptor degeneration. *Neuron* **50**, 23–33 (2006).
 203. Douglass, A. D., Kraves, S., Deisseroth, K., Schier, A. F. & Englert, F. Report escape behavior elicited by single Channelrhodopsin-2-evoked spikes in zebrafish somatosensory neurons. *Curr. Biol.* **18**, 1133–1137 (2008).
 204. Klapoetke, N. C. *et al.* Independent optical excitation of distinct neural populations. *Nat. Methods* **11**, 338–346 (2014).
 205. Schild, L. C. & Glauser, D. A. Dual color neural activation and behavior control with Chrimson and CoChR in *Caenorhabditis elegans*. *Genetics* **200**, 1029–1034 (2015).
 206. Berndt, A., Yizhar, O., Gunaydin, L. A., Hegemann, P. & Deisseroth, K. Bi-stable neural state switches. *Nat. Neurosci.* **12**, 229–234 (2009).
 207. Schultheis, C., Liewald, J. F., Bamberg, E., Nagel, G. & Gottschalk, A. Optogenetic long-term manipulation of behavior and animal development. *PLoS One* **6**, e18766 (2011).
 208. Kolbe, M., Besir, H., Essen, L. O. & Oesterhelt, D. Structure of the light-driven chloride pump halorhodopsin at 1.8 Å Resolution. *Science* **288**, 1390–1396 (2000).
 209. Chow, B. Y. *et al.* High-performance genetically targetable optical neural silencing by light-driven proton pumps. *Nature* **463**, 98–102 (2010).
 210. Govorunova, E. G., Sineshchekov, O. A., Janz, R., Liu, X. & Spudich, J. L. Natural light-gated anion channels: A family of microbial rhodopsins for advanced optogenetics. *Science* **349**, 647 LP – 650 (2015).
 211. Mohammad, F. *et al.* Optogenetic inhibition of behavior with anion channelrhodopsins. *Nat. Methods* **14**, 271–274 (2017).
 212. Tolstenkov, O. *et al.* Functionally asymmetric motor neurons contribute to coordinating locomotion of *Caenorhabditis elegans*. *ELife* **7**, 1–28 (2018).
 213. Zhang, F. *et al.* Multimodal fast optical interrogation of neural circuitry. *Nature* **446**, 633–639 (2007).
 214. Bergs, A. *et al.* Rhodopsin optogenetic toolbox v2.0 for light-sensitive excitation and inhibition in *Caenorhabditis elegans*. *PLoS One* **13**, 1–24 (2018).
 215. Fenno, L., Yizhar, O. & Deisseroth, K. The development and application of optogenetics. *Annu. Rev. Neurosci.* **34**, 389–412 (2011).
 216. Tischer, D. & Weiner, O. D. Illuminating cell signalling with optogenetic tools. *Nat. Rev. Mol. Cell Biol.* **15**, 551–558 (2014).
 217. Kwon, E. & Heo, W. Do. Optogenetic tools for dissecting complex intracellular signaling pathways. *Biochem. Biophys. Res. Commun.* (2020). doi:10.1016/j.bbrc.2019.12.132
 218. Yamada, M., Nagasaki, S. C., Ozawa, T. & Imayoshi, I. Light-mediated control of gene expression in mammalian cells. *Neurosci. Res.* **152**, 66–77 (2020).
 219. Airan, R. D., Thompson, K. R., Fenno, L. E., Bernstein, H. & Deisseroth, K. Temporally precise *in vivo* control of intracellular signalling. *Nature* **458**, 1025–1029 (2009).
 220. Eickelbeck, D. *et al.* Lamprey Parapainopsin (“UVLamp”): a bistable UV-sensitive optogenetic switch for ultrafast control of GPCR Pathways. *ChemBioChem* **21**, 612–617 (2020).

221. Schröder-Lang, S. *et al.* Fast manipulation of cellular cAMP level by light in vivo. *Nat. Methods* **4**, 39–42 (2007).
222. Steuer Costa, W., Yu, S. chieh, Liewald, J. F. & Gottschalk, A. Fast cAMP Modulation of Neurotransmission via Neuropeptide Signals and Vesicle Loading. *Curr. Biol.* **27**, 495–507 (2017).
223. Gao, S. *et al.* Optogenetic manipulation of cGMP in cells and animals by the tightly light-regulated guanylyl-cyclase opsin CyclOp. *Nat. Commun.* **6**, 1–12 (2015).
224. Stirman, J. N. *et al.* Real-time multimodal optical control of neurons and muscles in freely behaving *Caenorhabditis elegans*. *Nat. Methods* **8**, 153–158 (2011).
225. Guo, Z. V., Hart, A. C. & Ramanathan, S. Optical interrogation of neural circuits in *Caenorhabditis elegans*. *Nat. Methods* **6**, 891–896 (2009).
226. Husson, S. J., Gottschalk, A. & Leifer, A. M. Optogenetic manipulation of neural activity in *C. elegans*: From synapse to circuits and behaviour. *Biol. Cell* **105**, 235–250 (2013).
227. Kim, H. K., Alexander, A. L. & Soltesz, I. Optogenetics: Lighting a path from the laboratory to the clinic. in *Optogenetics: A Roadmap* (ed. Stroh, A.) 277–300 (Springer New York, 2018). doi:10.1007/978-1-4939-7417-7_14
228. Watteyne, J. *et al.* Neuromedin U signaling regulates retrieval of circuit of learned salt avoidance in a *C. elegans* gustatory circuit. *Nature Communications*, **11**, 2076 (2020).
229. Van der Auwera, P. *et al.* RPamide neuropeptides NLP-22 and NLP-2 act through GnRH-like receptors to promote sleep and wakefulness in *C. elegans*. *Sci. Rep.* **10**, 9929 (2020).
230. Kingsford, M. J. *et al.* Sensory environments, larval abilities and local self-recruitment. *Bulletin of Marine Science* **70**, 309–340 (2002).
231. Cresci, A. *et al.* The relationship between the moon cycle and the orientation of glass eels (*Anguilla anguilla*) at sea. *R. Soc. Open Sci.* **6**, (2019).
232. Gray, J. The movement of fish with special reference to the eel. *J. Exp. Biol.* **10**, 88–104 (1933).
233. Dickinson, M. H. *et al.* How animals move: An integrative view. *Science* **288**, 100–106 (2000).
234. Guzman, H. M., Gomez, C. G., Hearn, A. & Eckert, S. A. Longest recorded trans-Pacific migration of a whale shark (*Rhincodon typus*). *Mar. Biodivers. Rec.* **11**, 4–9 (2018).
235. Reppert, S. M. & de Roode, J. C. Demystifying monarch butterfly migration. *Curr. Biol.* **28**, R1009–R1022 (2018).
236. Lankester, E. R. XXXV.—On the primitive cell-layers of the embryo as the basis of genealogical classification of animals, and on the origin of vascular and lymph systems. *J. Nat. Hist.* **11**, 321–338 (1873).
237. Brunet, T. *et al.* The evolutionary origin of bilaterian smooth and striated myocytes. *ELife* **5**, 1–24 (2016).
238. Dos Reis, M. *et al.* Uncertainty in the timing of origin of animals and the limits of precision in molecular timescales. *Curr. Biol.* **25**, 2939–2950 (2015).
239. Peters, M. A., Teramoto, T., White, J. Q., Iwasaki, K. & Jorgensen, E. M. A calcium wave mediated by gap junctions coordinates a rhythmic behavior in *C. elegans*. *Curr. Biol.* **17**, 1601–1608 (2007).
240. Gemmell, B. J., Troolin, D. R., Costello, J. H., Colin, S. P. & Satterlie, R. A. Control of vortex rings for manoeuvrability. *J. R. Soc. Interface* **12**, (2015).
241. Jordano, M. de A., Morandini, A. C. & Nagata, R. M. Is phenotypic plasticity determined by temperature and fluid regime in filter-feeding gelatinous organisms? *J. Exp. Mar. Bio. Ecol.* **522**, (2020).
242. Wang, W. *et al.* Kinematics of gecko climbing: the lateral undulation pattern. *Zoology* **140**, 125768 (2020).
243. Bode-Oke, A. T., Zeyghami, S. & Dong, H. Flying in reverse: Kinematics and aerodynamics of a dragonfly in backward free flight. *J. R. Soc. Interface* **15**, (2018).
244. Sapir, N. & Dudley, R. Backward flight in hummingbirds employs unique kinematic adjustments and entails low metabolic cost. *J. Exp. Biol.* **215**, 3603–3611 (2012).
245. Gray, J. & Lissmann, H. W. The locomotion of Nematodes. *J. Exp. Biol.* **41**, 135–154 (1964).
246. Shen, X. N., Sznitman, J., Krajacic, P., Lamitina, T. & Arratia, P. E. Undulatory locomotion of *Caenorhabditis elegans* on wet surfaces. *Biophys. J.* **102**, 2772–2781 (2012).
247. Gillis, G. B. Undulatory locomotion in elongate aquatic vertebrates: anguilliform swimming since sir james gray. *Am. Zool.* **36**, 656–665 (1996).
248. Butler, V. J. *et al.* A consistent muscle activation strategy underlies crawling and swimming in *Caenorhabditis elegans*. *J. R. Soc. Interface* **12**, (2015).
249. Jayne, B. C. Muscular mechanisms of snake locomotion: An electromyographic study of lateral undulation of the florida banded water snake (*Nerodia fasciata*) and the yellow rat snake (*Elaphe obsoleta*). *J. Morphol.* **197**, 159–181 (1988).
250. Kusakabe, R. & Kuratani, S. Evolution and developmental patterning of the vertebrate skeletal muscles: Perspectives from the lamprey. *Dev. Dyn.* **234**, 824–834 (2005).
251. Stokes, M. D. Larval locomotion of the lancelet *Branchiostoma floridae*. *J. Exp. Biol.* **200**, 1661–1680 (1997).
252. Bergmann, P. J., Mann, S. D. W., Morinaga, G., Freitas, E. S. & Siler, C. D. Convergent evolution of elongate forms in Craniates and of locomotion in elongate Squamate reptiles. *Integr. Comp. Biol.* icaa015 (2020). doi:10.1093/icb/icaa015
253. Katz, P. S. Evolution of central pattern generators and rhythmic behaviours. *Philos. Trans. R. Soc. B Biol. Sci.* **371**, (2016).
254. Dasen, J. S. Evolution of Locomotor Rhythms. *Trends Neurosci.* **41**, 648–651 (2018).
255. Machado, T. A., Pnevmatikakis, E., Paninski, L., Jessell, T. M. & Miri, A. Primacy of flexor locomotor pattern revealed by ancestral reversion of motor neuron identity. *Cell* **162**, 338–350 (2015).
256. Jung, H. *et al.* The ancient origins of neural substrates for land walking. *Cell* **172**, 667–682.e15 (2018).
257. Buchanan, J. T. & Grillner, S. Newly identified 'glutamate interneurons' and their role in locomotion in the lamprey spinal cord. *Science* **236**, 312 LP – 314 (1987).
258. Kiehn, O. Development and functional organization of spinal locomotor circuits. *Curr. Opin. Neurobiol.* **21**, 100–109 (2011).

259. Grillner, S. & El Manira, A. Current principles of motor control, with special reference to vertebrate locomotion. *Physiol. Rev.* **100**, 271–320 (2020).
260. Marder, E. & Calabrese, R. L. Principles of rhythmic motor pattern generation. *Physiol. Rev.* **76**, 687–717 (1996).
261. Marder, E., Bucher, D., Schulz, D. J. & Taylor, A. L. Invertebrate central pattern generation moves along. *Curr. Biol.* **15**, 685–699 (2005).
262. Berkowitz, A. Expanding our horizons: Central pattern generation in the context of complex activity sequences. *J. Exp. Biol.* **222**, (2019).
263. Grätsch, S., Büschges, A. & Dubuc, R. Descending control of locomotor circuits. *Curr. Opin. Physiol.* **8**, 94–98 (2019).
264. Bringmann, H. Sleep-active neurons: Conserved motors of sleep. *Genetics* **208**, 1279–1289 (2018).
265. Ewer, J. & Reynolds, S. Neuropeptide control of molting in insects. in *Hormones, Brain and Behavior* (eds. Pfaff, D. W., Arnold, A. P., Fahrbach, S. E., Etgen, A. M. & Rubin Brain and Behavior, R. T. B. T.-H.) 1–92 (Academic Press, 2002). doi:<https://doi.org/10.1016/B978-012532104-4/50037-8>
266. Fendt, M. & Fanselow, M. S. The neuroanatomical and neurochemical basis of conditioned fear. *Neurosci. Biobehav. Rev.* **23**, 743–760 (1999).
267. Liu, X. *et al.* Optogenetic stimulation of a hippocampal engram activates fear memory recall. *Nature* **484**, 381–385 (2012).
268. Bezares-Calderón, L. A. *et al.* Neural circuitry of a polycystin-mediated hydrodynamic startle response for predator avoidance. *ELife* **7**, 1–28 (2018).
269. Xu, T. *et al.* Descending pathway facilitates undulatory wave propagation in *Caenorhabditis elegans* through gap junctions. *Proc. Natl. Acad. Sci. U. S. A.* **115**, E4493–E4502 (2018).
270. Wen, Q. *et al.* Proprioceptive coupling within motor neurons drives *C. elegans* forward locomotion. *Neuron* **76**, 750–761 (2012).
271. Cohen, N. & Denham, J. E. Whole animal modeling: piecing together nematode locomotion. *Curr. Opin. Syst. Biol.* **13**, 150–160 (2019).
272. Kaplan, H. S., Salazar Thula, O., Khoss, N. & Zimmer, M. Nested neuronal dynamics orchestrate a behavioral hierarchy across timescales. *Neuron* **105**, 562–576.e9 (2020).
273. Kaplan, H. S., Nichols, A. L. A. & Zimmer, M. Sensorimotor integration in *Caenorhabditis elegans*: A reappraisal towards dynamic and distributed computations. *Philos. Trans. R. Soc. B Biol. Sci.* **373**, (2018).
274. Roberts, William M., *et al.* A stochastic neuronal model predicts random search behaviors at multiple spatial scales in *C. elegans*. *Elife* **5**, e12572 (2016) DOI: 10.7554/eLife.12572.
275. Bouvier, J. *et al.* Descending command neurons in the brainstem that halt locomotion. *Cell* **163**, 1191–1203 (2015).
276. Kim, L. H. *et al.* Integration of descending command systems for the generation of context-specific locomotor behaviors. *Front. Neurosci.* **11**, 1–19 (2017).
277. Aulsebrook, A. E., Jones, T. M., Rattenborg, N. C., Roth, T. C. & Lesku, J. A. Sleep ecophysiology: Integrating neuroscience and ecology. *Trends Ecol. Evol.* **31**, 590–599 (2016).
278. Drew, K. L. *et al.* Central nervous system regulation of mammalian hibernation: Implications for metabolic suppression and ischemia tolerance. *J. Neurochem.* **102**, 1713–1726 (2007).
279. Hahn, D. A. & Denlinger, D. L. Energetics of insect diapause. *Annu. Rev. Entomol.* **56**, 103–121 (2011).
280. Fadok, J. P. *et al.* A competitive inhibitory circuit for selection of active and passive fear responses. *Nature* **542**, 96–99 (2017).
281. Lesku, J. A. & Ly, L. M. T. Sleep origins: Restful jellyfish are sleeping jellyfish. *Curr. Biol.* **27**, R1060–R1062 (2017).
282. Anafi, R. C., Kayser, M. S. & Raizen, D. M. Exploring phylogeny to find the function of sleep. *Nat. Rev. Neurosci.* **20**, 109–116 (2019).
283. Juvin, L. *et al.* A specific population of reticulospinal neurons controls the termination of locomotion. *Cell Rep.* **15**, 2377–2386 (2016).
284. Schwenkgrub, J., Harrell, E. R., Bathellier, B. & Bouvier, J. Deep imaging in the brainstem reveals functional heterogeneity in V2a neurons controlling locomotion. *Sci. Adv.* **6**, eabc6309 (2020).
285. Capelli, P., Pivetta, C., Esposito, M. S. & Arber, S. Locomotor speed control circuits in the caudal brainstem. *Nature* **551**, 373–377 (2017).
286. Grätsch, S. *et al.* A brainstem neural substrate for stopping locomotion. *J. Neurosci.* **39**, 1044–1057 (2019).
287. Roseberry, T. K. *et al.* Cell-type-specific control of brainstem locomotor circuits by basal ganglia. *Cell* **164**, 526–537 (2016).
288. Luppi, P. H. *et al.* The neuronal network responsible for paradoxical sleep and its dysfunctions causing narcolepsy and rapid eye movement (REM) behavior disorder. *Sleep Med. Rev.* **15**, 153–163 (2011).
289. Kayser, M. S. & Biron, D. Sleep and development in genetically tractable model organisms. *Genetics* **203**, 21–33 (2016).
290. Tastekin, I. *et al.* Sensorimotor pathway controlling stopping behavior during chemotaxis in the drosophila melanogaster larva. *ELife* **7**, 1–38 (2018).
291. Katz, M., Corson, F., Iwanir, S., Biron, D. & Shaham, S. Glia modulate a neuronal circuit for locomotion suppression during sleep in *C. elegans*. *Cell Rep.* **22**, 2601–2614 (2018).
292. Nelson, M. D. *et al.* FMRFamide-like FLP-13 neuropeptides promote quiescence following heat stress in *Caenorhabditis elegans*. *Curr. Biol.* **24**, 2406–2410 (2014).
293. Fry, A. L., Laboy, J. T. & Norman, K. R. VAV-1 acts in a single interneuron to inhibit motor circuit activity in *Caenorhabditis elegans*. *Nat. Commun.* **5**, 1–13 (2014).
294. Shaw, P. J., Cirelli, C., Greenspan, R. J. & Tononi, G. Correlates of sleep and waking in *Drosophila melanogaster*. *Science* **287**, 1834–1837 (2000).

295. Trojanowski, N. F. & Raizen, D. M. Call it worm sleep. *Trends Neurosci.* **39**, 54–62 (2016).
296. Rasch, B. & Born, J. About sleep's role in memory. *Physiol. Rev.* **93**, 681–766 (2013).
297. Ray, S. & Reddy, A. B. Cross-talk between circadian clocks, sleep-wake cycles, and metabolic networks: Dispelling the darkness. *BioEssays* **38**, 394–405 (2016).
298. Blum, I. D., Bell, B. & Wu, M. N. Time for Bed : Genetic mechanisms mediating the circadian regulation of sleep. *Trends Genet.* **34**, 379–388 (2018).
299. Saper, C. B., Fuller, P. M., Pedersen, N. P., Lu, J. & Scammell, T. E. Sleep state switching. *Neuron* **68**, 1023–1042 (2010).
300. Liu, D. & Dan, Y. A motor theory of sleep-wake control: arousal-action circuit. *Annu. Rev. Neurosci.* **42**, 27–46 (2019).
301. Cirelli, C. & Tononi, G. Is sleep essential? *PLoS Biol.* **6**, e216 (2008).
302. Xie, L. *et al.* Sleep drives metabolite clearance from adult brain. *Science* **342**, 373–377 (2013).
303. Tononi, G. & Cirelli, C. Sleep and the price of plasticity: from synaptic and cellular homeostasis to memory consolidation and integration. *Neuron* **81**, 12–34 (2014).
304. Freiberg, A. S. Why we sleep: A hypothesis for an ultimate or evolutionary origin for sleep and other physiological rhythms. *J. Circadian Rhythms* **18**, 1–5 (2020).
305. Hauglund, N. L., Pavan, C. & Nedergaard, M. Cleaning the sleeping brain – the potential restorative function of the glymphatic system. *Curr. Opin. Physiol.* **15**, 1–6 (2020).
306. Richter, C., Woods, I. G. & Schier, A. F. Neuropeptidergic control of sleep and wakefulness. *Annu. Rev. Neurosci.* **37**, 503–531 (2014).
307. Lüthi, A. Sleep: The very long posited (VLPO) synaptic pathways of arousal. *Curr. Biol.* **29**, R1310–R1312 (2019).
308. Lu, J., Sherman, D., Devor, M. & Saper, C. B. A putative flip-flop switch for control of REM sleep. *Nature* **441**, 589–594 (2006).
309. Dauvilliers, Y. *et al.* REM sleep behaviour disorder. *Nat. Rev. Dis. Prim.* **4**, (2018).
310. Luppi, P. H. *et al.* Brainstem mechanisms of paradoxical (REM) sleep generation. *Pflugers Arch. J. Physiol.* **463**, 43–52 (2012).
311. Limousin, N. *et al.* A brainstem inflammatory lesion causing REM sleep behavior disorder and sleepwalking (parasomnia overlap disorder). *Sleep Med.* **10**, 1059–1062 (2009).
312. Mahoney, C. E., Cogswell, A., Korálnik, I. J. & Scammell, T. E. The neurobiological basis of narcolepsy. *Nat. Rev. Neurosci.* **20**, 83–93 (2019).
313. Sapin, E. *et al.* Localization of the brainstem GABAergic neurons controlling paradoxical (REM) sleep. *PLoS One* **4**, (2009).
314. Sirieix, C., Gervasoni, D., Luppi, P. H. & Léger, L. Role of the lateral paragigantocellular nucleus in the network of paradoxical (REM) sleep: An electrophysiological and anatomical study in the rat. *PLoS One* **7**, (2012).
315. Brownstone, R. M. & Chopek, J. W. Reticulospinal systems for tuning motor commands. *Front. Neural Circuits* **12**, 30 (2018).
316. Brooks, P. L. & Peever, J. H. Identification of the transmitter and receptor mechanisms responsible for REM sleep paralysis. *J. Neurosci.* **32**, 9785–9795 (2012).
317. Liang, H., Watson, C. & Paxinos, G. Terminations of reticulospinal fibers originating from the gigantocellular reticular formation in the mouse spinal cord. *Brain Struct. Funct.* **221**, 1623–1633 (2016).
318. Valencia Garcia, S. *et al.* Ventromedial medulla inhibitory neuron inactivation induces REM sleep without atonia and REM sleep behavior disorder. *Nat. Commun.* **9**, 1–11 (2018).
319. Turek, M., Lewandrowski, I. & Bringmann, H. An AP2 transcription factor is required for a sleep-active neuron to induce sleep-like quiescence in *C. elegans*. *Curr. Biol.* **23**, 2215–2223 (2013).
320. Turek, M., Besseling, J., Spies, J. P., König, S. & Bringmann, H. Sleep-active neuron specification and sleep induction require FLP-11 neuropeptides to systemically induce sleep. *eLife* **5**, e12499 (2016).
321. Nelson, M. D. *et al.* The neuropeptide NLP-22 regulates a sleep-like state in *Caenorhabditis elegans*. *Nat. Commun.* **4**, 2846 (2013).
322. Van Buskirk, C. & Sternberg, P. W. Epidermal growth factor signaling induces behavioral quiescence in *Caenorhabditis elegans*. *Nat. Neurosci.* **10**, 1300–1307 (2007).
323. Van Buskirk, C. & Sternberg, P. W. Paired and LIM class homeodomain proteins coordinate differentiation of the *C. elegans* ALA neuron. *Development* **137**, 2065–2074 (2010).
324. Hill, A. J., Mansfield, R., Lopez, J. M. N. G., Raizen, D. M. & Van Buskirk, C. Cellular stress induces a protective sleep-like state in *C. elegans*. *Curr. Biol.* **24**, 2399–2405 (2014).
325. Nath, R. D., Chow, E. S., Wang, H., Schwarz, E. M. & Sternberg, P. W. *C. elegans* stress-induced sleep emerges from the collective action of multiple neuropeptides. *Curr. Biol.* **26**, 2446–2455 (2016).
326. Goetting, D. L., Soto, R. & Buskirk, C. Van. Food-dependent plasticity in *Caenorhabditis elegans* stress-induced sleep is mediated by TOR – FOXA and TGF- β signaling. *Genetics* **209**, 1183–1195 (2018).
327. Nichols, A. L. A., Eichler, T., Latham, R. & Zimmer, M. A global brain state underlies *C. elegans* sleep behavior. *Science* **356**, 1277–1279 (2017).
328. Skora, S., Mende, F. & Zimmer, M. Energy scarcity promotes a brain-wide sleep state modulated by insulin signaling in *C. elegans*. *Cell Rep.* **22**, 953–966 (2018).
329. Helfrich-Förster, C. Sleep in insects. *Annu. Rev. Entomol.* **63**, 69–86 (2018).
330. Nässel, D. R. & Zandawala, M. Recent advances in neuropeptide signaling in *Drosophila*, from genes to physiology and behavior. *Prog. Neurobiol.* **179**, 101607 (2019).
331. Burbach, J. P. H. What are neuropeptides? in *Neuropeptides. Methods in Molecular Biology (Methods and Protocols)*, vol 789. (ed. Merighi, A.) 1–36 (Humana Press, 2011). doi:10.1007/978-1-61779-310-3_1
332. van den Pol, A. N. Neuropeptide transmission in brain circuits. *Neuron* **76**, 98–115 (2012).

333. Frooninckx, L. *et al.* Neuropeptide GPCRs in *C. elegans*. *Front. Endocrinol. (Lausanne)*. **3**, 1–19 (2012).
334. Jékely, G. Global view of the evolution and diversity of metazoan neuropeptide signaling. *Proc. Natl. Acad. Sci.* **110**, 8702–8707 (2013).
335. Mirabeau, O. & Joly, J. Molecular evolution of peptidergic signaling systems in bilaterians. *Proc. Natl. Acad. Sci.* **110**, 2028–2037 (2013).
336. Elphick, M. R., Mirabeau, O. & Larhammar, D. Evolution of neuropeptide signalling systems. *J. Exp. Biol.* **221**, jeb193342 (2018).
337. Van Bael, S. *et al.* Mass spectrometric evidence for neuropeptide-amidating enzymes in *C. elegans*. *J. Biol. Chem.* jbc.RA117.000731 (2018). doi:10.1074/jbc.RA117.000731
338. Schoofs, L., De Loof, A. & Van Hiel, M. B. Neuropeptides as regulators of behavior in insects. *Annu. Rev. Entomol.* **62**, 35–52 (2017).
339. Li, C. & Kim, K. Neuropeptides. *WormBook* 1–36 (2008). doi:10.1895/wormbook.1.142.1
340. Peymen, K., Watteyne, J., Frooninckx, L., Schoofs, L. & Beets, I. The FMRFamide-like peptide family in nematodes. *Front. Endocrinol. (Lausanne)*. **5**, (2014).
341. Suchecki, D. & Elias, C. F. Neuropeptides and behavior: From motivation to psychopathology. *Frontiers in Endocrinology* **8**, 210 (2017).
342. Zhang, L., Vaudry, D., Brown, C. H. & Eiden, L. E. Regulatory peptides in neuroscience and endocrinology: A new era begins. in *Frontiers in Endocrinology* **10**, 793 (2019).
343. Rosenbaum, D. M., Rasmussen, S. G. F. & Kobilka, B. K. The structure and function of G-protein-coupled receptors. *Nature* **459**, 356–363 (2009).
344. de Mendoza, A., Sebé-Pedrós, A. & Ruiz-Trillo, I. The evolution of the GPCR signaling system in eukaryotes: Modularity, conservation, and the transition to metazoan multicellularity. *Genome Biol. Evol.* **6**, 606–619 (2014).
345. Palczewski, K. G Protein–Coupled Receptor Rhodopsin. *Annu. Rev. Biochem.* **75**, 743–767 (2006).
346. Xu, J. *et al.* GPR68 senses flow and is essential for vascular physiology. *Cell* **173**, 762–775.e16 (2018).
347. Ritter, S. L. & Hall, R. A. Fine-tuning of GPCR activity by receptor-interacting proteins. *Nat. Rev. Mol. Cell Biol.* **10**, 819–830 (2009).
348. Janssen, T., Lindemans, M., Meelkop, E., Temmerman, L. & Schoofs, L. Coevolution of neuropeptidergic signaling systems: from worm to man. *Ann. N. Y. Acad. Sci.* **1200**, 1–14 (2010).
349. Arendt, D. The evolution of cell types in animals: emerging principles from molecular studies. *Nat. Rev. Genet.* **9**, 868–882 (2008).
350. Schoofs, L. & Beets, I. Neuropeptides control life-phase transitions. *Proc. Natl. Acad. Sci.* **110**, 7973–7974 (2013).
351. Borbély, É., Scheich, B. & Helyes, Z. Neuropeptides in learning and memory. *Neuropeptides* **47**, 439–450 (2013).
352. Marder, E., O’Leary, T. & Shruti, S. Neuromodulation of circuits with variable parameters: single neurons and small circuits reveal principles of state-dependent and robust neuromodulation. *Annu. Rev. Neurosci.* **37**, 329–346 (2014).
353. Zhen, M. & Samuel, A. D. T. *C. elegans* locomotion: Small circuits, complex functions. *Curr. Opin. Neurobiol.* **33**, 117–126 (2015).
354. Lim, M. A. *et al.* Neuroendocrine modulation sustains the *C. elegans* forward motor state. *ELife* **5**, 1–33 (2016).
355. Hums, I. *et al.* Regulation of two motor patterns enables the gradual adjustment of locomotion strategy in *Caenorhabditis elegans*. *ELife* **5**, e14116 (2016).
356. Chew, Y. L., Grundy, L. J., Brown, A. E. X., Beets, I. & Schafer, W. R. Neuropeptides encoded by *nlp-49* modulate locomotion, arousal and egg-laying behaviours in *Caenorhabditis elegans* via the receptor SEB-3. *Philos. Trans. R. Soc. B Biol. Sci.* **373**, 20170368 (2018).
357. Oranath, A. *et al.* Food sensation modulates locomotion by dopamine and neuropeptide signaling in a distributed neuronal network. *Neuron* **100**, 1414–1428.e10 (2018).
358. Hauser, A. S., Attwood, M. M., Rask-Andersen, M., Schiöth, H. B. & Gloriam, D. E. Trends in GPCR drug discovery: New agents, targets and indications. *Nat. Rev. Drug Discov.* **16**, 829–842 (2017).
359. Ramachandran, S. *et al.* A conserved neuropeptide system links head and body motor circuits to enable adaptive behavior. *bioRxiv* 2020.04.27.064550 (2020). doi:10.1101/2020.04.27.064550
360. Nelson, M. D. *et al.* FRPR-4 is a G-protein coupled neuropeptide receptor that regulates behavioral quiescence and posture in *Caenorhabditis elegans*. *PLoS One* **10**, 1–19 (2015).
361. Tao, L. *et al.* Parallel processing of two mechanosensory modalities by a single neuron in *C. elegans*. *Dev. Cell* **51**, 617–631.e3 (2019).
362. Iannaccone, M. J. *et al.* The RFamide receptor DMSR-1 regulates stress-induced sleep in *C. elegans*. *ELife* **6**, 1–20 (2017).
363. Cianciulli, A. *et al.* Interneurons regulate locomotion quiescence via cyclic adenosine monophosphate signaling during stress-induced sleep in *Caenorhabditis elegans*. *Genetics* **213**, 267–279 (2019).
364. Choi, S., Chatzigeorgiou, M., Taylor, K. P., Schafer, W. R. & Kaplan, J. M. Analysis of NPR-1 reveals a circuit mechanism for behavioral quiescence in *C. elegans*. *Neuron* **78**, 869–880 (2013).
365. Soto, R., Goetting, D. L. & Van Buskirk, C. NPR-1 modulates plasticity in *C. elegans* stress-induced sleep. *iScience* **19**, 1037–1047 (2019).
366. Yew, J. Y. *et al.* Peptide products of the *afp-6* gene of the nematode *Ascaris suum* have different biological actions. *J. Comp. Neurol.* **502**, 872–882 (2007).
367. Konop, C. J. *et al.* Mass spectrometry of single GABAergic somatic motoneurons identifies a novel inhibitory peptide, As-NLP-22, in the Nematode *Ascaris suum*. *J. Am. Soc. Mass Spectrom.* **26**, 2009–2023 (2015).
368. Shang, Y. *et al.* Short neuropeptide F is a sleep-promoting inhibitory modulator. *Neuron* **80**, 171–183 (2013).
369. Lenz, O., Xiong, J., Nelson, M. D., Raizen, D. M. & Williams, J. A. FMRFamide signaling promotes stress-

- induced sleep in *Drosophila*. *Brain. Behav. Immun.* **47**, 141–148 (2015).
370. Lee, D. A. *et al.* Genetic and neuronal regulation of sleep by neuropeptide VF. *ELife* **6**, e25727 (2017).

Chapter 2:

A GABAergic and peptidergic sleep neuron also functions as a locomotion stop neuron with compartmentalized Ca²⁺ dynamics

The content of this chapter was published in the open access, scientifically peer-reviewed journal *Nature Communications*:

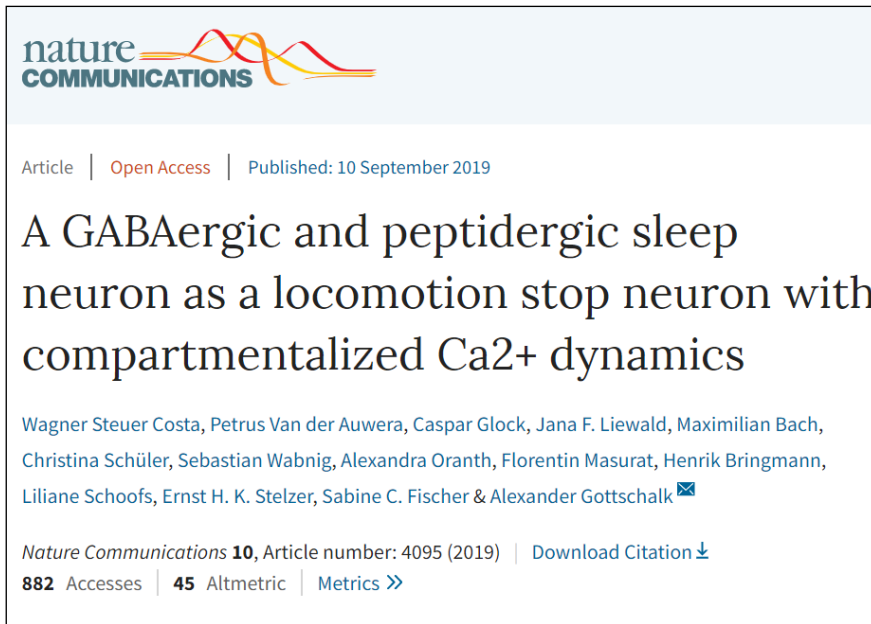
Wagner Steuer Costa^{1,2,10}, Petrus Van der Auwera^{1,2,5,10}, Caspar Glock^{1,2,6}, Jana F. Liewald^{1,2}, Maximilian Bach^{1,2}, Christina Schüler^{1,2}, Sebastian Wabnig^{1,2,7}, Alexandra Oranth^{1,2}, Florentin Masurat³, Henrik Bringmann^{3,4}, Liliane Schoofs⁵, Ernst H. K. Stelzer^{1,8}, Sabine C. Fischer^{1,8,9}, Alexander Gottschalk^{1,2,11} (2019) A GABAergic and peptidergic sleep neuron as a locomotion stop neuron with compartmentalized Ca²⁺ dynamics. *Nature Communications*, 10, 4095. <https://doi.org/10.1038/s41467-019-12098-5>

General author contributions

Conceptualization: WSC, PVdA, CG, SCF, AG; Data curation, analysis and visualization: WSC, PVdA, CG, JFL, CS, MB, SW, AO, SCF, AG; Software: WSC, PVdA, SCF; Reagents: FM, HB; wrote the paper: WSC, PVdA, AG, with help from the other authors; Supervision, funding acquisition: LS, EHKS, AG.

Extended contribution statement of PVdA.

The introduction was written by WSC and AG with additions of PVdA. PVdA performed most of the experiments represented in Figures 4 to 7. He made the graphics in figure panel A of Fig. 4 as well as Fig. 8 and he made both Fig. 5 and Fig. 6 (except for panel 6I) as well as Supplementary Fig. 5 & 6. He mainly wrote Results sections 2.3.5 – 2.3.8 (together with WSC and with adjustments of AG). WSC, PVdA and AG contributed equally to the discussion and all proofread the full manuscript multiple times.



This is a RoMEO Green journal. <http://sherpa.ac.uk/romeo/search.php>

Author affiliations

¹ Buchmann Institute for Molecular Life Sciences (BMLS), Goethe University, Max-von-Laue-Strasse 15, D-60438 Frankfurt, Germany

² Institute for Biophysical Chemistry, Goethe University, Max-von-Laue-Strasse 9, D-60438 Frankfurt, Germany

³ Max Planck Institute for Biophysical Chemistry, Am Fassberg 11, 37077 Göttingen, Germany

⁴ Department of Biology, University of Marburg, Karl-von-Frisch-Strasse 8, D-35043 Marburg, Germany

⁵ Functional Genomics and Proteomics Group, Department of Biology, KU Leuven, Naamsestraat 59 - box 2465, 3000 Leuven, Belgium

⁶ present address: Max-Planck-Institute for Brain Research, Max-von-Laue-Strasse 4, D-60438 Frankfurt, Germany

⁷ present address: od green GmbH, Passauerstrasse 34, A-4780 Schärding am Inn, Austria

⁸ Institute of Cell Biology and Neuroscience, Goethe University, Max-von-Laue-Strasse 13, D-60439 Frankfurt, Germany

⁹ present address: Center for Computational and Theoretical Biology (CCTB), University of Würzburg, Campus Hubland Nord 32, D-97074 Würzburg, Germany

¹⁰ these authors contributed equally

¹¹ to whom correspondence should be addressed

The authors declare no competing interests.

“

2.1 Abstract

Animals must slow or halt locomotion to integrate sensory inputs or to change direction. In *Caenorhabditis elegans*, the GABAergic and peptidergic neuron RIS mediates developmentally timed quiescence. Here, we show RIS functions additionally as a locomotion stop neuron. RIS optogenetic stimulation caused acute and persistent inhibition of locomotion and pharyngeal pumping, phenotypes requiring FLP-11 neuropeptides and GABA. RIS photoactivation allows the animal to maintain its body posture by sustaining muscle tone, yet inactivating motor neuron oscillatory activity. During locomotion, RIS axonal Ca²⁺ signals revealed functional compartmentalization: Activity in the nerve ring process correlated with locomotion stop, while activity in a branch correlated with induced reversals. GABA was required to induce, and FLP-11 neuropeptides were required to sustain locomotion stop. RIS attenuates neuronal activity and inhibits movement, possibly enabling sensory integration and decision making, and exemplifies dual use of one cell across development in a compact nervous system.

2.2 Introduction

Animals actively stop locomotion, in order to await certain events, or to avoid potentially dangerous situations. In order to quickly resume locomotion after the stop, they must keep their muscle tone. This is in contrast to phases of behavioral quiescence, or sleep, where vertebrates typically lose their muscle tone and assume a relaxed body posture^{1,2}. In limbed animals, multi-layered neuronal systems control locomotion³. Central pattern generators (CPGs) in the spinal cord mediate 1) rhythm generation, usually by networks of excitatory neurons that oscillate and cause mutual inhibition via interneurons, and 2) pattern generation that regulates motor neurons (MNs), and thus muscle action, to orchestrate coordinated movements underlying locomotion. For left-right coordination during walking, inhibitory and excitatory commissural interneurons are required^{4,5}. Locomotion is triggered by excitatory signals descending from supraspinal regions of the mid- or hindbrain (in mammals⁶) or of the brain stem (in tadpoles⁷), which ‘call’ the spinal CPG networks into action. Recently, a class of interneurons in the murine brainstem was shown to induce a stop command for the pattern generation systems⁸. These V2a ‘stop’ neurons project to excitatory and inhibitory spinal cord neurons, inducing locomotion halt likely via inhibition of rhythm-generating neurons. The stop neurons do not reduce muscle tone, and do not inhibit MNs. Thus, the animal does not collapse, but rather can quickly resume locomotion.

Equivalents of these ‘stop neurons’ and systems for slowing were identified in non-limbed vertebrates^{9, 10}, and recently also in *Drosophila*¹¹, where descending interneurons induce locomotion stop during navigation of odorant gradients, while activity of other neurons causes slowing¹². However, molecular identities of stop cells are only partly known, and also different organisms appear to use different mechanisms and partly redundant circuitry to induce locomotion stop¹³. Thus it is unclear whether ‘stop’ systems evolved several times, or whether a primordial locomotion stop system diversified into the different systems present today in different organisms.

In the nematode *Caenorhabditis elegans* with its much smaller number of neurons, rhythm generation resides in the MNs. Ventral cord excitatory MNs coordinate the undulatory behavior for forward and backward locomotion (B- and A-class, respectively). They exhibit oscillatory activity patterns that are entrained by proprioceptive feedback as well as bi-directional coupling by premotor interneurons (PINs) in the ventral nerve cord^{14, 15, 16, 17}. In addition, the AS-class of asymmetric MNs exhibits oscillatory activity, interacts with PINs and contributes to propagation of the body wave¹⁸.

Activity of vertebrate stop neurons contrasts descending pathways that are active during sleep, which halt locomotion and affect muscle relaxation through inhibitory reticulospinal neurons¹⁹. Sleep also occurs in *C. elegans*: 1) Lethargus, also called developmentally timed sleep (DTS), occurring during larval molt transitions²⁰, and 2) stress-induced sleep (SIS), in response to cellular insults^{21, 22}. Both states are similar with a lack of locomotion and feeding, as well as increased arousal threshold. They are regulated by distinct neuropeptidergic pathways and neurons, i.e. NLP-8, FLP-24, FLP-13 (neuropeptide like protein, FMRFamide like peptide) neuropeptides and the ALA (anterior lateral A) neuron for SIS^{20, 23}, while the GABAergic and neuropeptidergic RIS (ring interneuron S) neuron, as well as NLP-22 neuropeptides, are required for DTS^{24, 25}. RIS photoactivation induced lethargus in larvae, independent of GABA, while FLP-11 neuropeptides were required for RIS-induced sleep, and their over-expression sufficed to cause lethargus²⁶. In *Ascaris*, FLP-11 was shown to be inhibitory to muscle cells²⁷. Also in other species, sleep and arousal are encoded by neuropeptidergic and biogenic amine neurotransmitters²⁸. In mammals, sleep is mainly regulated in the ventrolateral preoptic nucleus, where GABAergic and galanin-releasing neurons inhibit orexin/hypocretin releasing neurons during sleep, while these modulators are released during (and promote) wakefulness²⁹. Mutations in the orexin receptor or abnormal activity in the hypothalamic area may lead to narcolepsy or catalepsy³⁰. Orexin

homologues were found in insects (allatotropin), but not in *C. elegans*, where instead FLP-21 and NLP-49 neuropeptides as well as pigment dispersing factor mediate arousal^{31, 32, 33, 34}. Stop neurons were not identified in *C. elegans* to date.

Adult *C. elegans* show behavioral quiescence during satiety, starvation or recovery from stress, e.g. heat shock^{22, 23, 35}. These states are associated with the RIS and ALA neurons, but it is unclear whether RIS has function other than as a pure sleep neuron. In the compact *C. elegans* nervous system, neurons often multitask, thus RIS might be utilized for additional functions. *C. elegans* frequently interrupts its predominantly forward locomotion by brief reversals, then resumes forward locomotion with a change in direction. It is only partially understood which neurons orchestrate this pirouette behavior, and in which sequence they may act^{36, 37}. Forward locomotion slows down before the animal briefly stops, and this part of the pirouette could be actively controlled by neuronal activity³⁸. Thus, may the RIS neuron function like vertebrate stop neurons, i.e. inducing a brief locomotion stop while maintaining muscle tone, to enable directional changes? Furthermore, may functions of sleep and stop neurons have been combined in one cell in the compact worm nervous system, and could this thus represent an evolutionary ancient mechanism from which sleep and stop systems diversified into distinct systems?

We address this by (opto-)genetics and by imaging activity of RIS during locomotion. Genetic ablation of RIS reduces reversal- and stop-events. Specific RIS photoactivation induces a full locomotion stop and also affects other rhythmic behaviors like pharyngeal pumping. RIS stimulation is accompanied by sustained Ca^{2+} levels in body wall muscle (BWM) cells, and inhibition of oscillatory activity in MNs. RIS-dependent behavioral responses are largely blocked without neuropeptidergic transmission, while interfering with GABA transmission affects their kinetics, and eliminating gap junctions uncovers further functions of RIS within circuits coordinating forward/backward transitions. The major determinant of RIS effects in adults, just as in larval sleep, is the FLP-11 neuropeptide. RIS shows compartmentalized axonal Ca^{2+} transients. In the nerve ring process, the onset of these signals correlates with the onset of locomotion slowing, while in an axonal branch, they are correlated with the induction of reversals, and require FLP-11 signaling. Our work dissects the function of a *C. elegans* 'stop' neuron, providing new insights into the roles and circuits of such neurons. It may help to understand such neurons, identified only phenotypically¹², and emphasizes that stop cells may exist widely across locomotion systems.

2.3 Results

2.3.1 Single-cell specific expression and photoactivation of ChR2 in RIS induces locomotion stop

We achieved conditional expression of channelrhodopsin-2 (ChR2) and GFP in the single RIS neuron. Animals showed fluorescence in a single cell body located in the ventral ganglion, next to the pharyngeal posterior bulb, on the right side of the head. RIS has a single process extending anteriorly towards the nerve ring, with a short branch reaching into the ventral nerve cord, while the axonal process wraps around the isthmus of the pharynx (**Fig. 1A**). When animals expressing RIS::ChR2 were cultivated in presence of all-*trans* retinal (ATR) and illuminated with blue light, all locomotion behavior stopped: On average, velocity dropped by 80% within 4-5s ($\tau = 1.67\text{s}$; **Fig. 1B**; [Supplementary Movie 1](#)), but also quite immediate for individual animals, i.e. 1-2 s ([Supplementary Fig. 1A](#)). We analyzed the body posture of the animals, i.e. bending angles demarcated by three adjacent points along the body axis (**Fig. 1C**)³⁹. Forward locomotion (sinusoidal body wave propagating antero-posteriorly) stopped upon RIS photostimulation: During the 10 s light stimulation, bending angles were 'frozen', i.e. the body posture was maintained. This contrasts the stop in locomotion upon photostimulation of all GABAergic MNs⁴⁰, where animals resumed behavior after a few seconds of photostimulation, though being uncoordinated ([Supplementary Movie 2](#)). GABA neuron photostimulation causes overall body elongation by 4%⁴⁰. Also RIS photoactivation induced body elongation, however only ca. 2.5%, affecting only the anterior third, which elongated ca. 10% (**Fig. 1D**). Thus, RIS may inhibit neurons driving the undulations, with some anterior muscle relaxation. RIS photoactivation also attenuated responses to mechanical stimulation, where a harsh touch to the head region led mostly to short reversals smaller than one body length; conversely, after RIS photoactivation, almost all animals reacted with a long reversal (**Fig. 1E**). During DTS, mechanical stimulation was shown to activate RIS, likely to suppress wake behaviors⁴¹, thus RIS photoactivation might mimic this larval behavior inhibition. To ask whether RIS is sufficient or required for reversals and stops, we ablated it using cell-specific overexpression of the apoptosis inducer EGL-1 ('egg-laying defective'), with GFP as a marker²². Animals lacking RIS showed significantly fewer long reversals and stops than wild type (WT; **Fig. 1F**), demonstrating a requirement of RIS for these behaviors.

Last, rhythmic pumping of the pharynx, the muscular feeding organ, ceased during 30s RIS photoactivation, depending on light intensity ([Supplementary Fig. 1B](#)).

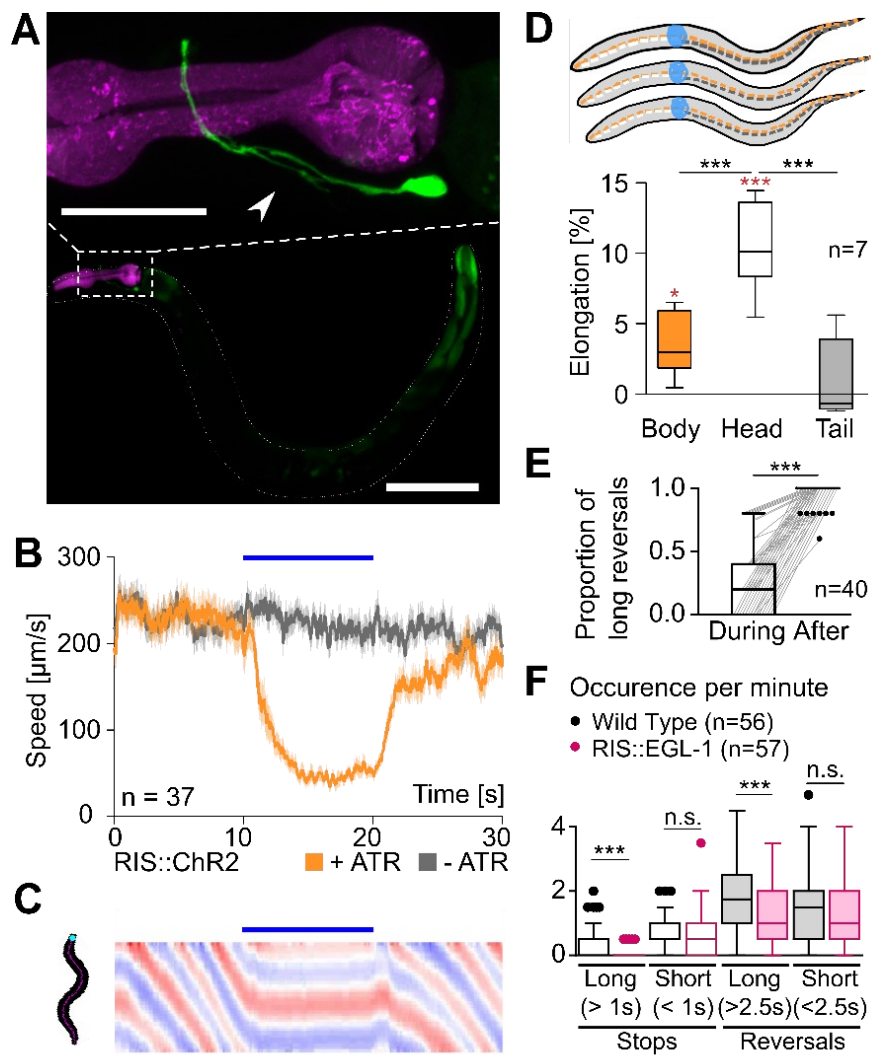


Figure 1: Photo-depolarization of the RIS neuron inhibits locomotion. **A**) Maximum intensity projection showing single-cell GFP expression in RIS. The pharynx expressing mCherry is shown in magenta. Scale bar = 100 μm . Inset: Enlarged head region. Arrowhead: RIS axonal branch region. Scale bar = 25 μm . **B**) Mean locomotion speed before, during and after RIS::ChR2 photoactivation (blue bar). Data: mean \pm SEM; n animals, cultivated with or without ATR, as indicated. **C**) Kymographic representation of bending angles along the spine of a single animal (top: head, bottom: tail, blue to red scale encodes the ventral to dorsal bending). Scale bar is 5 s, blue bar indicates illumination. **D**) Analysis of anterior or posterior body elongation during RIS photoactivation, demarcated by a dot painted on the body of the animal (pictogram: blue paint; dotted lines represent entire body (orange), head (white), or tail (grey) lengths along body mid line) in comparison to whole body analysis. Boxplot with Tukey whiskers; comparisons are to the no light condition (red asterisks) or between body regions (black asterisks). **E**) Fraction of reversals larger than one body length after mechanical stimulation to the head region during and after RIS photoactivation. Each animal was tested five times during both conditions (N=40). **F**) Frequency of long and short (shorter or longer than 1 s or 2.5 s, respectively) stops and reversals was compared in wild type animals, as well as in animals lacking RIS due to expression of the apoptosis inducer EGL-1. Boxplot with Tukey whiskers. n = number of animals. *** $p \leq 0.001$; ** $p \leq 0.01$; * $p \leq 0.05$; statistical significance tested by 1-way ANOVA with Tukey's Multiple Comparison test in (D) and Wilcoxon matched pairs test in (E), as well as by unpaired t-test in (F).

In electropharyngeograms, i.e. extracellular recordings of electrical activity associated with pharyngeal contractions⁴², RIS photostimulation generally evoked a complete absence of electrical transients, and on average significantly reduced the number of pump events ([Supplementary Fig. 1C, D](#)). Thus, RIS activation, presumably through GABA and

neuropeptide release, may inhibit pharyngeal pumping during locomotion reversals, in parallel to another established pathway for pumping inhibition using serotonin, the SER-2 receptor, and $G_{\alpha o}$ signaling³⁷.

2.3.2 RIS suppresses oscillatory activation of body wall muscle by affecting cholinergic neurons

To explore effects of RIS on the locomotion system, we used Ca^{2+} imaging. RCaMP1h, a red-fluorescent genetically encoded Ca^{2+} indicator⁴³, was specifically expressed in body wall muscles in addition to ChR2 in RIS, and animals were physically immobilized⁴⁴ (**Fig. 2A** and [Supplementary Movie 3](#)). Ca^{2+} signals were monitored over time, either in dorso-ventrally opposite regions (**Fig. 2A, B**), or in line scans along the animals' dorsal muscles, assessed as 'kymograms' spanning the body length (**Fig. 2A, C**). Despite absence of dynamic proprioceptive feedback, muscular Ca^{2+} levels visibly fluctuated along the body. Ca^{2+} levels were high in bent regions, in line with muscular activity underlying the body bend, and with the proprioceptive coupling of MNs in one body segment to the anterior segment⁴⁵. The Ca^{2+} signals oscillated at low frequency (ca. 0.12 Hz), in a dorso-ventrally reciprocal fashion (**Fig. 2B**). They could thus reflect rhythmic activity of the cholinergic MNs innervating the respective muscle cells. Oscillations were much slower than in free-moving animals (~0.36 Hz⁴⁶; note that further, due to immobilization, no traveling of the Ca^{2+} wave is observed). During RIS ChR2-activation, this oscillatory activity essentially stopped, while BWM Ca^{2+} levels did not obviously change (**Fig. 2C**; for $\Delta [Ca^{2+}]$ over time, see [Supplementary Movie 3B](#)). Since oscillations were asynchronous across animals, and to enable comparisons independent of actual signal intensities, we used sample auto-correlation, where the auto-correlation period reflects the extent of oscillatory activity (**Fig. 2D**). For animals grown without ATR, the period duration did not differ between the dark and lit periods, while it significantly increased with ATR present (**Fig. 2E**), indicating robust slowing of oscillations (since during 20 s stimulation often no full oscillations occurred, we assumed a 20s minimum of the period).

Next, we assessed these effects in body muscle, i.e., downstream of MNs, by electrophysiology. Miniature postsynaptic currents (mPSCs) report on release of neurotransmitter from single synaptic vesicles (**Fig. 3A**). If RIS photodepolarization reduced muscle activity by inhibiting MNs, we would expect reduced mPSC rates. However, RIS::ChR2 photoactivation neither abolished nor reduced mPSCs, their frequency or amplitude (**Fig. 3A-C**). This indicates that MNs did not reduce their activity during RIS

signaling and released the same amount of transmitter. Possibly they altered their relative activities, e.g. if the frequency of oscillation of the CPGs they constitute is altered, and thus MN activity may have become asynchronous. We thus analyzed the frequencies of the observed mPSCs (**Fig. 3D**).

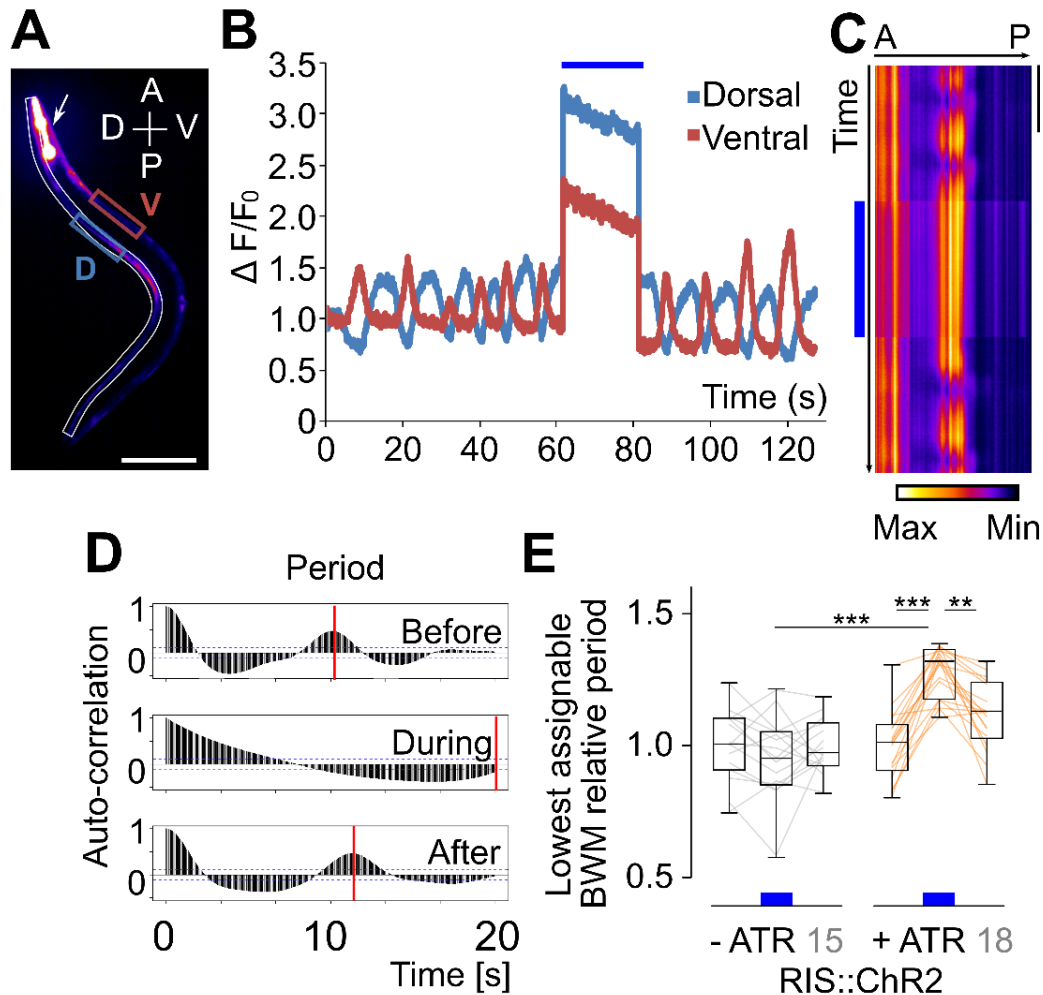


Figure 2: RIS photoactivation stopped muscular Ca^{2+} -dynamics. **A**) Maximum intensity projection of RCaMP imaging in BWM cells of an immobilized animal (arrow: pharynx, *pmyo-2::mCherry* marker). Boxed regions: Violet, blue: regions of interest for dorso-ventrally alternating activity; white: region of interest for kymographic analysis of dorsal muscle Ca^{2+} signals along the body in C, scale bar = 100 μm , A, P, V, D: anterior, posterior, ventral, dorsal, respectively. **B**) Ca^{2+} dynamics in both regions of interest from panel (A) (V = ventral, D = dorsal muscle cells) measured before, during, and after RIS::ChR2 photostimulation, denoted by the blue bar. F_0 defined as the mean RCaMP intensity during the first 4.5 s of the recording. **C**) Kymograph representation of the Ca^{2+} dynamics along the dorsal side. The RCaMP signal was normalized for visualization purposes. RIS photoactivation: blue bar. Scale bar = 10 s. **D**) Example of the RCaMP signal auto-correlation for a specific point in the BWM over time, before, during and following illumination. Ventral and dorsal BWMs were analyzed. Red lines: Peak auto-correlation of two consecutive Ca^{2+} waves and their time lag (if no consecutive Ca^{2+} signals were detected during the stimulation period, stimulus duration was taken as lower bound). **E**) Distribution of the mean change in the muscular Ca^{2+} oscillation period per animal, compared to before RIS photoactivation. When no oscillations occurred, the duration of photostimulation (20 s) was assumed as minimal period. Compared are animals without and with ATR, number of animals indicated in grey numbers. *** $p \leq 0.001$; ** $p \leq 0.01$; statistical significance tested by ANOVA, Barlett's test, Bonferroni's multiple comparison test.

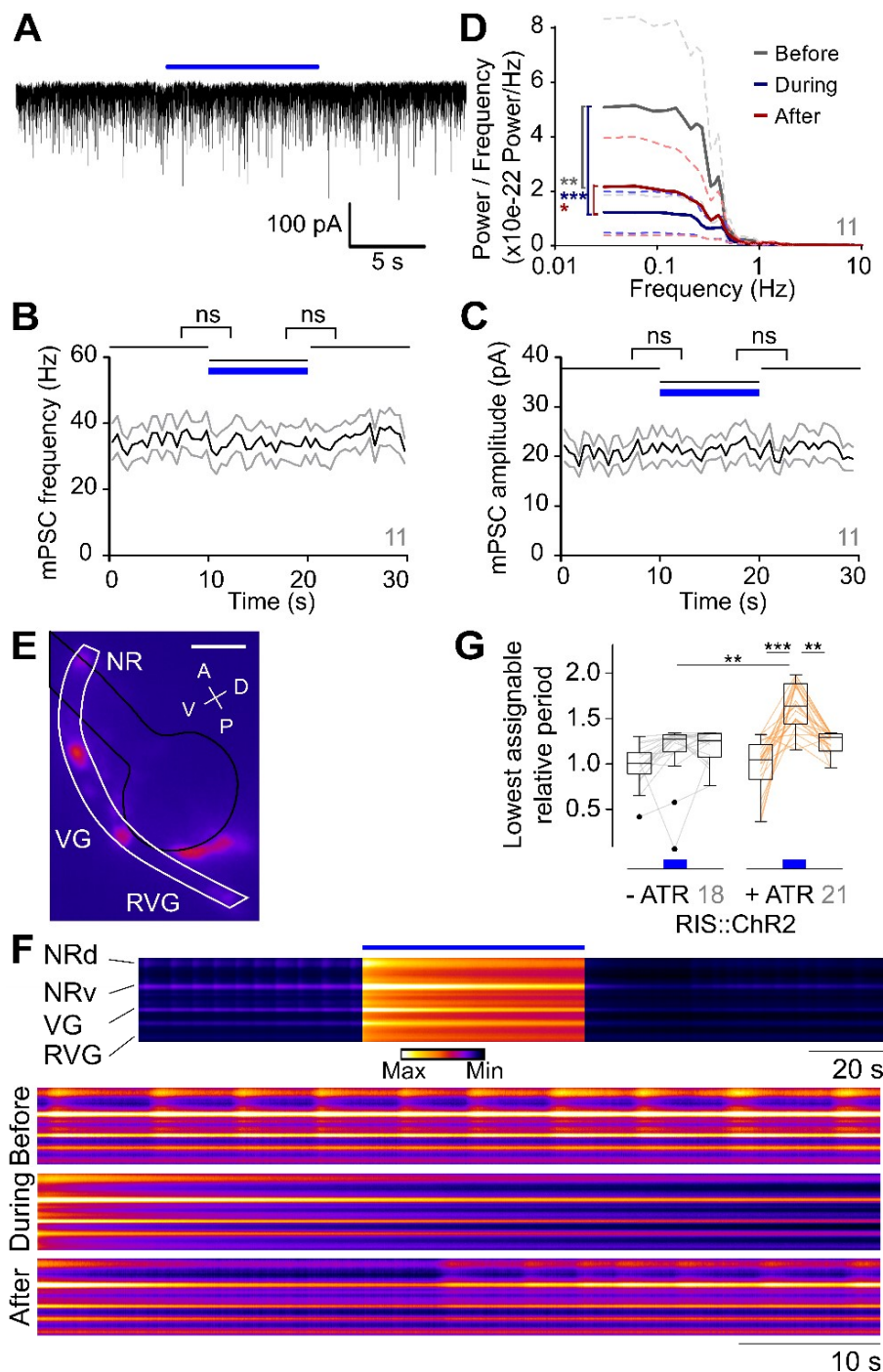


Figure 3: RIS photoactivation suppressed motor neuron (MN) synchrony and Ca^{2+} oscillations. **A)** Exemplary voltage clamp recording of BWM cell, postsynaptic to MNs. Blue bar denotes RIS::ChR2 photostimulation **B, C)** Analysis (Mean \pm SEM) of mPSC frequency (B) and amplitude (C). Blue bar: Illumination period; $n = 11$ animals. **D)** Fourier transform with multi-taper analysis of mPSC events across the observed frequencies. Mean (solid lines) \pm SEM (dashed lines) of the periods before, during and after RIS photostimulation of $n = 11$ animals. **E)** RCaMP fluorescence in cholinergic neurons in the head with region of interest from dorsal nerve ring (NR; d and v denote dorsal and ventral portions in **F)** through ventral to retrovesicular ganglia (VG, RVG) marked in white; black: pharynx outline. Scale bar = 25 μm . For identity of cells imaged, see [Supplementary Fig. 3A.F](#) **F)** Kymograph representation of cholinergic neuron Ca^{2+} dynamics from the dorsal NR to posterior RVG. Scale bars, upper = 20 s, lower = 10 s; blue bar: illumination period, Lower three panels show expanded views. **G)** Autocorrelation analysis (as in [Fig. 2E](#)); distribution of mean change in Ca^{2+} oscillation period, in cholinergic neurons, per animal, relative to before RIS photoactivation. When no oscillations occurred, the duration of photostimulation (60 s) was assumed as minimal period. Number of animals indicated in grey. *** $p \leq 0.001$; ** $p \leq 0.01$; * $p \leq 0.05$; statistical significance tested by two-way ANOVA in (D) and ANOVA, Barlett's test, Bonferroni's multiple comparison test in (G).

Predominantly low frequencies were populated in this analysis, and RIS photoactivation caused a significant reduction of their power. We also assessed muscular action potentials (APs), which occurred at low frequency, not obvious silenced by RIS photostimulation ([Supplementary Fig. 2](#)). Thus, muscle tone is maintained during RIS activity, while MN activity is desynchronized. As the observed muscle activity is evoked by MNs even in restrained animals⁴⁷, we wanted to analyze MNs directly. If RIS effects on BWM Ca^{2+} fluctuations occur at the MN level, Ca^{2+} fluctuations in MNs may seize during RIS photoactivation. We expressed RCaMP in a large subset (132/160) of cholinergic neurons, encompassing all synaptic cholinergic partners of RIS (VB, DB, AS, RMD, SMD, SDQ, PVC, AVE, including cells in the head ganglia, but excluding SAB; [Supplementary Fig. 3A](#); see methods), and analyzed Ca^{2+} dynamics before and during RIS photoactivation (**Fig. 3E, F**; [Supplementary Movie 4](#)). We observed spontaneous fluctuations in the signals across head MNs of ~0.17 Hz. RIS photoactivation increased the mean relative auto-correlation period 1.6 fold (**Fig. 3G**), i.e. activity in the head cholinergic nervous system was significantly reduced. No such effect was seen in animals raised without ATR. Thus, RIS::ChR2 activity reduced Ca^{2+} oscillations in cholinergic neurons, by slowing oscillatory activity in the neuronal network, which is the likely reason for the observed reduction of muscle oscillations.

2.3.3 RIS photostimulation effects are accelerated by GABA transmission

Effects of RIS on various behaviors could depend on different types of neurotransmission: RIS is GABAergic, peptidergic, and makes gap junctions, which may all be driven by ChR2 stimulation. In RIS' control of DTS, GABA played no role, as lethargus still occurred in GABA-defective mutants, and was instead instructed by neuropeptidergic transmission²⁶. We tested mutants of these signaling pathways by analyzing the locomotion state as forward, reverse or stop categories, defined by a threshold of $\pm 45 \mu\text{m/s}$ on the velocity trajectory. WT animals stopped locomotion during RIS photoactivation (**Fig. 4A**). After the stimulus ended, a significant proportion the animals resumed locomotion within 2 s, however, inducing reversals, from which they gradually returned to mostly forward locomotion. Mutants lacking the vesicular GABA transporter ('uncoordinated' *unc-47(e307)* animals), still exhibited the RIS-induced stop response, with delayed onset, and the post-stimulation reversal. RIS-induced body elongation that was significantly stronger in *unc-47* mutants than in WT (**Fig. 4B**). This appears paradoxical, yet, compared to WT, *unc-47* animals are pre-contracted due to absence of GABA at the neuromuscular junction, thus

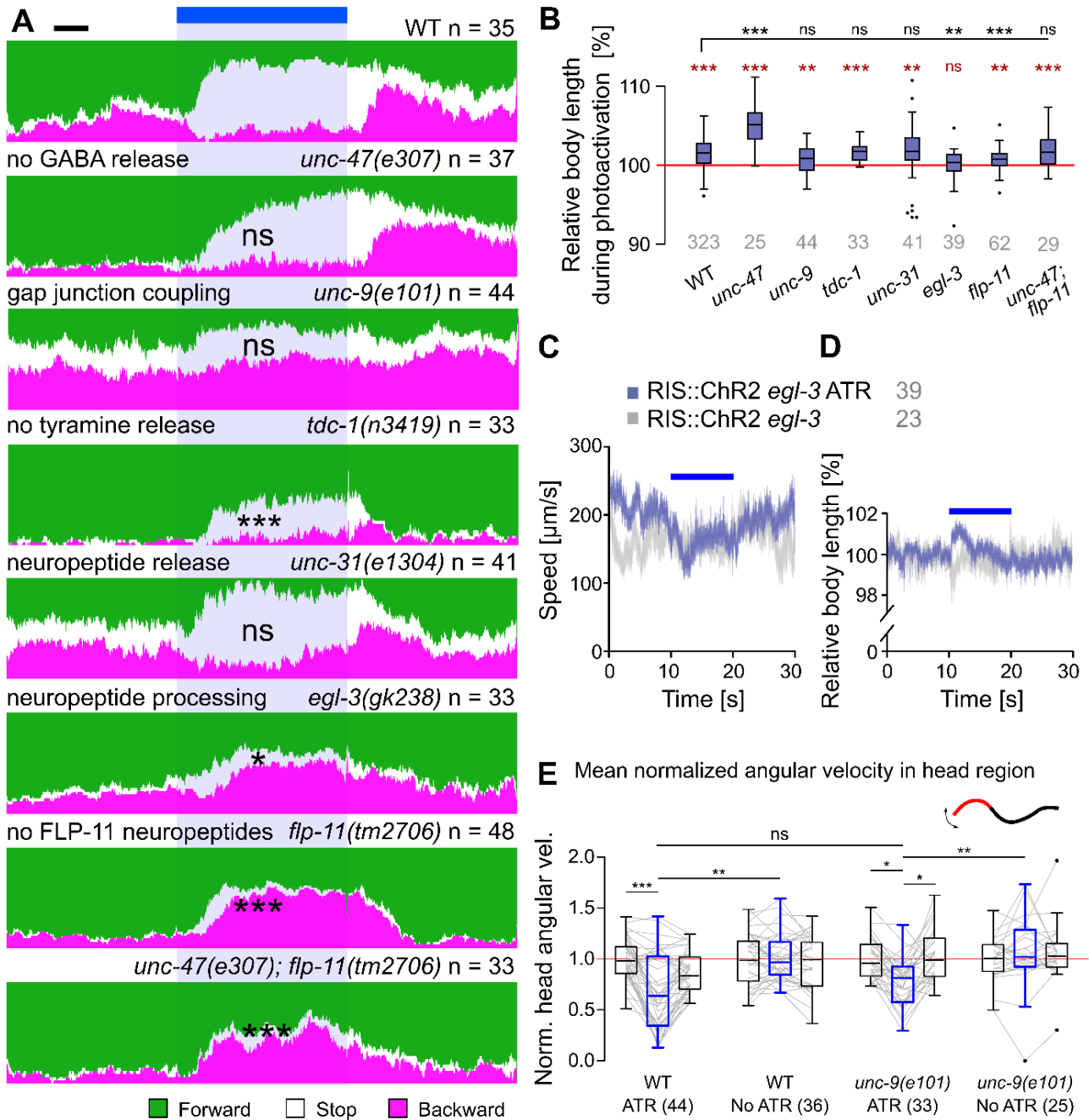


Figure 4: The stop phenotype induced by RIS photoactivation requires GABA and neuropeptide signaling. **A**) Animal locomotion analyzed before, during and after photoactivation of RIS (in *lite-1(ce314)* background, to eliminate unspecific photophobic responses), and the proportion of animals in distinct state (forward (green), stop (white), reversal (magenta)), deduced from the animal velocities, is represented in color, over time, across all animals analyzed (number of animals and genotypes indicated above each data set). Significant change in stop proportion during RIS photoactivation versus WT indicated; blue bar and blue shade: illumination period; scale bar: 2 s. **B**) Relative body elongation during RIS photoactivation; box plot with Tukey whiskers, numbers of animals and genotypes are indicated below. **C, D**) Mean \pm SEM locomotion speed (C) or body length (D), before, during or after photoactivation of RIS::Chr2 (blue bars), compared in *egl-3(gk238)* mutants raised with or without ATR. Number of animals depicted in grey. **E**) Mean normalized angular velocity in anterior quarter of the animal for WT and *unc-9(e101)* mutants expressing RIS::Chr2, with and without ATR. Box plot with Tukey whiskers. *** $p \leq 0.001$; ** $p \leq 0.01$; * $p \leq 0.05$; ns: non significant; statistical significance tested by ANOVA, Kruskal-Wallis with Dunn's Multiple Comparison Test in (A; black, vs. WT in B, and E) or Wilcoxon Signed Rank Test, versus no body length change (red, in B).

inhibition of cholinergic dynamics by RIS (**Fig. 3**) likely causes more pronounced body elongation. In sum, GABA is not involved in maintaining RIS induced locomotion stop phenotypes, nor the post-stimulation reversal, but rather speeds up the slowing and stopping effects induced by RIS activation. This may be via RIB neurons, that were shown to increase locomotion speed, and to which RIS makes synapses^{48, 49}([Supplementary Fig. 3B](#)).

2.3.4 RIS photostimulation induces subsequent reversals via gap junctions

RIS forms electrical synapses with five neuron types⁴⁹ ([Supplementary Fig. 3B](#)): AIB, AVJ, DB, RIM and SMD. We analyzed if effects observed during and after RIS::ChR2 activation may be due to concomitant depolarization of these neurons, in mutants lacking the innexin (gap junction subunit) UNC-9, expressed in RIS and forming homo- or heterotypic gap junctions with itself or with UNC-7^{50, 51}. Based on its expression pattern, lack of UNC-9 should affect gap junctions between RIS and AIB, AVJ, DB, SMD, and RIM⁵²(**Fig. S3C**). RIM inhibits reversals⁵³. Conversely, reversals can be induced by AIB neurons, which inhibit RIM, via disinhibition⁵⁴. *unc-9(e101)* mutants showed a transient body elongation during RIS photoactivation (**Fig. 4B**), possibly due to RIS inhibitory transmitter release. However, *unc-9* mutants neither increased stop probability upon RIS photostimulation, nor did they induce reversals following RIS stimulation (**Fig. 4A**). Thus, reversals mediated via AIB may be induced through RIS activation and gap junctions to AIB, and inhibitory transmission from AIB to RIM might overcome the putative electrical activation of RIM by RIS. Reversals following RIS stimulation may result from rebound activity upon offset of RIS-RIM electrical stimulation, and a longer-lasting RIS-AIB stimulation, disinhibiting RIM. Our findings for *unc-9* animals are complicated by their low basal locomotion speed. Thus, we assessed the angular speed of the head region, before, during, and after RIS photoactivation, as a proxy for speed (**Fig. 4E**). RIS activation inhibited head movements in WT and in *unc-9(e101)* mutants. We further analyzed if RIS may evoke behavior via RIM, which is tyramineric⁵³, thus RIS depolarization could affect RIM tyramine release. SMD neurons together with RMD neurons control head movements by activating muscles. RIM/tyramine inhibits RMD, SMD and head muscles^{49, 55}, thus changing locomotion stop probability⁵⁶. The tyramine-deficient mutant *tdc-1(n3419)* moved almost only forward, and upon RIS photoactivation, animals displayed a significantly reduced propensity to stop (**Fig. 3A**). Also these animals showed no reversals after the RIS photostimulation period, yet the body elongated (**Fig. 3B**). In sum, RIS stimulation may affect slowing and subsequent reversals in part via RIM neurons.

2.3.5 RIS photostimulation effects require neuropeptides

We next assessed the role of neuropeptides in photoevoked RIS::ChR2 signaling by analyzing mutants lacking the Ca^{2+} -dependent activator protein for secretion (CAPS, encoded by *unc-31*), or the pro-protein convertase EGL-3. UNC-31 is required for secretion of (many of the) mature neuropeptides, while EGL-3 mediates processing of most if not all neuropeptide precursors⁵⁷. RIS photostimulation in *unc-31(e1304)* mutants still evoked stopping (**Fig. 4A**), thus release of neuropeptides mediating RIS effects may require factors other than UNC-31⁵⁸. However, *egl-3(gk238)* mutants were largely affected, and stopped significantly less than WT: Only a very transient (ca. 2 s) and minor speed reduction (~28%) was observed (**Fig. 4C**), while WT slowed down by ~72% and stopped for the entire 10 s illumination period (**Fig. 1B**). After a transient elongation during the first 2 s of RIS photoactivation (presumably due to GABA; **Fig. 4D**), *egl-3(gk238)* mutants on average showed no relaxation (**Fig. 4B**). RIS was previously shown to regulate DTS using FLP-11 neuropeptides²⁶. *flp-11(tm2706)* mutants showed diminished RIS-induced elongation (**Fig. 4B**), and almost no stops. Instead, *flp-11* animals reversed more, right after RIS stimulus onset (**Fig. 4A**), as observed for *egl-3* mutants. FLP-11 peptides may inhibit AVE backward command interneurons via chemical synapses ([Supplementary Fig. 3B](#)), and without FLP-11 neuropeptides, AVE may more readily induce reversals, as also the AIB-RIM disinhibitory pathway is activated by RIS. The slowing response was much briefer in *flp-11* mutants, and albeit transient stops were observed, no *flp-11* animal stopped locomotion for the entire stimulus period. RIS activation in *flp-11* mutants also caused no pharyngeal pumping inhibition (N = 3, 150 < n < 200 animals per trial). Since *unc-47* GABA mutants had delayed stop phenotypes, while *flp-11* mutants displayed transient stops at the start of RIS photoactivation, we wondered if their phenotypes were independent. In *unc-47; flp-11* double mutants, the RIS::ChR2 induced stop was completely abolished, however, reversals still occurred (**Fig. 4A**). In sum, efficient RIS mediated locomotion stop is jointly induced by GABAergic and FLP-11 peptidergic signaling. The former modality evokes fast slowing, the latter causes sustained stops.

2.3.6 Recording of Ca^{2+} activity in the RIS axon and soma in freely moving animals

Photostimulated RIS affects locomotion, pharyngeal pumping, and withdrawal after mechanical stimuli, via GABA, FLP-11 and possibly other neuropeptides, acting on different cells. During intrinsic behavior, RIS is active along with other neurons. Singular stimulation of RIS, evoking the observed phenotypes, could thus artificially exaggerate only aspects of

behaviors that occur when RIS is (co-)activated with/by other cells. We explored this by analyzing RIS activity in free-moving animals by Ca^{2+} imaging. We modified a previously described tracking system⁵⁹. A four-quadrant photomultiplier controls a stage, keeping a fluorescent spot in the center, and a high-magnification fluorescence video is acquired. An infrared behavior video is acquired at low-magnification, stage positions are recorded, and the combined data streams allow behavioral quantification and correlation with neuron activity. We expressed GCaMP6s in RIS, along with a red fluorescent protein in the pharyngeal terminal bulb (TB), to track the head region (**Fig. 5A**). As not RIS, but the TB was tracked, the RIS image rotates around the center of the picture, while the animal changes direction. Custom-written software for image processing 1) registered images on the RIS cell body, 2) cropped a region of interest (ROI) containing the entire RIS morphology and rotated it such that the axon was oriented (**Fig. 5B**, [Supplementary Fig. 5](#) and [Videos 5, 7](#)), 3) defined a smaller ROI for each image, depicting only the RIS soma and axonal, 4) fitted, along the spline of this ROI, a parabola, defined 100 equally spaced perpendicular segments and quantified their fluorescence.

2.3.7 RIS axonal Ca^{2+} activity during locomotion is correlated with slowing and the onset of reversals

RIS Ca^{2+} activity, assessed on short time scales (in contrast to previous analyses during sleep), was transient, or lasted for several seconds, and coincided with slowing and/or reversals (**Fig. 5C**), for which the magnitude of the Ca^{2+} signal was indicative. Ca^{2+} rose stepwise while the animal slowed, until high levels were reached (**Fig. 5D**; [Supplementary Movie 6](#)) and the animals exhibited subsequent reversals. During those, Ca^{2+} dropped and forward movement resumed a few seconds later. Across all events recorded, the main change in Ca^{2+} signal was observed in the nerve ring region of the RIS axon (**Fig. 5E**); sometimes, activity was also observed in the branch (**Fig. 5C, D**; [Supplementary Movies 7, 8](#)). Axonal Ca^{2+} transients are expected to be most indicative of relevant neuronal activity, likely correlated with transmitter release. Analyzing axonal events further helped to exclude noise from intestinal fluorescence.

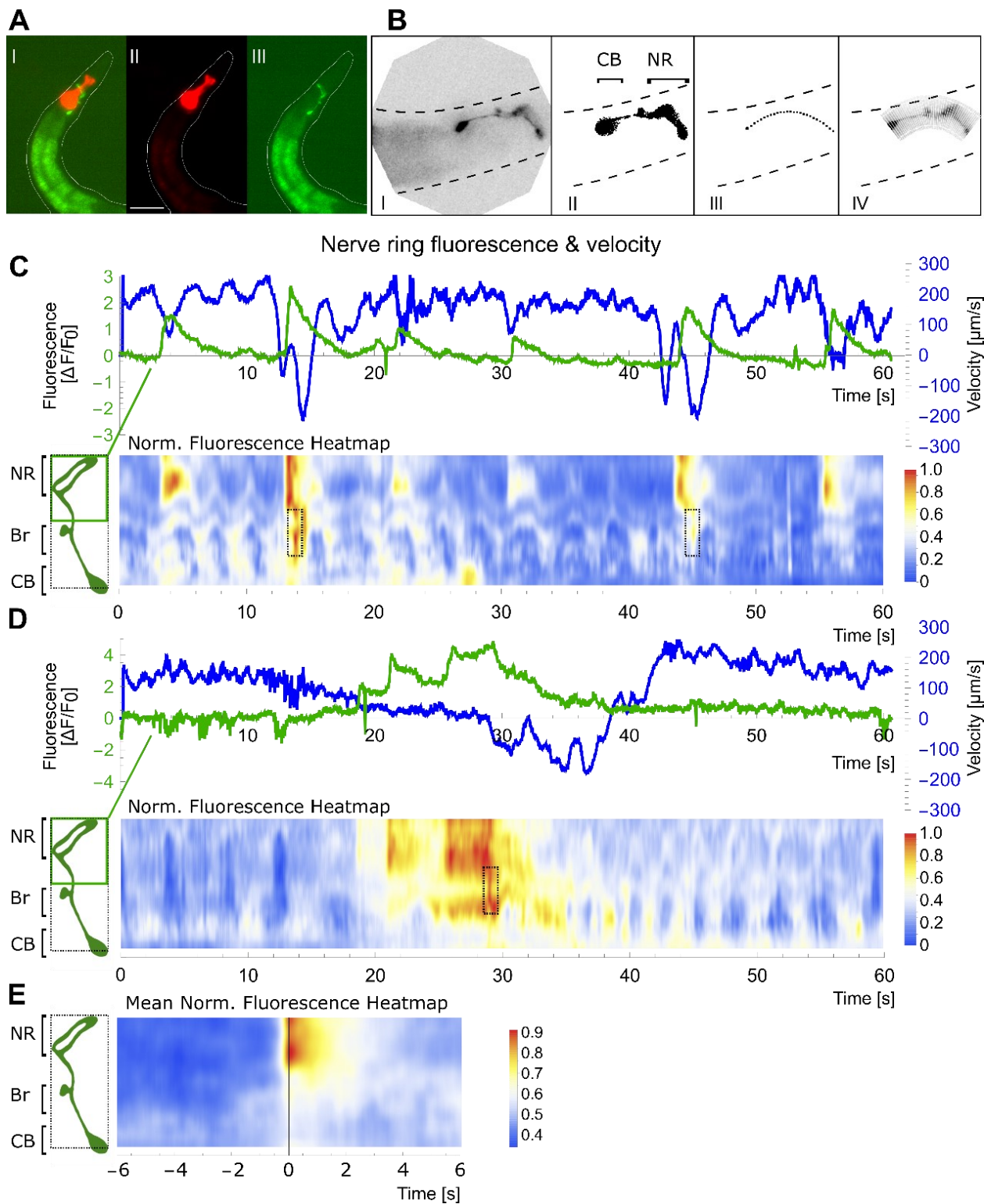


Figure 5: Ca^{2+} activity measured along the RIS axon in freely moving animals correlates with slowing and reversals: **A**) Strain used for tracking and Ca^{2+} imaging RIS in moving animals, expressing a red fluorescent marker in the pharyngeal terminal bulb (for tracking) and GCaMP6s in RIS. Micrographs of red (II) and green (III) fluorescence, and merged color channels (I). Scale bar: 50 μm . **B**) Image analysis after binarization and repositioning the soma, involved reorienting the raw image (I), masking unspecific gut fluorescence (II), fitting a parabola (III), and measuring fluorescence intensity in perpendicular rectangular ROIs (IV). Dorsal is up, anterior to the left; CB, cell body; NR, nerve ring. **C**, **D**) Upper panels: Representative traces of animal velocity (blue) and fluorescence intensity in the RIS nerve ring portion (green). Lower panels: Corresponding heat maps displaying the normalized fluorescence dynamics along the axon over time. RIS pictograms on the left indicate morphology including nerve ring (NR), branch (Br) and cell body (CB), the distance along the axon as well as the region of the nerve ring (green box) used for calculating the $\Delta F/F_0$ traces

in the upper panels, while dashed region shows extent of ROIs analyzed in lower panels (also in E). Distinct Ca^{2+} rise events in the branch region are boxed. **E)** Mean normalized fluorescence heat map of $n = 45$ acquired Ca^{2+} events along the entire length of RIS, partially excluding the soma, by aligning time windows 6 s prior and post Ca^{2+} peaks ($N = 11$ animals).

Thus, we used only the fluorescence of the anterior half of the neuronal ROI, comprising the axon around the nerve ring, unless we also analyzed the axonal branch. Slowing and reversal events (as shown in **Fig. 5C**) were identified by analyzing locomotion based on the x,y- position of the tracked animal and its body posture, allowing to derive directional velocity along the mid-body axis.

The relative occurrence of reversals and Ca^{2+} peaks are shown in **Fig. 6A**, as probability distributions, aligned to the nearest Ca^{2+} peak or nearest reversal, respectively. The skew of these distributions suggested that reversals followed the onset of a Ca^{2+} rise. We aligned events recorded from 20 animals, either to Ca^{2+} peaks (**Fig. 6B, D**, 45 events) or to the moment of reversal ([Supplementary Fig. 5A](#), 75 reversals). For Ca^{2+} peak-aligned data, we either analyzed velocity (becoming negative upon reversal), to probe if RIS Ca^{2+} may be a determinant of reversals (**Fig. 6B**), or absolute speed, to explore if RIS may be a speed sensor ([Supplementary Fig. 6A](#)).

RIS Ca^{2+} signals required ~ 1.2 s from detectable onset to peak (**Fig. 6B**). Concomitantly, a drop in velocity occurred, which in 80% of cases led to a reversal (mean velocity thus approached zero, but remained positive). Animals significantly decreased velocity (**Fig. 6B**, box plot). We also assessed the onset of Ca^{2+} rise (determined from dF/dt), which likely coincides with transmitter release (**Fig. 6B**). Cross-correlation of the Ca^{2+} rise rate and velocity drop showed a low but significant coefficient of -0.15 , and a time lag of -0.8 s (**Fig. 6C**). Thus, the onset of the Ca^{2+} rise (green vertical line, **Fig. 6B**) preceded slowing, which is likely regulated by RIS. Correlating the moment of reversal and the Ca^{2+} signal indicated that RIS Ca^{2+} determines duration of reversals ([Supplementary Fig. 5A](#)). In sum, a rise in RIS Ca^{2+} preceded slowing and reversals, as also indicated by the event probabilities (**Fig. 6A**). We conclude that RIS activity precedes the behavioral change, and may determine it.

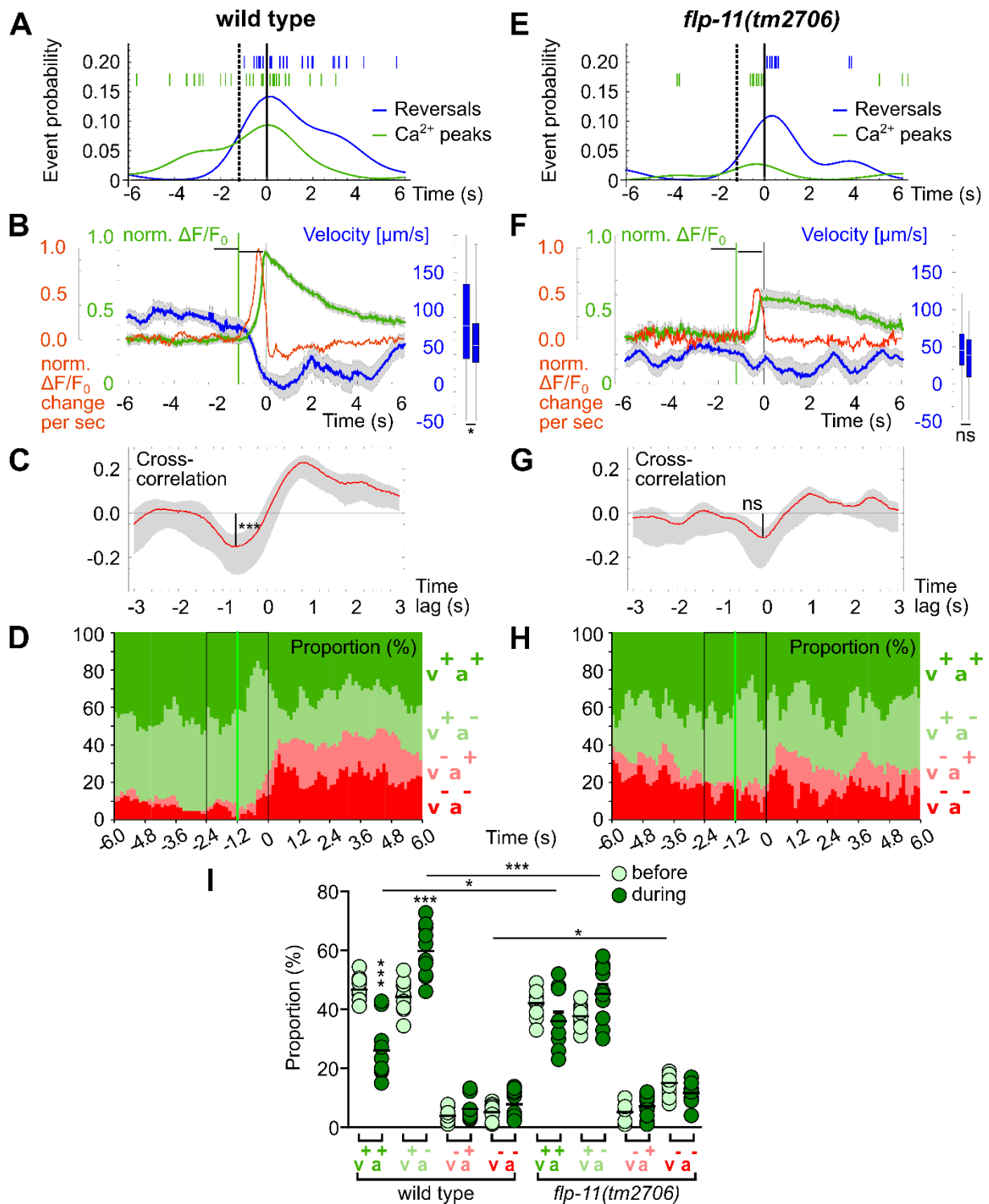


Figure 6: RIS Ca²⁺ activity induces decreased forward locomotion and increased reversal probability, which requires FLP-11 neuropeptides: **A)** Conditional probability density function of the shortest unbiased time lag to a reversal given a Ca²⁺ peak event (aligned nearest reversal events depicted as blue lines) and vice versa for the probability of a Ca²⁺ peak event given a reversal (green lines: time lag to the nearest reversal), in WT animals. The dotted vertical line indicates the mean onset of a Ca²⁺ rise, the black solid line indicates peak Ca²⁺. **B)** Ca²⁺ peak-aligned normalized GCaMP intensity (green, mean \pm SEM) in the nerve ring region of the RIS axon (as depicted in **Fig. 4C**) and animal velocity in $\mu\text{m/s}$ (blue, mean \pm SEM, n=45; a significant reduction in the two periods before and during the Ca²⁺ rise is shown on the right, boxplot, p < 0.001). Shown in red is the mean first derivative (dF/dt rise rate, s⁻¹) of all Ca²⁺ signals. **C)** Mean \pm confidence intervals of time-shifted cross-correlation (red) of animal velocity aligned to Ca²⁺ signal rise rate, (as in B). Anticorrelation is significantly different from 0, and shows a negative time lag (n=45, Pearson's r = -0.15). **D)** Ca²⁺ peak aligned analysis of the proportion of the animal population in one of 4 behavioral states: 1) moving forward and accelerating (v+a+, positive velocity and acceleration, dark green; for acceleration data, see

[Supplementary Fig. 6C, D](#)), 2) moving forward and decelerating (v^+a , light green), 3) moving backwards, but accelerating (v^-a^+ , pink) and 4) moving backwards and increasing their negative velocity (v^-a , dark red). Number of reversing animals increased significantly during RIS Ca^{2+} events (T-test, $p < 0.001$). Green line indicates mean onset of RIS Ca^{2+} rise. **I**) Scatter plot with means of the data in (D, H), statistical differences analyzed for the time periods indicated by black boxes (before and during Ca^{2+} rise). **E-H**) As in A-D, but in *flp-11(tm2706)* background. Boxplots in B and F compare the average in the time windows indicated by black brackets below the traces. *** $p \leq 0.001$; ** $p \leq 0.01$; * $p \leq 0.05$; ns: not significant; statistical significance tested by paired T-test in B, F and unpaired T-test in C, G; ANOVA with Tukey multiple comparisons test in I.

We further analyzed how RIS activity is associated with behavioral changes by assessing the fraction of animals performing particular locomotion behaviors at and around the timing of RIS Ca^{2+} peaks (**Fig. 6D, I**). Before RIS became active, there was a similar propensity for animals to accelerate or to slow down. During the Ca^{2+} rise, animals were more likely to decelerate, and following the Ca^{2+} peak, reversal probability increased. Thus, the likely moment of RIS releasing GABA and FLP-11 neuropeptides is correlated with, and most likely induces, inhibition of locomotion, preceding reversals, analogous to our observations upon RIS photostimulation (**Fig. 1B**). We conclude that RIS fulfills a crucial role in neuronal programs controlling forward-backward transitions.

2.3.8 FLP-11 neuropeptides are required for RIS' effects on locomotion speed

RIS affects locomotion slowing, and is particularly active before reversals. As FLP-11 neuropeptides were required for stopping, we asked if in *flp-11* mutants RIS Ca^{2+} activity occurs but may be unable to evoke behaviors. From 24 *flp-11* animals, we recorded 100 reversals ([Supplementary Fig. 5B](#)) and 25 Ca^{2+} events (**Fig 6E-H**). Overall occurrence of reversals or Ca^{2+} events did not differ between WT and *flp-11* (Fisher's exact tests, two sided, $p = 0.865$ and 0.055 respectively, n.s.), thus network functions appeared normal. As in WT, *flp-11* mutants displayed similarly skewed probability distributions for reversals and Ca^{2+} peaks (**Fig. 6E**). Reversal induction per se is independent of FLP-11. Slowing, on average, was less pronounced during RIS Ca^{2+} rise events, which were less frequently paired to slowing or reversals; thus reversal velocity (**Fig. 6F**) and speed ([Supplementary Fig. 6B](#)), were not significantly different before and during the Ca^{2+} rise. No significant cross-correlation of the Ca^{2+} rise rate and velocity was found (**Fig. 6G**). *flp-11* mutants did not show significant changes in the proportion of forward, reverse, accelerating or slowing subsequent to a Ca^{2+} transient, while these proportions were significantly different between WT and *flp-11*, and *flp-11* animals reversed more prior to RIS Ca^{2+} signals (**Fig. 6D, H, I**). In sum, locomotion, particularly slowing, is abnormally regulated in *flp-11* mutants. RIS' tight control of the timing of reversals after a stop requires FLP-11 release, which also aids in sustaining stops (**Fig. 4A**), while it elicits fast slowing by GABA. Yet, as reversals occur after

RIS photostimulation even without GABA and FLP-11, additional neurons must partake in inducing reversals.

2.3.9 Compartmentalized Ca²⁺ dynamics in the RIS axon

In *flp-11* mutants, RIS was on average less efficient in causing slowing. This was intriguing, since we could still observe occasional reversal events. We asked whether there is a specific feature of RIS Ca²⁺ activity that distinguishes such events. We segregated the RIS Ca²⁺-aligned events into those paired with a reversal, and those that merely led to a velocity reduction or stop. We then assessed Ca²⁺ signals spatiotemporally, from soma to nerve ring, encompassing also the branch, focusing on the 2 s centered on the Ca²⁺ event. To capture dynamic changes, Ca²⁺ signals were normalized to the first 150 ms of this time window, and significantly different Ca²⁺ levels were color coded (**Fig. 7**). In the RIS nerve ring region, we observed Ca²⁺ signals for both types of events, i.e. paired (**Fig. 5D**, e.g. sec 28-30; **Fig. 7A**) or unpaired to a reversal (**Fig. 5D**, e.g. sec 21-23; **Fig. 7B**). Interestingly, events paired to a reversal showed significantly increased Ca²⁺ dynamics in the branch region (**Fig. 7A**; [Supplementary Movies 7, 8A](#)), which were absent when animals only slowed or stopped (**Fig. 7B**; [Supplementary Movies 7, 8B](#)). Furthermore, reversal-unpaired events showed a significant reduction in branch Ca²⁺ signals ~750 ms preceding the maximal nerve ring Ca²⁺ signal. In these events, no significant activity was observable in the branch, even when the nerve ring region was active (**Fig. 7B**). We conclude that RIS axonal Ca²⁺ dynamics are compartmentalized, and that the branch region has a specific function in induction of, or concomitant with, reversals. RIS axonal Ca²⁺ dynamics in *flp-11(tm2706)* mutants had no significant Ca²⁺ dynamics during reversals (**Fig. 7C**), while events paired only to a stop still showed nerve ring activity, though no significant reduction in branch activity was observed (**Fig. 7D**). FLP-11 neuropeptides may directly or indirectly provide positive feedback to RIS during reversals.

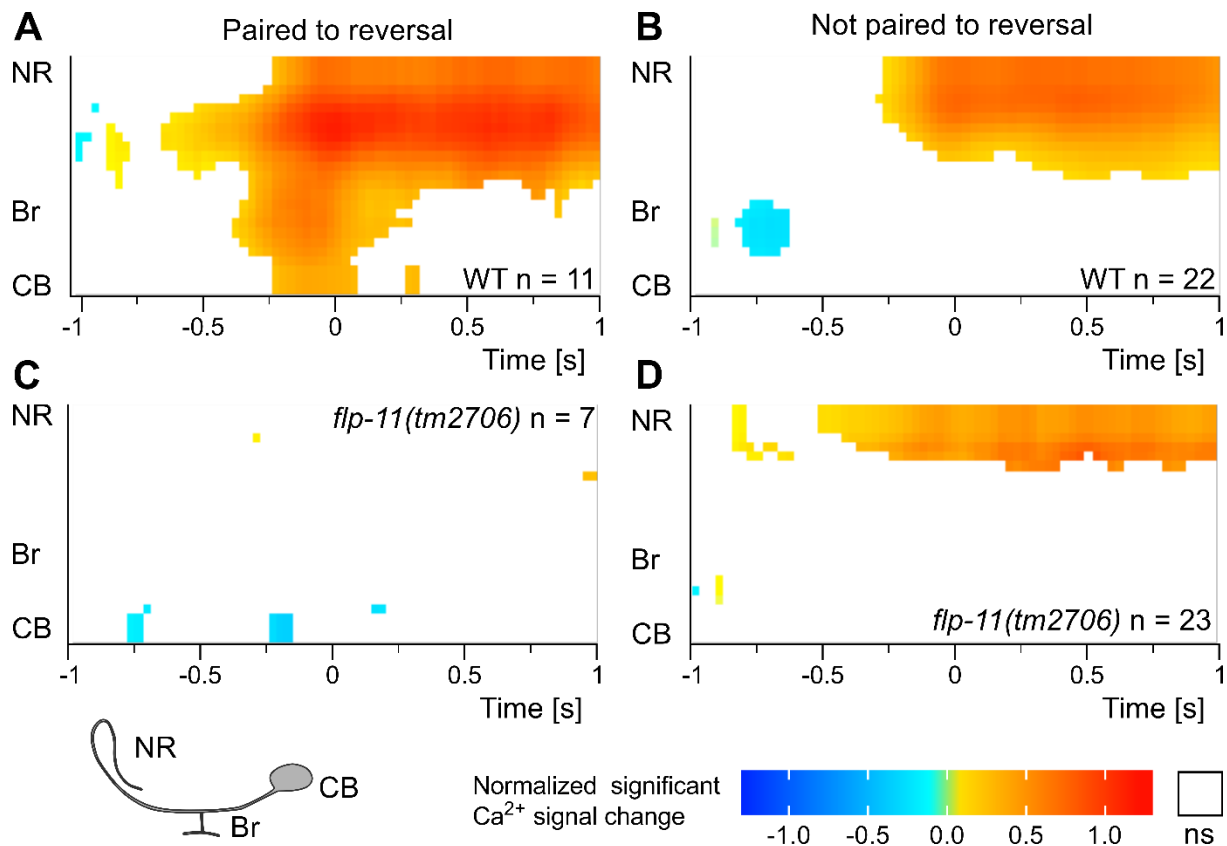


Figure 7: Compartmentalized Ca^{2+} dynamics in the RIS process. **A, C**) Ca^{2+} events paired to a reversal in the 2 s time window flanking a Ca^{2+} signal obtained from freely behaving animals (WT in **A**, *flp-11(tm2706)* in **C**). Top is the dorsal nerve ring (NR) region, passing through the branch region (Br) to the center of the cell body (CB). Only events significantly different from inactivity are shown, color coded for intensity, normalized to the mean of the first 150 ms depicted. Blue and red hues indicate significant reductions and increases, respectively. Non-significant dynamics are omitted and shown in white. **B, D**) Ca^{2+} events unpaired to a reversal in the 2 s time window flanking a Ca^{2+} signal, as in (**A**, **C**). Number of events indicated. Significance level: T-Test, $p < 0.05$.

2.4 Discussion

Neuronal circuits regulate and fine-tune locomotion. While in mammals this is orchestrated by whole brain systems like motor- and prefrontal cortex, cerebellum and spinal cord neurons, much fewer neurons must fulfill these tasks in compressed nervous systems. Here, we analyzed the role of one neuron, RIS, which orchestrates locomotion slowing and reversals in *C. elegans*. RIS does this by re-employing a peptidergic pathway used in sleep control, e.g. after larval molts or in response to stress. Here, RIS uses also GABAergic signaling, not required during DTS induction²⁶. During optogenetic stimulation, GABAergic signaling from RIS induces the locomotion stop within seconds, possibly by inhibiting RIB neurons⁴⁸ ([Supplementary Fig. 3B, C](#)), and sustains it by FLP-11 signaling (**Fig. 8A**). The observed axonal compartmentalization of Ca^{2+} dynamics during locomotion (**Fig. 8B**), jointly with the requirement of peptidergic and GABAergic signaling suggest that RIS uses both modalities in a spatiotemporally defined manner to control locomotion. RIS' role in both

locomotion and sleep control represent two types of temporally different activity: 1) where RIS is employed to control locomotion with brief activity bouts (seconds), in coordination with other locomotion neurons, and 2) where DTS and SIS involve long-term RIS activity (minutes to hours), together with the sleep neuron ALA²².

RIS depolarization in the nerve ring results in fast GABA- and FLP-11 neuropeptide-mediated inhibition of neuronal activity and locomotion. Suppression of branch depolarization is permissive for locomotion halting, and conversely, if the RIS axon is not hyperpolarized in the branch before depolarization in the nerve ring, the most likely behavioral outcome is a reversal. This coincides with optogenetic experiments where RIS depolarization led to reversals and required both, GABA and FLP-11 release. These transmitter(s) dampened cholinergic MN oscillations and synchronized acetylcholine release, and suppressed oscillations of body muscle activity. Occasionally reversals occurred also without RIS activity, or in the absence of FLP-11. Thus, RIS is sufficient, but not essential for reversals, and must act in coordination with other neurons. Roberts et al.³⁸ described a four-state model of *C. elegans* locomotion, where forward-reverse and vice versa transitions were connected by brief pause states. RIS may induce this brief stop. Hints of this are found in our analyses, e.g. pause events at seconds 13, 44, 56 in Fig. 5C, accompanied by RIS Ca²⁺ peaks. Also, in analyses of mean Ca²⁺ events, a brief phase of zero acceleration followed the moment of maximal slowing ([Supplementary Fig. 6C](#)).

The functional compartmentalization of the RIS axon indicated that the branch is instructive for reversal onset. Since the effects of RIS activation are rather fast, and the RIS axon extends only in the nerve ring, the targets of transmitters released by RIS are likely in the head ganglia. RIS synaptic output and input segregate between its nerve ring and branch regions⁴⁹, with the branch being mainly postsynaptic, and the nerve ring process being dominated by output synapses. The branch connects to only three neuron types: AVJ, PVC and SMD. SMD neurons are part of the network encoding the amplitude of Ω -turns (named after the body posture adopted transiently during turning)⁶⁰. No behavior was yet associated with AVJ, while PVC is a PIN inducing forward movement⁶¹. In the locomotion state model³⁸, PVC and AVE drive forward and backward locomotion, respectively. PVC innervates RIS and RIS has synaptic output to AVE⁴⁹, implying a possible sequence of signaling leading from forward (PVC) to a pause (RIS), e.g. mediated by GABA inhibition of the speed neuron RIB, and transition to a reversal, by gap junctions to AIB and possibly by activating AVE (the latter would imply, however, an excitatory connection, possibly through excitatory GABA

receptors (like the EXP-2 channel involved in control of the defecation motor program⁶²). However, such speculative models will have to be clarified in animals lacking such receptors cell-specifically. During pure slowing events, branch Ca^{2+} activity was suppressed prior to RIS activation. PVC activity, which may inhibit RIS (e.g. via mAChRs, as PVC is cholinergic), could alter RIS output such that the evoked behavior is a stop instead of a reversal. Lack of FLP-11 neuropeptides uncoupled reversals from RIS Ca^{2+} activity and was permissive for reversal induction during RIS photoactivation. This suggests that RIS contributes to coordinating reversals by controlling the halt duration, and that it uses FLP-11 peptides for this purpose.

The kinetics of RIS::ChR2 elicited behaviors may be due to the different diffusion properties of GABA and FLP-11 neuropeptides (GABA is much smaller than FLP-11 neuropeptides). GABA was required for fast slowing within 1 s, while FLP-11 sustained the locomotion stop. RIS::ChR2 depolarization in WT animals increased reversal probability at the stimulus offset, while *flp-11* mutants increased their reversal probability already during the photostimulation period. Hence, FLP-11 is required to maintain behavior inhibition during RIS activity. The requirement for GABA and FLP-11 signaling for fast induction of a stop and for its maintenance, respectively, is in line with activities of stop neurons in vertebrates in regulating locomotion inhibition and body posture^{8, 10}.

In the mouse, behavior stop signals are not controlled by a single cell type in striatum⁶³, but by the activity of stop neurons in the brainstem that project to the spinal cord and depress locomotor rhythm generation^{8, 64}. Similarly, RIS de-synchronized motor neuron activity. Conservation of RIS and of FLP-11 neuropeptides in nematodes⁶⁵, but also the neuropeptide VF (NPVF) in fish, that can suppress escape behaviors⁶⁶, suggests that RIS acts as a stop neuron in parallel to / upstream of the ventral nerve cord CPG system¹⁷. A comparison among worm, fly, leech, tadpole, zebrafish, lamprey, mouse (**Fig. 8C**) of stop and sleep neurons may suggest that in compact brains like *C. elegans*, both activities are coalescing in one neuron type, RIS, which effects locomotion stop during brief activity, and sleep during prolonged activity. In more complex brains, such functions dissociate into different systems, distinct for sleep control and locomotion stop, which reside in different cell types (molecular identities still need to be determined for most systems) and brain structures, and use different mechanisms. Here, more elaborate control regimes have evolved, where sleep neurons induce relaxation, while stop neurons halt locomotion but do not relax muscle. RIS makes this distinction by brief and short signaling via the same

molecules. RIS may thus represent a primordial neuronal pathway, e.g. for fast sensory integration, and may have evolved to more finely tuned stop neurons in vertebrates.

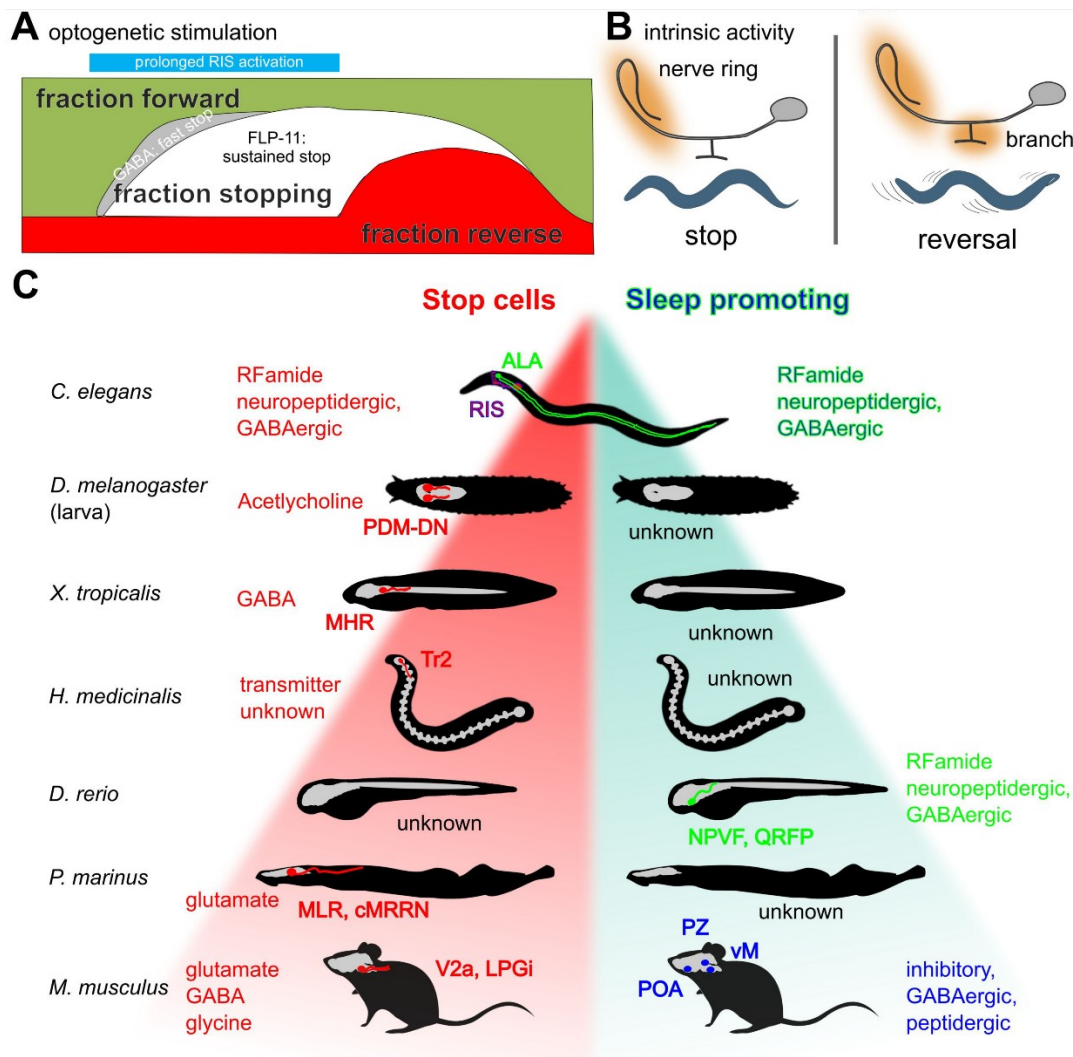


Figure 8: Models summarizing stimulated and intrinsic activities of RIS, and comparison of sleep and stop neurons across model systems. A) Fraction of behaviors found in animals before, during and following optogenetic RIS stimulation (blue bar), categorized as forward (green), stop (grey and white) and reversal (red) movement. Also indicated is the contribution of RIS neurotransmitters to fast and sustained phases of induced stops. **B)** Ca^{2+} activities of nerve ring and branch regions of the RIS axon, accompanying locomotion behaviors. The nerve ring region is active to induce slowing, while the branch region is additionally active when reversals are induced. **C)** Comparison of stop cells¹³ and sleep neurons/systems in various model organisms. Hierarchy indicates complexity of the respective brains, but implies no phylogenetic relationships. Left: Cells that stop or slow down locomotion when activated, in *C. elegans* (RIS), *D. melanogaster* larvae (PDM-DNs; posterior dorso-medial brain lobe descending neurons¹¹), *X. tropicalis* tadpoles (GABAergic MHRs, mid-hindbrain reticulospinal neurons), Tr2 cells⁷⁰ in the anterior brain of the leech *H. medicinalis*, glutamatergic neurons in the MLR (mesencephalic locomotion region) and RS stop cells of the cMRRN (reticulospinal cells of caudal middle rhombencephalic reticular nucleus) of the lamprey *P. marinus*^{10, 71}, and several types of mammalian stop cells: V2a reticulospinal interneurons in rostral medulla or caudal pons⁸, GABAergic neurons in the MLR, GABAergic and glycinergic neurons in the gigantocellular nucleus (GiA) and glycinergic neurons in the lateral paragigantocellular nucleus (LPGi)⁷². No stop cells were identified in zebrafish. Right: Sleep promoting neurons/systems (green: directly, and blue, indirectly promoting sleep, reviewed in ⁷³) are peptidergic and GABAergic RIS and ALA cells in *C. elegans* (thus combining functions of stop and sleep neurons in RIS); in zebrafish larvae RFamide neuropeptide VF (NPVF), similar to *C. elegans flp-11* derived peptides, inhibits serotonergic neurons in the ventral raphe nucleus; and in the mouse, GABAergic/peptidergic neurons in the

preoptic area (POA), inhibitory neurons of the parafacial zone (PZ) of the brain stem and GABAergic neurons of the ventral medulla (vM) are involved in sleep control. Transmitters used by each cell type are indicated. No sleep systems are known yet for fly larvae, tadpoles, leech or lamprey. Animal silhouettes were acquired from <http://phylopic.org/>.

2.5 Methods

Molecular biology

pCoS6 (p_{glr-1::flox::Chr2(H134R)::mCherry::SL2::GFP}) was a gift from Cornelia Schmitt⁶⁷. The following plasmids were kindly provided by Navin Pokala (Bargmann lab, Rockefeller University, USA): **pNP165** (pSM::p_{glr-1::flox::Chr2(H134R)::mCherry}), **pNP260** (pSM::p_{nmr1::flox::Chr2::STAR::mCherry}) and **pNP259** (pSM::p_{gpa-14::Cre}). **pPD95.79** was a gift from Andrew Fire (Addgene plasmid # 1496; <http://n2t.net/addgene:1496> ; RRID:Addgene_1496). **pOT15** (QUAS::jRCaMP1b), **pOT6** (punc-17::QF) and **pOT7** (punc-4::QS::mCherry) were provided by Oleg Tolstikov¹⁸. We used the plasmid **pmyo-3::RCaMP1h** for RCaMP expression in BWM cells⁴³. **pmyo-2::GCaMP3** was kindly provided by Karen Erbguth. **pGP** (p_{mec-4::GCaMP6::SL2::GFP}) was kindly provided by Douglas S. Kim. **pCG02** (p_{ggr-2::GCaMP6s::SL2::RFP}): pGP backbone was ligated to the p_{ggr-2} sequence from pWSC28, both cut with SphI and NotI-HF. **pCG03** (p_{ggr-2::flox::GCaMP6s::SL2::RFP}): pCG02 was linearized with SacII and ligated to the PCR product of pWSC24 with forward primer oCG11 (AAAGAATTCGGTACCGATAACTTCGTATAGCATACA) and reverse primer oCG12 (TGGCGCGCCGGCCCCGATAACTTCGTATAATGTATGC). **pWSC05** (p_{pnpr-9}): pPD95.79 was cut with Sall and PstI and ligated to a PCR product of a p_{pnpr-9} from N2 genomic DNA (forward primer, oWSC09: AGACTGCAGCGTCAAATGGAAAGGTTCCGCGCAT, reverse primer, oWSC10: GTCGACTTCTACGACATTTCCAGGAAGTAGCTCTAA), cut with PstI and Sall. A nested PCR protocol was run for the promoter fragment with the following outer primers: forward, oWSC13: ACGGAATGTGTCTGCAAAAGAAACGG, reverse, oWSC14: ACATTTCCCAACGACATTTCCAGG. **pWSC15** (p_{ggr-1::GFP}): pWSC05 was cut with Sall and HindIII and ligated to a PCR product of p_{grr-1} from N2 genomic DNA (forward primer, oWSC37: GAAATGAAATAAGCTTAGGCAACCGTGTGCTCTGGC, reverse primer, oWSC38: ATCCTCTAGAGTCGACTCAATAATTAAGTATGCAGTTGA), cut with HindIII and Sall. A nested PCR protocol was run for the promoter fragment with the following outer primers: forward, oWSC42: AGTGGGGTAAAGCTTGTCTAGGC, reverse, oWSC43: TCTGCCTGACCCAGGACGCA. **pWSC17** (p_{ggr-2::GFP}): pWSC05 was cut with Sall and SphI and ligated to a PCR product of p_{grr-2} from N2 genomic DNA (forward primer, oWSC40: AATGAAATAAGCTTGCATGCTCTTCCGGCAGATGCGCTGTT, reverse primer, oWSC41: ATCCTCTAGAGTCGACCGCTCGTGGTAAGACGTTATAGTT), cut with SphI and Sall. A nested PCR protocol was run for the promoter fragment with the following outer primers: forward, oWSC44: TCTCTCCGCGCTGACCAAGT, reverse, oWSC45: TGGCACCGGTTGCTCCTACT. **pWSC19** (p_{ggr-1::Cre}): pNP259 was cut with KpnI and HindIII and ligated to pWSC15, cut with HindIII and KpnI. **pWSC20** (p_{ggr-1::mCherry}): pWSC15 was cut with HindIII and Sall and ligated to pNP165, cut with XhoI and HindIII. **pWSC24** (p_{ggr-2::flox::Chr2(H134R)::mCherry::SL2::GFP}): pCoS6 was cut with Sall and SphI and ligated to pWSC17, cut with SphI and Sall. **pWSC28** (p_{ggr-2::GCaMP3}) pmyo-2::GCaMP3 was cut with MscI and SphI and ligated to the fragment of pWSC17, cut with SphI and MscI.

PCR for pharyngeal terminal bulb marker

The red fluorescent mCherry marker in the pharyngeal bulb of the pharynx (driven by the p_{ncx-10} promoter), used for tracking of the region containing RIS, was injected as a linear DNA construct, generated by fusion PCR with these primers: A (GTTCTTTCAACATTGCAAAAAGGCACCA), A' (TACACAGTTGCA GAGCGCTTTAATCAGA), B (ATCTTCTTACCCTTTGAGACCATTACCTGAAAAAGAAACAGTTG ATAAGCGGGT), C (ATGGTCTCAAAGGGTGAAG), D (ACGACGGCCAGTGAATTATC), D' (GGAAACAGTTATGTTTGGTATATTGGG).

C. elegans cultivation and transgenesis

C. elegans wild type (N2, Bristol strain) and transgenic animals were cultivated on either nematode growth medium (NGM) or high growth medium (HGM) plates seeded with *E. coli* OP-50-1 strain. We noted that at elevated temperature of 25°C, conditional transgene expression for RIS was observed also in additional, unwanted neurons, thus we kept animals (including larval stages) at 20°C at all times. In addition, 100 µM all-trans retinal (ATR; Sigma-Aldrich) were supplemented to *E. coli* prior to seeding for optogenetic experiments⁴⁰. Transgenic animals were generated following standard protocols. Extra-chromosomal array integration was performed by UV-exposure following standard protocols.

C. elegans strains

The following strains were used or generated for this study: **N2** (wild type isolate, Bristol strain), **HBR1777**: *goIs384[pflp-11::egl-1::SL2-mkate2-flp-11-3'utr, unc-119(+)]²²*, **ZX1466**: *lite-1(ce314)X; zxls55[p_{ggr-2::flox::Chr2(H134R)::mCherry::SL2::GFP}; p_{ggr-1::Cre}]*, **ZX1468**: *unc-47(e307)III; lite-1(ce314)X; zxls55[p_{ggr-2::flox::Chr2(H134R)::mCherry::SL2::GFP}; p_{ggr-1::Cre}]*, **ZX1469**: *unc-31(n1304)IV, lite-1(ce314)X; zxls55[p_{ggr-2::flox::Chr2(H134R)::mCherry::SL2::GFP}; p_{ggr-1::Cre}]*, **ZX1470**: *lite-1(ce314)X, zxls55[p_{ggr-2::flox::Chr2(H134R)::mCherry::SL2::GFP}; p_{ggr-1::Cre}]; pmyo-2::mCherry*]; *zxls52[pmyo-3::RCaMP]*, **ZX1561**: *zxls55[p_{ggr-2::flox::Chr2(H134R)::mCherry::SL2::GFP}; p_{ggr-1::Cre}]*, **ZX1577**: *lite-1(ce314)X; zEx360[p_{ggr-2::flox::Chr2(H134R)::mCherry::SL2::GFP}; p_{ggr-1::Cre}]*, **ZX1891**: *egl-3(gk238)X; lite-1(ce314)X; zEx360[p_{ggr-2::flox::Chr2(H134R)::mCherry::SL2::GFP}; p_{ggr-1::Cre}]*, **ZX2017**: *zxls60[p_{ggr-2::flox::GCaMP6s::SL2::tagRFP}; p_{ggr-1::nCre}]; zEx378[p_{ncx-10::mCherry}]*, **ZX2099**: *flp-11(tm2706)X, lite-1(ce314)X, zEx360[p_{ggr-2::flox::Chr2(H134R)::mCherry::SL2::GFP}; p_{ggr-1::Cre}]*, **ZX2140**: *unc-47(e307)III; flp-11(tm2706)X; lite-1(ce314)X; zEx360[p_{ggr-2::flox::Chr2(H134R)::mCherry::SL2::GFP}; p_{ggr-1::Cre}]*, **ZX2223**: *flp-11(tm2706)X, zEx1173[p_{ggr-2::flox::GCaMP6s::SL2::tagRFP}; p_{ggr-1::nCre}]; p_{ncx-10::mCherry}]*, **ZX2297**: *lite-1(ce314)X, zEx371[p_{ggr-1::Cre}, p_{ggr-2::flox::Chr2(H134R)::mCherry::SL2::GFP}, QUAS::jRCaMP1b, punc-17::QF, punc-4::QS]*.

Optogenetic stimulation and behavioral analysis

Locomotion parameters of freely moving animals were measured with a single worm tracking and illumination device described earlier⁶⁸. This tracking set up enabled accurately targeted illumination to specific body segments by a modified

liquid crystal display (LCD) projector, integrated with an inverted epifluorescence microscope. For optogenetics experiments animals were cultivated in the dark on NGM plates with *E. coli* OP50-1 and all-*trans*-retinal (ATR). NGM plates were freshly seeded a day in advance with 250 μ l of OP50 bacterial culture supplemented with ATR dissolved in 100% ethanol to a final concentration of 100 μ M. 5 minutes prior to analysis young adult animals were gently picked with an eyelash to unseeded NGM plates under dim red light (>600 nm) and maintained in the dark. Blue light of 470 nm and 1.8 mW/mm² intensity was used to stimulate ChR2 expressed in RIS. Light power quantification was performed with a power meter (PM100, Thorlabs, Newton, NY, USA) at the sample focal plane. All optogenetic experiments followed the same illumination protocol: 10 s tracking and behavioral acquisition (without blue light), subsequently 10 s targeted blue light illumination, followed by another 10 s of tracking without blue illumination. Only the anterior half of the animal was illuminated. Tracks were quality controlled by censoring data points from erroneously evaluated video frames. Briefly, a specialized workflow in KNIME (KNIME Desktop version 3.5, KNIME.com AG, Zurich, Switzerland) allowed data that passed the constraints (animals' speed below 1.25 mm/s and length deviation below 25 %, relative to the first five seconds of acquisition). Animals with more than 15 % of the data points censored were excluded from analysis.

Anterior and Posterior body length analysis

Single animals were picked onto the center of an unseeded NGM plate and a small spot of ink was painted with an eyelash on the cuticle of the worm, about 1/3 of the length of the animal relative to the head. Worms were recorded during unrestrained locomotion, using a 10x objective on an Axio Scope A1 (Zeiss). Videos were acquired by a DCC1545M camera (Thorlabs) with 3 s pre-stimulation, 5 s 470 nm at 0.9 mW/mm² RIS photoactivation and 3 s post-stimulation. Analysis was performed in ImageJ, blind to condition, where three frames were manually annotated: one frame before photostimulation, one in the middle of the 5 s photostimulation period and the last frame of post-stimulation. Two splines were tagged to the center line of the animal, ranging from the head or tail to the ink dot. The length of the dot was also quantified, as well as the length from head to tail. The relative elongation of the head, tail and full body splines were calculated in reference to the data before RIS photostimulation.

Ca²⁺ imaging microscope setup

An inverted fluorescence microscope (Axiovert 200, Zeiss, Germany) equipped with an MS 2000 motorized stage and PhotoTrack quadrant photomultiplier tube (both Applied Scientific Instrumentation, USA) was utilized for Ca²⁺ imaging, similar to a system described earlier. As excitation light sources two high-power light emitting diodes (LEDs; 470 and 590 nm wavelength, KSL 70, Rapp Optoelektronik, Germany) or a 100 W HBO mercury lamp were used. Simultaneous dual-wavelength acquisition was enabled by a Photometrics DualView- Λ beam splitter in combination with a Hamamatsu Orca Flash 4.0 sCMOS camera controlled by HCLImage Live (Hamamatsu) or MicroManager (version 1.4.13, <http://micro-manager.org>) software.

Ca²⁺ imaging in immobilized worms

Animals were immobilized on 10% M9 agar pads with polystyrene beads (Polysciences, USA) and imaged either by 25x (BWM) or 40x (Nerve Ring) oil objective lenses. The following light filter settings were used: GFP/mCherry Dualband ET Filterset (F56-019, AHF Analysentechnik, Germany), was combined with 532/18 nm and 625/15 nm emission filters and a 565 longpass beamsplitter (F39-833, F39-624 and F48-567, respectively, all AHF). ChR2 stimulation was performed using 1 mW/mm² blue light. To measure RCaMP fluorescence, 590 nm, 0.6 mW/mm² yellow light was used. The 4x4 binned images were acquired at 31 ms exposure time and 20 fps. Light illumination protocols were generated by a Lambda SC Smart shutter controller unit (Sutter Instruments, USA), using its TTL output to drive the LED power supply or to open a shutter when using the HBO lamp. Video synchronization was achieved by cropping the acquisition to obtain equally sized time bins before, during and after blue light exposure. Image analysis was performed in ImageJ (NIH), called by a custom KNIME workflow, after manual annotation of regions of interest (ROIs). Spline ROIs were selected for the BWM cells or ventral nerve cord to nerve ring region and the kymographs were generated by averaging a 7x7x7 moving voxel across the ROI. A ventral and a dorsal BWM ROI were defined, and their periodicity data was averaged for the analysis of a single animal. Additionally, an elliptic ROI was selected for background fluorescence exclusion. Mean intensity values for each video frame were obtained and background fluorescence values were subtracted from the fluorescence values derived for RCaMP. Subtracted data was normalized to $\Delta F/F_0 = (F_i - F_0)/F_0$, where F_i represents the intensity at the given time point and F_0 represents the average fluorescence of the first second of the acquisition.

Signal autocorrelation analysis

Since spontaneous activity was not synchronized between animals, we introduced the metric of signal autocorrelation for calcium imaging as a means of describing perturbations in the Ca²⁺ dynamics of both, BWM and neurons. We observed that Ca²⁺ dynamics in undisturbed animals were periodic, albeit without a fixed frequency. This periodicity could be obtained by analyzing the signal correlation to itself, where peaks in the autocorrelation function were indicative of the period of Ca²⁺ dynamics. This was performed by a custom script in R called by a KNIME workflow. The R script calculated the autocorrelation of a smooth spline fit of the $\Delta F/F_0$ signal and searched for its peaks in window of 20 s of data to calculate the period of the autocorrelation. If no period could be found, it was set as the maximum of 1 in every 20 s. Hence, this function returned the period lower bound where confidence in the result can be guaranteed. Note that for the autocorrelation analysis only the signal differences over time, and not the absolute values, are taken into account. Thus, this analysis does not require prior signal normalization.

Axonal Ca²⁺ imaging of RIS in moving animals

For measuring spontaneous Ca^{2+} activity, a tracking system for single neuron Ca^{2+} imaging in moving animals¹³ was modified to allow axonal visualization with an improved temporal accuracy and signal to noise ratio. Animals expressing a GCaMP6 indicator exclusively in RIS were imaged for 60 seconds while moving undisturbed on transparent 1.5% agar pads in M9 buffer. A 25x/0.6 NeoFluar long-range air objective (Zeiss, Germany) was used to visualize the RIS neuron. Fluorescent measurements of GCaMP6 and mCherry were enabled using a GFP/mCherry Dualband ET Filterset (F56-019, AHF Analysentechnik, Germany), combined with 532/18 nm and 625/15 nm emission filters and a 565 longpass beamsplitter (F39-833, F39-624 and F48-567, respectively, all AHF). Tracking the animal's head was established by the PhotoTrack system (Applied Scientific Instrumentation, USA) that automatically repositions the motorized XY stage to keep a bright fluorescent marker in center of the field of view (FOV). By keeping the relative signal strength from each of the 4 sensors in a 4-quadrant photomultiplier tube (PMT) equal, via an analog system, millisecond precision is achieved⁵³. An oblique 625 shortpass beamsplitter (F38-625, AHF) was inserted in the light path to divert the long red wavelengths to the PMT. Pncx-10::mCherry was expressed in the terminal pharyngeal bulb to allow for robust tracking. To exclude longer wavelengths necessary for behavioral analysis, a 615/20 bandpass filter (F39-616, AHF) was also added in the lightpath to the PMT, thus improving tracking performance. Behavioral images to deduce the animals' body shape and orientation were obtained under far red illumination with a far-red 740nm LED filtered with a 690/50 bandpass filter (F47-690, AHF), and magnified with a 4x/0.1 long range objective positioned above the sample, optimized with an additional 0.5x demagnification tube lens. Data was acquired through the transparent agarose pad with a DCC1545M USB CCD camera (Thorlabs, Newton, NY, USA) controlled via uc480 ThorCam Software on a separate PC. To exclude the bright blue and yellow excitation light (necessary for calcium imaging) a 610-675nm bandpass filter was added in the behavioral acquisition light path. Synchronization of both camera's running with 30ms exposure time and the stage position reporting was done with a TTL start and stop trigger pulse sent by a Lambda SC Smart shutter controller unit (Sutter Instruments, USA). The synchronized combined data of 60s acquisitions enable behavioral quantification of parameters such as speed, velocity and acceleration along the midbody axis. This axis was determined by the pharyngeal bulb (kept in the center of the FOV of the behavioral camera due to tracking) and the centroid of the animal's body shape. Prior to differentiation, the stage coordinates of the fluorescent pharyngeal bulb in the moving head were corrected by the deviation of body centroid of the complete animal. The normalized velocity or speed in Fig. 6B, F and [Supplementary Fig. 5](#) were calculated by pairwise subtracting the mean values of the corresponding time periods for individual animals and dividing this by the average speed over the full 60s acquisition of that animal.

Image processing

Video files containing data of both fluorescent channels (for GCaMP6 and mCherry) were processed with custom written Mathematica notebooks (Wolfram Research, Inc., Champaign, IL, USA) as also depicted in Fig. 5B and [Supplementary Movie S5](#). Green and red fluorescent channels were digitally overlaid to accurately correct the spatial alignment. As the structure tracked was not the cell body of RIS, but the pharyngeal terminal bulb of a moving animal, the RIS neuron image rotates around the center of the image. A data analysis pipeline was programmed to allow parallelized processing of multiple videos. First, the green fluorescent channel was cropped to around the respective position of the pharyngeal bulb. Next, images were thresholded to locate the centroid of the moving neuronal cell bodies in every frame of the video. The cell body was then repositioned to overlay its position in all frames and rotated after measuring the angular orientation to horizontal of both gut autofluorescence, as well as the brightest regions of the axon (by binarizing a smaller ROI after masking the gut). Subsequently, also the dorso-ventral axis was determined. In this way, a ROI containing the entire RIS morphology was cropped and rotated in each image such that the axon is always oriented in the same direction. At last, a parabola was fitted through the neuronally shaped image components. Alongside this parabola about 25 equally spaced points were determined to generate rectangular ROIs perpendicular to it. Mean fluorescent intensity was measured in these sub-ROIs (5x25 pixels) and subtracted by the median intensity of two adjacent smaller regions above and below each of these (3x5 pixels) to correct for local differences in background along the axon. Finally, these values were resampled to 100 values representing the percentagewise segments along the axon to correct for stretching of the axon. The $\Delta F/F$ traces in Fig. 5C, D are the mean values of the 50 most anterior segments of RIS covering the nerve ring region represented as $\Delta F/F = (F_i - F_{\text{mean}})/F_{\text{mean}}$, where F_{mean} is the mean fluorescent intensity during the first 2 seconds of acquisition. Fluorescent heatmaps in Fig. 5C, D display min-max normalized values (for each segment of each video normalized over time by $F_{\text{norm},i} = (F_i - F_{\text{min}})/(F_{\text{min}} - F_{\text{max}})$ to account for variation in the mean intensity of each segment) that are smoothed over 4 frames with a meanfilter. Fig. 5E displays the mean of 45 aligned normalized fluorescence time windows 6 seconds prior and post manually assigned Ca^{2+} peak events. The normalized fluorescent traces in Fig. 6B, F are the means \pm SEM of event-aligned 6 s time windows of min-max normalized traces that consists of the mean fluorescence intensity of the 50 nerve ring segments.

Calcium dynamics to behavior correlation analysis

Conditional probability density functions (in Fig. 6A, E) of the shortest unbiased time lag to either a reversal or a given Ca^{2+} peak event or vice versa, were found by Gaussian kernel density estimation with bandwidth 1s and aligned to the conditional event (Ca^{2+} peak or reversal respectively). Cross-correlation analyses (Fig. 6C, G) were performed in Mathematica by calculating Pearson's correlation functions for equally sized 6 s time windows of both normalized fluorescent change and acceleration time shifted up to 3 s time lags.

Electrophysiology

Recordings from dissected body wall muscle cells anterior to the vulva at the ventral side are described in⁴⁰. Light activation was performed using an LED lamp (KSL-70, Rapp OptoElectronic, Hamburg, Germany; 470 nm, 8 mW/mm²) and controlled by an EPC10 amplifier and Patchmaster software (HEKA, Germany). mPSC analysis was done by Mini Analysis software (Synaptosoft, Decatur, GA, USA, version 6.0.7). Amplitude and mean number of mPSC events per second were analyzed for each 10 s before, 10 s during and 10 s after illumination.

Electropharyngeograms

Electropharyngeogram recording was performed as previously described⁶⁹. Animals were selected on the day prior to measurement as L4 larvae. The head was cut away from the body with a scalpel at about one third to half of the body length. The tip of the worm head was sucked under 100-fold magnification into an EPG-suction electrode, connected via a silver-chloride coated silver wire to an EPC-10 amplifier (Heka, Germany). Prior to measurement, the preparation was incubated in 2 μ M serotonin for 5 min to induce pharyngeal pumping. EPG recordings were performed by PatchMaster software (Heka). We recorded spontaneous pumping for 30 s prior to 30 s of RIS::ChR2 depolarization via 3 mW/mm² (470 nm) light and further 30 s post stimulus. We used Review software (Buxton Corporation, USA) to convert from PatchMaster to ABF files. Pump rate and duration were analyzed by AutoEPG58 (kindly provided by C. James, Embody Biosignals Ltd., UK).

Statistics

Statistical analysis was performed in Prism (Version 5.01, GraphPad Software, Inc.), Mathematica (version 10, Wolfram Research, Inc., Champaign, IL, USA), OriginPro 2015G (OriginLab Corporation, Northampton, USA), or R (version 3.3.2), the latter called by RStudio (version 1.0.136, RStudio, Inc.) or KNIME (Desktop version 3.5, KNIME.com AG, Zurich, Switzerland). No statistical methods were applied to predetermine sample size. However, sample sizes reported here are consistent to data presented in previous publications. Data was tested for normality prior to statistical inference. Data is given as means \pm SEM when not otherwise stated. Significance between data sets after paired or two-tailed Student's t-test is given as p-value (* $p \leq 0.05$; ** $p \leq 0.01$; *** $p \leq 0.001$), when not otherwise stated. For other statistical test used, see figure legends.

Data, reagent and code availability

All data are provided as supplementary information. Reagents and code are available upon request.

2.6 References

1. Vetrivelan R, Chang C, Lu J. Muscle tone regulation during REM sleep: neural circuitry and clinical significance. *Arch Ital Biol* **149**, 348-366 (2011).
2. Clément O, *et al.* The lateral hypothalamic area controls paradoxical (REM) sleep by means of descending projections to brainstem GABAergic neurons. *J Neurosci* **32**, 16763–16774 (2012).
3. Kiehn O. Development and functional organization of spinal locomotor circuits. *Curr Opin Neurobiol* **21**, 100-109 (2011).
4. Talpalar AE, Bouvier J, Borgius L, Fortin G, Pierani A, Kiehn O. Dual-mode operation of neuronal networks involved in left-right alternation. *Nature* **500**, 85-88 (2013).
5. Kiehn O. Decoding the organization of spinal circuits that control locomotion. *Nat Rev Neurosci* **17**, 224-238 (2016).
6. Caggiano V, *et al.* Midbrain circuits that set locomotor speed and gait selection. *Nature* **553**, 455-460 (2018).
7. Li WC, Roberts A, Soffe SR. Locomotor rhythm maintenance: electrical coupling among premotor excitatory interneurons in the brainstem and spinal cord of young *Xenopus* tadpoles. *J Physiol* **587**, 1677-1693 (2009).
8. Bouvier J, *et al.* Descending command neurons in the brainstem that halt locomotion. *Cell* **163**, 1191-1203 (2015).
9. Ampatzis K, Song J, Ausborn J, El Manira A. Separate microcircuit modules of distinct V2a interneurons and motoneurons control the speed of locomotion. *Neuron* **83**, 934–943 (2014).
10. Juvin L, Grätsch S, Trillaud-Doppia E, Gariépy J-F, Büschges A, Dubuc R. A specific population of reticulospinal neurons controls the termination of locomotion. *Cell reports* **15**, 2377–2386 (2016).
11. Tastekin I, *et al.* Sensorimotor pathway controlling stopping behavior during chemotaxis in the *Drosophila melanogaster* larva. *eLife* **7**, e38740 (2018).
12. Cande J, *et al.* Optogenetic dissection of descending behavioral control in *Drosophila*. *eLife* **7**, e34275 (2018).
13. Ritson EJ, Li W-C. The neuronal mechanisms underlying locomotion termination. *Curr Opin Physiol* **8**, 109-115 (2019).
14. Fouad AD, *et al.* Distributed rhythm generators underlie *Caenorhabditis elegans* forward locomotion. *eLife* **7**, e29913 (2018).
15. Gao S, *et al.* Excitatory motor neurons are local oscillators for backward locomotion. *eLife* **7**, e29915 (2018).
16. Xu T, *et al.* Descending pathway facilitates undulatory wave propagation in *Caenorhabditis elegans* through gap junctions. *Proc Natl Acad Sci U S A* **115**, E4493-E4502 (2018).
17. Wen Q, Gao S, Zhen M. *Caenorhabditis elegans* excitatory ventral cord motor neurons derive rhythm for body undulation. *Philos Trans R Soc Lond B Biol Sci* **373**, (2018).
18. Tolstenkov O, *et al.* Functionally asymmetric motor neurons contribute to coordinating locomotion of *Caenorhabditis elegans*. *eLife* **7**, e34997 (2018).
19. Luppi PH, *et al.* The neuronal network responsible for paradoxical sleep and its dysfunctions causing narcolepsy and rapid eye movement (REM) behavior disorder. *Sleep medicine reviews* **15**, 153-163 (2011).
20. Raizen DM, *et al.* Lethargus is a *Caenorhabditis elegans* sleep-like state. *Nature* **451**, 569–572 (2008).
21. Hill AJ, Mansfield R, Lopez JMNG, Raizen DM, van Buskirk C. Cellular stress induces a protective sleep-like state in *C. elegans*. *Curr Biol* **24**, 2399–2405 (2014).
22. Wu Y, Masurat F, Preis J, Bringmann H. Sleep counteracts aging phenotypes to survive starvation-induced developmental arrest in *C. elegans*. *Curr Biol*, 3610-3624 (2018).
23. Nath RD, Chow ES, Wang H, Schwarz EM, Sternberg PW. *C. elegans* stress-induced sleep emerges from the collective action of multiple neuropeptides. *Curr Biol* **26**, 2446–2455 (2016).
24. Nelson MD, *et al.* The neuropeptide NLP-22 regulates a sleep-like state in *Caenorhabditis elegans*. *Nature communications* **4**, 2846 (2013).
25. Turek M, Lewandrowski I, Bringmann H. An AP2 transcription factor is required for a sleep-active neuron to induce sleep-like quiescence in *C. elegans*. *Curr Biol* **23**, 2215-2223 (2013).
26. Turek M, Besseling J, Spies JP, König S, Bringmann H. Sleep-active neuron specification and sleep induction require FLP-11 neuropeptides to systemically induce sleep. *eLife* **5**, e12499 (2016).
27. Yew JY, Davis R, Dikler S, Nanda J, Reinders B, Stretton AO. Peptide products of the *afp-6* gene of the nematode *Ascaris suum* have different biological actions. *J Comp Neurol* **502**, 872-882 (2007).
28. Appelbaum L, *et al.* Sleep-wake regulation and hypocretin-melatonin interaction in zebrafish. *Proc Natl Acad Sci U S A* **106**, 21942–21947 (2009).
29. Saper CB, Chou TC, Scammell TE. The sleep switch: hypothalamic control of sleep and wakefulness. *Trends Neurosci* **24**, 726–731 (2001).
30. Lin L, *et al.* The sleep disorder canine narcolepsy is caused by a mutation in the hypocretin (orexin) receptor 2 gene. *Cell* **98**, 365–376 (1999).
31. Caers J, Verlinden H, Zels S, Vandersmissen HP, Vuerinckx K, Schoofs L. More than two decades of research on insect neuropeptide GPCRs: an overview. *Frontiers in endocrinology* **3**, 151 (2012).
32. Choi S, Chatzigeorgiou M, Taylor KP, Schafer WR, Kaplan JM. Analysis of NPR-1 reveals a circuit mechanism for behavioral quiescence in *C. elegans*. *Neuron* **78**, 869–880 (2013).
33. Chen D, Taylor KP, Hall Q, Kaplan JM. The neuropeptides FLP-2 and PDF-1 act in concert to arouse *Caenorhabditis elegans* locomotion. *Genetics* **204**, 1151-1159 (2016).
34. Chew YL, *et al.* An afferent neuropeptide system transmits mechanosensory signals triggering sensitization and arousal in *C. elegans*. *Neuron* **99**, 1233-1246.e1236 (2018).
35. You Y-j, Kim J, Raizen DM, Avery L. Insulin, cGMP, and TGF-beta signals regulate food intake and quiescence in *C. elegans*: a model for satiety. *Cell metabolism* **7**, 249–257 (2008).
36. Pierce-Shimomura JT, Morse TM, Lockery SR. The fundamental role of pirouettes in *Caenorhabditis elegans* chemotaxis. *J Neurosci* **19**, 9557-9569 (1999).

37. Donnelly JL, *et al.* Monoaminergic orchestration of motor programs in a complex *C. elegans* behavior. *PLoS Biol* **11**, e1001529 (2013).
38. Roberts WM, *et al.* A stochastic neuronal model predicts random search behaviors at multiple spatial scales in *C. elegans*. *eLife* **5**, e12572 (2016).
39. Stephens GJ, Johnson-Kerner B, Bialek W, Ryu WS. Dimensionality and dynamics in the behavior of *C. elegans*. *PLoS Comput Biol* **4**, e1000028 (2008).
40. Liewald JF, *et al.* Optogenetic analysis of synaptic function. *Nat Methods* **5**, 895-902 (2008).
41. Spies J, Bringmann H. Automated detection and manipulation of sleep in *C. elegans* reveals depolarization of a sleep-active neuron during mechanical stimulation-induced sleep deprivation. *Scientific reports* **8**, 9732 (2018).
42. Raizen DM, Avery L. Electrical activity and behavior in the pharynx of *C. elegans*. *Neuron* **12**, 483-495 (1994).
43. Akerboom J, *et al.* Genetically encoded calcium indicators for multi-color neural activity imaging and combination with optogenetics. *Frontiers in molecular neuroscience* **6**, 2 (2013).
44. Fang-Yen C, Wasserman SM, Sengupta P, Samuel ADT. Agarose immobilization of *C. elegans*. *Worm Breeder's Gazette* **18**, (2009).
45. Wen Q, *et al.* Proprioceptive coupling within motor neurons drives *C. elegans* forward locomotion. *Neuron* **76**, 750-761 (2012).
46. Karbowski J, Cronin CJ, Seah A, Mendel JE, Cleary D, Sternberg PW. Conservation rules, their breakdown, and optimality in *Caenorhabditis* sinusoidal locomotion. *Journal of theoretical biology* **242**, 652-669 (2006).
47. Prevedel R, *et al.* Simultaneous whole-animal 3D imaging of neuronal activity using light-field microscopy. *Nat Methods* **11**, 727-730 (2014).
48. Li Z, Liu J, Zheng M, Xu XZ. Encoding of both analog- and digital-like behavioral outputs by one *C. elegans* interneuron. *Cell* **159**, 751-765 (2014).
49. White JG, Southgate E, Thomson JN, Brenner S. The structure of the nervous system of the nematode *Caenorhabditis elegans*. *Philos Trans R Soc Lond B Biol Sci* **314**, 1-340 (1986).
50. Altun ZF, Chen BJ, Wang ZW, Hall DH. High resolution map of *Caenorhabditis elegans* gap junction proteins. *Dev Dynam* **238**, 1936-1950 (2009).
51. Starich TA, Xu J, Skerrett IM, Nicholson BJ, Shaw JE. Interactions between innexins UNC-7 and UNC-9 mediate electrical synapse specificity in the *Caenorhabditis elegans* locomotory nervous system. *Neural Dev* **4**, 16 (2009).
52. Bhattacharya A, Aghayeva U, Berghoff EG, Hobert O. Plasticity of the electrical connectome of *C. elegans*. *Cell* **176**, 1174-1189 e1116 (2019).
53. Alkema MJ, Hunter-Ensor M, Ringstad N, Horvitz HR. Tyramine functions independently of octopamine in the *Caenorhabditis elegans* nervous system. *Neuron* **46**, 247-260 (2005).
54. Piggott BJ, Liu J, Feng Z, Wescott SA, Xu XZS. The neural circuits and synaptic mechanisms underlying motor initiation in *C. elegans*. *Cell* **147**, 922-933 (2011).
55. Pirri JK, McPherson AD, Donnelly JL, Francis MM, Alkema MJ. A tyramine-gated chloride channel coordinates distinct motor programs of a *Caenorhabditis elegans* escape response. *Neuron* **62**, 526-538 (2009).
56. Gordus A, Pokala N, Levy S, Flavell SW, Bargmann CI. Feedback from network states generates variability in a probabilistic olfactory circuit. *Cell* **161**, 215-227 (2015).
57. Husson SJ, Clynen E, Baggerman G, Janssen T, Schoofs L. Defective processing of neuropeptide precursors in *Caenorhabditis elegans* lacking proprotein convertase 2 (KPC-2/EGL-3): mutant analysis by mass spectrometry. *J Neurochem* **98**, 1999-2012 (2006).
58. Sieburth D, Madison JM, Kaplan JM. PKC-1 regulates secretion of neuropeptides. *Nat Neurosci* **10**, 49-57 (2007).
59. Faumont S, *et al.* An image-free opto-mechanical system for creating virtual environments and imaging neuronal activity in freely moving *Caenorhabditis elegans*. *PLoS One* **6**, e24666 (2011).
60. Gray JM, Hill JJ, Bargmann CI. A circuit for navigation in *Caenorhabditis elegans*. *Proc Natl Acad Sci U S A* **102**, 3184-3191 (2005).
61. Wicks SR, Rankin CH. Integration of mechanosensory stimuli in *Caenorhabditis elegans*. *J Neurosci* **15**, 2434-2444 (1995).
62. Beg AA, Jorgensen EM. EXP-1 is an excitatory GABA-gated cation channel. *Nat Neurosci* **6**, 1145-1152 (2003).
63. Sales-Carbonell C, *et al.* No discrete start/stop signals in the dorsal striatum of mice performing a learned action. *Curr Biol* **28**, 3044-3055.e3045 (2018).
64. Ferreira-Pinto MJ, Ruder L, Capelli P, Arber S. Connecting circuits for supraspinal control of locomotion. *Neuron* **100**, 361-374 (2018).
65. Atkinson LE, *et al.* Unraveling flp-11/flp-32 dichotomy in nematodes. *Int J Parasitol* **46**, 723-736 (2016).
66. Madelaine R, *et al.* The hypothalamic NPVF circuit modulates ventral raphe activity during nociception. *Scientific reports* **7**, 41528 (2017).
67. Schmitt C, *et al.* Specific expression of channelrhodopsin-2 in single neurons of *Caenorhabditis elegans*. *PLoS ONE* **7**, e43164 (2012).
68. Stirman JN, *et al.* Real-time multimodal optical control of neurons and muscles in freely behaving *Caenorhabditis elegans*. *Nat Methods* **8**, 153-158 (2011).
69. Schuler C, Fischer E, Shalitel L, Steuer Costa W, Gottschalk A. Arrhythmogenic effects of mutated L-type Ca(2+)-channels on an optogenetically paced muscular pump in *Caenorhabditis elegans*. *Scientific reports* **5**, 14427 (2015).
70. O'Gara BA, Friesen WO. Termination of leech swimming activity by a previously identified swim trigger neuron. *J Comp Physiol A* **177**, 627-636 (1995).
71. Gratsch S, *et al.* A brainstem neural substrate for stopping locomotion. *J Neurosci* **39**, 1044-1057 (2019).
72. Capelli P, Pivetta C, Soledad Esposito M, Arber S. Locomotor speed control circuits in the caudal brainstem. *Nature* **551**, 373-377 (2017).
73. Bringmann H. Sleep-active neurons: Conserved motors of sleep. *Genetics* **208**, 1279-1289 (2018).

”

Chapter 3:

RPamide neuropeptides NLP-22 and NLP-2 act through GnRH-like receptors to promote sleep and wakefulness in *C. elegans*

The content of this chapter was published in the open access, scientifically peer-reviewed journal *Scientific Reports*:

Petrus Van der Auwera^{1,4¶}, Lotte Frooninckx^{1¶}, Kristen Buscemi², Ryan T. Vance², Jan Watteyne¹, Olivier Mirabeau³, Liesbet Temmerman¹, Wouter De Haes¹, Luca Fancsalszky¹, Alexander Gottschalk⁴, David M. Raizen⁵, Matthew D. Nelson², Liliane Schoofs^{1*}, Isabel Beets^{1*} (2020). RPamide neuropeptides NLP-22 and NLP-2 act through GnRH-like receptors to promote sleep and wakefulness in *C. elegans*. *Scientific Reports*, 10, 9929. <https://doi.org/10.1038/s41598-020-66536-2>

General author contributions:

LF, PVdA, OM, MDN, DMR, LS and IB conceived the study. LF, PVdA, OM, MDN, RTV, KB, JW, LF performed the experiments. PVdA, LF, OM, MDN, JW, LT and WDH analysed the data. PVdA, LF, LS, IB wrote the paper. All authors revised and edited the paper. MDN, AG, DMR, LS, and IB supervised the study and secured funding.



Extended contribution statement of PVdA.

PVdA wrote the complete manuscript (starting from an initial draft from LF) and he proofread it multiple times with additions of MDN, AG, DMR, LS and IB. PVdA made the following figures in the manuscript: Figs. 2, 3, 4, 5a-d, 5g-j and 6 as well as Supplementary Figs. S1, S2, S3, S4b, S5, S6, S8 and S10. PVdA performed the preparations for experimental data in Figs. 4, 5a-d and 5g-j and performed experiments in Fig. 6A and Supplementary Figs. S4b and S6 himself. He also did all the statistics except for data in Fig. 1.

SCIENTIFIC REPORTS

Article | [Open Access](#) | Published: 18 June 2020

RPamide neuropeptides NLP-22 and NLP-2 act through GnRH-like receptors to promote sleep and wakefulness in *C. elegans*

Petrus Van der Auwera, Lotte Froominckx, Kristen Buscemi, Ryan T. Vance, Jan Watteyne, Olivier Mirabeau, Liesbet Temmerman, Wouter De Haes, Luca Fancsalszky, Alexander Gottschalk, David M. Raizen, Matthew D. Nelson, Liliane Schoofs  & Isabel Beets 

Scientific Reports **10**, Article number: 9929 (2020) | [Cite this article](#)

This is a RoMEO Green journal. <http://sherpa.ac.uk/romeo/search.php>

Author affiliations

¹Department of Biology, KU Leuven, Naamsestraat 59, 3000 Leuven, Belgium

²Department of Biology, Saint Joseph's University, 5600 City Ave, Philadelphia, PA 19131, USA

³Institut Curie, Inserm U830, 26 rue d'Ulm, 75248 Paris, France

⁴Buchmann Institute for Molecular Life Sciences (BMLS), Goethe University, Max-von-Laue-Strasse 15, D-60438 Frankfurt, Germany

⁵Department of Neurology, Perelman School of Medicine, University of Pennsylvania, 415 Curie Blvd, Philadelphia, PA 19104, USA

† These authors contributed equally.

* Corresponding authors contributed equally.

The authors declare no competing interests.

“

3.1 Abstract

Sleep and wakefulness are fundamental behavioral states of which the underlying molecular principles are becoming slowly elucidated. Transitions between these states require the coordination of multiple neurochemical and modulatory systems. In *Caenorhabditis elegans* sleep occurs during a larval transition stage called lethargus and is induced by somnogenic neuropeptides. Here, we identify two opposing neuropeptide/receptor signaling pathways: NLP-22 promotes behavioral quiescence, whereas NLP-2 promotes movement during lethargus, by signaling through gonadotropin-releasing hormone (GnRH) related receptors. Both NLP-2 and NLP-22 belong to the RPamide neuropeptide family and share sequence similarities with neuropeptides of the bilaterian GnRH, adipokinetic hormone (AKH) and corazonin family. RPamide neuropeptides dose-dependently activate the GnRH/AKH-like receptors GNRR-3 and GNRR-6 in a cellular receptor activation assay. In addition, *nlp-22*-induced locomotion quiescence requires the receptor *gnrr-6*. By contrast, wakefulness induced by *nlp-2* overexpression is diminished by deletion of either *gnrr-3* or *gnrr-6*. *nlp-2* is expressed in a pair of olfactory AWA neurons and cycles with larval periodicity, as reported for *nlp-22*, which is expressed in RIA. Our data suggest that the somnogenic NLP-22 neuropeptide signals through GNRR-6, and that both GNRR-3 and GNRR-6 are required for the wake-promoting action of NLP-2 neuropeptides.

3.2 Introduction

Sleep is an essential quiescent state, conserved at the molecular level across distantly related animals¹⁻⁵. Because animals display a remarkable diversity of sleep traits, a consensus definition for sleep-like states has been set based on behavioral changes shared with human sleep. These include behavioral quiescence, reduced sensory responsiveness, reversibility, the assumption of a specific posture, and homeostatic regulation^{1,4,6,7}. Sleep deprivation is detrimental to diverse biological processes, including metabolism, longevity, and memory formation⁸⁻¹¹.

Genetic studies in model organisms such as mice, zebrafish, *Drosophila* and *C. elegans* have provided powerful ways to dissect core mechanisms of sleep-like states that are evolutionarily conserved across these species^{1-3,6,10}. A well-known example is the circadian protein PERIOD that regulates the timing of sleep^{12,13}. Other conserved sleep pathways include epidermal growth factor (EGF) and notch signaling¹⁴⁻¹⁶. Conserved wake-promoting pathways include dopamine and pigment dispersing factor (PDF) signaling¹⁷⁻¹⁹. How these

sleep and wake pathways interact is still unclear (for review, see^{3,4,18}). Mounting evidence indicates that sleep-wake transitions require the coordination of several brain regions and engage multiple neurochemical systems, including biogenic amines^{1,17,20} and neuropeptides^{19,21}. In mammals, hypothalamic orexin/hypocretin neuropeptides promote wakefulness, while galanin neuropeptides and melanin-concentrating hormone (MCH) are involved in REM sleep^{22,23}. In zebrafish, the neuropeptides neuromedin U and neuropeptide Y are wake- and sleep-promoting, respectively^{24,25}. In *Drosophila*, the neuropeptides amnesiac, myoinhibitory peptide, neuropeptide F, short neuropeptide F and SIFamide all promote sleep^{19,26,27}, whereas PDF promotes arousal^{28–30}.

The nematode *Caenorhabditis elegans* sleeps during lethargus, a period of behavioral quiescence that occurs before each larval molt and that meets behavioral criteria of sleep^{2,31–37}. *C. elegans* lethargus has been characterized as a global quiescent brain state with distinct gene expression in sleep-active neurons^{37–39}. Many of the sleep-regulatory pathways identified in vertebrates and insects are conserved in *C. elegans* and sleep-like quiescence during lethargus shows fundamental similarities to sleep in other animals⁴. Neuropeptidergic signaling systems conserved in *C. elegans* comprise the PDF orthologous system PDF-1/PDFR-1 and the RFamide neuropeptide system FLP-2/FRPR-18, which promote arousal by increasing sensory activity^{30,40}. Inhibition of these wake-promoting neuropeptides by FLP-18/NPR-1 and FLP-21/NPR-1 signaling reduces sensory responsiveness during lethargus²¹. Two other neuropeptides are known to play a somnogenic role in lethargus: FLP-11, expressed in the GABAergic RIS interneuron, and NLP-22, expressed in the glutamatergic RIA interneurons^{39,41}. FLP-11 seems to signal through multiple receptors including FRPR-3, NPR-4 and NPR-22³⁹, whereas the molecular target(s) of NLP-22 have remained elusive.

The established role of RFamide neuropeptides as regulators of sleep in both *C. elegans* and *Drosophila* led to the discovery of a sleep-promoting function for the hypothalamic RFamide neuropeptide VF (NPVF also known as RFRP-1/2/3) in zebrafish larvae⁴². NPVF is also called Gonadotropin-Inhibitory Hormone (GnIH) because it suppresses Gonadotropin-Releasing Hormone (GnRH) synthesis and release⁴³. Accumulating evidence indicates that also GnRH-like signaling regulates sleep in the central nervous system. In *Drosophila*, GnRH-like signaling is required for starvation-induced sleep suppression^{44,45}. In addition, a likely downstream effector of this GnRH-like signaling pathway, salt-inducible kinase 3 (SIK3), is a conserved regulator of sleep^{46–48}. Strong interconnections between

GnRH signaling and the hypocretin/orexin neuronal circuits controlling sleep/wake states have been reported in vertebrates^{49,50}. Human patients with primary insomnia also display altered GnRH levels⁵¹.

In 2009, we discovered that an adipokinetic hormone (AKH)-like neuropeptide signals through a GnRH-like receptor in *C. elegans*.⁵² Based on this finding, we postulated that the insect AKH and the vertebrate GnRH systems share a common evolutionary origin in bilaterian animals^{52,53}. Additional studies later confirmed that AKH, corazonin and GnRH indeed belong to the same superfamily of GnRH-like neuropeptides, members of which occur in all bilaterian animals^{54–56}. GnRH/AKH-like peptides are involved in energy homeostasis⁵⁷ and control carbohydrate and lipid metabolism in insects⁵⁸. In *C. elegans* a recent study showed that lipid mobilization promotes sleep⁵⁹. These data, together with the growing evidence for a role of vertebrate GnRH in the regulation of sleep, led us to hypothesize that *C. elegans* GnRH-like signaling may be involved in sleep regulation. The *C. elegans* genome encodes eight GnRH-like G protein-coupled receptors (GPCRs)^{60,61}, the majority of which is still orphan, i.e. an endogenous ligand has not yet been identified. Here we show that two of these GNRRs are activated by the RPamide neuropeptides NLP-22 and NLP-2, displaying sequence similarities to GnRH/AKH-like peptides, and demonstrate that they act opposingly to control sleep and wakefulness in *C. elegans*.

3.3 Results

3.3.1 The *C. elegans* genome encodes eight GnRH/AKH-related receptors

Using characterized GnRH/AKH receptors as a query in a protein BLAST search⁶², we identified eight putative GnRH/AKH-like receptors in *C. elegans* (GNRR-1 to GNRR-7 and DAF-38/GNRR-8). Phylogenetic analysis showed that these receptors are orthologs of the GnRH/AKH receptor family, as they cluster together with other ecdysozoan GnRH/AKH receptors (**Fig. 1**). The nematode cluster can be subdivided in two groups consisting of GNRR-1, which is located more basal to the clade node, and a paralogous group formed by 7 other GnRH/AKH-like receptors. GNRR-1 was identified as a receptor for NLP-47, a GnRH/AKH neuropeptide ortholog in *C. elegans*, and has been the only characterized GNRR so far⁵². The other GnRH/AKH-like receptors are still orphan receptors, i.e. GPCRs with no known peptide ligand. Only DAF-38/GNRR-8 is known to mediate the response to ascaroside pheromones that control dauer entry when it heterodimerizes with the DAF-37 chemoreceptor⁶³.

3.3.2 RPamide neuropeptides activate GNRR-3 and GNRR-6 *in vitro*

Transmembrane topology prediction revealed that GNRR-1 to -3, GNRR-5 to -7 and DAF-38/GNRR-8 have seven alpha-helical transmembrane domains, typical for GPCRs ([Supplementary Fig. S1 online](#)). We tested a *C. elegans* peptide library for the ability to activate these seven receptors using an *in vitro* calcium mobilization assay. We cloned and transiently expressed each of the seven GNRRs in Chinese hamster ovary (CHO) cells stably expressing apo-aequorin and the human promiscuous $G\alpha_{16}$ protein. These cells were challenged with a synthetic library of over 340 *C. elegans* peptides of the RFamide (FLP) and neuropeptide-like protein (NLP) families⁶⁴. Besides the known NLP-47/GNRR-1 interaction⁵², only GNRR-3 and GNRR-6 displayed a functional response in this assay (**Fig. 2**). Of all peptides tested, only peptides encoded by the genes *nlp-2* (NLP-2-1, NLP-2-2, NLP-2-3), *nlp-22* (NLP-22) and *nlp-23* (NLP-23-2) activated these receptors in a dose-dependent manner, although with different potencies.

Peptides encoded by *nlp-2* and *nlp-23* potently activated GNRR-3 with EC_{50} values in the nanomolar range. By contrast, NLP-22 activated GNRR-3 with far lower potency (EC_{50} value > 6 μ M), which may be physiologically irrelevant. GNRR-6 was potently activated by NLP-22 and NLP-23 peptides. Peptides encoded by *nlp-2* also activated GNRR-6, although with a higher EC_{50} value than NLP-22 and NLP-23. None of these neuropeptides elicited a calcium response in cells transfected with an empty vector as a negative control, indicating that the responses are specific to the expressed receptors ([Supplementary Fig. S2 online](#)). When GNRR-3 or GNRR-6 were expressed in cells devoid of the promiscuous $G\alpha_{16}$ subunit, a dose-dependent increase in aequorin luminescence was still observed upon addition of their peptide ligands, suggesting that GNRR-3 and GNRR-6 can couple to $G\alpha_q$ proteins expressed in these cells to elicit a calcium response ([Supplementary Fig. S3 online](#)). In short, we identified the neuropeptides encoded by *nlp-2*, *nlp-22* and *nlp-23* as bioactive ligands of the GnRH/AKH-like receptors GNRR-3 and GNRR-6 *in vitro*.

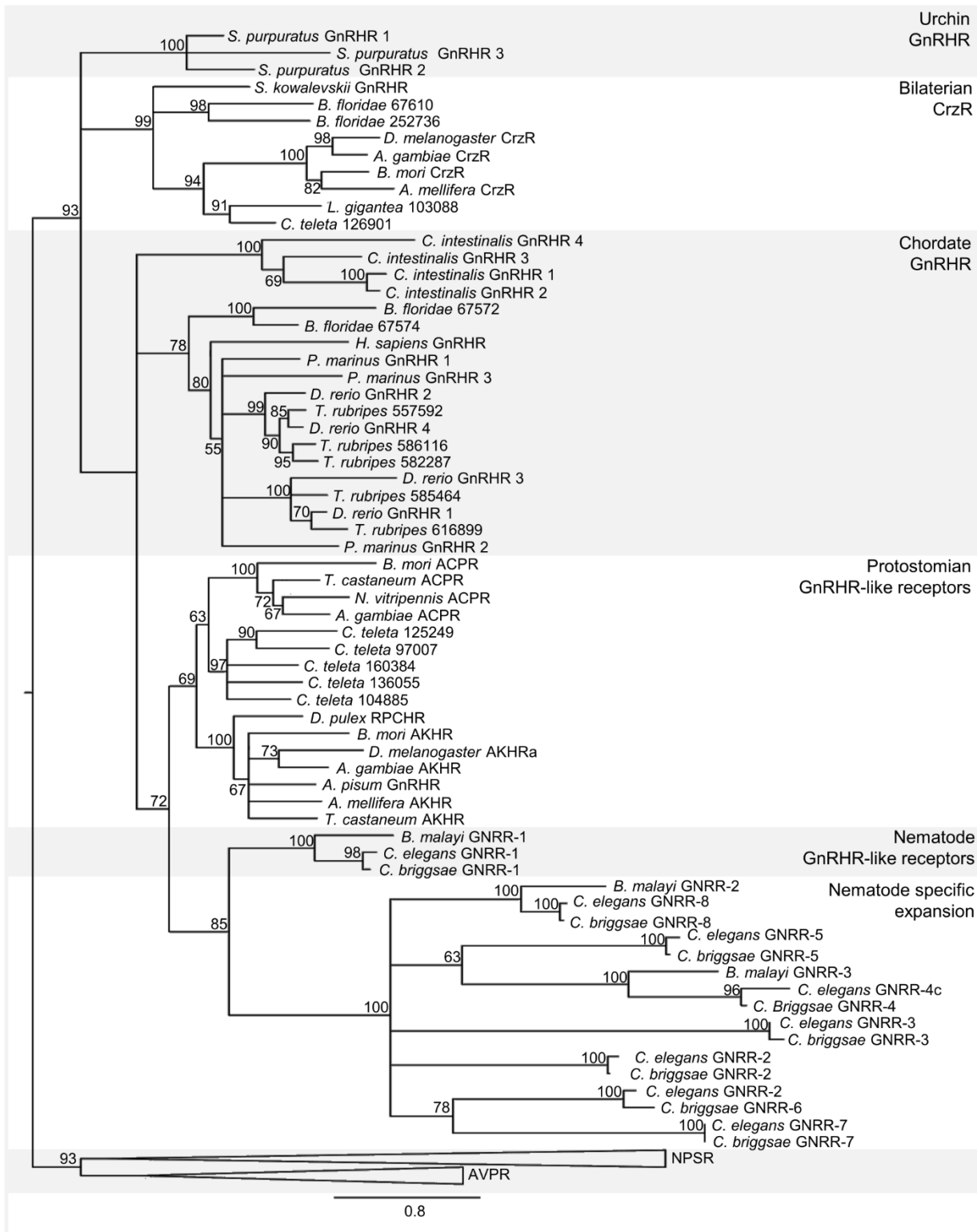


Figure 1: Maximum likelihood tree of vertebrate and invertebrate GnRH/AKH receptors.

Branch lengths indicate the expected number of substitutions per site. Node numbers are branch support values (%) derived from 100 non-parametric bootstraps. Accession numbers are provided in Materials and Methods. ACPR, adipokinetic hormone/corazonin related peptide receptor; AKHR, adipokinetic hormone receptor; AVPR, arginine vasopressin receptor; CrzR, corazonin receptor; GnRHR, gonadotropin-releasing hormone receptor; GNRR, gonadotropin-releasing hormone receptor related receptor; RPCHR, red-pigment concentrating hormone receptor; NPSR, neuropeptide S receptor.

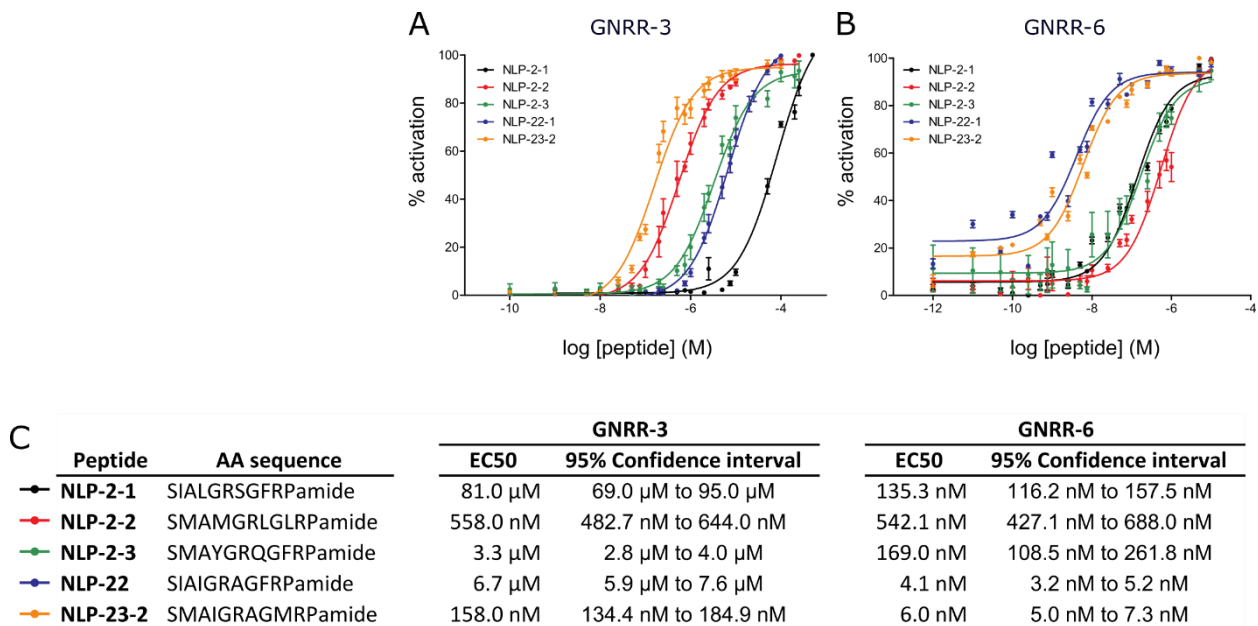


Figure 2: NLP-2, NLP-22, and NLP-23 peptides activate GNRR-3 and GNRR-6 *in vitro*.

Dose-response curves for GNRR-3 (**A**) and GNRR-6 (**B**) co-expressed in CHO cells with a promiscuous $G\alpha_{16}$ protein are shown as relative (%) to the highest value (100 % activation) after normalization to the total calcium response. Each data point represents the mean \pm SEM of N = 5-7 replicates for each peptide. (**C**) Amino acid (AA) sequences of RPamide neuropeptides activating GNRR-3 and GNRR-6 with their respective mean EC₅₀ values and 95% Confidence intervals.

Pattern and BLAST analyses of the FRPamides highlighted that also NLP-46 is a possible member of this RPamide neuropeptide family, which is evolutionarily well conserved among nematodes (**Fig. 3a**) and characterized by a C-terminal RPamide motif. The predicted neuropeptides encoded by *nlp-2*, *nlp-22*, *nlp-23* and *nlp-46* have recently been identified by mass spectrometry analysis⁶⁵, indicating that the predictions are correct. Besides the conserved C-terminus, nematode RPamides typically have an alanine residue at position three and conserved glycine and arginine residues at positions five and six, respectively (**Fig. 3a**). Many neuropeptidergic signaling systems are conserved throughout the Animal Kingdom and several orthologous neuropeptide-receptor pairs have been identified^{64,66–68}. In an attempt to deduce the phylogenetic origin of the nematode RPamides, we looked for degenerate motifs shared between RPamides and members of other known neuropeptide families. This search revealed a motif (G[F/W]XPG) near the C-terminus that is found in several members of the urbilaterian conserved GnRH/AKH neuropeptide family (**Fig. 3b** and [Supplementary Fig. S5 online](#)). Nematode GnRH/AKH-like neuropeptides derived from NLP-47, which activate the GnRH/AKH receptor ortholog GNRR-1⁵², lack this characteristic C-terminal motif. By contrast, NLP-47 peptides share an N-terminal pyroglutamate residue and [FW]-[ST]-X2-W motif with the GnRH/AKH peptide family that is absent in RPamides (**Fig. 3c**).

A

Nematoda RPamides	<i>C. elegans</i> NLP-2-1	S	I	A	L	G	R	S	-	G	F	R	P	G	-
	<i>C. elegans</i> NLP-2-2	S	M	A	M	G	R	L	-	G	L	R	P	G	-
	<i>C. elegans</i> NLP-2-3	S	M	A	Y	G	R	Q	-	G	F	R	P	G	-
	<i>C. elegans</i> NLP-22	S	I	A	I	G	R	A	-	G	F	R	P	G	-
	<i>C. elegans</i> NLP-23-2	S	M	A	I	G	R	A	-	G	M	R	P	G	-
	<i>C. elegans</i> NLP-46	N	I	A	I	G	R	G	D	G	L	R	P	G	-
	<i>A. suum</i> NLP-2-1	S	M	A	L	G	R	L	-	A	F	R	P	G	-
	<i>A. suum</i> NLP-2-2	S	L	A	L	G	R	V	-	D	F	R	P	G	-
	<i>A. suum</i> NLP-2-3	S	A	A	F	G	R	F	-	H	F	R	P	G	-
	<i>A. suum</i> NLP-2-4	S	L	A	L	G	R	S	-	G	F	R	P	G	-
	<i>A. suum</i> NLP-2-5	S	L	A	L	G	R	V	-	G	F	R	P	G	-
	<i>A. suum</i> NLP-22	S	L	A	S	G	R	W	-	G	L	R	P	G	-
	<i>A. suum</i> 05724	S	I	A	L	G	R	F	-	S	L	R	P	G	-
	<i>A. suum</i> 09524	N	I	A	I	G	R	G	D	G	F	R	P	G	-
	<i>P. pacificus</i> 172383	S	L	A	L	G	R	N	-	G	F	R	P	G	-
	<i>B. malayi</i> 52160	N	I	A	I	G	R	A	D	G	F	R	P	G	-

B

		C-terminal similarity													
Chordata	<i>H. sapiens</i> GnRH-1	Q	-	-	H	W	S	Y	-	G	L	R	P	G	G
	<i>H. sapiens</i> GnRH-2	Q	-	-	H	W	S	H	-	G	W	Y	P	G	G
	<i>D. rerio</i> GnRH-3	Q	-	-	H	W	S	Y	-	G	W	L	P	G	G
	<i>P. marinus</i> GnRH-1	Q	-	-	H	Y	S	L	-	E	W	K	P	G	G
	<i>P. marinus</i> GnRH-2	Q	-	-	H	W	S	H	-	G	W	F	P	G	G
	<i>B. floridae</i> GnRH	Q	-	E	H	W	Q	Y	G	H	W	-	Y	G	-
Echinodermata	<i>S. purpuratus</i> GnRH-1	Q	V	H	H	F	S	-	-	G	W	R	P	G	G
	<i>A. filiformis</i> GnRH	Q	-	I	H	G	R	I	-	G	W	K	P	G	G
	<i>A. rubens</i> GnRH-1	Q	-	I	H	Y	K	N	P	G	W	G	P	G	G
	<i>O. victoriae</i> GnRH	Q	-	L	H	-	S	R	M	R	W	E	P	G	G
Rotifera	<i>B. calyciflorus</i> GnRH	Q	-	L	T	F	S	S	-	D	W	S	G	G	-
Annelida	<i>H. robusta</i> GnRH	Q	S	I	H	F	S	R	-	S	W	Q	P	G	-
	<i>A. californica</i> GnRH	Q	-	I	H	F	S	P	-	D	W	G	T	G	-
Mollusca	<i>L. gigantea</i>	Q	-	I	H	F	S	P	-	T	W	G	S	G	-
	<i>T. diomedea</i> GnRH	Q	-	I	H	F	S	P	-	G	W	E	P	G	-
Priapulida	<i>P. caudatus</i> GnRH	Q	-	I	F	F	S	K	-	G	W	R	G	G	-
Tardigrada	<i>H. dujardini</i> GnRH	Q	-	L	S	F	S	T	-	G	W	G	H	G	-
	<i>C. maenas</i> RPCH	Q	-	L	N	F	S	P	-	G	W	-	-	G	-
	<i>D. melanogaster</i> AKH	Q	-	L	T	F	S	P	-	D	W	-	-	G	-
Arthropoda	<i>L. migratoria</i> AKH-1	Q	-	L	N	F	T	P	-	N	W	G	T	G	-

C

		N-terminal similarity												
Nematoda GnRH/AKH-like peptides	<i>C. elegans</i> NLP-47	Q	-	M	T	F	T	D	-	Q	W	T	-	-
	<i>A. costaricensis</i> 58181	Q	-	M	T	F	T	D	-	R	W	N	-	-
	<i>W. bancrofti</i> 21668	Q	-	M	T	F	T	D	-	N	W	D	-	-
	<i>H. contortus</i> 98198	Q	-	M	T	F	S	D	-	Q	W	N	-	-

identical AA
conserved AA
pyroglutamate
aromatic AA
amidated Gly

Figure 3: RPamide peptides are conserved among nematodes and share sequence similarity with GnRH/AKH peptides.

(A) Amino acid sequence alignment of nematode RPamide neuropeptides. All have a C-terminal glycine amidation target but lack an N-terminal pyroglutamate. (B) Amino acid sequence alignment of GnRH/AKH peptides across major animal phyla. (C) Amino acid sequence alignment of nematode GnRH/AKH-like NLP-47 peptides lacking the C-terminal glycine amidation target. For A-C, residues with a colored background are conserved in at least 50% of the sequences. Identical residues are depicted in black, conserved residues in grey and conserved aromatic residues in green. Pyroglutamate residues are indicated in blue and amidated glycine residues are indicated in orange. Absence of these modifications in nematode RPamide or GnRH peptides, respectively, are indicated by red boxes. Hyphens indicate gaps and a more elaborate alignment is depicted in [Supplementary Fig. S5 online](#).

One of the NLP-23 derived peptides (NLP-23-1, LYISRQGFRPA) also lacks the C-terminal glycine residue of RPamides. In contrast to amidated NLP-2, NLP-22 and NLP-23 derived neuropeptides, NLP-23-1 and GnRH-like neuropeptides derived from NLP-46 and NLP-47 did not activate GNRR-3 or GNRR-6 *in vitro* (data not shown).

3.3.4 NLP-22 RPamide neuropeptides induce locomotion quiescence through GNRR-6

The RPamide neuropeptide NLP-22 promotes movement and feeding quiescence in *C. elegans*⁴¹. Since GNRR-3 and GNRR-6 are activated by RPamide neuropeptides *in vitro*, we asked whether these GPCRs are involved in sleep regulation. If NLP-22 transduces its behavioral effects through GNRR-3 and/or GNRR-6, loss-of-function of *gnrr-3* and/or *gnrr-6* should abrogate the somnogenic effects of *nlp-22*. To test this, we quantified the effect of *gnrr-3* and *gnrr-6* mutations ([Supplementary Figure S4a online](#)) on behavioral quiescence of adult worms overexpressing *nlp-22* from a heat-shock inducible promoter⁴¹, by counting the number of body bends and pharyngeal pumps. Overexpression of *nlp-22* in *gnrr-3* mutant adults reduced pharyngeal pumping and body bending activity to the same degree as observed in a wild-type background (**Fig. 4a-b**), suggesting that GNRR-3 is not an endogenous receptor for NLP-22 in the regulation of behavioral quiescence. Similarly, the suppression of pharyngeal pumping induced by *nlp-22* was not affected in mutants of *gnrr-6* (**Fig. 4a**). By contrast, adult *gnrr-6* mutants overexpressing *nlp-22* had a small but significant elevation of body bend frequency in comparison to animals overexpressing *nlp-22* in a wild-type background (**Fig. 4b**). We further examined the potential effect of *gnrr-6* on *nlp-22*-induced locomotion quiescence by quantifying movement before and after heat shock-induced expression of *nlp-22* using the WorMotel, an automated machine vision-based platform for analysis of movement^{69,70}. Before heat shock, mutants of *gnrr-6* behaved like animals with a wild-type background (**Fig. 4c**). However, loss of *gnrr-6* attenuated the somnogenic effect of *nlp-22* overexpression on locomotion (**Fig. 4c**). We conclude that GNRR-6, but not GNRR-3, is a receptor for NLP-22 in the regulation of body movement. This conclusion is supported by our *in vitro* data (**Fig. 2b**) showing that NLP-22 is a potent ligand for GNRR-6, but activates GNRR-3 only at physiologically irrelevant concentrations.

Translational reporter transgenes for *gnrr-6* revealed expression of this gene in neurons involved in locomotory control. Expression of *gnrr-6* localized to SIA sublateral motor neurons and AVB forward command interneurons, which is in agreement with single-cell RNA-Seq data⁷¹. In addition, we observed expression in PDB and PHC neurons in the tail and few sensory neurons in the head ([Supplementary Fig. S6a-h online](#)). Available single-cell RNA-Seq data suggests that additional neurons, including OLL, URB and AWC neurons, may express *gnrr-6*⁷¹. Expression of *gnrr-3* was observed in several inhibitory GABAergic motor neurons of the ventral nerve cord (VNC) in the distal tail ([Supplementary Fig. S6i-j](#)

[online](#)). These distinct expression patterns suggest that GNRR-3 and GNRR-6 act in different locomotory circuits, which is in line with our finding that NLP-22 affects locomotion quiescence through GNRR-6 but not GNRR-3.

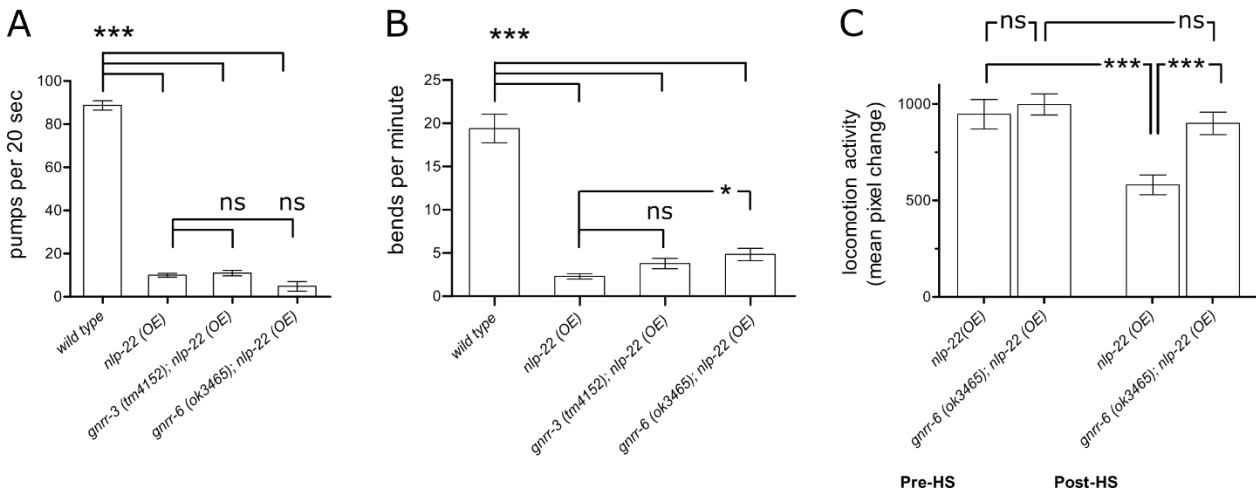


Figure 4: GNRR-6, but not GNRR-3, is required for *nlp-22* induced locomotion quiescence.

(A-B) Heat-shock induced overexpression of *nlp-22* reduces both pharyngeal pumping (A) ($N > 10$ animals) and body bending (B) ($N > 18$ animals) compared to wild-type animals. These *nlp-22* induced quiescence phenotypes are unaffected in *gnrr-3* mutant animals. Overexpression of *nlp-22* in *gnrr-6* mutants attenuates locomotory activity, showing significantly more body bends, while *nlp-22* induced feeding quiescence is still adequate in *gnrr-6* mutants. (C) Long-term behavioral tracking before and after heat shock (HS) induction of *nlp-22* overexpression shows that *gnrr-6* mutants display deficient movement quiescence compared to *nlp-22* overexpression in wild-type animals ($N = 24$ animals). Error bars indicate SEM. One-way ANOVA and Tukey test; *** $P < 0.001$; * $P < 0.05$; ns, not significant ($P > 0.05$).

3.3.5 NLP-2 RPamide neuropeptides reduce locomotion quiescence during L4 lethargus

Since NLP-2 and NLP-23 neuropeptides activated the same receptors *in vitro* as NLP-22, we asked whether genetically manipulating genes encoding these neuropeptides affects locomotion quiescence. We measured total movement quiescence and quiescence duration during L4 lethargus of *nlp-2* and *nlp-23* loss-of-function mutants. *nlp-23* mutants displayed no difference in quiescence compared to wild-type animals ([Supplementary Fig. S7](#)). By contrast, *nlp-2* mutants showed increased movement quiescence and quiescence duration during L4 lethargus (**Fig. 5a-b**). The opposite phenotypes, a decrease in total quiescence and quiescence duration (**Fig. 5c-d**), were induced by multi-copy overexpression of *nlp-2* from its endogenous promoter. These data suggest that NLP-2 peptides promote wakefulness during L4 lethargus. In adult animals, both *nlp-2* overexpression and loss-of-function reduced locomotion activity ([Supplementary Fig. S8 online](#)), suggesting that concentrations of NLP-2 peptides below or above physiological levels alter locomotion

differently during adulthood and lethargus. Although *nlp-2* derived peptides activate the same receptors *in vitro* as the somnogenic NLP-22 neuropeptides, our *in vivo* experiments suggest that NLP-2 neuropeptides promote movement rather than quiescence during lethargus.

3.3.6 GNRR-3 and GNRR-6 are required for wake-promoting effects of *nlp-2* overexpression

If NLP-2 peptides were signaling through GNRR-3 and/or GNRR-6, then loss of these receptors' functions may have the same phenotype as *nlp-2* loss-of-function. Total quiescence and quiescence duration during L4 lethargus in *gnrr-3* and *gnrr-6* mutants were not different from wild-type controls (**Fig. 5e-h**). Since overexpression of *nlp-2* decreased behavioral quiescence (**Fig. 5c-d**), an effect opposite to that of NLP-22/GNRR-6 signaling, we hypothesized that NLP-2 signals through a different receptor than NLP-22. Our *in vitro* data indicated that NLP-2 neuropeptides are potent ligands of both GNRR-3 and GNRR-6 (**Fig. 2a**), in contrast to NLP-22 which signals via GNRR-6 and not via GNRR-3. If GNRR-3 or GNRR-6 is a receptor for NLP-2 in regulating quiescence, then *gnrr-3* and/or *gnrr-6* loss-of-function should abrogate the wake-promoting effects of *nlp-2* overexpression. We found that disrupting either *gnrr-3* or *gnrr-6* abolished the reduced quiescence in animals overexpressing *nlp-2* (**Fig. 5i-j**). Thus, both *gnrr-3* and *gnrr-6* are required for the wake-promoting effects of *nlp-2* overexpression during lethargus.

Our behavioral data suggests that the RPamide receptor GNRR-6 is required for the regulation of lethargus quiescence by both NLP-2 and NLP-22 neuropeptides, whereas NLP-2/GNRR-3 signaling is additionally required in order to increase wakefulness rather than quiescence. As these receptors seem to be expressed in non-overlapping subsets of neurons ([Supplementary Fig. S6 online](#)), we asked if overexpression of *gnrr-3* alone is sufficient to decrease lethargus quiescence. Overexpression of *gnrr-3* indeed decreased total quiescence and quiescence duration during L4 lethargus (**Fig. 5k-l**). Thus, overexpression of *nlp-2* and *gnrr-3* result in similar wake-promoting phenotypes.

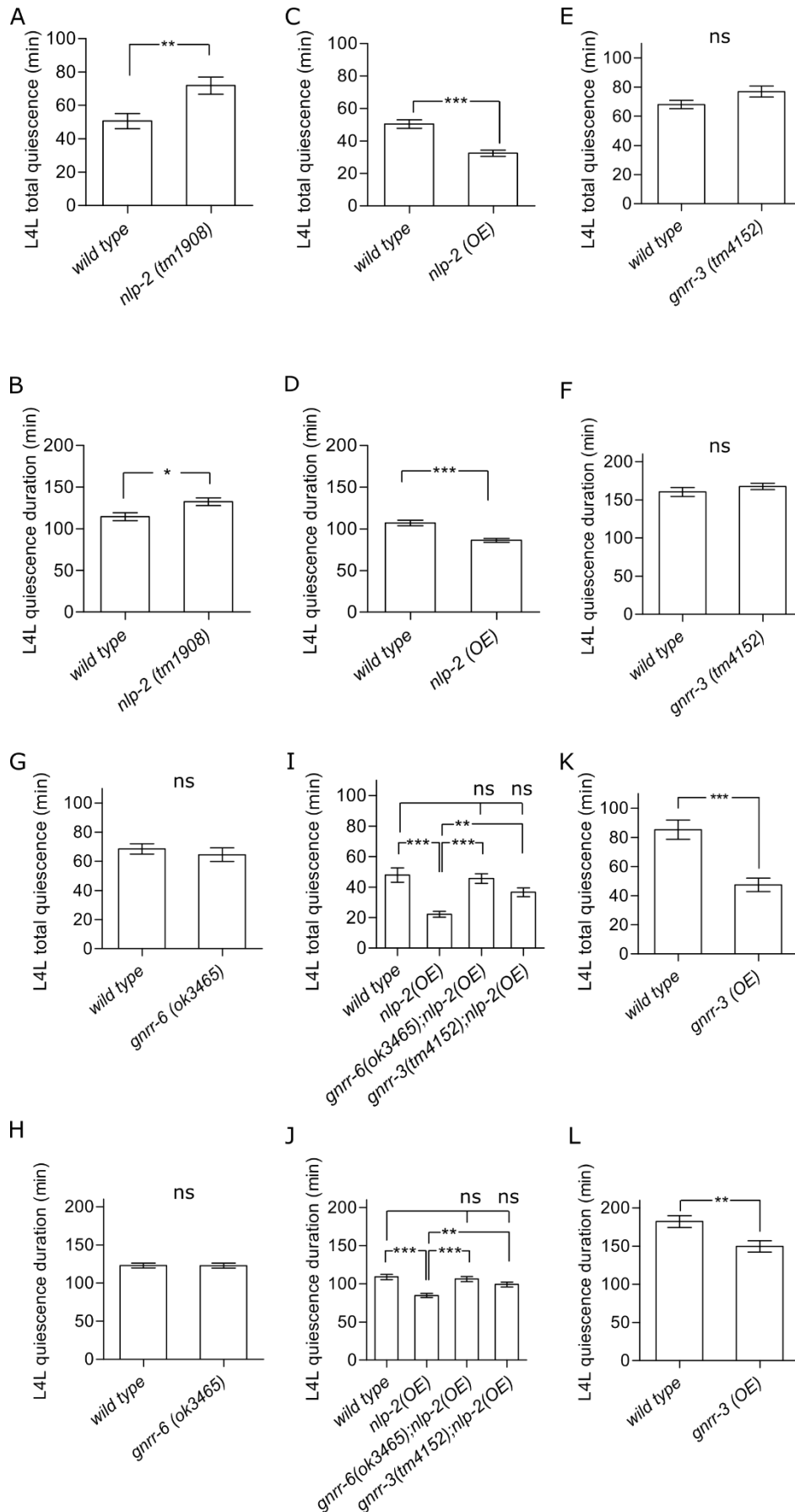


Figure 5: GNRR-3 and GNRR-6 are required for the wake-promoting effects of *nlp-2* overexpression. Average total quiescence during L4 lethargus (L4L) and average quiescence duration of L4L for (A, B) *nlp-2* mutants (N ≥ 20 animals) and (C, D) animals overexpressing *nlp-2* from an *nlp-2p::nlp-2* transgene (N > 27

animals). **(E, F)** Mutants for *gnrr-3* (N > 15 animals) and **(G, H)** *gnrr-6* (N > 21 animals) are not defective in lethargus quiescence. **(I, J)** Disrupting *gnrr-3* or *gnrr-6* abolishes locomotory quiescence in animals overexpressing *nlp-2* (N ≥ 31 animals). **(K, L)** Animals overexpressing *gnrr-3* show increased movement quiescence during L4L (N = 18 animals). Student's two-tailed t-tests or One-way ANOVA and Tukey test; ****P* < 0.001; ***P* < 0.01; **P* < 0.05; ns, not significant (*P* > 0.05); error bars represent SEM.

This effect on movement was restricted to lethargus as adult worms that lacked *gnrr-3* or that overexpressed *gnrr-3* did not show altered locomotory activity ([Supplementary Fig. S8 online](#)). In sum, GNRR-6 signaling is required for the RPamide-mediated regulation of movement during lethargus, while NLP-2/GNRR-3 signaling is additionally required to mediate *nlp-2*-induced wakefulness rather than quiescence.

3.3.7 NLP-2 peptides do not modulate feeding quiescence and sensory arousal threshold during L4 lethargus

Behavior during lethargus is characterized by locomotion quiescence, feeding quiescence, and reduced responsiveness to external stimuli^{2,31}. To assess whether NLP-2 signaling affects feeding quiescence, we analyzed the duration of feeding quiescence during L4 lethargus for *nlp-2* mutants and for animals overexpressing *nlp-2*. There was no difference in the duration of feeding quiescence, indicating that NLP-2 signaling controls movement quiescence but not feeding quiescence ([Supplementary Fig. S9a online](#)).

Other mutants with reduced quiescence during lethargus, such as *egl-4* and *npr-1* mutants, show increased responsiveness to sensory stimuli during lethargus^{2,21,31}, possibly explaining their arousal phenotype. To test whether the reduction of movement quiescence can be explained by an increased sensitivity to arousing stimuli, we measured the latency required for animals to be aroused by blue light during lethargus. There was no significant difference in response latency between wild type worms and animals lacking or overexpressing *nlp-2* ([Supplementary Fig. S9b online](#)). Thus, the reduced quiescence phenotype of worms overexpressing *nlp-2* appears specific for movement quiescence, although increased sensitivity to other sensory cues (like chemicals or touch) cannot be excluded.

3.3.8 *nlp-2* expression cycles with a developmental clock

To identify the cells that express *nlp-2*, we generated a transcriptional green fluorescent protein (GFP) reporter construct. Expression of the *nlp-2p::gfp* reporter transgene was restricted to one pair of head neurons and four uterine cells. Based on their location and sensory cilia morphology, we identified the head neurons as the olfactory AWA neurons (**Fig. 6a**). The uterus cells were identified as the neurosecretory uv1 cells⁷². The somnogenic

RPamide NLP-22 has a cyclical mRNA expression pattern concurrent with peaks in the mid larval stages prior to lethargus⁴¹. Therefore, we investigated whether the expression pattern of *nlp-2* mRNA also cycles throughout development. We used quantitative reverse-transcription PCR (qRT-PCR) to analyze *nlp-2* mRNA expression over a 30h time frame, which covered both L3 and L4 lethargus periods.

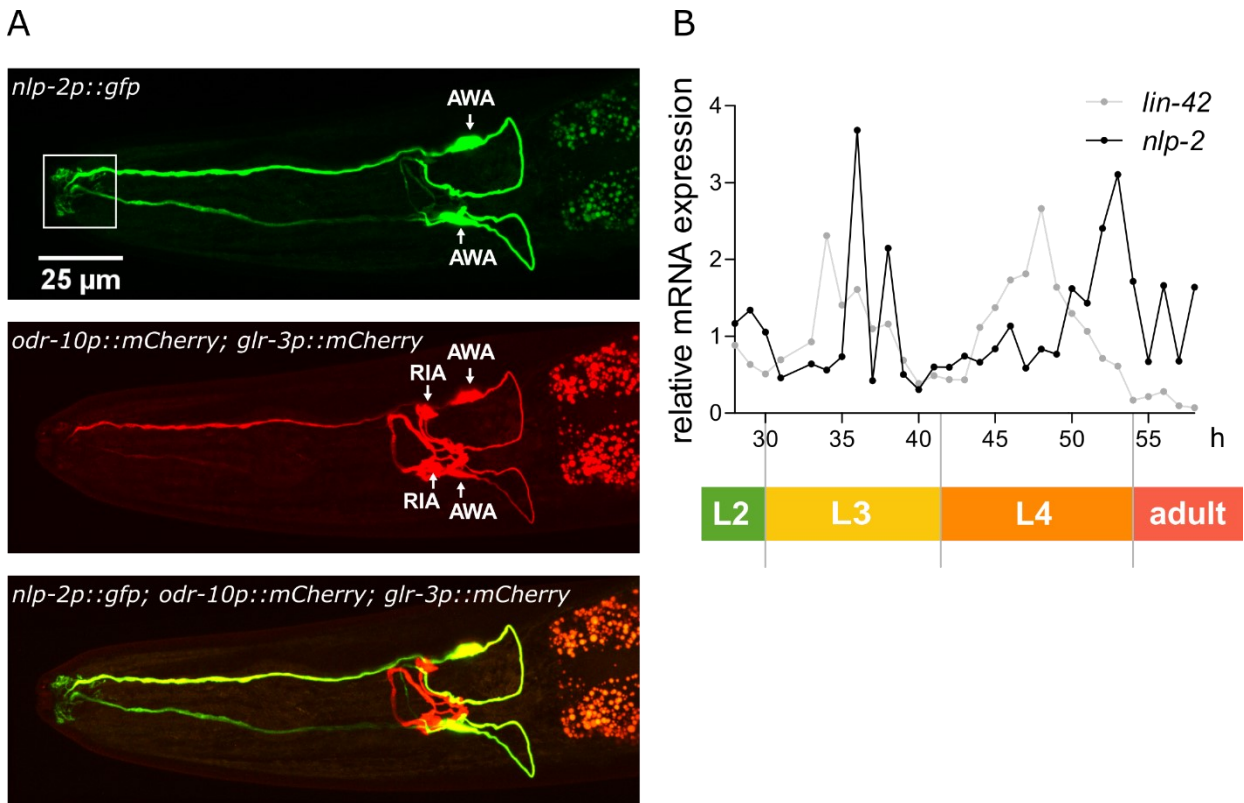


Figure 6: Expression of *nlp-2* localizes to AWA neurons and cycles with larval periodicity.

(A) Expression pattern of a transcriptional *nlp-2* reporter transgene [*nlp-2p::gfp*] in the head region. The upper panel shows the green fluorescent channel displaying [*nlp-2p::gfp*] transgene expression. The middle panel shows the red fluorescent channel with expression of two marker transgenes: [*odr-10p::mCherry*] in AWA and [*glr-3p::mCherry*] in RIA. The lower panel shows an overlay between the green and red channels, demonstrating that the expression of [*nlp-2p::gfp*] colocalizes with the AWA marker construct [*odr-10p::mCherry*], but not with the [*glr-3p::mCherry*]. The white box in the upper panel indicates the characteristic cilia at the dendrite tips of the AWA amphid sensory neurons expressing GFP. **(B)** Relative qRT PCR expression of *nlp-2* during larval development. The *nlp-2* and *lin-42* expression levels are plotted during one-hour time intervals of postembryonic development at 20°C after L1 larval arrest. Larval stage indications are based on the complete temporal *lin-42* expression profile (ranging from 0 to 75 hours after hatching).

Developmental progression was timed by the transcript profiles of *lin-42*, the *C. elegans* ortholog of the core circadian regulator PERIOD. Similar to PERIOD, which shows cyclic expression with a circadian periodicity in mammals and insects^{12,73}, *lin-42* transcript levels cycle with *C. elegans* larval stages, being lowest during each molt¹³. We found that *nlp-2* expression cycles with a constant phase relationship to *lin-42* during larval development (**Fig. 6b**). *nlp-2* mRNA expression peaked in preparation of the L3 and L4 molts, when *lin-*

42 levels are low, suggesting that *nlp-2* expression is regulated, at least partially, at the transcriptional level.

3.4 Discussion

Sleep, wakefulness and the transition between these behavioral states are regulated by the coordinated interplay of neuronal circuits in which neuropeptide signaling plays an essential role^{19,23,74}. Neuropeptides, such as mammalian hypocretin/orexin and melanin-concentrating hormone, can have arousing or somnogenic effects, respectively^{22,75,76}, suggesting that the balanced action of sleep- and wake-promoting neuropeptides is a conserved mechanism for regulating sleep/wake cycles.

Here, we provide evidence for two GnRH-like neuropeptidergic systems promoting sleep and wakefulness in *C. elegans*. NLP-2 RPamide signaling impairs movement quiescence during lethargus, which is opposite to the effect of the somnogenic NLP-22 RPamide neuropeptide that induces behavioral quiescence. RPamide neuropeptides – comprising *nlp-2*, *nlp-22*, *nlp-23* and *nlp-46* encoded peptides – are highly conserved in nematodes and share subtle sequence similarities to members of the bilaterian GnRH/AKH peptide family. GnRH-like signaling displays urbilaterian conservation and has well-established roles in reproductive maturation and behavior as well as in energy homeostasis^{52–56,77–81}. To date, a direct role for GnRH/AKH systems in the regulation of sleep and wakefulness has been described only in *D. melanogaster*, where neuronal AKH/AKHR signaling is required for starvation-induced sleep suppression^{45,82}. While *Drosophila* uses hyperactivity as a survival strategy to prevent starvation, *C. elegans* larvae respond to extended starvation by increased sleep and developmental arrest to prolong healthy lifespan⁸³. In adult *C. elegans*, however, food deprivation also leads to suppression of heat stress-induced quiescence and this suppression is increased with population density⁸⁴.

Our results suggest a model in which the RPamide neuropeptides NLP-2 and NLP-22 signal through GNRR-3 and GNRR-6 with opposing effects on locomotory quiescence during lethargus. Consistent with a neuropeptide system sufficient for promoting movement, we found that overexpression of either *nlp-2* or *gnrr-3* reduces quiescence during L4 lethargus. Although overexpression of a peptide may result in levels higher than those normally present *in vivo*, *nlp-2*-induced wakefulness during L4 lethargus requires both *gnrr-3* and *gnrr-6*. This finding suggests that NLP-2 neuropeptides signal through these receptors *in vivo* and is in agreement with our cell-culture experiments, in which NLP-2 peptides activated both GNRR-3 and GNRR-6. By contrast, the somnogenic NLP-22 peptide increases quiescence by

signaling via GNRR-6 but not via GNRR-3. Taken together, these results suggest that GNRR-6 is required for the regulation of lethargus quiescence by RPamide neuropeptides. We propose that NLP-22 activates GNRR-6, but not GNRR-3, resulting in quiescence, whereas NLP-2 peptides additionally activate GNRR-3, which promotes wakefulness rather than sleep. As *gnrr-3* and *gnrr-6* seem to be expressed in non-overlapping subsets of neurons, NLP-2/GNRR-3 signaling may indirectly interfere with NLP-22 pathways, although the mechanisms underlying such interactions remain unclear. While disrupting *nlp-2* or *nlp-22* affects quiescence during lethargus, *gnrr-3* and *gnrr-6* mutants display normal lethargus, which might be explained by additional as yet unidentified RPamide receptors. The observation that both GNRR-3 and GNRR-6 elicit a cellular calcium response *in vitro* without $G\alpha_{16}$ suggests signaling via $G\alpha_q$, which is in agreement with a previous study reporting that $G\alpha_q$ signaling controls sleep/wake-like states in *C. elegans*⁸⁵. The role of NLP-2, GNRR-3 and GNRR-6 in behavioral quiescence seems restricted to locomotion, as neither feeding quiescence, nor *nlp-22*-induced pharyngeal pumping quiescence is affected in animals with altered *nlp-2* expression levels or lacking these receptor systems, respectively. Disrupting NLP-2 signaling also leads to the preservation of a normal threshold for sensory arousal, in contrast to other neuropeptidergic systems, like NPR-1 and its ligands FLP-18 and FLP-21, that stimulate both sensory and locomotory activity during lethargus⁸⁶.

Our results suggest that lethargus in *C. elegans* is regulated by the balanced and cyclic action of sleep- and wake-promoting neuropeptides. Signaling by NLP-2 neuropeptides, like NLP-22⁴¹, is at least partially regulated at the level of mRNA transcripts, which cycle relative to a LIN-42/PERIOD-based larval clock that controls the synchronization of lethargus quiescence¹³. Peak expression of *nlp-2* is delayed compared to the expression of the *lin-42* gene, the *C. elegans* ortholog of the circadian clock gene *period*, which sets the timing for sleep-like behavior. This observation is in line with our evidence for the wake-promoting effects of NLP-2. How might the cyclic expression of *nlp-2* be regulated? The upregulation of *nlp-2* transcripts when *lin-42* expression is high suggests that *nlp-2* expression can be a clock output signal, regulated by the activity of LIN-42. Interestingly, a similar mechanism has been described for regulating the expression of *nlp-22*, which oscillates in response to the LIN-42/PERIOD-based larval clock⁴¹. The *nlp-2* and *nlp-22* genes are clustered on the X chromosome, suggesting a transcriptional co-regulation of these wake- and sleep-promoting signals. Both literature⁴¹ and our locomotion quiescence data (**Fig. 4**) suggest that RPamide peptide concentrations are tightly regulated, as both decreasing them below or increasing them above physiological levels alters locomotion. For *nlp-2*, deviation from

this set-point in either direction reduces locomotion in adults, but how this occurs mechanistically remains unclear. We propose that elevated levels of NLP-2 increases locomotion during larval sleep, possibly by acting as a molecular switch to wakefulness via its additional activation of GNRR-3, and that NLP-2 levels are subsequently maintained within a physiological range during normal locomotion in adults.

Expression of *nlp-2* was restricted to a pair of olfactory AWA neurons and vulval uv1 cells, consistent with previously reported expression patterns⁸⁷. The *nlp-2*-expressing AWA neurons have ciliated sensory endings and are known to display pulsatile calcium transients, which are elicited by action potential bursts^{88,89}. AWA neurons display sex-specific pheromone responses⁹⁰ and may share some functional similarity to chordate GnRH neurons that arise from the olfactory placode^{91,92} and are also presumed to regulate non-reproductive functions in larval stages.^{93,94} Our expression data suggest that NLP-2 neuropeptides from AWA neurons may act on GNRR-3 and GNRR-6 in neurons of the motor circuit to mediate wakefulness. The integration of environmental and intrinsic signals enables the coordination of sleep-wake states with competing and complementary animal behaviors, such as foraging and mating^{95,96}. The release of NLP-2 from sensory neurons in response to environmental and/or internal stimuli may therefore contribute to a switch between sleep-wake states.

The somnogenic RPamide NLP-22 is expressed in a different site, the glutamatergic RIA interneurons⁴¹, which have no direct synaptic connections to AWA sensory neurons, but are also involved in sensorimotor integration and olfactory steering ([Supplementary Fig. S10 online](#))^{97,98}. The NLP-22 receptor GNRR-6 is expressed in sublateral motor neurons and interneurons that project along the ventral nerve cord, which suggests a role in locomotion quiescence. NLP-22-induced feeding quiescence is indeed unaffected in *gnrr-6* mutants, suggesting that NLP-22 signals through an additional thus far unidentified receptor to inhibit feeding during sleep.

Reported GnRH-associated phenotypes together with the data presented here may hint at a conserved role for GnRH/AKH-like signaling in circadian and developmental clock-mediated metabolic and locomotion activity patterns.⁹⁹ In mammals, reduced sleep during the proestrus phase, when GnRH pulse frequency increases, suggests a role in wakefulness^{100,101}. GnRH-like neuropeptides have also been implicated in the timing of insect pupariation/ecdysis¹⁰². Like *C. elegans* lethargus, ecdysis is characterized by reduced feeding and locomotion quiescence and eventually leads to sexual maturation. The role of GnRH-like signaling in the cyclic regulation of metabolism and reproduction, such as

cyclic larval/juvenile ecdysis, seasonal breeding and estrous cycle, can be reconciled with its role in sleep-wake behavior as coordinating and coupling diverse metabolic cycles to behavioral responses across Bilateria.

3.5 Materials and Methods

Strains and cultivation

Strains were cultured at 20°C under standard conditions on NGM agar plates seeded with *Escherichia coli* OP50¹⁰³. The following wild type and mutant strains were used: N2 (Bristol), LSC509 [*gnrr-6 (ok3465) X*] (x2), LSC714 [*gnrr-3 (tm4152) X*] (x8), FX01908 [*nlp-2 (tm1908) X*] and NQ638 [*nlp-23 (tm5531) X*] (x2) (x# indicated times outcrossed to N2). Transgenic strains used in this study are listed in [Supplementary Table S1 online](#).

Phylogenetic analysis

For the phylogenetic analysis of GnRH/AKH-like receptors, the protein dataset was composed of deuterostomian GnRH receptors, bilaterian corazonin (Crz) receptors, protostomian GnRH/AKH receptors and nematode GnRH/AKH-like receptors. Arginine vasopressin (AVP) and neuropeptide S (NPS) receptor sequences were used as outgroup. Accession numbers of the sequences are listed in [Supplementary Table S2 online](#). Sequence alignments were generated using the Simultaneous Alignment and Tree Estimation (SATé) software package, which uses an iterative greedy search heuristic to sequentially align sequences and compute a maximum likelihood phylogenetic tree from alignments¹⁰⁴. The final maximum likelihood phylogeny was estimated using PhyML. The following parameters were used: LG as the amino-acid replacement matrix¹⁰⁵, Subtree Pruning and Regrafting (SPR) and Nearest Neighbor Interchange (NNI) for topological moves¹⁰⁶, and a number of discrete gamma rate categories equal to 4. Branch support values were generated using nonparametric bootstrapping (100 bootstraps). Branches with bootstrap values below 50% were collapsed.

Peptide sequence alignments in [Supplementary Figure S5 online \(A,B\)](#) were generated using the MUSCLE algorithm in MEGA 7. Panel C was first aligned with the MUSCLE algorithm and afterwards adjusted manually into separated boxes of similar sequences to avoid larger gaps in the multiple sequence alignment, though predicted color coding was maintained. Full species names and Genbank sequence accession numbers are listed in [Supplementary Table S3 online](#).

Molecular biology

For receptor deorphanization, the open reading frame of each receptor was cloned into the pcDNA3.1D/V5-His TOPO mammalian expression vector. Only receptors with a seven alpha-helical transmembrane topology, predicted using TMHMM 2.0 software, were cloned¹⁰⁷. Sequences of receptor cDNAs (GNRR-1a, GNRR-2a, GNRR-3, GNRR-5, GNRR-6, GNRR-7 and DAF-38/GNRR-8) were verified to yield identical protein sequences as the corresponding translated cDNA sequences on WormBase (WS235). Expression plasmids were isolated for transfection of mammalian cells using the EndoFree Plasmid Maxi Kit (Qiagen).

For the *nlp-22* heat shock-inducible overexpression strains, *gnrr-3* and *gnrr-6* mutants were crossed with NQ251 carrying a [*hsp16.2p::nlp-22; hsp16.2p::gfp; myo-2p::mCherry*] transgene⁴¹. For *nlp-2* and *gnrr-3* overexpression, a linear *nlp-2p::nlp-2* and *gnrr-3p::gnrr-3* PCR construct was amplified from wild type *C. elegans* genomic DNA using Herculase Enhanced DNA polymerase (Agilent Technologies). Primers used for PCR amplification are listed in [Supplementary Table S4 online](#).

Transcriptional GFP reporter constructs for *nlp-2* and *gnrr-3* were created using overlap-extension PCR as described¹⁰⁸. A translational GFP reporter construct for *gnrr-6* was PCR amplified from a commercially available fosmid vector (TransgeneOme clone 9914866399944241 D12; Source BioScience). A translational *gnrr-6p::gnrr-6::SL2-mKate* reporter construct was generated using the Multisite Gateway Three-Fragment cloning system (12537-023, Invitrogen) into pDEST4R3 II. The respective promoter lengths upstream of the predicted start codon used for *nlp-2* and *gnrr-3* transcriptional reporter constructs were 2062 bp and 1877 bp. The translational reporter construct for *gnrr-6* consisted of 2960 bp promoter, the *gnrr-6* coding sequence without stop codon, and a *gfp* sequence inserted 66 bp after the *gnrr-6* coding sequence or an SL2::mKate sequence. Primers used for PCR amplification are listed in [Supplementary Table S5 online](#).

Transgenesis

Transgenic worms were created by microinjection using a Leica DMIRB inverted DIC microscope equipped with an Eppendorf Femtojet microinjection system. Each construct was injected at a concentration of 50 ng/μl together with 1kb DNA ladder as carrier DNA and 5 ng/μl pCFJ90 (*myo-2p::mCherry*) or a combination of 5 ng/μl (*rol-6p::rol-6(d)*) and *glr-3p::mCherry* as co-injection marker.

Peptide synthesis and purification

Peptides were custom-synthesized by GL Biochem Ltd. All peptides were initially tested at a concentration of 10 μM. Receptor activating peptides were purified using reverse-phase HPLC and verified using MALDI TOF mass spectrometry. Peptide concentrations were determined with a bicinchoninic acid (BCA) assay¹⁰⁹. For receptor activation assays, peptides were first lyophilized and then diluted to the desired concentrations.

Receptor activation assay

Chinese hamster ovary (CHO) cells stably expressing apo-aequorin and the promiscuous Gα₁₆ subunit were used for receptor deorphanization (ES-000-A24, Perkin-Elmer). To characterize downstream signaling, CHO cells stably expressing apo-aequorin but lacking the promiscuous Gα₁₆ protein were used (ES-000-A12, Perkin-Elmer). Cells were cultured in Dulbecco's Modified Eagle's Medium Nutrient Mixture Ham F-12 (DMEM/F-12, Invitrogen) to which 1% penicillin/streptomycin, 2.5 μg/ml amphotericin B, and 10% fetal bovine serum (Sigma-Aldrich) were added. Growth medium was supplemented with 250 μg/ml zeocin or 5 μg/ml puromycin, which serves as a selection reagent for CHO cells with or without the promiscuous Gα₁₆ subunit, respectively. Cells were grown as a monolayer at 37°C, 5% CO₂ and high humidity. For transfection, 3.75 ml Opti-MEM I (Invitrogen), 7.5 μg pcDNA3.1 construct and 18.75 μl Plus reagent (Invitrogen) were gently mixed in a polystyrene tube. After incubation for 5 minutes at room temperature, 45 μl

Lipofectamine LTX (Invitrogen) was added and gently mixed. The transfection reagent was incubated for 30 min at room temperature. Growth medium was removed leaving 3 ml and the transfection reagents were added dropwise to the cells. Transfected cells were grown overnight and 20 ml growth medium was added the next day. Cells were grown one more day before the assay at 28°C.

Two days after transfection, CHO cells were detached from the surface of the culture flask using phosphate buffered saline with 0.2% EDTA and collected in 10 ml colorless DMEM/F-12 (11039, Gibco). Cell viability was measured using a NucleoCounter NC-100 (Chemometric). Cells were pelleted for 4 min at 800 rpm at room temperature and resuspended to a concentration of 5×10^6 cells/ml in colorless DMEM/F12 with 0.1 % bovine serum albumin (BSA). 5 μ M coelenterazine H (Invitrogen) was added to the cell suspension. Cells were incubated by gentle shaking for 4 hours in the dark at room temperature, allowing the aequorin holoenzyme to be reconstituted. After a 10-fold dilution in DMEM/F12 with 0.1 % BSA, the cells were incubated for another 30 min. Peptides were dissolved in DMEM/F12 with 0.1 % BSA and 50 μ l of the peptide solution was added to the wells of a white flat bottom 96-well plate. Wells containing DMEM/F12 with 0.1 % BSA were used as a negative control, while wells containing 1 μ M ATP were used as a positive control. Incubated cells were added to the wells at a density of 25,000 cells/well and luminescence was monitored for 30 s on a Mithras LB 940 luminometer (Berthold Technologies). After 30 seconds, 0.2 % Triton X-100 dissolved in DMEM/F12 with 0.1 % BSA was added to lyse the cells and light emission was recorded for another 8 seconds. Light emission from each well was calculated relative to the total calcium response (ligand + Triton X-100). EC50 values were calculated from dose-response curves that were constructed using a nonlinear regression analysis with a sigmoidal dose-response equation (Graphpad Prism 5).

Fluorescence microscopy

Transgenic reporter animals were mounted on 2 % agarose pads and immobilized with 5 mM sodium azide. Fluorescence was observed on an Olympus Fluoview FV1000 (IX81) confocal microscope. Confocal Z-stack images were processed using Imaris 7.2 (Olympus).

The *nlp-2p::gfp* localization construct was co-injected with a red fluorescent *glr-3p::mCherry* marker construct that cell-specifically expresses in the RIA neurons and a *rol-6* dominant *roller* co-injection marker. The resulting NQ744 *qnEx423 [nlp-2p::gfp; glr-3p::mCherry; rol-6]* strain was then crossed with LSC1298 *lstEx682 [odr-10p::mCherry::3'UTR odr-10; unc-122p::gfp]* to colocalize its expression in AWA.

To identify expression in amphid sensory neurons, LSC1687 *lstEx1023 [gnrr-6p::gnrr-6::gfp; unc-122p::mCherry]* animals were stained with Dil. Similarly, a second *gnrr-6* reporter strain LSC1904 *lstEx1048 [gnrr-6p::gnrr-6::SL2::mKate; unc-122p::gfp]* was stained with DiO to confirm expression of *gnrr-6* in ASK. To colocalize transgene expression or to exclude *gnrr-6* expression in specific neurons, LSC1904 was also crossed with the following marker strains: for PHC neurons BL5717 *inls179 [ida-1p::gfp] II; him-8(e1489) I*, for AVB neurons AQ2529 *ljEx286 [sra-11p::YC3.60]*, for SMB neurons AQ3642 *ynls25 [flp-12p::gfp; rol-6d]*, for SMD neurons AQ3848 *kyls123 [trp-1p::gfp]*, and for glutamatergic neurons OH12312 *otls388 [eat-4(fosmid)::SL2::yfp::H2B; pha-1(e2123)]; him 5(e1490)*. GFP-positive cells in LSC1091 *lstEx556 [gnrr-3p::gnrr-3::gfp; unc-122p::mCherry]* were identified by crossing with a red fluorescent GABAergic reporter strain, XE1375 *wpls36 [unc-47p::mCherry]*.

Developmental time course of mRNA expression

Developmental mRNA expression was analyzed using qRT-PCR as described¹¹⁰. Wild type *C. elegans* were synchronized as L1 diapause larvae and cultured in S-medium¹⁰³ with *E. coli* K12 as food source, while gently shaking at 20°C. Worms were sampled every hour. mRNA was isolated (Rneasy Mini kit, Qiagen) and reverse transcribed to cDNA (SuperScript III Reverse Transcriptase, Invitrogen) using random primers (Invitrogen). Primer pairs for *nlp-2* were designed with Primer Express (Applied Biosystems) and VectorNTI (Invitrogen). The specific primers used for qPCR of *nlp-2* transcripts were: forward 5'-CTGAAGGAGCAATGGGCAAA -3' and reverse 5'-ATGATGAGATCACTAACATCCACAG -3'. The transcript profile of *lin-42b/c* was used as a marker for developmental timing¹³, using *lin-42 fwd* TGTGCCCAACGCCAATC and *lin-42 rev* CACCTTCCTCAGCATTGC. A melt curve analysis confirmed the absence of primer dimers and other non-specific products. Fast SYBR Green Master Mix (Applied Biosystems) was used for qRT-PCR and performed using the StepOnePlus Real-Time PCR system (Applied Biosystems). Cycling parameters were 600 s at 95°C, followed by 40 cycles of 3 s at 95°C and 30 seconds at 60°C. Each sample was analyzed in triplicate to assess technical variation. A no template control consisting of milli-Q water instead of cDNA was added as a negative control. The normalized relative quantity of cDNA was calculated using the geometric mean of three reference genes (*cdc-42*, *tba-1* and *pmp-3* as the three best performing out of *cdc-42*, *tba-1*, *pmp-3*, *rpb-12*, *gpd-2* and *Y45F10D.4* using geNorm¹¹¹).

Behavioral assays

Measurements of feeding and locomotion quiescence after heat-shock induced expression of *nlp-22* (Fig. 4a-b) were performed according to Nelson *et al.* (2013)⁴¹. Day one adult worms were placed on a 55 mm diameter NGM agar plate seeded with *E. coli* OP50. Plates were double wrapped with parafilm and incubated in a water bath at 33°C for 30 min. After heat-shock, worms were recovered at 20°C for 2-3 hrs. To quantify feeding quiescence, pharyngeal pumps were counted for 20 s. A pump was counted as one complete phase of contraction and relaxation, based on the anterior-posterior movement of the grinder in the terminal bulb. This was done at 80X on a stereomicroscope. For locomotion quiescence, body bends were manually counted for 1-minute time intervals. A bend was counted as a single turn (i.e. half phase) in either direction during normal forward movement. This was done at 40-80X on a stereomicroscope. Long-term behavioral tracking of locomotory quiescence pre- and post-heat shock (Fig. 4c) was measured with the WorMotel system as described below.

For measurements of total quiescence and quiescence duration during L4 lethargus, worms were monitored beginning in the L4 stage for 9 hrs in 2 concave wells (3 mm diameter, 2.5 mm depth) of a polydimethylsiloxane (PDMS) chip filled with 15 μ l NGM agar and seeded with *E. coli* OP50¹¹². For each measurement, one control and one experimental animal were manually placed in adjacent wells. The PDMS chip was placed on a microscope base (Diagnostics Instruments) with a fiber optic cable DCR III light source (Schott) for bright-field illumination. Worms were monitored by a camera (659 x 494

pixels, scA640-70fm, Basler Vision Technologies) which was mounted on a stereomicroscope (Zeiss Stemi 2000). 8-bit grayscale images with a spatial resolution of 12.5 μm per pixel were captured every 10 s. The quiescence parameters “total quiescence” and “quiescence duration” are defined as in Raizen *et al.* (2008)². Quiescence was quantified using a machine vision frame subtraction method² and statistically compared to wild-type control animals with paired t-tests. All quiescence experiments using this method (Fig. 5e-f, k-l and [Supplementary Fig. S7 online](#)) were done in a temperature-controlled room at 20°C.

Locomotion quiescence during L4 lethargus (Fig. 5a-d, g-j) and adult locomotion activity (Fig. 4c) was also quantified using a medium-throughput WorMotel system. WorMotel analyses were conducted as described previously⁶⁹. Briefly, 24-wells of a polydimethylsiloxane (PDMS) chip (gifts from Chris Fang-Yen, University of Pennsylvania) were filled with NGM/agar and allowed to cool to room temperature. L4 animals were identified to be pre-lethargus due to their active feeding behavior (i.e. pharyngeal pumping) and transferred to a freshly seeded plate. Moving them to a plate prior to the WorMotel prevented the accidental transfer of eggs and other larvae. Individual active L4 animals were then transferred to the surface of the agar in the 24-welled chip. A small amount of DA837 bacteria was transferred with the animal at this time, using a worm pick. The chip was placed in a petri-dish, which was sealed with parafilm and transferred into the WorMotel imaging system. Images were taken every 10 seconds for 12 hours. Using published MatLab software⁶⁹, pixel subtraction followed by quiescence analyses were conducted to produce the total amount of quiescence every 10-minutes during the 12-hour period. Lethargus periods were manually identified based on an identifiable 1-2-hour peak of quiescence, which usually occurred within the first 2-4 hours of imaging. If a peak was not detected because of high background, the images were manually observed for the absence or death of an animal, and these data point were censored. We also censored data in which the animals appeared to fall asleep during the preparation of the chip. This was evident by the peak of quiescence beginning immediately after the start of the recording. WorMotel assays were performed at temperatures ranging from 22.5 to 24 °C. Quiescence was statistically compared to wild type control animals with unpaired t-tests. Statistical analysis was always performed with internal wild-type controls.

To measure the duration of L4 lethargus feeding quiescence ([Supplementary Fig. S9a online](#)), late L4 worms, which had not yet entered lethargus, were individually transferred to freshly seeded NGM agar plates. Pharyngeal pumping was observed by stereomicroscopy every 10 min. Quiescence duration was measured as the time between the offset and onset of pharyngeal pumping.

For adult locomotion assays ([Supplementary Fig. S8 online](#)), synchronized day 1 adult animals were imaged for 10 min while moving on fresh NGM plates at 20°C that were seeded 24 hrs in advance with 200 μl of OP50 bacterial culture. High-resolution acquisition (56 pixels/mm) was performed with a 10 megapixel camera (GigE PRO GP11004M NET 1/2,3" CMOS 3840 x 2748; with matching lenses LM16JC10M Mp KOWA 2/3" F1.8) running at 2 frames per second. Animal tracking was achieved with a custom written MATLAB (MathWorks) script¹¹³. Background subtracted and denoised image frames were binarized to obtain worm shapes in each frame. Shape centroid tracks over time were quality controlled for collisions and smoothed by a rectangular sliding window of 3 centroid positions. The absolute speed was determined as the distance between consecutive centroid positions. Only speed values assigned as forward locomotion runs were averaged for each track. Each experimental day contained an internal wild type control to which other strains were normalized.

Arousal threshold was analyzed by measuring the response latency of individual worms to blue light during lethargus ([Supplementary Fig. S9b online](#)). A response to blue light was defined as a backward movement equal to one-half of the worm's length³⁵.

Statistical Analysis

Dose-response curves were constructed using a nonlinear regression analysis with a sigmoidal dose-response equation (GraphPad Prism 5). Statistical significance of behavioral assays was determined using (un)paired Student t-tests or one-way ANOVA and Tukey post-hoc for multiple comparisons (as indicated in each figure legend) with the GraphPad Prism version 5 software package. In graphs, error bars represent standard error of the mean (SEM) and significance levels are indicated as: *** $P < 0.001$; ** $P < 0.01$; * $P < 0.05$; ns (= not significant) $P > 0.05$. Experiments were performed on at least two independent days.

3.6 References

1. Zimmerman, J. E., Naidoo, N., Raizen, D. M. & Pack, A. I. Conservation of sleep: insights from non-mammalian model systems. *Trends Neurosci.* **31**, 371–376 (2008).
2. Raizen, D. M. *et al.* Lethargus is a *Caenorhabditis elegans* sleep-like state. *Nature* **451**, 569–572 (2008).
3. Allada, R. & Siegel, J. M. Unearthing the phylogenetic roots of sleep. *Curr. Biol.* **18**, 670–679 (2010).
4. Trojanowski, N. F. & Raizen, D. M. Call it worm sleep. *Trends Neurosci.* **39**, 54–62 (2016).
5. Ly, S., Pack, A. I. & Naidoo, N. The neurobiological basis of sleep : Insights from *Drosophila*. *Neurosci. Biobehav. Rev.* **87**, 67–86 (2018).
6. Crocker, A. & Sehgal, A. Genetic analysis of sleep. *Genes Dev.* **24**, 1220–1235 (2010).
7. Hendricks, J. C., Sehgal, A. & Pack, a I. The need for a simple animal model to understand sleep. *Prog. Neurobiol.* **61**, 339–351 (2000).
8. Shaw, P. J., Tononi, G., Greenspan, R. J. & Robinson, D. F. Stress response genes protect against lethal effects of sleep deprivation in *Drosophila*. *Nature* **417**, 287–291 (2002).
9. Knutson, K. L., Spiegel, K., Penev, P. & Van Cauter, E. The metabolic consequences of sleep deprivation. *Sleep Med. Rev.* **11**, 163–178 (2007).
10. Cirelli, C. & Tononi, G. Is sleep essential? *PLoS Biol.* **6**, e216 (2008).
11. Palma, J.-A., Urrestarazu, E. & Iriarte, J. Sleep loss as risk factor for neurologic disorders: a review. *Sleep Med.* **14**, 229–236 (2013).
12. Hardin, P. E., Hall, J. C. & Rosbash, M. Feedback of the *Drosophila* period gene product on circadian cycling of its messenger RNA levels. *Nature* **343**, 536–540 (1990).
13. Jeon, M., Gardner, E. A., Miller, E. A., Deshler, J. & E., R. A. Similarity of the *C. elegans* developmental timing protein LIN-42 to circadian rhythm proteins. *Science* **286**, 1141–1146 (1999).
14. Van Buskirk, C. & Sternberg, P. W. Epidermal growth factor signaling induces behavioral quiescence in *Caenorhabditis elegans*. *Nat. Neurosci.* **10**, 1300–1307 (2007).
15. Singh, K. *et al.* *C. elegans* Notch signaling regulates adult chemosensory response and larval molting Quiescence. *Curr. Biol.* **21**, 825–834 (2011).
16. Blum, I. D., Bell, B. & Wu, M. N. Time for bed : Genetic mechanisms mediating the circadian regulation of sleep. *Trends Genet.* **34**, 379–388 (2018).
17. Singh, K., Ju, J. Y., Walsh, M. B., Dilorio, M. A. & Hart, A. C. Deep conservation of genes required for both *Drosophila melanogaster* and *Caenorhabditis elegans* sleep includes a role for dopaminergic signaling. *Sleep* **37**, 1439–1451 (2014).
18. Herrero, A. *et al.* Pigment-dispersing factor signaling in the circadian system of *Caenorhabditis elegans*. *Genes, Brain Behav.* **2**, 493–501 (2015).
19. Richter, C., Woods, I. G. & Schier, A. F. Neuropeptidergic control of sleep and wakefulness. *Annu. Rev. Neurosci.* **37**, 503–531 (2014).
20. Choi, S. *et al.* Sensory neurons arouse *C. elegans* locomotion via both glutamate and neuropeptide release. *PLOS Genet.* **11**, e1005359 (2015).
21. Choi, S., Chatzigeorgiou, M., Taylor, K. P., Schafer, W. R. & Kaplan, J. M. Analysis of NPR-1 reveals a circuit mechanism for behavioral quiescence in *C.elegans*. *Neuron* **78**, 869–880 (2013).
22. Gao, X.-B. & Horvath, T. Function and dysfunction of hypocretin/orexin: an energetics point of view. *Annu. Rev. Neurosci.* **37**, 101–116 (2014).
23. Saper, C. B., Fuller, P. M., Pedersen, N. P., Lu, J. & Scammell, T. E. Sleep state switching. *Neuron* **68**, 1023–1042 (2010).
24. Chiu, C. N. *et al.* A zebrafish genetic screen identifies neuromedin U as a regulator of sleep / wake states. *Neuron* **89**, 842–856 (2016).
25. Singh, C., Rihel, J. & Prober, D. A. Neuropeptide Y regulates sleep by modulating noradrenergic signaling. *Curr. Biol.* **27**, 3796-3811.e5 (2017).
26. Park, S., Sonn, J. Y., Oh, Y., Lim, C. & Choe, J. SIFamide and SIFamide receptor define a novel neuropeptide signaling to promote sleep in *Drosophila*. *Mol. Cells* **37**, 295–301 (2014).
27. Lenz, O., Xiong, J., Nelson, M. D., Raizen, D. M. & Williams, J. A. FMRFamide signaling promotes stress-induced sleep in *Drosophila*. *Brain. Behav. Immun.* **47**, 141–148 (2015).
28. Meelkop, E., Temmerman, L., Schoofs, L. & Janssen, T. Signalling through pigment dispersing hormone-like peptides in invertebrates. *Prog. Neurobiol.* **93**, 125–147 (2011).
29. Parisky, K. M. *et al.* PDF cells are a GABA-responsive wake-promoting component of the *Drosophila* sleep circuit. *Neuron* **60**, 672–682 (2008).
30. Chen, D., Taylor, K. P., Hall, Q. & Kaplan, J. M. The neuropeptides FLP-2 and PDF-1 act in concert to arouse *Caenorhabditis elegans* locomotion. *Genetics* **204**, 1151–1159 (2016).
31. Nelson, M. D. & Raizen, D. M. A sleep state during *C. elegans* development. *Curr. Opin. Neurobiol.* **23**, 824–830 (2013).
32. Schwarz, J., Lewandrowski, I. & Bringmann, H. Reduced activity of a sensory neuron during a sleep-like state in *Caenorhabditis elegans*. *Curr. Biol.* **21**, R983–R984 (2011).
33. Cho, J. Y. & Sternberg, P. W. Multilevel modulation of a sensory motor circuit during *C. elegans* sleep and arousal. *Cell* **156**, 249–260 (2014).
34. Iwanir, S. *et al.* The microarchitecture of *C. elegans* behavior during lethargus: homeostatic bout dynamics, a typical body posture, and regulation by a central neuron. *Sleep* **36**, 385–395 (2013).
35. Driver, R. J., Lamb, A. L., Wyner, A. J. & Raizen, D. M. DAF-16/FOXO regulates homeostasis of essential sleep-

- like behavior during larval transitions in *C. elegans*. *Curr. Biol.* **23**, 501–506 (2013).
36. Nagy, S. *et al.* Homeostasis in *C. elegans* sleep is characterized by two behaviorally and genetically distinct mechanisms. *ELife* **3**, e04380 (2014).
 37. Nichols, A. L. A., Eichler, T., Latham, R. & Zimmer, M. A global brain state underlies *C. elegans* sleep behavior. *Science* **356**, 1277–1279 (2017).
 38. Turek, M. & Bringmann, H. Gene expression changes of *Caenorhabditis elegans* larvae during molting and sleep-like lethargus. *PLoS One* **9**, 25–28 (2014).
 39. Turek, M., Besseling, J., Spies, J. P., König, S. & Bringmann, H. Sleep-active neuron specification and sleep induction require FLP-11 neuropeptides to systemically induce sleep. *ELife* **5**, e12499 (2016).
 40. Chew, Y. L., Grundy, L. J., Brown, A. E. X., Beets, I. & Schafer, W. R. Neuropeptides encoded by *nlp-49* modulate locomotion, arousal and egg-laying behaviours in *Caenorhabditis elegans* via the receptor SEB-3. *Philos. Trans. R. Soc. B Biol. Sci.* **373**, 20170368 (2018).
 41. Nelson, M. D. *et al.* The neuropeptide NLP-22 regulates a sleep-like state in *Caenorhabditis elegans*. *Nat. Commun.* **4**, 2846 (2013).
 42. Lee, D. A. *et al.* Genetic and neuronal regulation of sleep by neuropeptide VF. *ELife* **6**, e25727 (2017).
 43. Kim, J. S. What's in a name? Roles of RFamide-related peptides beyond gonadotrophin inhibition. *J. Neuroendocrinol.* **28**, doi: 10.1111/jne.12407 (2016).
 44. Kubrak, O. I., Lushchak, O. V., Zandawala, M. & Nässel, D. R. Systemic corazonin signalling modulates stress responses and metabolism in *Drosophila*. *Open Biol.* **6**, 160152 (2016).
 45. Regalado, J. M. *et al.* Increased food intake after starvation enhances sleep in *Drosophila melanogaster*. *J. Genet. Genomics* **44**, 319–326 (2017).
 46. van der Linden, A. M. *et al.* The EGL-4 PKG acts with KIN-29 salt-inducible kinase and protein kinase A to regulate chemoreceptor gene expression and sensory behaviors in *Caenorhabditis elegans*. *Genetics* **180**, 1475–1491 (2008).
 47. Choi, S., Lim, D.-S. & Chung, J. Feeding and fasting signals converge on the LKB1-SIK3 pathway to regulate lipid metabolism in *Drosophila*. *PLoS Genet.* **11**, e1005263 (2015).
 48. Funato, H. *et al.* Forward-genetics analysis of sleep in randomly mutagenized mice. *Nature* **539**, 378–383 (2016).
 49. Hoskins, L. J., Xu, M. & Volkoff, H. Interactions between gonadotropin-releasing hormone (GnRH) and orexin in the regulation of feeding and reproduction in goldfish (*Carassius auratus*). *Horm. Behav.* **54**, 379–385 (2008).
 50. Zhao, Y., Singh, C., Prober, D. A. & Wayne, N. L. Morphological and physiological interactions between GnRH3 and hypocretin/orexin neuronal systems in zebrafish (*Danio rerio*). *Endocrinology* **157**, 4012–4020 (2016).
 51. Xia, L., Chen, G.-H., Li, Z.-H., Jiang, S. & Shen, J. Alterations in hypothalamus-pituitary-adrenal/thyroid axes and gonadotropin-releasing hormone in the patients with primary insomnia: a clinical research. *PLoS One* **8**, e71065 (2013).
 52. Lindemans, M. *et al.* Adipokinetic hormone signaling through the gonadotropin-releasing hormone receptor modulates egg-laying in *Caenorhabditis elegans*. *Proc. Natl. Acad. Sci.* **106**, 1642–1647 (2009).
 53. Lindemans, M. *et al.* Gonadotropin-releasing hormone and adipokinetic hormone signaling systems share a common evolutionary origin. *Front. Endocrinol.* **2**, 16 (2011).
 54. Hauser, F. & Grimmelikhuijzen, C. J. P. Evolution of the AKH/corazonin/ACP/GnRH receptor superfamily and their ligands in the Protostomia. *Gen. Comp. Endocrinol.* **209**, 35–49 (2014).
 55. Roch, G. J., Tello, J. A. & Sherwood, N. M. At the transition from invertebrates to vertebrates, a novel gnrh-like peptide emerges in amphioxus. *Mol. Biol. Evol.* **31**, 765–778 (2014).
 56. Zandawala, M., Tian, S. & Elphick, M. R. The evolution and nomenclature of GnRH-type and corazonin-type neuropeptide signaling systems. *Gen. Comp. Endocrinol.* **264**, 64–77 (2018).
 57. Johnson, J. I., Kavanaugh, S. I., Nguyen, C. & Tsai, P. S. Localization and functional characterization of a novel adipokinetic hormone in the mollusk, *Aplysia californica*. *PLoS One* **9**, e106014 (2014).
 58. Gálíková, M. *et al.* Energy homeostasis control in *Drosophila* adipokinetic hormone mutants. *Genetics* **201**, 665–683 (2015).
 59. Grubbs, J. J., Lopes, L. E., van der Linden, A. M. & Raizen, D. M. A salt-induced kinase is required for the metabolic regulation of sleep. *PLoS Biol.* **18**, e3000220 (2020).
 60. Vadakkadath Meethal, S. *et al.* Identification of a gonadotropin-releasing hormone receptor orthologue in *Caenorhabditis elegans*. *BMC Evol. Biol.* **6**, 103 (2006).
 61. Froominckx, L. *et al.* Neuropeptide GPCRs in *C. elegans*. *Front. Endocrinol. (Lausanne)*. **3**, 1–19 (2012).
 62. Altschul, S. F., Gish, W., Miller, W., Myers, E. W. & Lipman, D. J. Basic local alignment search tool. *J. Mol. Biol.* **215**, 403–410 (1990).
 63. Park, D. *et al.* Interaction of structure-specific and promiscuous G-protein-coupled receptors mediates small-molecule signaling in *Caenorhabditis elegans*. *Proc. Natl. Acad. Sci.* **109**, 9917–9922 (2012).
 64. Van Sinay, E. *et al.* Evolutionarily conserved TRH neuropeptide pathway regulates growth in *Caenorhabditis elegans*. *Proc. Natl. Acad. Sci.* **114**, E4065–E4074 (2017).
 65. Van Bael, S. *et al.* Mass spectrometric evidence for neuropeptide-amidating enzymes in *C. elegans*. *J. Biol. Chem.* jbc.RA117.000731 (2018). doi:10.1074/jbc.RA117.000731
 66. Mirabeau, O. & Joly, J. Molecular evolution of peptidergic signaling systems in bilaterians. *Proc. Natl. Acad. Sci.* **110**, 2028–2037 (2013).
 67. Jékely, G. Global view of the evolution and diversity of metazoan neuropeptide signaling. *Proc. Natl. Acad. Sci.* **110**, 8702–8707 (2013).
 68. Lindemans, M. *et al.* A neuromedin-pyrokinin-like neuropeptide signaling system in *Caenorhabditis elegans*. *Biochem. Biophys. Res. Commun.* **379**, 760–764 (2009).
 69. Churgin, M. A. *et al.* Longitudinal imaging of *Caenorhabditis elegans* in a microfabricated device reveals variation

- in behavioral decline during aging. *ELife* **6**, e26652 (2017).
70. Iannaccone, M. J. *et al.* The RFamide receptor DMSR-1 regulates stress-induced sleep in *C. elegans*. *ELife* **6**, 1–20 (2017).
 71. Taylor, S. R. *et al.* Expression profiling of the mature *C. elegans* nervous system by single-cell RNA-Sequencing. *bioRxiv* 737577 (2019). doi:10.1101/737577
 72. Webb Chasser, A. M., Johnson, R. W. & Chamberlin, H. M. EGL-38 / Pax coordinates development in the *Caenorhabditis elegans* egg-laying system through EGF pathway dependent and independent functions. *Mech. Dev.* **159**, 103566 (2019).
 73. Takahashi, J. S. Transcriptional architecture of the mammalian circadian clock. *Nat. Rev. Genet.* **18**, 164–179 (2016).
 74. Brown, R. E., Basheer, R., Mckenna, J. T., Strecker, R. E. & Robert, W. Control of sleep and wakefulness. *Physiol. Rev.* **92**, 1087–1187 (2013).
 75. Ono, D. & Yamanaka, A. Hypothalamic regulation of the sleep/wake cycle. *Neurosci. Res.* **118**, 74–81 (2017).
 76. Monti, J. M., Torterolo, P. & Lagos, P. Melanin-concentrating hormone control of sleep/wake behavior. *Sleep Med. Rev.* **17**, 293–298 (2013).
 77. Herbison, A. E. Control of puberty onset and fertility by gonadotropin-releasing hormone neurons. *Nat. Rev. Endocrinol.* **12**, 452–466 (2016).
 78. Tayler, T. D., Pacheco, D. A., Hergarden, A. C., Murthy, M. & Anderson, D. J. A neuropeptide circuit that coordinates sperm transfer and copulation duration in *Drosophila*. *Proc. Natl. Acad. Sci.* **109**, 20697–20702 (2012).
 79. Treen, N. *et al.* Mollusc gonadotropin-releasing hormone directly regulates gonadal functions: a primitive endocrine system controlling reproduction. *Gen. Comp. Endocrinol.* **176**, 167–172 (2012).
 80. Twan, W. H. *et al.* The presence and ancestral role of gonadotropin-releasing hormone in the reproduction of scleractinian coral, *Euphyllia ancora*. *Endocrinology* **147**, 397–406 (2006).
 81. Artigas, G. Q. *et al.* A G protein-coupled receptor mediates neuropeptide-induced oocyte maturation in the jellyfish *Clytia*. *PLoS Biol.* **18**, 1–25 (2020).
 82. Yu, Y. *et al.* Regulation of starvation-induced hyperactivity by insulin and glucagon signaling in adult *Drosophila*. *ELife* **5**, e15693 (2016).
 83. Wu, Y., Masurat, F., Preis, J. & Bringmann, H. Sleep counteracts aging phenotypes to survive starvation-induced developmental arrest in *C. elegans*. *Curr. Biol.* **28**, 3610–3624.e8 (2018).
 84. Goetting, D. L., Soto, R. & Buskirk, C. Van. Food-dependent plasticity in *Caenorhabditis elegans* stress-induced sleep is mediated by TOR – FOXA and TGF- β signaling. *Genetics* **209**, 1183–1195 (2018).
 85. Schwarz, J. & Bringmann, H. Reduced sleep-like quiescence in both hyperactive and hypoactive mutants of the Galphaq gene *egl-30* during lethargus in *Caenorhabditis elegans*. *PLoS One* **8**, e75853 (2013).
 86. Nagy, S., Raizen, D. M. & Biron, D. Measurements of behavioral quiescence in *Caenorhabditis elegans*. *Methods* **68**, 500–507 (2014).
 87. Nathoo, A. N., Moeller, R. A., Westlund, B. A. & Hart, A. C. Identification of neuropeptide-like protein gene families in *Caenorhabditis elegans* and other species. *Proc. Natl. Acad. Sci.* **98**, 14000–14005 (2001).
 88. Itskovits, E., Ruach, R. & Zaslaver, A. Concerted pulsatile and graded neural dynamics enables efficient chemotaxis in *C. elegans*. *Nat. Commun.* **9**, 2866 (2018).
 89. Liu, Q., Kidd, P. B., Dobosiewicz, M. & Bargmann, C. I. *C. elegans* AWA olfactory neurons fire calcium-mediated all-or-none action potentials. *Cell* **175**, 57–70 (2018).
 90. Wan, X. *et al.* SRD-1 in AWA neurons is the receptor for female volatile sex pheromones in *C. elegans* males. *EMBO Rep.* **20**, 1–15 (2019).
 91. Abitua, P. B. *et al.* The pre-vertebrate origins of neurogenic placodes. *Nature* **524**, 462–465 (2015).
 92. Arendt, D. The evolution of cell types in animals: emerging principles from molecular studies. *Nat. Rev. Genet.* **9**, 868–882 (2008).
 93. Kusakabe, T. G. *et al.* A conserved non-reproductive GnRH system in Chordates. *PLoS One* **7**, (2012).
 94. Kamiya, C. *et al.* Nonreproductive role of gonadotropin-releasing hormone in the control of ascidian metamorphosis. *Dev. Dyn.* **243**, 1524–1535 (2014).
 95. Bargmann, C. I. Chemosensation in *C. elegans*. in *WormBook* (ed. The *C. elegans* Research Community) 1–29 (doi:10.1895/wormbook.1.123.1, 2006).
 96. Griffith, L. C. Neuromodulatory control of sleep in *Drosophila melanogaster*: Integration of competing and complementary behaviors. *Curr. Opin. Neurobiol.* **23**, 819–823 (2014).
 97. Yeon, J. *et al.* A sensory-motor neuron type mediates proprioceptive coordination of steering in *C. elegans* via two TRPC channels. *PLoS Biol.* **16**, e2004929 (2018).
 98. Liu, H. *et al.* Cholinergic sensorimotor integration regulates olfactory steering. *Neuron* **97**, 390–405.e3 (2018).
 99. Andreatta, G. *et al.* Corazonin signaling integrates energy homeostasis and lunar phase to regulate aspects of growth and sexual maturation in *Platynereis*. *Proc. Natl. Acad. Sci. U. S. A.* **117**, 1097–1106 (2020).
 100. Schwierin, B., Borbély, A. A. & Tobler, I. Sleep homeostasis in the female rat during the estrous cycle. *Brain Res.* **811**, 96–104 (1998).
 101. Stamatiades, G. A. & Kaiser, U. B. Gonadotropin regulation by pulsatile GnRH: Signaling and gene expression. *Mol. Cell. Endocrinol.* **463**, 131–141 (2018).
 102. Kim, Y.-J. *et al.* Corazonin receptor signaling in ecdysis initiation. *Proc. Natl. Acad. Sci.* **101**, 6704–6709 (2004).
 103. Stiernagle, T. Maintenance of *C. elegans*. in *WormBook* (eds. Fay, D. S. & Ambros, V.) (The *C. elegans* Research Community, 2006). doi:10.1895/wormbook.1.101.1
 104. Liu, K., Raghavan, S., Nelesen, S., Linder, C. R. & Warnow, T. Rapid and accurate large-scale coestimation of sequence alignments and phylogenetic trees. *Science* **324**, 1561–1564 (2009).
 105. Le, S. Q. & Gascuel, O. An improved general amino acid replacement matrix. *Mol. Biol. Evol.* **25**, 1307–1320

- (2008).
106. Guindon, S. *et al.* New algorithms and methods to estimate maximum-likelihood phylogenies: assessing the performance of PhyML 3.0. *Syst. Biol.* **59**, 307–321 (2010).
 107. Krogh, A., Larsson, È., Heijne, G. Von & Sonnhammer, E. L. L. Predicting transmembrane protein topology with a hidden Markov model : Application to complete genomes. *J. Mol. Biol.* **305**, 567–580 (2001).
 108. Nelson, M. D. & Fitch, D. H. A. Overlap extension PCR : An efficient method. *Methods Mol. Biol.* **772**, 459–470 (2011).
 109. Wiechelman, K. J., Braun, R. D. & Fitzpatrick, J. D. Investigation of the bicinchoninic acid protein assay: Identification of the groups responsible for color formation. *Anal. Biochem.* **175**, 231–237 (1988).
 110. Temmerman, L. *et al.* A proteomic approach to neuropeptide function elucidation. *Peptides* **34**, 3–9 (2012).
 111. Vandesompele, J., De Preter, K., Poppe, B., Van Roy, N. & De Paepe, A. Accurate normalization of real-time quantitative RT -PCR data by geometric averaging of multiple internal control genes. *Genome Biol.* **3**, research0034 (2002).
 112. Yu, C.-C. J., Raizen, D. M. & Fang-Yen, C. Multi-well imaging of development and behavior in *Caenorhabditis elegans*. *J. Neurosci. Methods* **223**, 35–9 (2014).
 113. Watteyne, J. *et al.* Neuromedin U signaling regulates retrieval of circuit of learned salt avoidance in a *C. elegans* gustatory circuit. *Nature Communications*, **11**, 2076 (2020).

”

Chapter 4:

Discussion

4.1 Discussion overview

Neuronal regulation tightly controls animal locomotion motifs by utilizing electrical, synaptic as well as neuroendocrine signals. While vertebrates utilize elaborate complex circuit architectures to achieve this, *C. elegans* compresses ample functionality in a compact nervous system.

On the other hand, the absence of animal locomotion is often regarded as the basic ground state to which an animal system returns if exciting neuronal inputs – required to instigate the rhythmic motor programs that enable propulsion through space – are lacking. However, animals do most certainly also display behavioral programs that actively prevent locomotion to increase their survival chances appropriately to the ecological context they inhabit. While the neuronal circuit mechanisms generating locomotion are being rapidly unraveled in increasing detail in multiple animal models, mechanisms inhibiting locomotion are only scarcely understood.^{1,2} Consequently, it still remains largely unknown to what extent the signaling molecules and neuronal circuits of different aspects of locomotion inhibition, like sleep and stopping behavior, differ or share similarities.

Neuropeptides are the most diverse group of signaling molecules in animals.³ In addition, their importance is illustrated by the broad variety of physiological processes and behavioral responses in which they are involved.⁴ Neuropeptidergic signaling pathways are primarily known to function as (extrasynaptic) neuroendocrine modulators of neurotransmission.⁵ In this manner, they contrast classical synaptic neurotransmitters that are mostly directly required for proper synaptic signal transmission, for instance in pattern generating neurocircuits that underlie motor patterns. By tweaking the electrical or biochemical properties of neurons that compose such circuits, neuropeptides are employed to tailor the resulting motor programs with the aim of adapting them to the animal's behavioral context.⁶

Therefore, mutational analysis of (only few) specific neuropeptides or neuropeptide receptors mostly reveals context-specific or relatively subtle defective behavioral phenotypes. For this reason, identification of their function on a cellular level is not straightforward and requires detailed quantitative analyses. Today, the exact functions of most neuropeptides are thus still poorly understood. Most of their cognate receptors were only very recently deorphanized, and their respective expression patterns are often still missing or only roughly delineated.⁷

The physiological importance of neuropeptidergic signaling hence urges us to develop a better scientific understanding of their *modus operandi* on a molecular level. All this led me to study the role of neuropeptides in an ancient, easily observable, and highly quantifiable animal behavior like locomotion. Specifically, my approach looked at locomotion from the alternative angle of its active prevention. I opted to make use of the benefits of the versatile model organism *C. elegans* as it enables extremely detailed mapping of genetic expression patterns and allows for experiments using cell-specific transgenic expression.

With the data of the articles in Chapters 2 and 3, presented above, we have clearly demonstrated a crucial role for neuropeptidergic signaling in locomotion inhibition in *C. elegans*. Furthermore, we have unraveled novel mechanistic insights of its molecular regulation on a (sub)cellular level. The focus of chapter 2 comprises the molecular mechanisms that are employed by a single neuron to elicit an organism-wide behavioral stopping response. In addition, chapter 3 characterises the role for GnRH-like neuropeptidergic signaling in sleep-wake regulation. Now, let me discuss and summarize the implications and potential broader consequences of both studies. As two behaviorally similar, but temporally and physiologically distinct aspects of locomotion inhibition (halting and sleep) were investigated in *C. elegans*, I will also elaborate on their similarities and speculate on how these behaviors might relate to one another.

4.2 Stop and sleep neurons in *C. elegans*

Out of the 302 neurons of the hermaphrodite connectome, only few are currently known to play a critical role in the active prevention of locomotion in *C. elegans* (see also **C1Fig. 11**). Obviously, motor neurons directly projecting to body wall muscle and which are required for generating motor programs might be involved. However, they are assumed to represent the executive layer that directly controls muscle tone, rather than being the neuron type dedicated to inducing the sophisticated action sequences that specifically inhibit locomotion, which is characteristic for dedicated stop or sleep neurons. Behavioral observations show that *C. elegans* nematodes can display locomotion arrest either with reduced muscle tone, for instance during prolonged sleep, or while simultaneously maintaining muscle tone, for instance during the brief stopping behavior accompanying the directional reorientation from forward to backward undulatory locomotion. To ensure proper motor execution only in suitable contexts, these stop/sleep neuron types or circuits would particularly be required to perceive upstream halting signals, to integrate such converging signals, and to counteract other locomotion activity promoting interneurons. How such neurons execute these functions on a molecular level is part of ongoing investigations in *C. elegans*.

4.2.1 RIS

In chapter 2 we show that the RIS interneuron fulfills the functionality of a stop neuron that rapidly halts locomotion in *C. elegans* (**C2Fig. 1**).⁸ Our data indicates that increased calcium activity in this single neuron is sufficient to induce transient stopping behavior (**C2Fig. 1, 5, 6b**). We find that RIS activity prevents calcium oscillations in cholinergic motor neurons, and thus inhibits their alternating activation of opposing body wall muscles (**C2Fig. 2, 3**). In this manner RIS activity could interfere in the pattern generating circuits underlying locomotion by desynchronizing the activity of excitatory motor neurons.

As shown in **C4Fig. 1**, RIS connects to many of its heavily connected neurons reciprocally, either via synapses or gap junctions. Presynaptic inputs that RIS receives from CEP, SDQL, AVJ, PVC and RIM neurons were recently shown to affect its calcium activity in L1 larvae and could thus signal the need to stop locomotion to RIS.⁹ AVJ neurons did not show such control of downstream RIS activity anymore during lethargus, indicating that RIS activity could be differentially regulated depending on the animal's sleep/wake state.

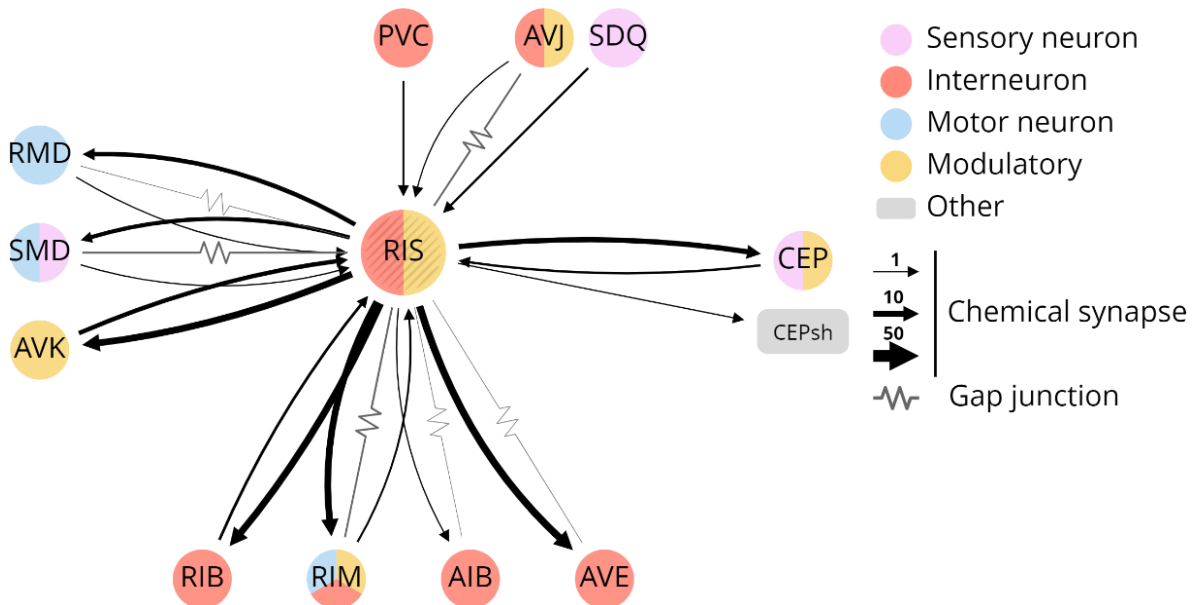


Figure 1: Connectome-based representation of neurons connected to RIS. Color codes of neuron types are indicated on the right. Black arrows represent the synaptic connections between neuron classes. Grey jagged lines represent gap junctions between neurons. The thickness of these symbols indicates the number of synapses or junctions, respectively. Generated with <http://nemanode.org> (built by <http://zhenlab.com>)¹⁰

We also find that the classical inhibitory neurotransmitter GABA facilitates the rapid onset of the RIS-induced stopping behavior (**C2Fig. 4a**), which establishes GABA as a contributing transmitter to rapidly induce locomotion stop. Direct release of GABA onto RIB interneurons (which are known to promote forward locomotion speed,¹¹ **C4Fig. 2**) and RMD head motor neurons could in part explain the accelerated stopping behavior. However, GABA is not required for stopping to occur in *C. elegans*, nor to maintain it. So, other neurotransmitters must also play a crucial role. Noteworthy, the SEZ-DN neurons that halt locomotion in fruit fly larvae by inhibiting the A27h premotor neuron network also synthesize GABA.¹² Known types of stop neurons in mammalian systems use a variety of neurotransmitters.^{13,14} Thus far, GABAergic neurons stopping locomotion have only been identified in the caudal brain stem of mice.¹⁴ While GABAergic neurons in the MLR are known to reduce locomotion speed by local inhibition of excitatory neurons.¹⁵

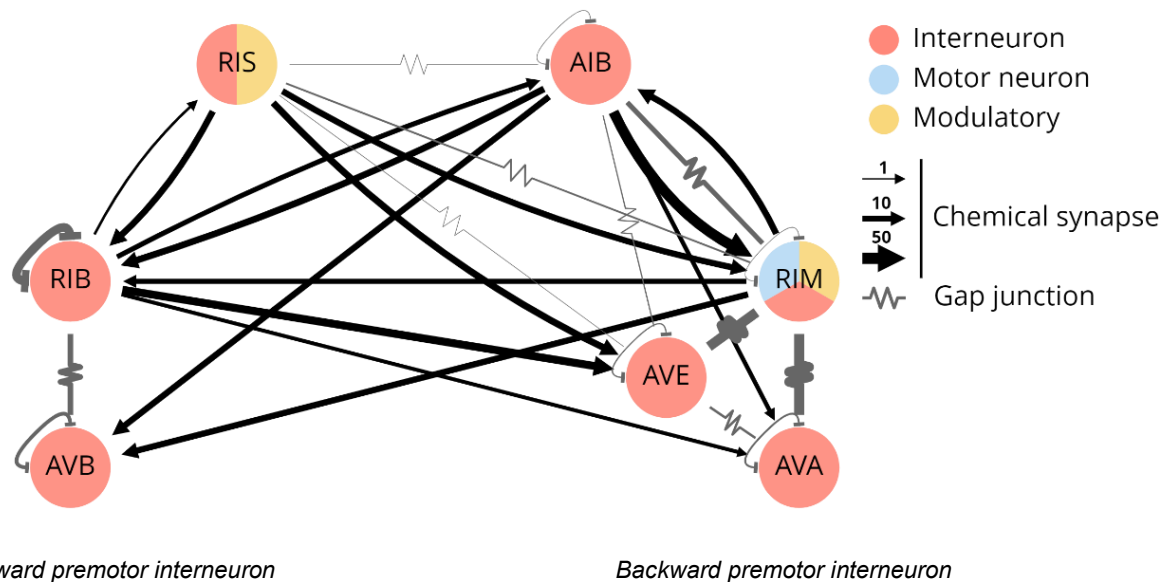


Figure 2: Simplified connectome-based neural circuit model of neurons instructive to understanding the neuronal regulation of stopping behavior. The activity of AVB and AVA premotor interneurons (PINs) are presumed to predominately determine either forward or backward locomotion state, respectively. Subsequently, these PINs both transmit their command inputs downstream via electrical gap junctions to differential local cholinergic motor neuron CPG circuits.¹⁶ As RIS is not directly connected to these major PINs we speculate that other connected interneurons are involved in relaying RIS activity further downstream to execute stopping behavior. We propose that RIS relays its halting functionality, at least in part, by inhibiting the forward-promoting RIB interneuron,¹¹ which is electrically coupled to the AVB forward PIN, by means of GABA. Simultaneously, electrical and neuropeptidergic RIS outputs could potentially prevent backward locomotion temporarily by affecting a coupled network of interneurons, such as AVE, AIB, RIM and AVA backward PINs which are known to promote and induce reversals.^{17–19} Color codes of neuron types are indicated on the right. Black arrows represent the synaptic connections between neuron classes. Grey jagged lines represent gap junctions between neurons. The thickness of these symbols indicates the number of synapses or junctions, respectively. Generated with <http://nemanode.org> (built by <http://zhenlab.com>)¹⁰

Besides its function as a stop neuron, we observe that the occurrence of reversal events increases following elevated RIS calcium levels (**C2Fig. 4, 6a, 6c**). We show that electrical connectivity via gap junctions is required for this increased reversal phenotype (**C2Fig. 4a,e**). However, RIS is not the sole neuron capable of inducing reversal events as animals are still able to perform backward locomotion even after genetic ablation of the RIS neuron (**C2Fig. 1f**). In this regard, evidence from multiple studies now support the proposition that AIB, RIM and AVA compose a coupled network that is crucial to control reversal behavior (**C4Fig. 2**).^{17–19} Similarly, the possibility also exists that RIS might not be the only dedicated stop neuron in *C. elegans* as there might be alternative means of halting locomotion. We suggest that RIS could potentially act via (AIB and) RIM neurons to favor shifting the global brain state from forward locomotion to reversing (**C2Fig. 4a** and **C4Fig. 2**). In this respect, I would like to mention the peculiar anatomical positioning of the RIS gap junctions in the ventral nerve ring where they connect to the most distal axonal endings of the contralateral RIM neurons. Similarly, AIB forms gap junctions near its most distal axonal endings that connect near the axonal branches of the contralateral RIM

neurons in the ventral ganglion.²⁰ Nuclear RIM and AIB calcium activity are both known to correlate with backward locomotion.¹⁸ However, (in contrast to RIM, which is heavily connected to AVA and AVE backward command neurons via gap junctions,) no strong correlation to reverse crawling speed is found for AIB neurons, while its calcium activity does often increase concomitantly with decelerating forward locomotion speed similar as to what we show here for RIS (**C2Fig. 5c**). Furthermore, it has also been suggested that AIB calcium transients initiate slightly prior to reversals.¹⁸ As a result, it would be interesting to investigate in more detail if and how these and our observations could be explained by gap junctions (or synapses) connecting AIB, RIS and RIM neurons. Particularly, further research on how the direction of locomotion is controlled in *C. elegans* could be informative for similar research in other invertebrate animals (or maybe even in lamprey or mice, as this research question still remains unanswered in vertebrates too).²

Next, I show that calcium activity in RIS correlates with decelerating forward locomotion and often precedes reversal events (**C2Fig. 5c-d, 6a-d**). When assigning compartments along the RIS axon this correlation becomes particularly clear around the nerve ring (**C2Fig. 5e**) where the majority of connections between RIS and its neighboring neurons are located.²⁰ We thus propose that RIS calcium dynamics are compartmentalized in its axon. Furthermore, we find that spontaneous axonal calcium activity around the characteristic branching region of the axon is significantly increased when calcium transients are paired with subsequent reversal events (**C2Fig. 7**). PVC and AVJ neurons exclusively connect to RIS at this branch region. PVC neurons have been shown to promote forward locomotion while little to nothing is known yet about the function of the AVJ neurons.^{21,22} (The left ventral SMD neuron also connects to RIS once in the branch region via a gap junction.²⁰) Increased calcium activity in the branch region of the RIS axon could indicate that synaptic or electrical inputs in this axonal region potentially contribute to initiation of reversals, although electrical outputs to AVJ or SMD neurons cannot be excluded (**C4Fig. 3**). The recent observation that presynaptic optogenetic depolarization of both PVC and AVJ neurons can increase RIS calcium levels in awake animals rather supports the former postulation.⁹ Compartmentalized calcium dynamics in RIA interneurons have already been demonstrated to control head bending behavior^{23,24}, but compartmentalization has not yet been looked into for AIB, nor for RIM neurons.

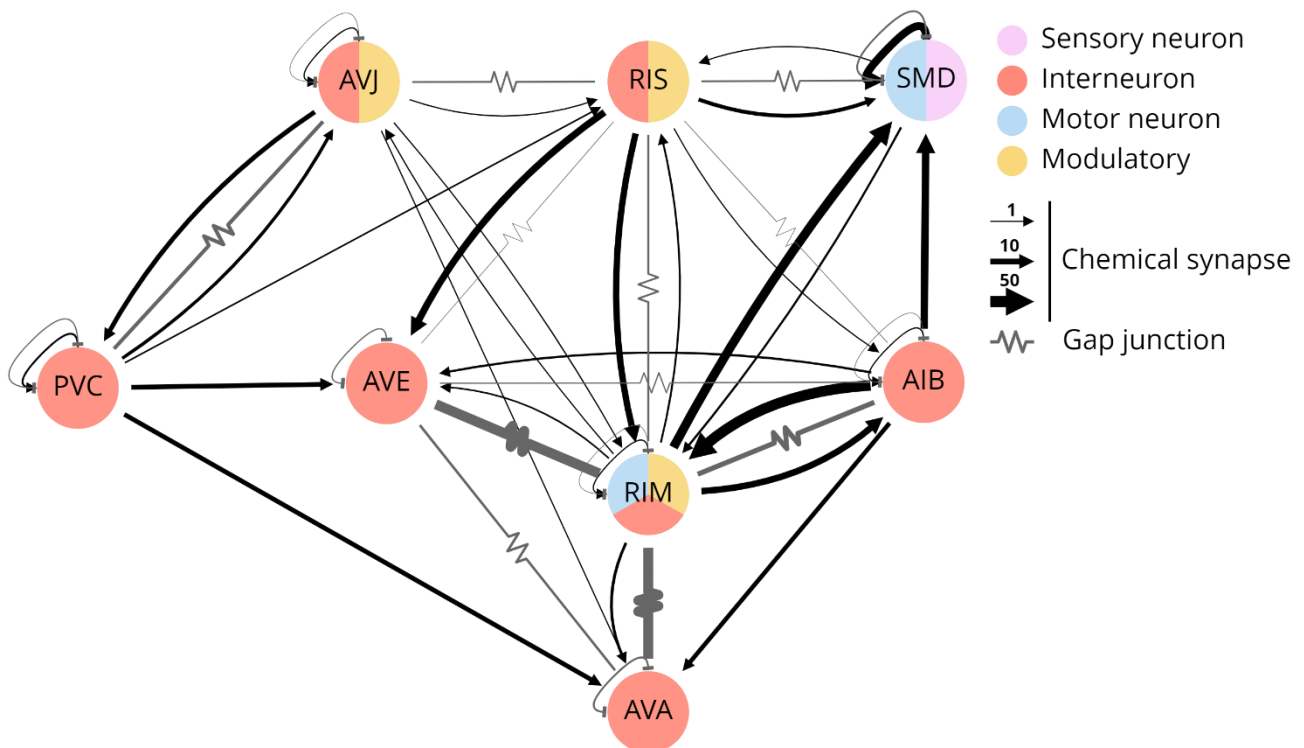


Figure 3: Connectome-based representation of major neurons involved in RIS-induced reversal behavior. AVJ and PVC neurons exclusively connect to RIS at the characteristic branch region of its axon. SMD neurons connect to RIS once in this branch region via a gap junction although the vast majority of their connections are located in the region of the RIS axon around the nerve ring.²⁰ AVE, AIB, RIM and AVA backward PINs compose a coupled network of interneurons inducing reversals.¹⁹ Color codes of neuron types are indicated on the right. Black arrows represent the synaptic connections between neuron classes. Grey jagged lines represent gap junctions between neurons. The thickness of these symbols indicates the number of synapses or junctions, respectively. Generated with <http://nemanode.org> (built by <http://zhenlab.com>)¹⁰

While compartmentalization of intraneuronal calcium has been heavily studied in sensory detection and mammalian synaptic plasticity, evidence for a role for compartmentalization in calcium-mediated neurotransmission in motor control is still limited or might even be lacking in other model systems.^{25,26} Further increasing the resolution of microscopic techniques for fluorescence calcium imaging in freely moving animals (by using spinning disk confocal^{27,28} or even more complex acquisition techniques^{29–31}), adding z-axis scanning to allow for volumetric imaging³¹ or using other improved genetically encoded biosensors could greatly benefit research to unravel the function of compartmentalized neuronal dynamics in more detail.

Our findings are consistent with the observation that RIS calcium activity in the nucleus was found to be strongly anticorrelated with activity of the major backward command interneurons.³² Supported by our data, I thus advocate that RIS activity might rapidly, but transiently suppress forward locomotion by briefly inhibiting forward command signals via GABAergic transmission, and that, once RIS activity decreases again, the electrical

consequences of these calcium transients, mostly favor backward locomotion presumably by effecting the coupled network of backward promoting interneurons to which RIS is connects via gap junctions. Whether the brief calcium transients in the RIS neuron could show similar functional features as the termination bursts of reticulospinal stop neurons observed in lamprey³³ might still be worth investigating.

In addition to this brief stopping behavior prior to reversals, the RIS interneuron is also known as the principal sleep-active neuron required for normal reduced locomotion activity during both lethargus and adulthood, when sleep can be induced in *C. elegans* by stress or pheromones.^{34–36} Remarkably, *C. elegans* is thus capable of inducing two distinct aspects of locomotion inhibition by means of the activity of a single interneuron. The noteworthy observation that the APTF-1 transcription factor (which is required for RIS-mediated locomotion quiescence) is exclusively expressed in RIS, AIB and RIB neurons, could potentially hint at a possible common role (involving these neuron classes) in initiating both brief stopping behaviour and sleep.³⁴

Strikingly, GABA was not found to play a significant role in RIS-mediated sleep in *C. elegans* while it has been posed as a potent sleep inducer in diverse model organisms (e. g. in the preoptic area of the mammalian hypothalamus) by inhibiting wake-promoting neurocircuits.^{34,37} In the light of our findings (**C2Fig. 4a**), a potential role for GABA in *C. elegans* sleep induction might have been masked in these previous studies (as they primarily focused on sleep/wake probability distribution data) if GABA would function to briefly accelerate onset of locomotion inhibition, but might not contribute to sustain it for longer periods of time.

All this clearly demonstrates the neuronal control of locomotion inhibition is a dynamic and modular regulatory process and not just the mathematical sum of logical ON/OFF switches to increase or decrease locomotion frequency. Besides RIS, only few other neurons, like the GABAergic neuron ALA, are known to be involved in *C. elegans* sleep induction.³⁵ Intriguingly, the glutamatergic RIA neurons, which are also known to display compartmentalized axonal calcium dynamics, release somnogenic NLP-22 neuropeptides.³⁸ Whether any of these neuron types also contribute to *C. elegans* stopping behaviour still remains to be determined.

Nonetheless, I expect that other neurocircuit mechanisms, independent of RIS, could still exist which are capable of suppressing locomotion as our data (in **C2Fig. 1f**) demonstrate

that animals are still able of stopping locomotion very briefly (or at least able to perform reversals) even after chemical ablation of RIS. Given the dual role of RIS, sleep neurons might be interesting candidates to investigate for their involvement in stopping behaviour. However, if neurocircuits orchestrating both sleep and stopping behaviour overlap (at least in part) in *C. elegans*, then the question still remains, to what extent these distinct behaviours are differentially regulated on a molecular level.

4.3 Neuropeptidergic modulation of locomotion inhibition

To investigate if neuropeptides can modulate the neuronal regulation of locomotion inhibition in *C. elegans*, we studied deletion mutant strains of neuropeptide precursor and GPCR genes in multiple behavioral assays. Based on their abundant dense core vesicle (DCV) content both RIS and ALA have been classified as modulatory neuron types.¹⁰ DCVs are known to contain neuropeptides. Because GABAergic transmission alone did not explain the full extent of RIS-mediated stopping behavior, neuropeptides were thus considered as alternative signaling molecules underlying its regulation. In **C2Fig. 4a-d**, I show that neuropeptides are indeed required to sustain the RIS-mediated optogenetic stopping phenotype.

4.3.1 FLP-11 neuropeptidergic signaling

Guided by literature³⁵ and a transcriptomic analysis of RIS³⁷, I identified that deletion of the *flp-11* gene in particular leads to disruption of RIS-mediated stopping behavior and is thus crucial to sustain animal halting prior to reversal initiation (**C2Fig. 4a-b**). In addition, publicly available sc-RNA-seq data sets confirm (the transcriptomic analysis, generated by our lab in collaboration with Prof. David Miller, by clearly demonstrating) that *flp-11* derived transcripts are most highly enriched in RIS neurons.³⁹⁻⁴¹ Furthermore, FLP-11 peptide homologs in *Ascaris suum* are also known to be expressed in a single interneuron in the posterior right lobe of the ventral ganglion, named (As-)RIS.^{42,43}

Subsequently, we show that increased RIS calcium activity is unable to induce concomitant decelerating locomotion when FLP-11 neuropeptides are lacking (**C2Fig. 6f,g**). In addition, we observed that spontaneous calcium activity transients in RIS do still occur normally when FLP-11 neuropeptides are not produced (**C2Fig. 6e,f**). The observation that FLP-11 neuropeptides are not required for RIS to increase backward locomotion further strengthens our model that gap junctions are presumably involved in inducing RIS-mediated reversals (**C2Fig. 4a,e**). This can then also imply that FLP-11 neuropeptides might potentially function

by simultaneously suppressing activity of both cholinergic interneurons that induce forward as well as those that induce backward locomotion, and that electrical connectivity via gap junctions indirectly leads to subsequent reversal independently of FLP-11 neuropeptides. Especially, as RIS calcium dynamics are more uncoupled from reversals when FLP-11 peptides are missing (**C2Fig. 7**).

Our data thus indicate that RIS regulates the prolonged duration of stopping behavior, via secretion of FLP-11 neuropeptides. FLP-11 neuropeptides are known to activate at least three different receptors promiscuously (albeit at relatively high EC_{50} values *in vitro*)⁴ that seem to act redundantly to regulate sleep.³⁵ All three these receptors show a relatively broad, primarily neuronal and mostly non-overlapping expression pattern. It might be interesting to validate the role of these receptors again in more detailed experiments that do not rely on neuropeptide overexpression strains. Potentially, more important receptors with a higher affinity for FLP-11 peptides could still await discovery as other somnogenic RFamide neuropeptides (like *flp-13* derived peptides) are now also known to exhibit similar promiscuous ligand-receptor interactions.^{44,45} However, if redundancy of either neuropeptides or receptors would be omnipresent in the peptidergic regulation of quiescence behavior,⁴⁶ it would become increasingly difficult to discern subtle quiescence defects in more detail with conventional mutational screening methods that might lack sufficient quantitative resolution.

Recently, it has been shown in immobilized L1 larvae that FLP-11 neuropeptides are required to strongly increase PVC calcium activity upon photodepolarization of RIS.⁹ This article also shows that RIS and PVC interneurons form a positive feedback loop and it suggests that concomitant activation of PVC (possibly due to FLP-11 peptide secretion) and RIM could function to prolong stops during the transition from forward to reverse states. In addition, it seems plausible that (transiently) increased electrical or synaptic inputs from multiple interneurons (f. i. PVC, RIM or AVJ) might finetune the release of FLP-11 neuropeptides from RIS to orchestrate appropriate stopping behavior.⁹ During stress-induced sleep, RIS activity is mediated by epidermal growth factor (EGF) signaling.³⁷ Whether EGF signaling could also regulate rapid FLP-11 neuropeptide secretion from RIS to induce brief stopping behavior still remains to be investigated.

Nevertheless, it would be interesting to further examine 1) if and how exactly FLP-11 neuropeptides can function via positive feedback to extend halting locomotion which could

eventually lead to prolonged locomotion quiescence during sleep and 2) whether they function by activating neuropeptide receptors on specific cholinergic neurons (resulting in their desynchronized activity, **C2Fig. 2, 3**) to maintain halting behavior. In accordance with the above, I thus speculate that FLP-11-mediated regulation of the duration of stopping behavior might potentially occur by simultaneous inhibition of several (both forward and backward promoting) neurons that express receptors activated by FLP-11 neuropeptides. Sufficiently strong FLP-11 inhibition of such neurons might extend stopping events to sleeping bouts via collective positive feedback to RIS.

In sum, RIS is a single, but fundamental modulatory neuron that can induce both brief stopping as well as prolonged locomotor arrest during sleep by controlling the duration of motor inhibition via peptidergic signaling. This indicates that these different aspects of locomotion inhibition can at least be partly shared on a cellular level. It also implies that is definitely worth investigating to what extent sleep and stopping neurons share similar downstream pathways in vertebrate systems or to what extent they remain functionally segregated in projecting to the executive level. Remarkably, also the vertebrate RFamide neuropeptide VF (NPVF, also known as gonadotropin-inhibitory hormone; GnIH), which is secreted by hypothalamic neurons that project to serotonergic raphe nuclei in the hindbrain, is involved in at least two distinct types of locomotion inhibition in larval fish: 1) suppressing escape behavior⁴⁷ and 2) sleep regulation.^{48,49}

4.3.2 RPamide neuropeptidergic signaling

In Chapter 3, we explore a novel role of two uncharacterized GnRH related receptors in the regulation of sleep-wake cycles during the larval development of *C. elegans*.⁵⁰ *In silico* sequence analysis revealed that eight such GNRR receptors are encoded in the *C. elegans* genome (**C3Fig. 1**). Previously, the ligand of only one of these GNRR receptors, GNRR-1, had been identified.⁵¹ Our phylogenetic tree indicates that the abundance of eight receptors originates from a nematode specific expansion of an ancestral GNRR predecessor resembling most to GNRR-1, which has the shortest branch lengths to other protostomian GnRH/AKH-like receptors, is activated by NLP-47 peptides, and is known to regulate reproduction.⁵¹ Surprisingly, we find that two of the GNRR receptors, GNRR-3 and GNRR-6, can be potently and dose-dependently activated *in vitro* by a group of neuropeptides encoded by the *nlp-2*, *nlp-22* and *nlp-23* genes (**C3Fig. 2**). This group of neuropeptides all contain a conserved C-terminal RPamide motif and are clustered on the same chromosome.

Due to the latter, we suggest that tandem gene duplications might have expanded these ligand genes in nematodes. Potentially, also the more dissimilar *nlp-45* and *nlp-46* genes might thus originate from these duplication events and could be interesting candidates for the remaining orphan GNRRs (GNRR-3/4/5/7). Alternatively, these receptors could possibly also be activated by pheromones via heterodimerization similar to what is known for DAF38/GNRR-8.⁵²

While RPamide neuropeptides display strong sequence conservation within the phylum *Nematoda*, clear sequence similarity to other peptides outside of the phylum had not yet been identified prior to this study. Based on their C-terminal conservation, the nematode RPamide neuropeptides most closely (albeit weakly) resemble both GnRH/AKH-like and Corazonin peptide families (out of all known bilaterian neuropeptides; **C3Fig. 3** and **C3Fig. S5** online). Together with the physiological receptor activation of GNRRs as well as with the lack of conservation of aromatic residues near the peptide N-terminus, I propose to classify the RPamide neuropeptides as GnRH-type peptides (in accordance with nomenclature recently proposed by Zandawala *et al.*, 2018).⁵³ However, as Corazonin(-like) peptides (or their receptors) have not been identified in the phylum *Nematoda*, I am unable to completely exclude the possibility that these genes could be remnants of ancestral Corazonin genes that are deemed lost. The phylogenetic data of their cognate receptors that we identified in this study, GNRR-3 and GNRR-6, (presented in our bioinformatic analysis; **C3Fig. 1**) also rather contradict this option as these *C. elegans* receptors do not cluster with other protostomian Corazonin receptors.

Nonetheless, the peculiar fact that RPamide peptides lack the characteristic N-terminal pyroglutamate modification, while the only other known *C. elegans* GnRH-type peptide (NLP-47) on the contrary lacks the conserved C-terminal amidation,⁵¹ rather urges me to speculate that (potentially following the tandem duplication event) differential selective pressures might have acted on their presumptive common ancestral gene to favor conservation of either terminus and resulting in differential gene functions. Sequencing genomes of uncharacterized bilaterian phyla and their addition to global sequence databases could shed more light on the evolution of the RPamides in the near future.⁵⁴

The only *C. elegans* RPamide neuropeptides that were previously studied in detail are encoded by *nlp-22* and are expressed in RIA interneurons. These NLP-22 neuropeptides display somnogenic properties during larval development and their overexpression is able to acutely induce sleep.³⁸ The identification of previously unstudied GNRRs as their cognate receptors *in vitro* led us to study their role in *C. elegans* sleep regulation in more detail.

Furthermore, exposure of *A. suum* to its synthetic orthologous neuropeptides (*As-NLP-22*) is known to suppress muscle contractions and decreases basal muscle tone which then both inhibit its locomotion as a consequence⁵⁵ This again strengthens the likelihood for a function of RPamide neuropeptides in motor control. However, the receptor that induces these physiological changes and where it is expressed still remained unknown in *A. suum*.

Next, we observed that *gnrr-3* is expressed in GABAergic motor neurons of the posterior ventral nerve cord in *C. elegans* which clearly points to a plausible role in regulating locomotion inhibition ([C3Fig. S6I,J online](#)). In addition, I determine the expression pattern of *gnrr-6* in a broader subset of neurons that also included multiple crucial neuron classes with shown functional relevance for motor behavior (**C3Fig. S6A-G** online).

We then show that NLP-22 neuropeptides signal through GNRR-6 to suppress *C. elegans* locomotion activity during sleep (**C3Fig. 4B,C**). Non-reproductive functions for GnRH signaling pathways have also been demonstrated in larvae of diverse chordates.^{56,57} In addition, we show that overexpression of *nlp-22* still induces pumping quiescence in the absence of GNRR-6 receptors (**C3Fig. 4A**) which indicates that other aspects of this sleeping behavior are not dependent on GNRR-6. Similarly, it would be interesting to investigate the role of FLP-11 neuropeptides in RIS-mediated feeding quiescence as photodepolarization of RIS also leads to reduced pharyngeal pumping (**C2Fig. S1B-D** online). Furthermore, it is definitely also worth exploring whether the release of NLP-22 peptides is regulated differentially in the distinct calcium compartments of RIA interneurons.²³

To the contrary, we also demonstrate that NLP-2 encoded neuropeptides instead promote wakefulness during lethargus (**C3Fig. 5A-D**) by signaling through both GNRR-3 as well as GNRR-6 receptors (**C3Fig. 5I,J**). The intriguing question how these RPamide peptides, only differing in up to 4 amino acid residues and both depending on GNRR-6 receptors, can mediate opposing activity phenotypes has not been elucidated yet in this study. Presumably, the differential activation potencies that they confer to specific receptors *in vivo* and the resulting extent of differential downstream pathway induction in the neurons expressing these two GNRRs might be crucial determinants for their opposing behavioral outcome.

Next, we show that *nlp-2* is predominantly expressed in a single pair of sensory AWA neurons (**C3Fig. 6A**) and that its transcripts cycle with larval periodicity (**C3Fig. 6B**). AWA neurons share some similar properties that are characteristic for GnRH neurons in

vertebrates; AWA neurons are olfactory sensory neurons which are known to detect sex-specific pheromones^{58,59} and display pulsatile electrochemical characteristics.^{60,61} Furthermore, our finding that *nlp-2* transcript abundance oscillates following the temporal expression cycles of developmental clock genes (**C3Fig. 6B**; similarly to what was found for *nlp-22*)³⁸ suggests that the expression levels of RPamide neuropeptides are tightly regulated throughout developmental maturation. Whether downstream feedback mechanisms also contribute to regulation of clock gene expression itself is still open for further investigation, but AWA neurons are known to be involved in odor-induced larval developmental arrest^{62,63} and one of their major sensory stimuli (the volatile attractive food odor diacetyl)^{58,64} was found to suppress sleep in adult nematodes.⁶⁵ In the light of our findings, the latter might possibly be mediated via peptidergic NLP-2 signaling. Whether or not NLP-2 peptides are indeed secreted by AWA neurons upon sensory stimulation of certain specific odorants or pheromones still remains to be determined, nonetheless it seems likely that the NLP-2 mediated induction of wake-promoting behavior is also dependent on more indirect internal clock signals regulating the cycling expression levels of RPamide neuropeptides.

The fact that *nlp-2* is also expressed in four neurosecretory uv1 uterine cells, might indicate that RPamides could also still be somehow implicated in the regulation of reproduction or egg-laying, in addition to sleep-wake regulation. A role for FLP-11 peptides in egg-laying has recently been demonstrated,⁶⁶ and also *nlp-49* encoded neuropeptides (which promote locomotor arousal upon overexpression) affect the timing of egg-laying behavior in addition.⁶⁷ We did not explore reproductive function further in our current study (cfr. PhD Thesis Lotte Froominckx), but determining whether the transcripts levels in either AWA neurons or uv1 cells or in both are regulated by the developmental clock would be interesting to pursue. In brief, we found that RPamide neuropeptides encoded by both *nlp-2* and *nlp-22* genes signal through GnRH-like receptors to promote either wakefulness or sleep, respectively.

In sum, we showed 1) that *C. elegans* employs electrical, synaptic as well as neuropeptidergic signaling of a stop neuron with compartmentalized Ca²⁺ dynamics, named RIS, to differentially regulate the active inhibition of locomotion and 2) that GnRH-like neuropeptidergic signaling pathways display non-reproductive functions in *C. elegans* in the regulation of its larval sleep-wake behavior. The combined data in the Results chapters of this dissertation together with recent scientific literature presented in the Introduction,

highlight that (RFamide) neuropeptides are evolutionary conserved regulators of sleeping behavior in a broad variety of animal systems. Furthermore, we pose that neuronal circuits with well-established functionality in the neuropeptidergic regulation of either reproductive function or sleep, might also display (thus far unstudied) functionality in vertebrates in either sleep or the inhibition of locomotion during wakefulness, respectively.

4.4 Outlook

Given the surprising findings in this thesis that 1) GnRH-like RPamide peptidergic signaling is involved in non-reproductive functions like larval sleep-wake regulation (in **Chapter 3**) and that 2) FLP-11 RFamide neuropeptides, known to regulate larval sleep, are subsequently also regulating brief stopping behavior in adults (in **Chapter 2**), I would like to highlight the importance of approaching behavioral research questions from a developmental perspective. This might allow us to narrow down the subtle behavioral functions of neuropeptidergic signaling pathways by taking into account that their functions could change throughout developmental stages as also the characteristic behaviors associated with these stages change.

Therefore, it might be informative to investigate in diverse model systems whether the known reproduction-centered function of the GnRH-like peptide family can be expanded to other physiological functions in non-reproductive larval stages or can potentially even be reconsidered to a broader role in the neuronal regulation of timing cyclic developmental maturation and the behavioral changes associated with this (such as larval molting, metamorphosis or adult reproductive behavior). Similarly, questions arise 1) whether *nlp-22* encoded peptides secreted by RIA interneurons could also play a role in the regulation of brief stopping behavior in adult *C. elegans*, similar to FLP-11 neuropeptides secreted by RIS, or 2) how somnogenic functions of RFamide neuropeptides like NPVF in larval vertebrates^{48,49} relate to adult functions in the regulation of either specific aspects of locomotion inhibition (like escape responses)⁴⁷ or rhythmic reproduction.^{68,69}

This thesis aimed to shed light on how specific neuropeptides secreted by stop or sleep neurons regulate locomotion inhibition behavior, specifically in *C. elegans*. However, many other intriguing animal research questions concerning locomotion inhibition still lie ahead. What the function of sleep encompasses, how somnogenic neuropeptides evolved, whether stop and sleep neurons had the same evolutionary ancestral cell type or which of both

phenotypes evolved first, all remain interesting and unsolved questions to taunt our imaginations for some time to come.

4.4 References

1. Xu, T. *et al.* Descending pathway facilitates undulatory wave propagation in *Caenorhabditis elegans* through gap junctions. *Proc. Natl. Acad. Sci. U. S. A.* **115**, E4493–E4502 (2018).
2. Grillner, S. & El Manira, A. Current principles of motor control, with special reference to vertebrate locomotion. *Physiol. Rev.* **100**, 271–320 (2020).
3. Schoofs, L., De Loof, A. & Van Hiel, M. B. Neuropeptides as regulators of behavior in insects. *Annu. Rev. Entomol.* **62**, 35–52 (2017).
4. Peymen, K., Watteyne, J., Frootinckx, L., Schoofs, L. & Beets, I. The FMRFamide-like peptide family in nematodes. *Front. Endocrinol. (Lausanne)*. **5**, (2014).
5. Bentley, B. *et al.* The multilayer connectome of *Caenorhabditis elegans*. *PLoS Computational Biology* **12**, (2016).
6. Marder, E., Bucher, D., Schulz, D. J. & Taylor, A. L. Invertebrate central pattern generation moves along. *Curr. Biol.* **15**, 685–699 (2005).
7. Frootinckx, L. *et al.* Neuropeptide GPCRs in *C. elegans*. *Front. Endocrinol. (Lausanne)*. **3**, 1–19 (2012).
8. Steuer Costa, W. *et al.* A GABAergic and peptidergic sleep neuron as a locomotion stop neuron with compartmentalized Ca²⁺ dynamics. *Nat. Commun.* **10**, (2019).
9. Maluck, E. *et al.* A wake-active locomotion circuit depolarizes a sleep-active neuron to switch on sleep. *PLoS Biol.* **18**, 1–41 (2020).
10. Witvliet, D. *et al.* Connectomes across development reveal principles of brain maturation. *Nature* **596**, 257–261 (2021).
11. Li, Z., Liu, J., Zheng, M. & Xu, X. Z. S. Encoding of both analog- and digital-like behavioral outputs by one *C. elegans* interneuron. *Cell* **159**, 751–765 (2014).
12. Tastekin, I. *et al.* Sensorimotor pathway controlling stopping behavior during chemotaxis in the *Drosophila melanogaster* larva. *Elife* **7**, 1–38 (2018).
13. Bouvier, J. *et al.* Descending command neurons in the brainstem that halt locomotion. *Cell* **163**, 1191–1203 (2015).
14. Capelli, P., Pivetta, C., Esposito, M. S. & Arber, S. Locomotor speed control circuits in the caudal brainstem. *Nature* **551**, 373–377 (2017).
15. Roseberry, T. K. *et al.* Cell-type-specific control of brainstem locomotor circuits by basal ganglia. *Cell* **164**, 526–537 (2016).
16. Wen, Q., Gao, S. & Zhen, M. *Caenorhabditis elegans* excitatory ventral cord motor neurons derive rhythm for body undulation. *Philos. Trans. R. Soc. B Biol. Sci.* **373**, 20170370 (2018).
17. Gordus, A., Pokala, N., Levy, S., Flavell, S. W. & Bargmann, C. I. Feedback from network states generates variability in a probabilistic olfactory circuit. *Cell* **161**, 215–227 (2015).
18. Kato, S. *et al.* Global brain dynamics embed the motor command sequence of *Caenorhabditis elegans*. *Cell* **163**, 656–669 (2015).
19. López-Cruz, A. *et al.* Parallel multimodal circuits control an innate foraging behavior. *Neuron* **102**, 407–419.e8 (2019).
20. White, J. G., Southgate, E., Thomson, J. N. & Brenner, S. The structure of the nervous system of the nematode *Caenorhabditis elegans*. *Philos. Trans. R. Soc. London* **314**, 1–340 (1986).
21. Husson, S. J. *et al.* Optogenetic analysis of a nociceptor neuron and network reveals ion channels acting downstream of primary sensors. *Curr. Biol.* **22**, 743–752 (2012).
22. Chalfie, M. *et al.* The neural circuit for touch sensitivity in *Caenorhabditis elegans*. *J. Neurosci.* **5**, 956–964 (1985).
23. Hendricks, M., Ha, H., Maffey, N. & Zhang, Y. Compartmentalized calcium dynamics in a *C. elegans* interneuron encode head movement. *Nature* **487**, 99–103 (2012).
24. Ouellette, M.-H., Desrochers, M. J., Gheta, I., Ramos, R. & Hendricks, M. A Gate-and-switch model for head orientation behaviors in *Caenorhabditis elegans*. *ENEURO* **5**, ENEURO.0121-18.2018 (2018).
25. Yang, H. H. H. *et al.* Subcellular imaging of voltage and calcium signals reveals neural processing *in vivo*. *Cell* **166**, 245–257 (2016).
26. Donato, A., Kagias, K., Zhang, Y. & Hilliard, M. A. Neuronal sub-compartmentalization: a strategy to optimize neuronal function. *Biol. Rev.* **94**, 1023–1037 (2019).
27. Nguyen, J. P. *et al.* Whole-brain calcium imaging with cellular resolution in freely behaving *Caenorhabditis elegans*. *Proc. Natl. Acad. Sci. U. S. A.* **113**, E1074–E1081 (2016).
28. Venkatachalam, V. *et al.* Pan-neuronal imaging in roaming *Caenorhabditis elegans*. *Proc. Natl. Acad. Sci. U. S. A.* **113**, E1082–E1088 (2016).
29. Schrödel, T., Prevedel, R., Aumayr, K., Zimmer, M. & Vaziri, A. Brain-wide 3D imaging of neuronal activity in *Caenorhabditis elegans* with sculpted light. *Nat. Methods* **10**, 1013–1020 (2013).
30. Prevedel, R. *et al.* Simultaneous whole-animal 3D imaging of neuronal activity using light-field microscopy. *Nat. Methods* **11**, 727–730 (2014).
31. Voleti, V. *et al.* Real-time volumetric microscopy of *in vivo* dynamics and large-scale samples with SCAPE 2.0. *Nat. Methods* **16**, 1054–1062 (2019).
32. Nichols, A. L. A., Eichler, T., Latham, R. & Zimmer, M. A global brain state underlies *C. elegans* sleep behavior. *Science* **356**, 1277–1279 (2017).
33. Juvin, L. *et al.* A specific population of reticulospinal neurons controls the termination of locomotion. *Cell Rep.* **15**, 2377–2386 (2016).
34. Turek, M., Lewandrowski, I. & Bringmann, H. An AP2 transcription factor is required for a sleep-active neuron to induce sleep-like quiescence in *C. elegans*. *Curr. Biol.* **23**, 2215–2223 (2013).
35. Turek, M., Besseling, J., Spies, J. P., König, S. & Bringmann, H. Sleep-active neuron specification and sleep induction require FLP-11 neuropeptides to systemically induce sleep. *Elife* **5**, e12499 (2016).
36. Wu, Y., Masurat, F., Preis, J. & Bringmann, H. Sleep counteracts aging phenotypes to survive starvation-induced developmental arrest in *C. elegans*. *Curr. Biol.* **28**, 3610–3624.e8 (2018).
37. Konietzka, J. *et al.* Epidermal growth factor signaling promotes sleep through a combined series and parallel neural circuit. *Curr. Biol.* **30**, 1–16.e13 (2020).
38. Nelson, M. D. *et al.* The neuropeptide NLP-22 regulates a sleep-like state in *Caenorhabditis elegans*. *Nat. Commun.* **4**, 2846 (2013).
39. Cao, J. *et al.* Comprehensive single-cell transcriptional profiling of a multicellular organism. *Science* **357**, 661–667 (2017).
40. Packer, J. S. *et al.* A lineage-resolved molecular atlas of *C. elegans* embryogenesis at single-cell resolution. *Science*, **365**, eaax1971 (2019).
41. Taylor, S. R. *et al.* Expression profiling of the mature *C. elegans* nervous system by single-cell RNA-Sequencing. *bioRxiv* 737577 (2019). doi:10.1101/737577

42. Yew, J. Y. *et al.* Peptide products of the *afp-6* gene of the nematode *Ascaris suum* have different biological actions. *J. Comp. Neurol.* **502**, 872–882 (2007).
43. Atkinson, L. E. *et al.* Unraveling flp-11/flp-32 dichotomy in nematodes. *Int. J. Parasitol.* **46**, 723–736 (2016).
44. Nelson, M. D. *et al.* FRPR-4 is a G-protein coupled neuropeptide receptor that regulates behavioral quiescence and posture in *Caenorhabditis elegans*. *PLoS One* **10**, 1–19 (2015).
45. Iannacone, M. J. *et al.* The RFamide receptor DMSR-1 regulates stress-induced sleep in *C. elegans*. *Elife* **6**, 1–20 (2017).
46. Nath, R. D., Chow, E. S., Wang, H., Schwarz, E. M. & Sternberg, P. W. *C. elegans* stress-induced sleep emerges from the collective action of multiple neuropeptides. *Curr. Biol.* **26**, 2446–2455 (2016).
47. Madelaine, R. *et al.* The hypothalamic NPVF circuit modulates ventral raphe activity during nociception. *Sci. Rep.* **7**, 41528 (2017).
48. Lee, D. A. *et al.* Genetic and neuronal regulation of sleep by neuropeptide VF. *Elife* **6**, e25727 (2017).
49. Lee, D. A. *et al.* Neuropeptide VF neurons promote sleep via the serotonergic raphe. *Elife* **9**, e54491 (2020).
50. Van der Auwera, P. *et al.* RPamide neuropeptides NLP-22 and NLP-2 act through GnRH-like receptors to promote sleep and wakefulness in *C. elegans*. *Sci. Rep.* **10**, 9929 (2020).
51. Lindemans, M. *et al.* Adipokinetic hormone signaling through the gonadotropin-releasing hormone receptor modulates egg-laying in *Caenorhabditis elegans*. *Proc. Natl. Acad. Sci.* **106**, 1642–1647 (2009).
52. Park, D. *et al.* Interaction of structure-specific and promiscuous G-protein-coupled receptors mediates small-molecule signaling in *Caenorhabditis elegans*. *Proc. Natl. Acad. Sci. U. S. A.* **109**, 9917–9922 (2012).
53. Zandawala, M. *et al.* Discovery of novel representatives of bilaterian neuropeptide families and reconstruction of neuropeptide precursor evolution in ophiuroid echinoderms. *Open Biol.* **7**, 170129 (2017).
54. Thiel, D., Franz-Wachtel, M., Aguilera, F. & Hejnal, A. Xenacoelomorph neuropeptidomes reveal a major expansion of neuropeptide systems during early bilaterian evolution. *Mol. Biol. Evol.* **35**, 2528–2543 (2018).
55. Konop, C. J. *et al.* Mass spectrometry of single GABAergic somatic motoneurons identifies a novel inhibitory peptide, As-NLP-22, in the nematode *Ascaris suum*. *J. Am. Soc. Mass Spectrom.* **26**, 2009–2023 (2015).
56. Kusakabe, T. G. *et al.* A conserved non-reproductive GnRH system in Chordates. *PLoS One* **7**, (2012).
57. Kamiya, C. *et al.* Nonreproductive role of gonadotropin-releasing hormone in the control of ascidian metamorphosis. *Dev. Dyn.* **243**, 1524–1535 (2014).
58. Bargmann, C. I., Hartweg, E. & Horvitz, H. R. Odorant-selective genes and neurons mediate olfaction in *C. elegans*. *Cell* **74**, 515–527 (1993).
59. Wan, X. *et al.* SRD-1 in AWA neurons is the receptor for female volatile sex pheromones in *C. elegans* males. *EMBO Rep.* **20**, 1–15 (2019).
60. Liu, Q., Kidd, P. B., Dobosiewicz, M. & Bargmann, C. I. *C. elegans* AWA olfactory neurons fire calcium-mediated all-or-none action potentials. *Cell* **175**, 57–70 (2018).
61. Itskovits, E., Ruach, R. & Zaslaver, A. Concerted pulsatile and graded neural dynamics enables efficient chemotaxis in *C. elegans*. *Nat. Commun.* **9**, 2866 (2018).
62. Sengupta, P., Chou, J. H. & Bargmann, C. I. odr-10 Encodes a seven transmembrane domain olfactory receptor required for responses to the odorant diacetyl. *Cell* **84**, 899–909 (1996).
63. Hoffmann, M. C., Sellings, L. H. L. & van der Kooy, D. A diacetyl-induced quiescence in young *Caenorhabditis elegans*. *Behav. Brain Res.* **214**, 12–17 (2010).
64. Larsch, J., Ventimiglia, D., Bargmann, C. I. & Albrecht, D. R. High-throughput imaging of neuronal activity in *Caenorhabditis elegans*. *Proc. Natl. Acad. Sci.* **110**, (2013).
65. Lawler, D. E. *et al.* Sleep analysis in adult *C. elegans* reveals state-dependent alteration of neural and behavioral responses. *J. Neurosci.* **41**, 1892 LP – 1907 (2021).
66. Banerjee, N., Bhattacharya, R., Gorczyca, M., Collins, K. M. & Francis, M. M. Local neuropeptide signaling modulates serotonergic transmission to shape the temporal organization of *C. elegans* egg-laying behavior. *PLoS Genet.* **13**, e1006697 (2017).
67. Chew, Y. L., Grundy, L. J., Brown, A. E. X., Beets, I. & Schafer, W. R. Neuropeptides encoded by *nlp-49* modulate locomotion, arousal and egg-laying behaviours in *Caenorhabditis elegans* via the receptor SEB-3. *Philos. Trans. R. Soc. B Biol. Sci.* **373**, 20170368 (2018).
68. Angelopoulou, E., Quignon, C., Kriegsfeld, L. J. & Simonneaux, V. Functional implications of RFRP-3 in the central control of daily and seasonal rhythms in reproduction. *Front. Endocrinol. (Lausanne)*. **10**, 1–15 (2019).
69. Dufour, S. *et al.* Origin and evolution of the neuroendocrine control of reproduction in Vertebrates, with special focus on genome and gene duplications. *Physiol. Rev.* **100**, 869–943 (2019).

Erweiterte Zusammenfassung in Deutsch

Die neuronale Regulation steuert die Fortbewegungsmuster von Tieren durch elektrische, synaptische und neuroendokrine Signale. Während Wirbeltiere dafür aufwendige, komplexe Schaltkreisarchitekturen verwenden, komprimiert *C. elegans* umfangreiche Funktionalität in einem kompakten Nervensystem.

Andererseits wird das Ausbleiben der Fortbewegung oft als der Grundzustand angesehen, zu dem ein tierisches (Nerven)System zurückkehrt, wenn erregende neuronale Eingangssignale fehlen. Letztere sind erforderlich, um die rhythmischen Motorprogramme zu initiieren, welche die räumliche Fortbewegung ermöglichen. Allerdings zeigen Tiere durchaus auch Verhaltensprogramme, die aktiv die Fortbewegung verhindern, um ihre Überlebenschancen entsprechend dem ökologischen Kontext, in dem sie leben, zu erhöhen. Während die neuronalen Schaltkreismechanismen, welche die Fortbewegung ermöglichen, in zahlreichen Tiermodellen immer detaillierter entschlüsselt werden, sind die Mechanismen, die die Fortbewegung hemmen, nur unzureichend bekannt. Folglich ist immer noch weitgehend unbekannt, inwieweit die Signalmoleküle und neuronalen Schaltkreise für die verschiedenen Aspekte der Bewegungshemmung, z.B. Schlaf und Stopverhalten, unterscheiden oder ob sie Ähnlichkeiten aufweisen.

Neuropeptide sind die vielfältigste Gruppe von Signalmolekülen bei Tieren, und ihre Bedeutung wird durch die große Vielfalt an physiologischen Prozessen und Verhaltensreaktionen deutlich, an denen sie beteiligt sind. Neuropeptiderge Signalwege sind in erster Linie dafür bekannt, dass sie als (extrasynaptische) neuroendokrine Modulatoren der Neurotransmission fungieren. Auf diese Weise stehen sie im Gegensatz zu den klassischen synaptischen Neurotransmittern, die meist direkt für die korrekte synaptische Signalübertragung benötigt werden, zum Beispiel in mustergenerierenden neuronalen Schaltkreisen, die motorischen Mustern zugrunde liegen. Durch Veränderung der elektrischen oder biochemischen Eigenschaften von Neuronen, die solche Schaltkreise bilden, passen Neuropeptide die resultierenden motorischen Programme an den Verhaltenskontext des Tieres an.

Die Mutationsanalyse von (einigen) spezifischen Neuropeptiden oder Neuropeptidrezeptoren zeigt meist nur kontextspezifische oder relativ subtile Defekte von Verhaltensphänotypen. Aus diesem Grund ist die Identifizierung ihrer Funktion auf zellulärer

Ebene nicht einfach und erfordert detaillierte quantitative Analysen. Die genauen Funktionen der meisten Neuropeptide sind daher bis heute nur unzureichend bekannt. Die meisten ihrer spezifischen Rezeptoren wurden erst vor kurzem deorphanisiert, und ihre jeweiligen Expressionsmuster sind oft noch nicht etabliert oder nur grob umrissen.

Die physiologische Bedeutung der neuropeptidergen Signalübertragung zwingt uns daher, ein besseres wissenschaftliches Verständnis ihrer Funktionsweise auf molekularer Ebene zu entwickeln. All dies hat mich dazu veranlasst, die Rolle der Neuropeptide bei einem evolutionär sehr alten, leicht zu beobachtenden und in hohem Maße quantifizierbaren Tierverhalten wie der Fortbewegung zu untersuchen. Konkret betrachtete ich die Fortbewegung aus dem alternativen Blickwinkel ihrer aktiven Unterbindung. Ich entschied mich, die Vorteile des vielseitigen Modellorganismus *C. elegans* zu nutzen, da er eine äußerst detaillierte Kartierung genetischer Expressionsmuster ermöglicht und Experimente mit zellspezifischer transgener Expression erlaubt.

Mit den Daten der Artikel in den Kapiteln 2 und 3 haben ich mit meinen KollegInnen eindeutig eine entscheidende Rolle der neuropeptidergen Signalübertragung bei der Bewegungshemmung in *C. elegans* nachgewiesen. Darüber hinaus haben wir neue mechanistische Erkenntnisse über die molekulare Regulation dieses Verhaltensaspektes auf (sub)zellulärer Ebene gewonnen. Der Schwerpunkt von Kapitel 2 liegt auf den molekularen Mechanismen, die von einem einzelnen Neuron eingesetzt werden, um eine organismusweite Verhaltensstopreaktion auszulösen. Darüber hinaus wird in Kapitel 3 die Rolle der GnRH-ähnlichen neuropeptidergen Signalübertragung bei der Schlaf-Wach-Regulation beschrieben. Hier möchte ich nun die Implikationen und möglichen weitergehenden Konsequenzen beider Studien diskutieren und zusammenfassen. Da in *C. elegans* zwei verhaltensmäßig ähnliche, aber zeitlich und physiologisch unterschiedliche Aspekte der Bewegungshemmung (Stop- und Schlafverhalten) untersucht wurden, werde ich auch auf ihre Ähnlichkeiten eingehen und eine Hypothese darüber formulieren, wie diese Verhaltensweisen miteinander zusammenhängen könnten.

Von den 302 Neuronen des hermaphroditischen Konnektoms von *C. elegans* sind derzeit nur wenige bekannt, die eine entscheidende Rolle beim aktiven Stop der Bewegung spielen. Offensichtlich könnten motorische Neuronen beteiligt sein, welche direkt die Körperwandmuskulatur innervieren und für die Erzeugung der Motorprogramme erforderlich

sind. Es wird angenommen, dass sie die ausführende Ebene darstellen, die den Muskeltonus direkt steuert. Jedoch sind sie wohl nicht der Neuronentyp, der die ausgefeilten motorischen Programme für spezifische Fortbewegungshemmung ausführt, welche für dezidierte Stopp- oder Schlafneuronen in anderen Tieren charakteristisch sind. Verhaltensanalysen zeigen, dass *C. elegans* zwei Arten von Bewegungsstillstand zeigen können: 1) mit reduziertem Muskeltonus, z. B. während eines verlängerten Schlafs, oder 2) mit gleichzeitiger Aufrechterhaltung des Muskeltonus, z. B. während des kurzen Stoppverhaltens, welches die Richtungsumkehr von vorwärts- zu rückwärtsgerichteter wellenförmiger Fortbewegung begleitet. Um eine ordnungsgemäße motorische Umsetzung ausschliesslich im geeigneten Kontext zu gewährleisten, müssten solche Stopp-/Schlafneuronen-Typen oder -Schaltkreise insbesondere in der Lage sein, stromauf gelegene Stoppsignale wahrzunehmen, solche konvergierenden Signale zu integrieren und anderen Interneuronen, welche die Fortbewegung fördern, entgegenzuwirken. Wie solche Neuronen diese Funktionen auf molekularer Ebene ausführen, ist Teil der laufenden Untersuchungen in *C. elegans*.

In Kapitel 2 zeigen wir, dass das RIS-Interneuron die Funktion eines Stopp-Neurons erfüllt, welches die Fortbewegung von *C. elegans* schnell anhalten kann. Unsere Daten deuten darauf hin, dass eine erhöhte Kalziumaktivität in diesem einzelnen Neuron ausreicht, um einen vorübergehenden Stop auszulösen. Wir fanden, dass die Aktivität von RIS die Kalzium-Oszillationen in cholinergen Motoneuronen verhindert und somit deren reziproke Stimulation der dorso-ventral gegenüber liegenden Körperwandmuskeln hemmt. Auf diese Weise könnte die RIS-Aktivität in die mustergenerierenden Schaltkreise eingreifen welche der Fortbewegung zugrunde liegen, indem sie die Aktivität erregender Motoneuronen desynchronisiert.

Weiterhin haben wir festgestellt, dass der klassische inhibitorische Neurotransmitter GABA für das schnelle Einsetzen des RIS-induzierten Stoppverhaltens förderlich ist, und ihn als Transmitter zur schnellen Einleitung des Lokomotionsstopps etabliert. GABA ist bei *C. elegans* jedoch weder für das Auftreten noch für die Aufrechterhaltung des Stoppverhaltens absolut erforderlich, weshalb auch andere Neurotransmitter eine entscheidende Rolle spielen müssen. Für RIS fanden wir, dass es neben seiner Funktion als Stoppneuron auch bei Umkehr der Bewegungsrichtung einen erhöhten Kalziumspiegel aufweist.

Wir zeigen, dass die (elektrische) Konnektivität von RIS über Gap Junctions für diesen erhöhten ‚Reversal‘-Phänotyp notwendig ist. RIS ist jedoch nicht das einzige Neuron, welches Reversals auslösen kann, da die Tiere auch nach genetischer Ablation des RIS-Neurons noch in der Lage sind, sich rückwärts zu bewegen.

Als nächstes zeige ich, dass die Kalziumaktivität in RIS mit der Verlangsamung der Vorwärtsbewegung korreliert und häufig den Umkehrereignissen vorausgeht. Bei der Analyse von möglichen funktionellen Kompartimenten entlang des RIS-Axons wird diese Korrelation besonders im Bereich des Nervenrings deutlich, wo sich die meisten Verbindungen zwischen RIS und seinen synaptischen Partnerneuronen befinden. Wir vermuten daher, dass die Kalziumdynamik von RIS in seinem Axon kompartimentiert ist.

Zusätzlich zu der Induzierung dieses kurzen Stoppverhaltens vor einer Bewegungsumkehr ist das RIS-Interneuron auch als das wichtigste schlafaktive Neuron in *C. elegans* bekannt. RIS ist für die reduzierte Fortbewegung sowohl im Zustand des Lethargus im Larvenstadium als auch im Erwachsenenalter erforderlich, in dem Schlafverhalten durch Stress oder Pheromone ausgelöst werden kann. Bemerkenswerterweise ist *C. elegans* also in der Lage, zwei unterschiedliche Aspekte der Bewegungshemmung durch die Aktivität eines einzigen Interneurons zu induzieren.

All dies zeigt deutlich, dass die neuronale Kontrolle der Lokomotionshemmung ein dynamischer und modularer Regulierungsprozess ist und nicht nur die mathematische Summe logischer Ein/Aus-Schalter zur Erhöhung oder Verringerung der Bewegungsfrequenz.

Um zu untersuchen, ob Neuropeptide die neuronale Regulierung der Lokomotionshemmung in *C. elegans* modulieren können, haben wir Stämme mit Deletionsmutanten von Neuropeptidvorläufer- und GPCR-Genen in verschiedenen Verhaltenstests untersucht. Da die GABAerge Übertragung allein nicht das gesamte Ausmaß des RIS-vermittelten Stopverhaltens erklärt, wurden Neuropeptide als alternative Signalmoleküle in Betracht gezogen. Wir konnten zeigen, dass Neuropeptide tatsächlich erforderlich sind, um den optogenetisch stimulierten RIS-vermittelten Stopp-Phänotyp aufrechtzuerhalten. Wie ich feststellte, führt insbesondere die Deletion des *flp-11*-Gens zu einer Unterbrechung des RIS-vermittelten Stopverhaltens. Somit ist FLP-11 entscheidend für die Aufrechterhaltung des Stops der Tiere, vor der Einleitung der Umkehrung der Bewegungsrichtung.

Anschließend konnten wir zeigen, dass ohne das Neuropeptide FLP-11 eine erhöhte RIS-Kalziumaktivität keine Verlangsamung der Fortbewegung bewirken kann. Unsere Daten deuten also darauf hin, dass RIS die verlängerte Dauer des Stopverhaltens über die Sekretion von FLP-11-Neuropeptiden reguliert.

Zusammenfassend lässt sich sagen, dass RIS ein einzelnes, aber grundlegendes modulatorisches Neuron ist, das sowohl ein kurzes Anhalten als auch einen längeren Bewegungsstillstand während des Schlafs bewirken kann, indem es die Dauer der motorischen Hemmung über peptiderge Signale steuert.

In Kapitel 3 untersuchen wir die neuartige Rolle von zwei bisher nicht charakterisierten, mit GnRH verwandten Rezeptoren bei der Regulierung der Schlaf-Wach-Zyklen während der Larvenentwicklung von *C. elegans*. *In silico*-Sequenzanalysen ergaben, dass acht solcher GNRR-Rezeptoren im Genom von *C. elegans* kodiert sind. Unser phylogenetischer Stammbaum deutet darauf hin, dass die Fülle von acht Rezeptoren aus einer nematodenspezifischen Expansion eines GNRR-Vorgängers stammt, der dem GNRR-1 am ähnlichsten ist. Der Stammbaum weist für GNRR-1 im Vergleich zu anderen protostomischen GnRH/AKH-ähnlichen Rezeptoren die kürzesten Zweiglängen auf. GNRR-1 wird durch NLP-47-Peptide aktiviert welche bekanntermaßen die Fortpflanzung regulieren. Überraschenderweise stellen wir fest, dass zwei der GNRR-Rezeptoren, GNRR-3 und GNRR-6, durch Neuropeptide, welche von den Genen *nlp-2*, *nlp-22* und *nlp-23* kodiert werden, *in vitro* stark und dosisabhängig aktiviert werden können. Diese Neuropeptide enthalten alle ein konserviertes C-terminales RPamid-Motiv und liegen auf demselben Chromosom nahe beieinander. Während die RPamide-Neuropeptide innerhalb des Stammes der *Nematoda* eine starke Sequenzkonservierung aufweisen, wurde vor dieser Studie noch keine eindeutige Sequenzähnlichkeit mit anderen Peptiden außerhalb des Stammes festgestellt. Wir schlagen vor, die RPamid-Neuropeptide als Peptide vom GnRH-Typ zu klassifizieren (in Übereinstimmung mit der kürzlich von Zandawala *et al.* (2018) vorgeschlagenen Nomenklatur).

Die einzigen RPamid-Neuropeptide von *C. elegans*, die bisher im Detail untersucht wurden, werden von *nlp-22* kodiert und in RIA-Interneuronen exprimiert. Diese NLP-22-Neuropeptide weisen während der Larvenentwicklung somnogene Eigenschaften auf, und ihre Überexpression ist in der Lage, akut Schlaf zu induzieren. Die Identifizierung von bisher nicht untersuchten GNRRs sowie ihrer kognitiven Rezeptoren *in vitro* veranlasste uns, ihre Rolle bei der Schlafregulation von *C. elegans* genauer zu untersuchen.

Wir stellen fest, dass *gnrr-3* in GABAergen Motoneuronen des hinteren ventralen Nervenstrangs von *C. elegans* exprimiert wird, was eindeutig auf eine plausible Rolle bei der Regulierung der Bewegungshemmung hinweist. Darüber hinaus ermittelte ich das Expressionsmuster von *gnrr-6* in einer größeren Untergruppe von Neuronen, die ebenfalls mehrere entscheidende Neuronenklassen mit Funktion im motorischen Verhalten umfasst. Wir zeigen dann, dass NLP-22-Neuropeptide durch GNRR-6 signalisieren, um die Fortbewegungsaktivität von *C. elegans* während des Schlafs zu unterdrücken. Darüber hinaus weisen wir nach, dass eine Überexpression von *nlp-22* auch in Abwesenheit von GNRR-6-Rezeptoren eine Inhibition des Pharynx induziert, was darauf hindeutet, dass Aspekte des Schlafverhaltens von GNRR-6 unabhängig sind. Andererseits zeigen wir auch, dass NLP-2 Neuropeptide während des Lethargus Wachzustände fördern, über GNRR-3- und GNRR-6-Rezeptoren.

Zuletzt wiesen wir nach, dass das *nlp-2* Gen vorwiegend in einem einzigen Paar sensorischer AWA-Neuronen exprimiert wird und dass seine Transkripte mit der Periodizität der larvalen Häutungen zyklisch zu- und abnehmen. Unsere Erkenntnisse, dass die *nlp-2*-Transkriptmenge den zeitlichen Expressionszyklen der Entwicklungszeitgene folgt, legen den Schluss nahe, dass die Expressionsniveaus der RPamid-Neuropeptide während der Entwicklungsreifung streng reguliert werden.

Somit haben wir herausgefunden, dass RPamid-Neuropeptide, die sowohl von *nlp-2*- als auch von *nlp-22*-Genen kodiert werden, über GnRH-ähnliche Rezeptoren Signale aussenden, die entweder Wachsein oder Schlaf fördern.

Zusammenfassend konnten wir zeigen, 1) dass *C. elegans* elektrische, synaptische und neuropeptiderge Signalwege von RIS, eines Stoppneurons mit kompartimentierter Ca^{2+} -Dynamik, nutzt, um die aktive Hemmung der Fortbewegung differenziert zu regulieren, und 2) dass GnRH-ähnliche neuropeptiderge Signalwege keine reproduktiven, sondern Funktionen bei der Regulierung des Schlaf-Wach-Verhaltens der Larven aufweisen. Diese Arbeit wirft somit ein neues Licht darauf, wie spezifische Neuropeptide von Stopp- oder Schlafneuronen das Verhalten der Bewegungshemmung in *C. elegans* regulieren.

Supplementary information and figures

I would like to refer to the online supplementary information and figures freely available at:

Chapter1: <https://doi.org/10.1038/s41467-019-12098-5>

Chapter2: <https://doi.org/10.1038/s41598-020-66536-2>

In addition, I added two additional publications to which I contributed to in lesser extent as annexes to this dissertation:

Annex I:

Tolstenkov, O., Van der Auwera, P., Steuer Costa, W., Bazhanova, O., Gemeinhardt, T. M., Bergs, A. C. & Gottschalk, A. (2018). Functionally asymmetric motor neurons contribute to coordinating locomotion of *Caenorhabditis elegans*. *eLife*, 7, e34997.

<https://doi.org/10.7554/eLife.34997.026>

I primarily contributed by optimizing the automated tracking microscope for calcium imaging in freely moving *C. elegans* animals, by writing computer code for scripts to analyse moving regions of interest in calcium imaging videos for Fig. 5 of this publication, by assisting in decision process for the preferential microscopic configuration for fluorescence microscopy set ups and discussing data interpretation in this publication.

Annex II:

Watteyne, J., Peymen, K., Van der Auwera, P., Borghgraef, C., Vandewyer, E., Van Damme, S., Rutten, I., Lammertyn, J., Jelier, R., Schoofs, L., Beets, I. (2020). Neuromedin U signaling regulates retrieval of learned salt avoidance in a *C. elegans* gustatory circuit. *Nature Communications*, 11, 2076.

<https://doi.org/10.1038/s41467-020-15964-9>

I primarily contributed by setting up and optimizing the microscope, microfluidic control system and work flow for calcium imaging animals that are simultaneously exposed to soluble stimulus sequences, by writing computer code for scripts to analyse moving regions of interest in calcium imaging videos and for scripts for automated generation of graphs for Fig. 6 of this publication, by (out)crossing multiple mutant *C. elegans* strains, by assisting in decision process for the preferential microscopic configuration for fluorescence microscopy set ups, by acquiring preliminary confocal fluorescence images of neuronal expression patterns and discussing data interpretation in this publication.

List of publications**Peer-reviewed articles**

Tolstenkov, O., Van der Auwera, P., Steuer Costa, W., Bazhanova, O., Gemeinhardt, T. M., Bergs, A. C. & Gottschalk, A. (2018). Functionally asymmetric motor neurons contribute to coordinating locomotion of *Caenorhabditis elegans*. *eLife*, 7, e34997.

<https://doi.org/10.7554/eLife.34997.026>

Steuer Costa, W.*, Van der Auwera, P.*, Glock, C., Liewald, J. F., Bach, M., Schüler, C., Wabnig, S., Oranth, A., Masurat, F., Bringmann, H., Schoofs, L., Stelzer, E. H. K., Fischer, S. C. & Gottschalk, A. (2019). A GABAergic and peptidergic sleep neuron as a locomotion stop neuron with compartmentalized Ca²⁺ dynamics. *Nature Communications*, 10, 4095.

<https://doi.org/10.1038/s41467-019-12098-5>

Watteyne, J., Peymen, K., Van der Auwera, P., Borghgraef, C., Vandeweyer, E., Van Damme, S., Rutten, I., Lammertyn, J., Jelier, R., Schoofs, L., Beets, I. (2020). Neuromedin U signaling regulates retrieval of learned salt avoidance in a *C. elegans* gustatory circuit. *Nature Communications*, 11, 1-16 (2020).

<https://doi.org/10.1038/s41467-020-15964-9>

Van der Auwera, P.*, Frooninckx, L.*, Buscemi, K., Vance, R. T., Nelson, M. D., Watteyne, J., Mirabeau, O., De Haes, W., Fancsalszky, L., Gottschalk, A., Raizen, D. M., Schoofs, L.* & Beets, I.* (2020). RPamide neuropeptides NLP-22 and NLP-2 act through GnRH-like receptors to promote sleep and wakefulness in *C. elegans*. *Scientific Reports*, 10, 9929,

<https://doi.org/10.1038/s41598-020-66536-2>

(* These authors contributed equally.)

Conference posters

Watteyne, J., Van der Auwera, P., Foley, C., Peymen, K., Schoofs, L., & Beets, I. (2018). Neuromedin U signaling in experience-dependent salt chemotaxis. In *C. elegans topics meeting 'CeNeuro 2018'*. Madison, WI, USA.

Watteyne, J., Van der Auwera, P., Peymen, K., Schoofs, L., & Beets, I. (2018). Neuromedin U signaling in experience-dependent salt chemotaxis. In *Royal Society Meeting on Connectome to Behavior: Modelling C. elegans at cellular resolution*. London - United Kingdom.

Van der Auwera, P., Steuer Costa, W., Fisher, S. C., Glock, C., Tolstenkov, O., Beets, I., Stelzer, E. H. K., Schoofs, L. & Gottschalk, A. (2018). Axonal calcium imaging of a GABAergic interneuron in freely moving *C. elegans*. In *The Royal Society Meeting*. London - United Kingdom.

Steuer Costa, W., Van der Auwera, P., Glock, C., Mandal, J., Oranth, A., Tolstenkov, O., Schüler, C., Liewald, J., Fischer, S., Beets, I., Miller, D. & Gottschalk, A. (2017). The peptidergic RIS neuron acts as a locomotion stop neuron in the adult. In *21st International C. elegans meeting*. Los Angeles, USA.

Steuer Costa, W., Van der Auwera, P., Glock, C., McWhirter, R., Tolstenkov, O., Beets, I., Mandal, J., Schüler, C., Liewald, J., Fischer, S., Schoofs, L., Stelzer, E. H. K., Miller, D. & Gottschalk, A. (2017). Neuropeptidergic control of the forward to reverse locomotion switch. In *EMBO/EMBL Symposia*. Heidelberg, Germany.

Tolstenkov, O., Bazhanova, O., Van der Auwera, P., Bergs, A., & Gottschalk, A. (2016). Optogenetic analysis of previously unstudied AS neurons in the locomotor circuit. In *European Worm Meeting*. Berlin, Germany.

Oranth, A., Schultheis, C., Erbguth, K., Liewald, J., Tolstenkov, O., Van der Auwera, P., Wabnig, S., Steuer Costa, W., Beets, I., Miller, D. & Gottschalk, A. (2016). Optogenetic analysis of peptidergic neuronal network controlling a food related navigation behavior. In *European Worm Meeting*. Berlin, Germany.

Van der Auwera, P., Steuer Costa, W., Fischer, S. C., Glock, C., Tolstenkov, O., Oranth, A., Stelzer, E. H. K., Schoofs, L. & Gottschalk, A. (2016). Axonal calcium imaging in freely moving animals. In *European Worm Meeting*. Berlin, Germany.

Van der Auwera, P., Steuer Costa, W., Fischer, S. C., Glock, C., Tolstenkov, O., Oranth, A., Stelzer, E. H. K., Schoofs, L. & Gottschalk, A. (2016). Axonal calcium imaging in freely moving *C. elegans* nematodes. In *The Brain Conference; The Brain in Focus: New Approaches to Imaging Neurons and Neural Circuits*. Rungstedgaard - North Copenhagen, Denmark.

Frooninckx, L., Watteyne, J., Van Sinay, E., Van der Auwera, P., Janssen, T., Mirabeau, O., Schoofs, L. & Beets, I. (2014). Pharmacological and functional characterization of a conserved tachykinin signaling system in *C. elegans*. In *Congress of the European Comparative Endocrinologists (CECE)*. Rennes, France.

Watteyne, J., Frooninckx, L., Van der Auwera, P., Beets, I., Temmerman, L., Husson, S., & Schoofs, L. (2014). Optogenetic analysis of the nociceptor ASH in *Caenorhabditis elegans*. In *FENS Forum of Neuroscience*. Milan, Italy.

Curriculum vitae

Petrus Van der Auwera

Born: 02/05/1991, Diest, Belgium

Current address:

Groot Park 1d bus 5
B-3360, Lovenjoel, BELGIUM

Nationality: Belg

Gender: male

petrus.vanderauwera@kuleuven.be

petrus.vanderauwera@outlook.com

ORCID: [0000-0001-7540-4788](https://orcid.org/0000-0001-7540-4788)



KU Leuven

Faculty of Science

Department Biology

Division of Animal Physiology and Neurobiology

Research Group of Functional Genomics & Proteomics (Schoofs lab)

Naamsestraat 59 - bus 2465

B-3000 Leuven, BELGIUM

Room: 91.44

tel. + 32 16 32 92 34

<https://bio.kuleuven.be/df/lis>

KU LEUVEN

Johann Wolfgang Goethe -Universität in Frankfurt am Main

Fachbereich Biochemie, Chemie und Pharmazie

Institute of Biochemistry

Buchmann Institute for Molecular Life Sciences

Cellular and Molecular Neurobiology Group (Gottschalk lab)

Max-von-Laue-straße 15

D-60438 Frankfurt am Main, GERMANY

tel. + 49(0)69 798-42518

https://www.bmls.de/Cellular_and_Molecular_Neurobiology/people.html



2003-2009: Algemeen secundair onderwijs (ASO), Sint-Jozefscollege, Aarschot, Belgium.

2009-2012: Bachelor of Science in Biology (minor Geology), KU Leuven, Leuven, Belgium.
Overall result: Magna cum laude with 78,17%

2012-2014: Master of Science: Biology, KU Leuven, Leuven, Belgium.
Overall result: Magna cum laude with 82,25%

Master Thesis (17,2 / 20): "An optogenetic analysis of neuropeptidergic signaling components involved in nociception in *Caenorhabditis elegans*" in Research Group of Functional Genomics & Proteomics (Schoofs lab).

2014-2019: Joint PhD research stays:

2014-2016: Cellular and Molecular Neurobiology Group (Gottschalk lab),
Johann Wolfgang Goethe -Universität in Frankfurt am Main, Germany.

2017-2019: Research Group of Functional Genomics & Proteomics (Schoofs lab),
KU Leuven, Belgium.

Annexes

Annex I:

Tolstenkov, O., Van der Auwera, P., Steuer Costa, W., Bazhanova, O., Gemeinhardt, T. M., Bergs, A. C. & Gottschalk, A. (2018). Functionally asymmetric motor neurons contribute to coordinating locomotion of *Caenorhabditis elegans*. *eLife*, 7, e34997.
<https://doi.org/10.7554/eLife.34997.026>

I primarily contributed by optimizing the automated tracking microscope for calcium imaging in freely moving *C. elegans* animals, by writing computer code for scripts to analyse moving regions of interest in calcium imaging videos for Fig. 5 of this publication, by assisting in decision process for the preferential microscopic configuration for fluorescence microscopy set ups and discussing data interpretation in this publication.

Annex II:

Watteyne, J., Peymen, K., Van der Auwera, P., Borghgraef, C., Vandewyer, E., Van Damme, S., Rutten, I., Lammertyn, J., Jelier, R., Schoofs, L., Beets, I. (2020). Neuromedin U signaling regulates retrieval of learned salt avoidance in a *C. elegans* gustatory circuit. *Nature Communications*, 11, 2076 (2020).
<https://doi.org/10.1038/s41467-020-15964-9>

I primarily contributed by setting up and optimizing the microscope, and microfluidic control system and work flow for calcium imaging animals that are simultaneously exposed to soluble stimulus sequences, by writing computer code for scripts to analyse moving regions of interest in calcium imaging videos and for scripts for automated generation of graphs for Fig. 6 of this publication, by (out)crossing multiple mutant *C. elegans* strains, by assisting in decision process for the preferential microscopic configuration for fluorescence microscopy set ups, by acquiring preliminary confocal fluorescence images of neuronal expression patterns and discussing data interpretation in this publication.

